NOVEL HYDROGEL POLYMERS

PHILIP HAROLD CORKHILL

Doctor of Philosophy

THE UNIVERSITY OF ASTON IN BIRMINGHAM

March 1988

THE UNIVERSITY OF ASTON IN BIRMINGHAM

NOVEL HYDROGEL POLYMERS

PHILIP HAROLD CORKHILL

Submitted for the Degree
of Doctor of Philosophy

March 1988

SUMMARY

Hydrogels may be conveniently described as hydrophilic polymers that are swollen by, but do not dissolve in, water. In this work a series of copolymer hydrogels and semi-interpenetrating polymer networks based on the monomers 2-hydroxyethyl methacrylate, N-vinyl pyrrolidone and N'N' dimethyl acrylamide, together with some less hydrophilic hydroxyalkyl acrylates and methacrylates have been synthesised. Variations in structure and composition have been correlated both with the total equilibrium water content of the resultant hydrogel and with the more detailed water binding behaviour, as revealed by differential scanning calorimetry studies. The water binding characteristics of the hydrogels were found to be primarily a function of the water structuring groups present in gel. The water binding abilities of these groups were, however, modified by steric effects. The mechanical properties of the hydrogels were also investigated. These were found to be dependent on both the polymer composition and the amount and nature of the water present in the gels. In biological systems, composite formation provides a means of producing strong, high water content materials. As an analogy with these systems hydrogel composites were prepared. In an initial study of these materials the water binding and mechanical properties of semi-interpenetrating polymer networks of N'N'dimethyl acrylamide with cellulosic type materials,with polyurethanes and with ester containing polymers were examined.

A preliminary investigation of surface properties of both the copolymers and semi-interpenetrating polymer networks has been completed, using both contact angle measurements and anchorage dependent fibroblast cells. Measurable differences in surface properties attributable to structural variations in the polymers were detected by droplet techniques in the dehydrated state. However, in the hydrated state these differences were masked by the water in the gels. The use of cells enabled the underlying differences to be probed and the nature of the water structuring group was again found to be the dominant factor.

Keywords: **hydrogel, interpenetrating polymer network, freezing water, surface properties, N'N' dimethyl acrylamide.**

To my parents

ACKNOWLEDGEMENTS

I would like to take this opportunity to express my thanks to the following:

Firstly, I would like to thank my supervisor Dr. Brian Tighe for his advice, encouragement and enthusiasm throughout the course of this work.

Miss Karen Thomas for completing the cell adhesion studies described in this thesis.

Mr. Colin Hamilton and the rest of the "famous five" for their interesting and helpful discussions both during and after working hours.

Dr. Alan Jolly, Dr. Richard Raistrick and Dr. Sheila Murphy for their help during the early months of this work.

Mr. Mohammed Yasin and all the staff and students who have worked with me in labs. 248 and 358 for helping to make my time at Aston so enjoyable.

The occupants of Flat 21, Vauxhall Court during the past three years for their advice and encouragement.

The University of Aston for financial support.

Finally, special thanks go to Miss Helen Oxley for her patience, support and understanding while I have been 'writing up'.

LIST OF CONTENTS

LIST OF TABLES

LIST OF FIGURES

LIST OF ABBREVIATIONS

AZBN	Azo-bis-isobutyronitrile	ACM	Acrylamide
BHK	Baby hamster kidney	CA	Cellulose acetate
CAB	Cellulose acetate butyrate	E	Youngs modulus
ε_b	Elongation to break	EEMA	2-Ethoxyethyl methacrylate
EGDM	Ethylene glycol dimethacrylate	EPDCD	The epoxide of poly (1,2 dihydroxy cyclohexa 3,5 diene dimethyl carbonate)
EWC	Equilibrium water content	γ^d	Dispersive component of the surface free energy
γ^p	Polar component of the surface free energy	γ^t	Total surface free energy
HEA	2-Hydroxyethyl acrylate	HEMA	2-Hydroxyethyl methacrylate
HPA	2-Hydroxypropyl acrylate	HPMA	2-Hydroxypropyl methacrylate
LMA	Lauryl methacrylate	MAA	Methacrylic acid
MMA	Methyl methacrylate	MPEGMA	Methoxy poly (ethylene glycol)$_{350}$ methacrylate
NNDMA	N'N'-Dimethyl acrylamide	NMR	Nuclear magnetic resonance spectroscopy
NVP	N-Vinyl pyrrolidone	PMMA	Poly (methyl methacrylate)
PVAc	Poly (vinyl acetate)	σ_b	Tensile strength
SEM	Scanning electron microscopy	St	Styrene

CHAPTER 1

Introduction

1.1 General Introduction

Hydrogels may be conveniently described as hydrophilic polymers that are water swollen, containing 20% - 98% water by weight, but do not dissolve in water. Many naturally occurring polymers may be used as hydrogels, however, the structural versatility available in synthetic hydrogels has given them distinctive properties, which in turn has enhanced their practical utility. In 1960 the first synthetic hydrogel, a polymer of 2-hydroxyethyl methacrylate (HEMA), was developed by the Czechoslovakian workers Wichterle and Lim[1] who noted its use for the fabrication of soft contact lenses[2,3]. This has proved to be the most successful commercial application of hydrogels but they have been used for a wide variety of biomedical applications. Hydrogels occupy a unique position in the field of biomaterials as the imbibed water strongly influences the transport, surface and mechanical properties of the polymers. However, the mechanical strength of hydrogels often proves to be the limiting factor in several applications. In biological systems composites provide a method of producing materials with good mechanical properties and a high water content[4,5,6]. Articular cartilage is one such composite, based on a polysaccharide matrix, with collagen as the filler polymer. This material has a high water content (65% - 80%) but excellent mechanical properties. However, there has been very little work on hydrogel composites. Therefore, by gaining an understanding of the nature of composites, it may be possible to synthesise hydrogels which mimic the behaviour of biological composites. The existing interest in homogeneous hydrogels, for use in biomedical and other applications, is reflected in the substantial number of reviews of these areas[7-23].

1.2 The Structure of Water

Before examining the interaction of water with hydrogels it is helpful to first examine the structure of water in aqueous solution. Franks[24] has edited a comprehensive review on the structure and properties of water but only a brief resumé of the models proposed for the

structure of water will be discussed below. These models may be described in terms of the process of ice melting.

The first model proposed for the structure of liquid water was by Röntgen in 1892[25]. He suggested the first of the 'mixture models' for water; these models suggest that as ice begins to melt some of the ice is converted to a liquid in which the remaining ice molecules dissolve. Another suggestion as to the structure of water in solution is based on the assumption that as ice melts the hydrogen bonds present in the system bend, but do not break. Therefore, in solution each water molecule is still hydrogen bonded to the same number of neighbours as it was in the solid. However, because of the distortion introduced by the bending of hydrogen bonds, the water is in a liquid rather than crystalline state. This 'conformist class' model was first proposed by Bernal and Fowler in 1933[26].

The third type of model for water structure is the 'interstitial model', first suggested by Samoilov in 1946[27]. In this model, as ice melts water molecules are dislodged from the position which they occupy in the lattice in the solid and are relocated in the interstices of the lattice. However, as no long range order is possible in a liquid a further refinement must be added to this model. This suggests that although there is order in the lattice clusters, there must be areas of disordered i.e. non-hydrogen bonded water between the ordered areas. These three basic types of model for the structure of water have been the basis for numerous attempts to describe the structure of liquid water[28]. Frank and Wen[29] proposed the flickering cluster model for the structure of water in aqueous solution. This suggests that water consists of a mixture of clusters of hydrogen bonded water molecules, with an average lifetime of less than 10^{-10} seconds for each cluster. These ordered cluster 'swim' in regions of disordered i.e. non-hydrogen bonded water.

A review of the recent experimental data and computer simulations on water structure has suggested that interstitial models cannot form the basis for water structure[30]. An alternative model for liquid water is proposed which suggests that it "... consists of a macroscopically connected, random network of hydrogen bonds, that is constantly undergoing topological reformation".

1.3 Water in Hydrogels

The water absorbed by a hydrogel network is quantitatively described by the equilibrium water content, EWC, the ratio of the weight of water in the hydrogel to the weight of the hydrogel at equilibrium hydration, expressed as a percentage.

$$\text{E.W.C \%} = \frac{\text{Weight of water in gel}}{\text{Total weight of hydrated gel}} \times 100 \qquad (1.1)$$

The EWC is arguably the most important single property of a hydrogel influencing, as it does, the permeability, mechanical, surface and other properties of the gel.

1.4 Characterisation of the Hydrogel-Water Interface

As hydrogels are used extensively in biomedical applications the interfacial properties of these materials are important. Silberberg[31] has presented a theoretical description of the hydrogel water interface and Andrade *et. al.*[32] have used a variety of techniques to study the interface. Some of the more common techniques used for the characterisation of the hydrogel-water interface are discussed below.

1.4.1 Scanning Electron Microscopy

The rugosity of the hydrogel surface can be determined by scanning electron microscopy (SEM) examination but careful sample preparation is required. There are three general

methods of sample preparation for SEM studies:

i) air drying

ii) freeze drying or critical point drying

iii) freeze etching

The method of sample preparation does, however, have an effect on the topology of the surface. It has been known for many years that air drying of hydrogels causes significant changes in the structure of the polymer and recent work has shown that even when hydrogels are freeze dried, macrosyneresis of the samples occur[33]. Therefore, to obtain useful information about the surface topology in the natural state, freeze etching must be used to prepare the samples. In freeze etching the sample is frozen rapidly and then fractured under liquid nitrogen. The fractured surface of the gel can then be examined in a cold stage SEM (i.e. still in the frozen state).

1.4.2 Contact Angle Measurements

Contact angle measurements provide another method of probing the interfacial properties of hydrogel systems. These measurements enable the surface free energy of solid, in both the hydrated and dehydrated states, to be determined. The detailed theory behind contact angle measurements will be discussed in Chapter 5, however, at this stage a brief review of the technique will be presented. All contact angle measurements rely on the resolution of forces at the three phase interface of a drop of wetting liquid (or vapour) on a solid surface either immersed in a liquid or in air. Several techniques are available for the measurement of contact angles[34] these include: the tilting plate method, Wilhelmy slide technique and the sessile drop or sessile bubble methods.

Data obtained from contact angle measurements can be used to elucidate the solid-vapour interfacial free energy, γ_{SV}, which in most cases can be approximated to γ_S the surface free

energy of the solid in a vacuum. The value obtained for surface free energy can be split into polar (γ_s^p) and dispersive (γ_s^d) components. Both the total surface free energy and the magnitude of the polar and dispersive components have a strong influence on the biotolerance and blood compatibility of a material and this will be discussed in Section 1.7.2. However, problems can arise in the determination of accurate values for γ_s^p and γ_s^d. Contact angle hysteresis is one problem often encountered when measuring contact angles. Although this can be caused by surface rugosity or inhomogeneity[32] other suggestions have also been forwarded as the cause of this phenomena. A freeze-etch study of water droplets on poly HEMA suggests that gel deformation does occur under water droplets[35], while other workers[36] have suggested that contact angle hysteresis may be due to the reorientation of the polymer chains at the surface of the hydrogel. Thus, the conformation of the polymer changes in order that the surface free energy of the hydrogel moves towards the surface energy of the adjacent phase.

1.4.3 X-Ray Photoelectron Spectroscopy

X-ray photoelectron spectroscopy (XPS) or alternatively electron spectroscopy for chemical analysis (ESCA) is a very useful technique for probing the hydrogel-water interface, based on the photoelectric effect. The kinetic energies of electrons ejected from the sample when it is bombarded with monoenergetic X-rays of known energy are measured and the energies of the ejected photoelectrons are controlled by the equation

$$E_k = E_{h\nu} - E_b - \phi \qquad (1.2)$$

where E_k is the kinetic energy of the ejected electron, $E_{h\nu}$ is the energy of the exciting X-rays, E_b the binding energy of the ejected electron and ϕ is a work function, dependent on the spectrometer.

ESCA studies can be carried out on the hydrogel in either the dehydrated or hydrated

(frozen) state and the following information may be obtained about the hydrogel[37].

i) All elements present (except hydrogen and helium)

ii) Surface concentrations of elements

iii) Bonding state and/or oxidation level of most atoms

iv) Information on aromatic or unsaturated structures from shake up $\pi \rightarrow \pi^*$ transitions

v) Information on electrical properties from charging studies

vi) Non-destructive depth profiling and surface hetrogeneity assessments using photoelectrons with different escape depths and angular dependent ESCA studies

1.4.4 Protein Adsorption and Cell Adhesion Studies

Although protein adsorption studies are normally used to assess biocompatibility, workers in our laboratories have used this technique to probe the surface on a molecular level[38,39]. Protein adsorption studies have been completed on a range of HEMA, acrylamide (ACM) and N-vinyl pyrrolidone (NVP) based copolymer hydrogels with a variety of comonomers. This technique can be used as a probe of surface charge, for example, during the progressive incorporation of methacrylic acid (present in the form of the carboxylate anion in the physiological solutions used in these studies) into both HEMA and ACM copolymers which causes a dramatic decrease in both albumin and fibrinogen adsorption. As incorporation of even 1% of methacrylic acid (MAA) causes this decrease in protein adsorption, the sensitivity of this technique to surface charge is apparent. Water structuring in polymers also appears to influence protein adsorption. The change in albumin and fibrinogen adsorption on copolymers of varying compositions (HEMA-Styrene, ACM-methylene-bis-acrylamide, HEMA-NVP and HEMA-ethyl methacrylate) were investigated. In all the copolymer series, the albumin and fibrinogen adsorption on those compositions that had EWCs of greater than 25% mirrored the changes in freezing and non-freezing water

respectively. Thus, protein adsorption can be used as a sensitive surface probe to detect changes in surface properties which are undetected by conventional surface analysis techniques.

Another useful biological probe technique, which reflects changing surface properties in hydrogels with water contents between 40% and 80%, involves the use of anchorage dependent fibroblast cells. The cell adhesion and growth on a variety of synthetic polymer substrates has been examined[40-42], as a means of investigating the interfacial conversion process that occurs when synthetic materials are placed in contact with a biological environment. Interestingly, poly HEMA hydrogel itself is non cell adhesive. As the water content of hydrogel copolymers increases above the level of this material (~40%), the region of cell non-adhesion is followed by a steady increase in cell adhesion. The relationship of cell adhesion to water content is much more sigmoidal than linear and reflects the fact that interesting surface changes are occurring in this region. There is, however, a current lack of direct physicochemical techniques whereby they may be monitored.

1.5 Techniques used for the Study of Water in Polymers

A variety of techniques exists for the study of water binding in polymers. This may lead to confusion because the ratio of the various states of water present in the polymer will depend on the experimental technique used. Each technique can have some influence on the water structuring, together with the dynamic and thermodynamic properties of the water present in the polymer. A selection of the techniques used for the study of water binding in polymers are described overleaf.

1.5.1 Differential Scanning Calorimetry

The freezing behaviour of water in many polymers is anomalous as even when cooled to very low temperatures only part of the available water in the polymer network freezes. For many years workers have made use of this fact and used calorimetric techniques to study the water binding of cellulose and related materials[43]. A new calorimetric technique which can be used for the study of water binding in polymers, differential scanning calorimetry (DSC), was developed by Perkin-Elmer in 1964 and a schematic diagram of the instrument is shown in Figure 1.1[44]. Whilst in conventional differential thermal analysis (DTA) the difference in temperature between the sample and reference holders is measured, in DSC the energy required to keep both the sample and reference holders at the same temperature is measured. For endothermic transitions the energy to the sample holder is increased to equalise the temperature with the reference holder and for exothermic transitions the energy input to the reference holder is increased. Therefore, the energy input to the sample or reference holder is the energy of the transition and this can be measured directly as it is the area under the recorded peak. A typical melting endotherm for poly HEMA is illustrated in Figure 1.2 and further information about water binding states can be elucidated from the peak shape. Earlier work has shown that the heat of fusion for water in polymers is identical to that for pure water[45,46]. Therefore, using a calibration graph constructed by measuring the area under the melting endotherms of pure water, it is possible to obtain a quantitative determination of the amounts of freezing and non-freezing water present in the polymer.

1.5.2 Nuclear Magnetic Resonance Spectroscopy

Using nuclear magnetic resonance spectroscopy (NMR) the states of water in polymers may be investigated by changes in line widths or changes in the relaxation times of the hydroxyl protons. For liquid water the ^{1}H NMR signal is a tall, narrow peak whilst for ice, and polymers containing bound water, the signal is low and broad. The signal from a polymer

Figure 1.1 **Block diagram of a differential scanning calorimeter**

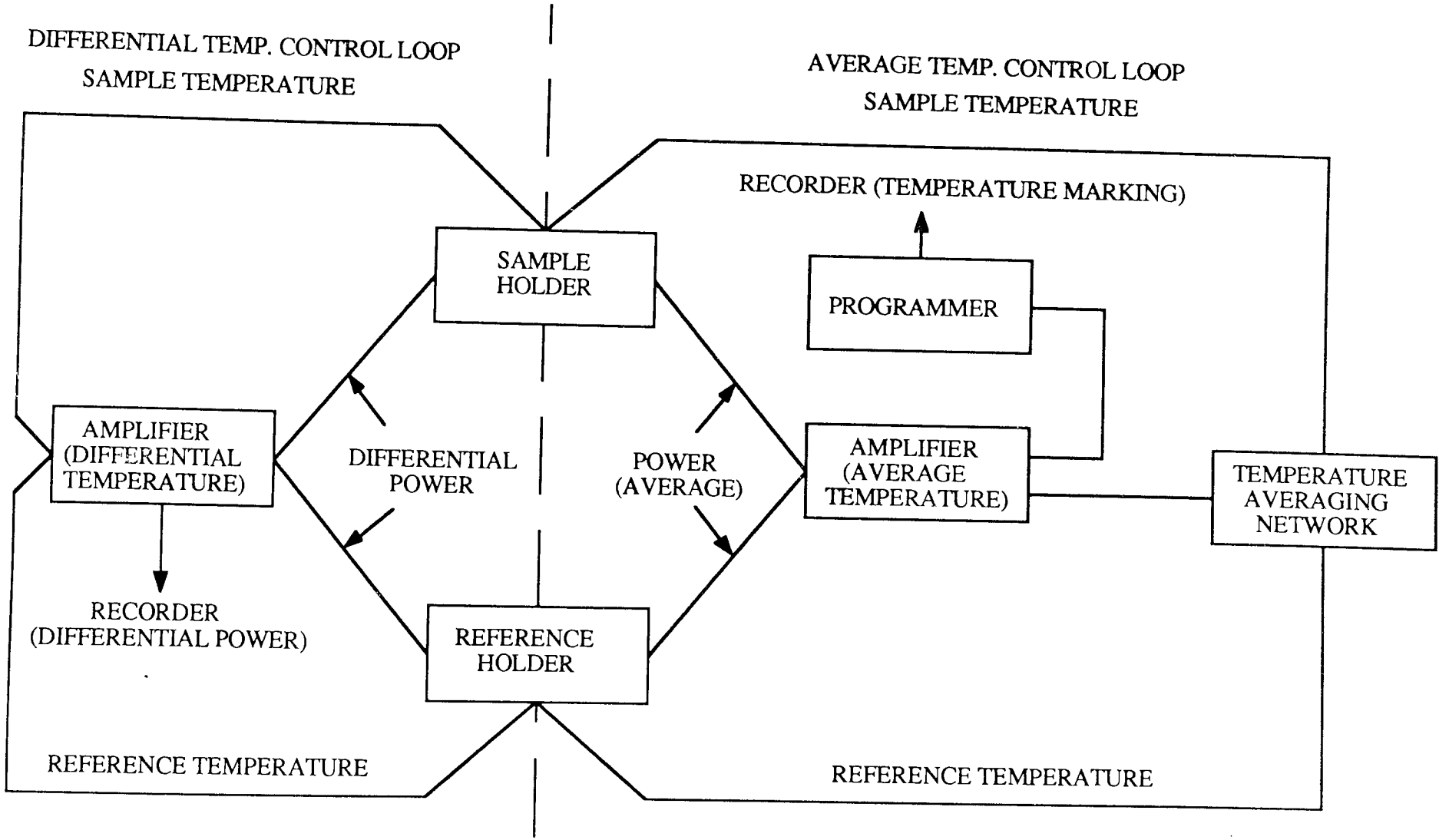

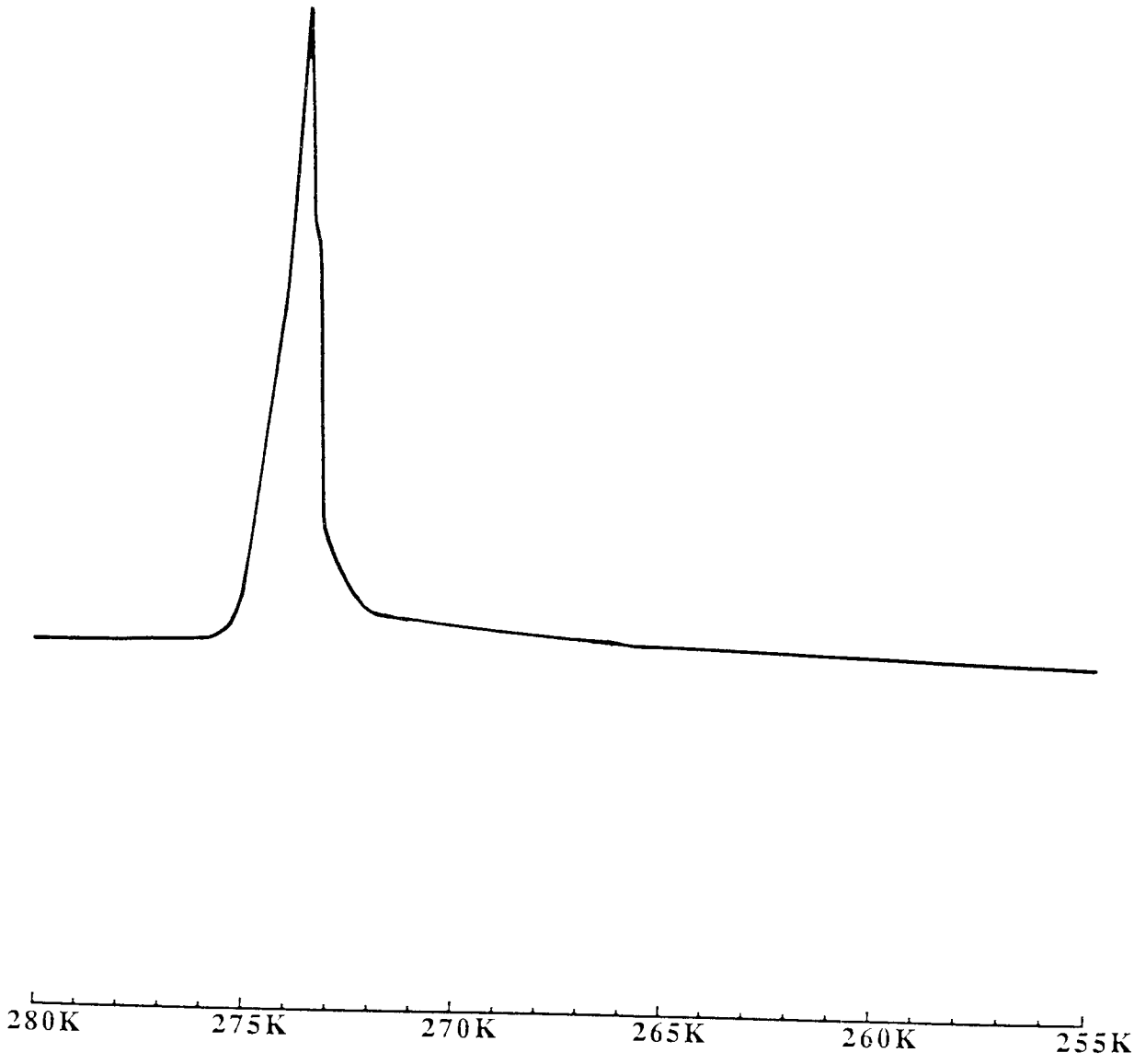

Figure 1.2 Typical melting endotherm of a poly HEMA hydrogel

containing water will be between these two extremes. Carbohydrate gels have been studied by NMR and the width of the signal from the hydroxyl protons investigated[47]. This signal can be interpreted to give the percentages of the various types of water present by assuming that, the free water in the system would produce a signal with a peak height and line width equivalent to that of pure water. Therefore the remaining peak area is due to the more closely associated water.

Andrade and his co-workers[48] have shown that the relaxation times of water present in poly HEMA hydrogel are much lower than those for bulk water. The spin-lattice relaxation time, T_1, involves conversion of spin energy to thermal energy and a reduction of T_1 indicates a reduction in the mobility of the water molecules in the hydrogel. T_2, the spin-spin relaxation time is the rate of transfer of spin energy between neighbouring nuclei. T_2 should increase with an increase in the number of mobile water molecules present in the gels. Therefore, the water content at which T_2 starts to increase corresponds to the point where "free" water begins to appear in the hydrogel.

1.5.3 Dilatometry

Another method used to study water structuring in gels is dilatometry[49]. Measuring the specific volume change over the range 243-298K and plotting specific volume against temperature, enables the states of water in gels to be determined. The shapes of the heating curves and the hysteresis between the heating and cooling curves are used as a basis for classifying the water in the gel into three states.

1.5.4 Specific Conductivity

Specific conductivity, K, has also been used to determine the nature of water present in hydrogels[50]. If the specific conductivity is measured over the range 258-293K a plot of log

K against 1/T shows a sharp discontinuity around 273K. The types of water present in the gel can be related to the magnitude of the change at the transition point. Activation energies, derived from specific conductivity measurements, are used as a method to determine the types of water present in the gel. If the activation energies of gels with a range of water contents are measured the activation energies are dependent upon the water contents of the gel[51]. Low water content gels (<20% EWC) have an activation energy similar to that of ice and this value may be assigned to "bound" water. Gels containing between 20% and 50% water have activation energies between ice and that of pure water and the activation energies in this region are, therefore, assigned to interfacial water. High water content (EWC>50%) have an activation energy similar to that of pure water and the large amount of "free" water which these gels contain is the overriding factor in determining the activation energy.

1.6 Water in Polymers

There is a great deal of evidence to suggest that water in polymers can exist in more than one state[45-70] and that these states of water in the polymers will affect its properties. Although of long standing interest in natural polymers, especially the cellulosics, water binding has only relatively recently attracted interest in synthetic systems of this type. Work on the water binding of cellulose and related materials has been in progress since 1932[71] and this early work, where there was much variation in the results, has been discussed by several authors[60,72]. There has also been interest in the water binding properties of cellulose acetate[55-58, 61] for use in reverse osmosis applications. All these studies have indicated that there are a minimum of two states of water in cellulose acetate membranes, although some workers have suggested that four states of water may be present[61]. Other work[58] has shown that the non-freezing water in cellulose acetate membranes increases with a decrease in the packing density of the polymer. However, in dense polymer films the polymer-polymer interactions increase, restricting the accessibility of the polymer chains to water

molecules. This results are important as when cellulose acetate membranes are used for reverse osmosis applications a low freezing water content has been shown to promote salt rejection. However, "bound" water is also important for the transport of pure water across the membrane[73].

In 1969 Baresová reported results from studies of the relaxation behaviour and phase separation in the HEMA-water system[74,75]. These indicated that, even at very low temperatures, some of the water in the system was strongly hydrogen bound to the polymer backbone and did not freeze. Therefore, it was suggested that water in poly HEMA existed in two different states.

An early NMR study of the water in agar gels noted anomalous relaxation times for the water in the gel[76]. This was due to the presence of "bound" water in the agar gel which, although comprising less than 1% of the gel[77], has a profound effect on the spin-spin relaxation time T_2 (as this is controlled by "relaxation interactions within the bound water molecules"). A subsequent NMR study of polyacrylamide gels demonstrated that factors other than the hydrophilicity of the substituent groups controlled the amount of non-freezing water in the gels[78]. The crosslink density and the length of crosslinks exerted a strong influence on the amount of non-freezing water present in the gel. It was also postulated that structural specificity played a part in determining the ratio of non-freezing to freezing water.

Aizawa et. al.[49,51,70] studied the states of water in agrose, Sephadex and other carbohydrate gels using several techniques. Their results obtained using electrical conductivity measurements, dilatometry and NMR (change in the proton line width with water content) enabled them to propose a model for the water structuring in these gels. They concluded that water in these gels existed in three states which they classified as W_1, W_2

and W_3. A similar method of classifying water in poly HEMA and hydroxyalkyl methacrylate copolymers was suggested by Andrade and co-workers[63]. The water present in hydrogels was classified into three types X, Y and Z water. This classification was based on a study of the water structuring in poly HEMA using specific conductivity, dilatometry and DSC . It was reported that poly HEMA gels contained up to 20% Z type water and 12% Y type water, with any remaining water in the gel present as X type water. Evidence for three types of water being present in gels of (2,3-dihydroxypropyl methacrylate) has also been presented[79] by these workers.

A three stage process for the absorption of water, by poly HEMA, has been suggested based on a DTA and NMR study of the water structuring in the hydrogel[48]. This is represented schematically in Figure 1.3.

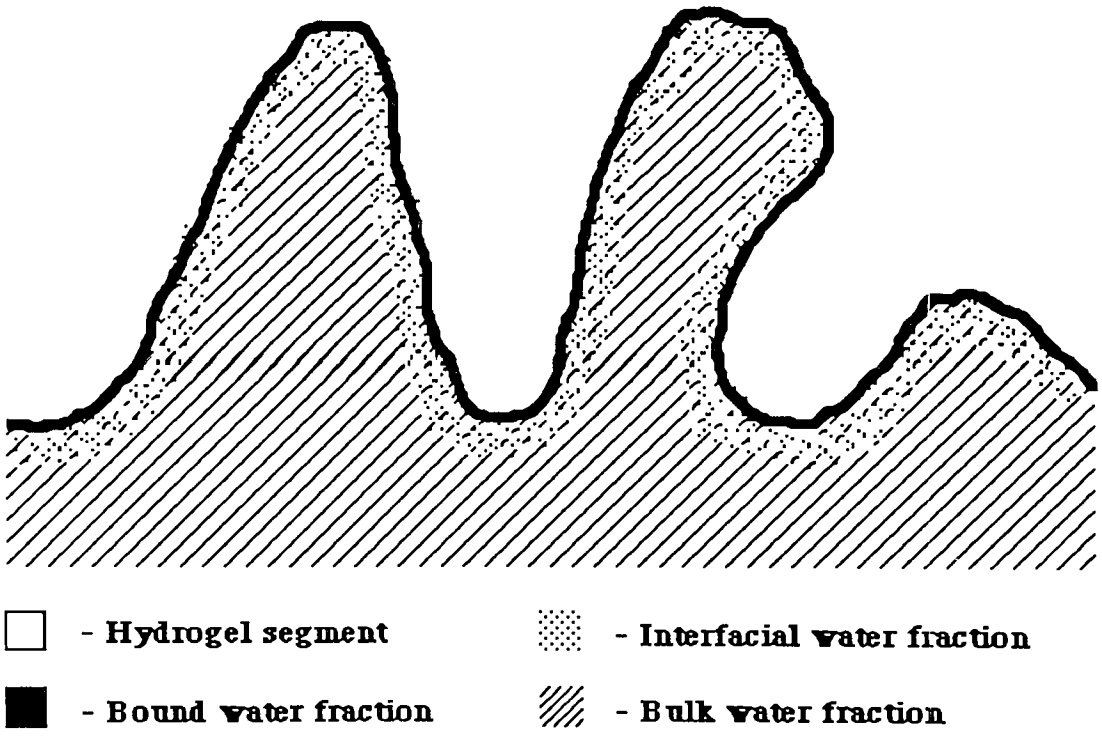

Figure 1.3 Three state model for water in swollen hydrogel membranes (redrawn from reference 80)

Initially water is strongly "bound" to specific sites on the polymer chains (e.g. the hydroxyl or ester groups). This water (up to 21.8% for poly HEMA crosslinked with 1% tetraethylene glycol dimethacrylate) behaves thermodynamically and dynamically as part of the polymer. Other water is preferentially structured around the polymer network, weakly bound to the hydrophilic sites in the polymer or the strongly "bound" water molecules (up to a maximum value of 17% in the poly HEMA hydrogel). Any remaining water behaves as bulk like water.

Work on stereoregular poly HEMA hydrogels[50,81] and HEMA copolymers[64] by Jhon and co-workers has given an insight into the way in which the various types of water in hydrogels are affected by changes in structure. It was shown that although the total water content of a system was changed by altering the crosslink density, the non-freezing water content remained constant. The interfacial water content increased with increasing crossslink density. The non-freezing water contents for isotactic and syndiotactic poly HEMA were reported as 21% and 19%, for example, while the EWCs were 38% and 31% respectively. These results are consistent with the hypothesis that the non-freezing water content is controlled mainly by the primary structure of the hydrogel. However, the secondary and tertiary structure has a great influence on the freezing (free and interfacial) water.

Pedley and Tighe[82] in their work on terpolymers of acrylamide, methacrylic acid and styrene demonstrated that, with this system, it was possible to control the percentage of freezing water in the polymer at a specific EWC. This was achieved by varying the molar ratio of the monomers and has applications in membranes for reverse osmosis. The shapes of the DSC melting endotherms were also investigated and it was found that the peak shapes and the areas under the peaks changed with temperature cycling. This was attributed to a move towards more ideal crystallisation behaviour. The relative amounts of each type of

water present in the hydrogel changed (with an increase in the amount of bulk like water) with temperature cycling, as the water within the polymer was reorganised. However, with poly (vinyl alcohol), PVA, hydrogels very different behaviour is observed with temperature cycling. A recent communication[83] on the effect of temperature cycling on PVA hydrogels indicated that the amount of freezing water in the gel decreased with temperature cycling. This was coupled with an increase in the non-freezing water present in the hydrogel. This behaviour was attributed to a decrease in the number or size of the crystalites in the PVA which enabled the water to interact more readily with the PVA molecules.

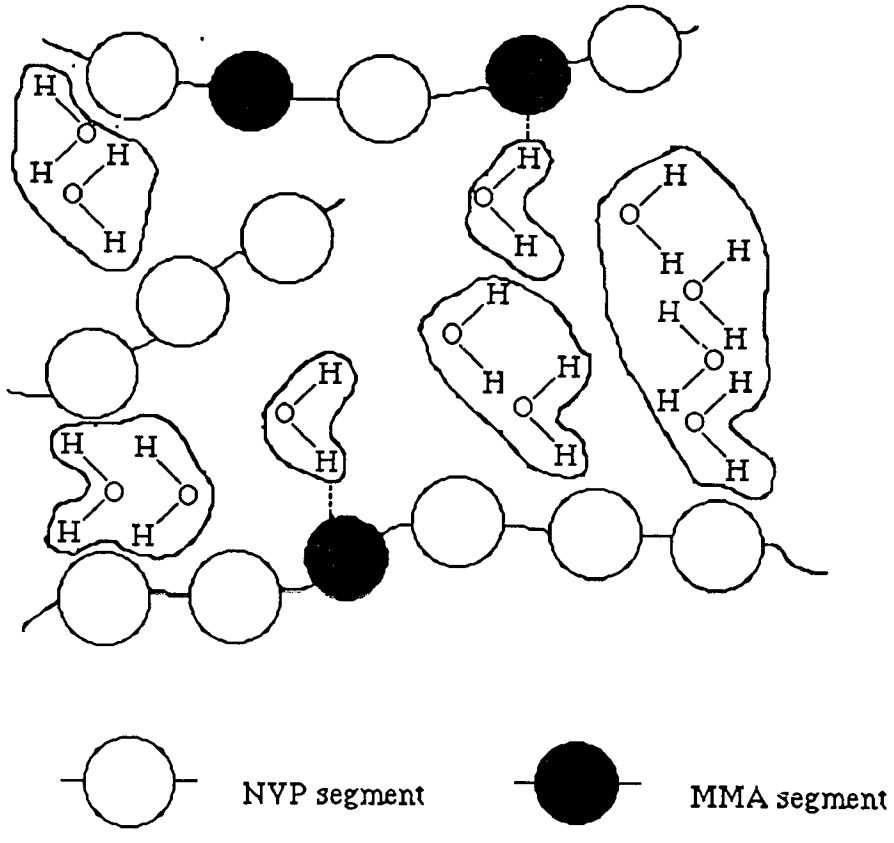

Figure 1.4 Water structuring in a MMA-NVP 80:20 hydrogel (redrawn from reference 84)

The water binding in copolymer hydrogels of methyl methacrylate and N-vinyl pyrrolidone has also been investigated. In membranes containing <27% NVP (i.e. those which contain no bulklike water) the water in the hydrogel was classified into two types; water hydrogen bound to the NVP segments in the backbone (i.e. non-freezing water) and hydrophobic hydration water which forms clusters near the MMA segments in the backbone. This is shown schematically in Figure 1.4. Andrade[85] has suggested that hydrophobic interactions are important in some hydrogel systems and they are known to contribute to the stabilisation of protiens[86]. Hydrophobic interactions arise in molecules with some degree of hydrophobic character, in which intramolecular or intermolecular interactions are more favourable than interaction with water. Refojo[87] has reported the existence of hydrophobic interactions in amphiphilic poly HEMA based on results from swelling experiments in various solvents. Introduction of organic solvents (e.g. acetone and alcohol) causes an increase of swelling in poly HEMA, relative to that in water. It is thought that these solvents break hydrophobic bonds by increasing the solubility of the non-polar groups, this would reduce the retractive force in the system and lead to increased swelling. Further work on the interaction between poly HEMA and organic solvents has also produced evidence (e.g a minimum in EWC and swelling at 55°C) which supports the theory that hydrophobic bonding is important in this system[88,89]. This will be discussed in more detail in Chapter 3.

The water present in a polymer network exists in a continuum of states between two extremes. These are, water strongly associated with the polymer network through hydrogen bonding, sometimes called 'bound' or non-freezing water and water with a much greater degree of mobility, unaffected by the polymeric environment and sometimes referred to as 'free' or freezing water. The properties of a hydrogel are, therefore, strongly influenced both by the EWC of the hydrogel and by the ratio of freezing to non-freezing water. The

technique used to study water binding will to some extent determine the number of states into which the water is classified and even the terms used to describe those states. A correlation of these descriptions has been assembled in Table 1.1.

Table 1.1 Comparison of terms used in water binding studies

				References
Primary		Secondary		52 - 54
Bound		Free		45, 55-57
Non-Freezing		Freezing		55, 58, 59
Primary bound	Secondary bound	Free	Bulk	46, 60
Bound Water which rejects salts	Bound Water which can contain salts with polymer	Free Water weakly interacting	Completely free water	61
Bound	Interfacial	Bulk		62, 33
Bound	Interfacial	Free		48, 50, 64
Non-Freezing	Freezable Bound	Free		65 - 69
X	Y	Z		50, 62 - 64
W_3	W_2	W_1		49, 70

1.6.1 Water Structuring at the Hydrogel-Water Interface

Evidence has previously been presented for the structuring of water in polymers, however, this water structuring is thought to extend into the bulk water adjacent to the polymer. Thermal anomalies are found in the interfacial tension, dielectric and other properties of water present at a solid or liquid interface in both biological and inorganic systems[90]. Drost-Hansen has reviewed all the evidence for these thermal anomalies near interfaces and concluded that water near interfaces is "significantly different" from bulk water[91]. He proposed the following model for the structure of water near a solid surface. Adjacent to the solid surface a layer of highly ordered water is present and this becomes more disordered as the distance from the surface increases until, at a sufficiently large distance from the surface, the water structure is that of normal bulk water. In the intermediate zone, there is a region of disordered transition between ordered and bulk water; the depths of these regions of order and disordered transition being dependent on the nature of the adjacent interface. This model is similar to that proposed by Frank and Wen for the structure of water in aqueous solution[29]

1.7 Biocompatibility

Over the past two decades there has been extensive research into the factors which render a material biocompatible or biotolerant. A complete discussion of this subject is outside the scope of this thesis. However, two areas which are particularly relevant to the applications of high water content hydrogels, protein adsorption on contact lenses and blood compatibility will be discussed here.

1.7.1 Protein Adsorption on Contact Lens Materials

One of the major commercial uses of high water content hydrogels is for the production of extended wear contact lenses. However, the formation of proteinaceous deposits on the

surface of these lenses may lead to lens spoilation[92,93]. Protein adsorption, on both hydrogel and non-hydrogel surfaces, has been studied extensively and Horbett has compiled two excellent reviews on this subject[94,95]. Baker and Tighe[96] have also discussed this problem and proposed a mechanism for the formation of protein deposits on lenses. Several studies on this phenomenon have been completed and some of these are discussed briefly below.

Castillo and co-workers[97] have used Fourier transform attenuated total reflectance infra-red spectroscopy to study protein adsorption on HEMA and HEMA-MAA lenses. Albumin denatured more slowly on the higher water content (HEMA-MAA) lenses, therefore, it was suggested that hydrophilicity affected the behaviour of proteins at interfaces. However, previous work on the analysis of deposits on high water content (HEMA-NVP) lenses indicated that they were identical to those on poly HEMA lenses, both in morphology and composition[98]. The main component of the deposits was a protein which was found only on the surface of the lens. A more detailed examination of the deposits revealed that the amino acid sequence of the protein was similar to lysozyme and that lipids and some inorganic material was also present. Finally, it was found that the deposits had often grown around a defect in the lens surface. Other studies of surface deposits on soft contact lenses[99-101] confirm that lysozyme (which accounts for only 17% of the protein in tears but is the major component of lens deposits) is selectively adsorbed and denatured by the lenses. A possible explanation for this is the low molecular weight of lysozyme (14,400 Da) which enables it to diffuse easily into the lens. A recent study has shown that mucin components are present on lenses with heavy protein deposits[102]. Mucin was not found on lenses with no (or only slight) deposits, therefore, it was suggested that the adsorption of mucin on top of the normally adsorbed tear proteins caused heavy protein deposits.

The amount of protein adsorbed is dependent on several factors, the primary one being the individual wearing the lens. However, the method of manufacture and lens composition also have an influence[103]. Thus, HEMA-MAA lenses with an EWC of 65% were found to absorb over thirty times more lysozyme than poly HEMA lenses, while lenses manufactured by lathe cutting adsorbed more protein than spin cast lenses. Although it is possible to remove protein deposits using cleaning solutions, it should be possible to eradicate this problem by careful design of the polymer and refinement of the techniques used in lens manufacture.

1.7.2 Blood Compatible Hydrogels

Many theories have been forwarded relating to the factors which render a surface non-thrombogenic (i.e. compatible with blood). In 1970 Baier and co-workers[104] suggested the moderate surface energy hypothesis for blood compatibility. This was based on measurements of the surface properties of materials which had shown some degree of biocompatibility. The critical surface tensions of all these materials were found to be in the range 20-30 mN/m, therefore, it was suggested that materials which have a critical surface tension in this range will exhibit biocompatibility (i.e. be fairly non-thrombogenic). However, several exceptions to this theory have now been discovered.

An alternative theory for blood compatibility, the minimum interfacial energy hypothesis, was proposed by Andrade[85]. This suggested that a low interfacial tension between the implant material and the host environment would improve biocompatibility. Ratner *et. al.*[105] studied the blood compatibility of several hydrogel materials and found that HEMA-ethyl methacrylate (EMA) copolymers were more non-thrombogenic than either of the homopolymers. Therefore, it was suggested that a balance of polar and apolar sites within the polymer increased its blood compatibility. In recent paper Andrade and co-workers[106],

investigated the interaction of HEMA-methyl methacrylate (MMA) copolymers, agarose, Avcothane and glass with blood. They concluded that the minimum free energy hypothesis did not explain their results. The results could be partly explained by the optimum polar-apolar hypothesis but they suggested a multi-parameter approach was necessary to define blood compatibility.

Okano and co-workers[107-109] consider that a microphase separated structure is important for blood compatibility. Block copolymers of HEMA with styrene (St), with poly (dimethyl siloxane) (PDMS), with poly (ethylene oxide) (PEO) and with poly (propylene oxide) (PPO) were synthesised.

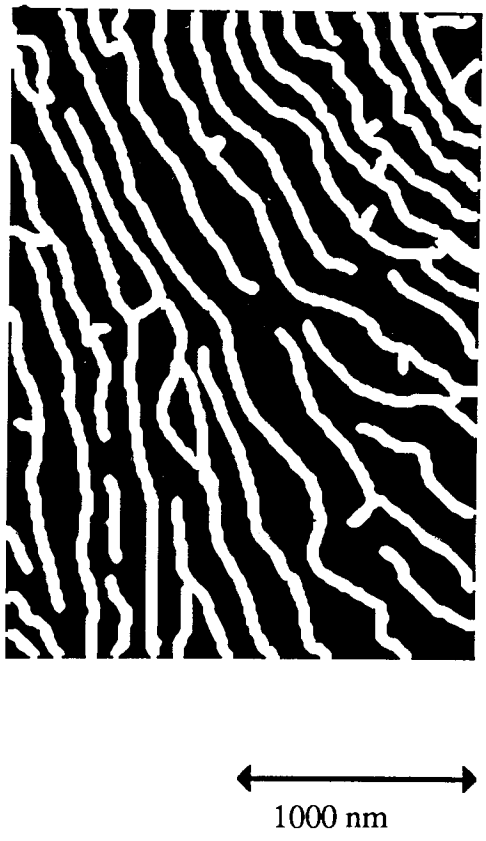

Figure 1.5 **Electron micrograph of a hydrophilic-hydrophobic block copolymer of HEMA-St with 0.61 mole fraction of HEMA. Dark areas represent HEMA microdomains (redrawn from reference 108)**

The composition of the block copolymers, which in turn influenced the morphology of the microdomains, controlled the thrombogenicity of the copolymers. Although all the copolymers synthesised were superior to the homopolymers in suppressing thrombus formation, HEMA-St and HEMA-PEO copolymers were the most successful. These copolymers exhibited a hydrophilic-hydrophobic lamalae structure, shown in Figure 1.5. In *in vivo* tests these copolymers had the ability to suppress the first stage in thrombus formation, platelet adhesion to the surface. The remaining microphase separated copolymers were anti-thrombogenic as they interfered with the second stage in thrombus formation (the change in shape of the adhered platelet, which leads to the release of a substance which triggers aggregation).

Previous work on protein adsorption to this system indicated that γ–globulin and fibrinogen adhered to the hydrophobic domains, whereas albumin adhered to the hydrophilic domains[110]. The formation of ordered areas of adsorbed protein was thought to suppress platelet adhesion. Horbett *et. al.*[111,112] studied the adsorption of fibrinogen, immunoglobin G, albumin and haemoglobin to a series of HEMA-EMA-PE graft copolymers. These polymers were also found to fractionate the plasma proteins and form an ordered adsorbed layer on their surface. They concluded that the formation of this protein layer was an important factor in determining *in vivo* compatibility. Ratner *et. al.*[105], in their work on HEMA-EMA graft copolymers, are one of the other groups that have suggested that the hydrophilic and hydrophobic sites at the surface controlled the composition of the absorbed protein layer. Early Japanese work on HEMA-MMA graft copolymers also showed a correlation between hydrophilic-hydrophobic microphase separated structure and blood compatibility[113]. Therefore, polymer morphology and the balance of hydrophilic and hydrophobic groups on the surface of the polymer appear to be important factors in controlling blood compatibility.

1.8 Biomedical Applications of Hydrogels

Hydrogels are used extensively as biomaterials and their use in contact lens[114], drug delivery[20] and other biomedical applications[8-14] has been well documented. One recent area of interest involves the use of hydrogels, often in the form of composites, some of which may be regarded as blends and interpenetrating networks, synthesised from hydrogels and other synthetic or naturally occurring polymers. Although there is little fundamental literature relating to this aspect of hydrogel chemistry, an examination of the clinical and patent literature reveals several examples of practical attempts to produce useful materials for specific applications using these approaches. One particular area in which this type of activity is apparent is that concerned with wound coverings.The literature in this area is reviewed below. Some of the fundamental aspects of the design of materials for wound dressings are also discussed and additionally, the factors which make hydrogels suitable for use in wound dressing applications are described.

1.8.1 Hydrogels as Wound Dressings

The development of synthetic occlusive wound dressings, used for the treatment of burns, granulation tissue, dermatitis, ulcerations, blisters, fissures, herpes and several other skin conditions is currently a subject of great commercial interest. Work on wound coverings has been in progress since last century and this early work, together with current work on the development of natural and synthetic wound dressings, was reviewed some ten years ago[115]. However, the last decade has seen significant movements in the field. Before examining the role of hydrogels in this area, it is appropriate to note the properties that a successful wound dresssing material should possess. Stated simply, the material should be flexible, strong, nonantigenic and permeable to water vapour and metabolites, whilst securely covering the wound to prevent bacterial infection. Hydrogels possess many of the above properties and because of this they have been used extensively as wound dressing

materials, sometimes alone but frequently in the form of composites, principally to enhance that property with which they are least well endowed-mechanical strength.

Several natural hydrogel polymers have been investigated to determine their suitability for use as wound dressings. Almost inevitably, however, poor mechanical strength necessitates the use of a fibre or polymer matrix as a support with these materials. Wang[116,117], for example, has produced a dextran hydrogel by first reducing dextran with sodium borohydride and then crosslinking the dextran with epichlorohydrin, to give a material which is claimed to have an EWC of 90-95 %. Thin films of the resulting hydrogel were reinforced with fine cotton gauze and the properties of this laminate examined. The hydrogel was loaded with insulin (1mg / ml) whose release from the system was gradual: a consequence of the low diffusion rate of macromolecules through swollen matrices. The hydrogel produced was demonstrated to deliver species of much lower molecular weight such as penicillin when immersed in saline, but the high porosity of the gel resulted in a relatively short delivery time coupled with non-linear penicillin delivery . No antigenic reaction was observed when the gel was implanted in rats and it is thought to have potential use as a skin substitute. Natural polymeric electrolytes have also undergone trials for use as dressings for burns and ulcers[118]. The dressing is formed from a copolymer of water soluble, linear, anionic and cationic polyelectrolytes. The anionic polyelectrolyte is a keratin derivative (eg. ammonium keratinate) and the cationic polyelectrolyte is a glucosaminoglycan (eg chitosin or collagen). When hydrated these hydrogels are malleable and, therefore, can be easily shaped to the contours of the wound. The hydrogels are also employed for the release of topical agents and a dressing containing gentamycin sulphate has been used successfully for the treatment of leg ulcers. A further group of high water content hydrogels have been prepared by radiation crosslinking of sugar and protein derivatives with a hydrophilic monomer such as acrylic acid[119]. These hydrogels are said

to be useful for wound dressing applications, particularly if they are bonded to a supporting film, which may be used to control their water content. Hydrogels prepared from glycerol and alkali metal alginates have also been patented for use as wound dressings[120]. The dressings produced are flexible, impermeable to bacteria and can easily be removed by water. Antibacterial agents can also be incorporated into the dressing, to counter infection. In trials with rats, treatment of 20% burn wounds infected with *Psuedomonas aeruginosa* with the dressing, reduced the mortality rate from 83% for the untreated controls to 11%.

One of the earliest and most widely studied hydrogel based wound dressings is the Hydron Burn Bandage (Hydro Med. Sciences Inc., New Brunswick, New Jersey). The dresssing is formed directly on the burn wound from a two component system, poly HEMA and poly ethylene glycol (PEG), the solvent. Alternate layers of poly ethylene glycol and poly HEMA are applied to the wound, either by spraying the components from a compressor or by direct application of PEG and powdered poly HEMA, until 3 or 4 layers have been built up. The PEG dissolves the poly HEMA forming a saturated solution, which solidifies after some 30 minutes[121,122]. There have been several clinical studies on this material with some conflicting reports on its suitability as a wound dressing material. Two studies[123,124] have concluded that although Hydron has some useful properties it has several disadvantages. These studies suggest that Hydron is difficult to apply, does not adhere well to the wound, especially if it is moist, and that cracking of the film is a problem in a significant number of cases. Additionally, as the dressing is translucent it is not possible to visually monitor the wound healing and the dressing must be cut away to check the wound for infection.

Several other clinical studies have, however, reported promising results using Hydron[125,126]. It has been described as a "valuable asset" in burn treatment, which is easy and painless to apply and reduces the pain for the patient after application. Hydron is

also fairly flexible and although the tensile strength is relatively low, the translucent dressing can remain in place for up to a week between changes. The rate of infection was found to be higher in wounds dressed with Hydron, than the control wounds, but the healing time was shorter. The permeability of Hydron enables the problem of infection in the wound to be countered by loading the dressing with an antibacterial agent. *In vivo* and *in vitro* studies in rats have confirmed the suitability of the dressing for the delivery of antimicrobial agents[127,128]. Thus, the mortality rate in rats with burns infected with *Pseudomonas aeruginosa* was reduced from 100% for the untreated controls, to 21% for rats treated with a HEMA / silver sulphadiazine dressing. Similarly, clinical trials[129,130] have shown that the dressing will release a variety of topical agents eg silver sulphadiazine, gentamicin, silver nitrate or nitro furazone over a period of up to 11 days thereby reducing patient discomfort. Additionally, Hydron containing an antibacterial agent provides an effective barrier to contamination from the environment. The inability to see the wound, or to obtain a wound culture, without removing the dressing were again regarded as the main disadvantages of Hydron in these trials, however. Further work with Hydron has included its use as a dressing for skin graft donor sites[131]. It was found to provide a good barrier to bacteria, showing a lower infection rate than gauze dressed graft sites, and although the dressing showed good adhesion to the sites, it was easy to remove after twelve days.

The relatively poor mechanical properties of poly HEMA inevitably present some problems during use. Migliaresi has attempted to improve these by forming a poly HEMA / polybutadiene laminate material, which can also be used as a skin graft. A mixture of HEMA and up to 60% by weight glycerol or diacetine (diluents), is polymerised in a mould in contact with a polybutadiene film to form the laminate[132-134]. The resulting laminates were permeable to oxygen but their water permeability was restricted by that of the polybutadiene film. The laminate was reinforced using a polyethylene terephthalate net for

trials with animals. The reinforced laminate has been tested in rabbits both as an implant, where it has shown good biocompatibility and as a skin graft, where promising results were also obtained. The laminate appears to have a potential for use as a burn wound covering and further work is being carried out on this material.

A novel hydrogel dressing, Geliperm (Geistlich, Wolhusen, Switzerland), has been developed by the Max-Planck-Institute for Immunobiology and Dermatology. Geliperm is synthesised from acrylamide and agar; the acrylamide being crosslinked in a solution of agar, using N'N' methylene-bis-acrylamide as a crosslinking agent, to produce an interpenetrating polymer network[135,136]. It has been demonstrated that interpenetrating polymer networks have significantly enhanced mechanical properties, compared to the individual strengths of the component polymers from which the material is fabricated[137]. Geliperm has many properties which make it an almost ideal wound dressing material. The gel has an equilibrium water content of 96% but is extremely elastic, with a high tensile strength (247 N / cm^2). The gel is claimed to be permeable to oxygen, water vapour and proteins with a molecular weight of up to one million, but impermeable to bacteria and cells. It is available in smooth, transparent (hydrated or dehydrated) sheets, is non-toxic, non-immunogenic and has a high capacity to absorb exudates from wounds. A more detailed examination of the properties and uses of Geliperm is given by Myers[138]. Geliperm is also available in granular form which is useful in the treatment of deep fissured wounds. The granular form has a much larger surface area than Geliperm film and is, therefore, able to absorb large amounts of exudate. Granular Geliperm also has the ability to absorb bacteria between the granules with the consequent advantage of removing bacteria from contaminated wounds.

Clinical trials with Geliperm[139] show that it improves the rate of wound healing and is easy

to apply and remove without causing pain to the patient. The dressing can be changed without damaging the new skin being formed beneath it and for this reason, Geliperm has proved useful in skin grafting[140], increasing the chance of the graft healing. In the first few critical days after grafting it maintains a sterile environment round the graft with optimum conditions for wound healing. Any problems with the graft can easily be seen through the transparent dressing, enabling them to be dealt with quickly. A recent study with rats[141] has indicated that wounds infected with *Escherichia coli* or *Staphylococcus aureus* will heal if left covered with Geliperm for ten days and the number of bacteria in the wound will begin to fall. However, in wounds infected with *Pseudomonas aeruginosa* after ten days the wound was not healing and there had been a tenfold increase in the number of bacteria. It appears, therefore, that in wounds infected with *Pseudomonas aeruginosa* frequent changes of dressing are necessary. It may be possible to overcome this problem by using Geliperm as a 'base' for the delivery of antibacterial agents.

An alternative approach to acrylamide based composite hydrogel wound dressings Omniderm (Omikron Scientific Ltd., Rehovot, Israel) has been synthesised by grafting acrylamide onto a polyurethane film, to give transparent, flexible gel with an EWC of approximately 50%[142,143]. The hydrated gel has a low modulus of elasticity, which improves the adherence of the gel to the wound, and high water permeability. Omniderm was found to have a higher permeability to antimicrobial agents than other occlusive dressings (Biobrane and Op site) and it's effectiveness as a base for antimicrobial agents was demonstrated in *in vivo* studies. Clinical trials on burns, ulcers and graft donor sites confirmed the potential of Omnidern as a wound dressing[144], although in some burn wounds fluid was found under the dressing.

It is apparent that these various composite hydrogel-based structures, differing as they do in

many respects, have many underlying similarities. The oxygen permeability is, in general, governed by two factors: the volume fraction of water in the dressing and its thickness. The surface properties are also greatly influenced by the water held within the composite dressing structure. Additionally, the importance of water structuring in the transport of large molecules through hydrogels has been discussed previously[145]. The mechanical properties of the range of materials described vary widely although some common features emerge. In general, it is the way in which the complex composite structure is formed rather than the simple fraction of water that determines this property. The combination of flexibility and good tear strength in the dressing seems to be of paramount importance, especially when the composite is first applied to the wound.

1.9 Scope and Objectives of Present Work

Although there have been several studies on the water binding of specific hydrogel copolymer series, no attempts have been made to correlate changes in water binding with changes in the mechanical or surface properties of copolymer hydrogels. Initially in this project, the water binding, surface and mechanical properties of high water content copolymer hydrogels were examined. It was thought that polymers of this type may prove useful for extended wear contact lens or wound dressing applications. High water content interpenetrating polymer network (IPN) hydrogels were also synthesised, in an attempt to improve the poor mechanical properties normally associated with high water content materials. The water binding, surface and mechanical properties of these materials were also elucidated and the differences between copolymer and IPN hydrogels of the same composition were investigated.

CHAPTER 2

Materials and Experimental Techniques

2.1 Reagents

The reagents used in this work are listed below in Tables 2.1 and 2.2 and their structures are shown in Figures 2.1 - 2.3. All monomer were purified by reduced pressure distillation, as described in the literature, before use[146].

Table 2.1 Molecular weights and suppliers of the monomers used.

Monomer	MWt. (g/mole)	Abbreviation	Supplier
2-Hydroxyethyl methacrylate	130	HEMA	Ubichem Ltd
Methyl methacrylate	100	MMA	B. D. H.
N-Vinyl pyrrolidone	111	NVP	B. D. H.
Styrene	104	St	B. D. H.
N'N'-Dimethyl acrylamide	99	NNDMA	Fluka
Lauryl methacrylate	254	LMA	Aldrich
Hydroxypropyl methacrylate	144	HPMA	Polysciences
Hydroxypropyl acrylate	130	HPA	Polysciences
Hydroxyethyl acrylate	116	HEA	Aldrich
2-Ethoxyethyl methacrylate	158	EEMA	Aldrich
MethoxyPEG$_{350}$ methacrylate	452	MPEGMA	Polysciences

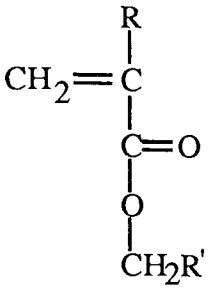

$R = CH_3$	$R' = CH_2OH$	2 - Hydroxyethyl methacrylate
$R = CH_3$	$R' = H$	Methyl methacrylate
$R = CH_3$	$R' = CH(OH)\,CH_3$	2- Hydroxypropyl methacrylate
$R = CH_3$	$R' = (CH_2)_{10}CH_3$	Lauryl methacrylate
$R = CH_3$	$R' = CH_2OCH_2CH_3$	2-Ethoxyethyl methacrylate
$R = H$	$R' = CH_2OH$	Hydroxyethyl acrylate
$R = H$	$R' = CH(OH)\,CH_3$	Hydroxypropyl acrylate

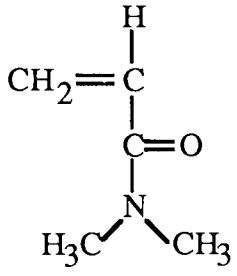

N'N' dimethyl acrylamide

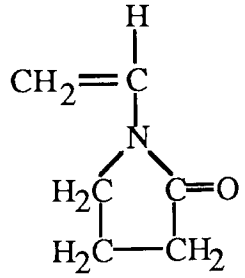

N - vinyl pyrrolidone

Figure 2.1 Structures of reagents listed in Table 2.1

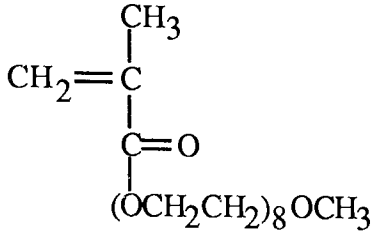

Methoxy poly (ethylene glycol)$_{350}$ methacrylate

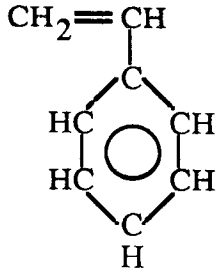

Styrene

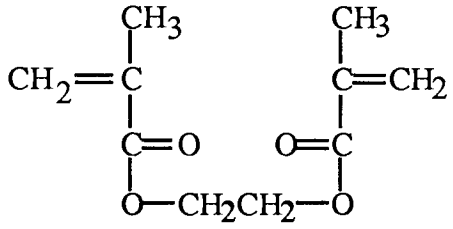

Ethylene glycol dimethacrylate

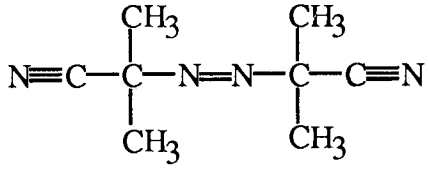

Azo-bis-isobutyronitrile

Figure 2.2 Structures of some reagents listed in Tables 2.1 and 2.2

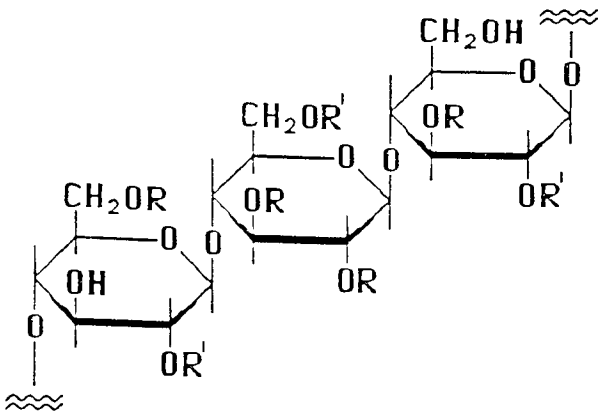

R = R' = $COCH_3$
Cellulose acetate

R = $COCH_3$ R'=$COCH_2CH_2CH_3$
Cellulose acetate butyrate

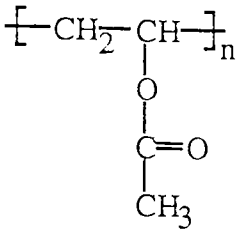

Poly (vinyl acetate)

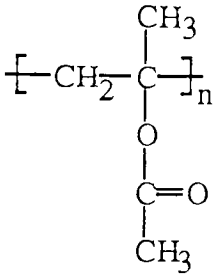

Poly (methyl methacrylate)

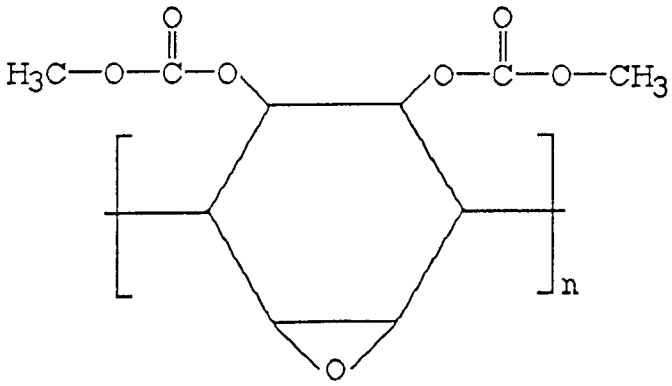

Epoxide of poly (1,2 dihydroxy cyclo hexa 3,5 diene dimethyl carbonate)

Figure 2.3 Structures of some polymers used in this work

Table 2.2 **Molecular weights and suppliers of the polymers, initiator and crosslinking agent used**

Reagent	MWt. (g/mole)	Abbreviation	Supplier
Ethylene glycol dimethacrylate	198	EGDM	B. D. H.
Azo-bis-isobutyronitrile	164	AZBN	Aldrich
Cellulose acetate	104,000*	CA	B. D. H.
Cellulose acetate butyrate	380,000*	CAB	P. C. L.
Poly methyl methacrylate	800,000*	PMMA	I. C. I.
Poly methyl methacrylate	103,000*	PMMA	I. C. I.
Poly vinyl acetate	100,000*	PVAc	Koch Light
Pellathane	37,000*	Pell	Upjohn
Biomer	+	Biomer	Ethicon Inc.
HPU25	180,000*	HPU25	Smith & Nephew
Epoxide of poly (1, 2 dihydroxy cyclohexa 3, 5 diene dimethyl carbonate)	+	EPDCD	I. C. I.
Polyoxyethylene sorbitan monolaurate	_	Tween 20	Sigma

(* values are polystyrene equivalent molecular weights determined by GPC using a Perkin Elmer series 10 liquid chromatogram, fitted with a Perkin Elmer LC-85D spectrophotometer variable wavelength detector and a Knauer differential refractometer detector. The columns used were 10^5, 10^4, 10^3 and 10^2 Å porosity 10μ gel from polymer laboratories 10PL gel.)

(+ insoluble in tetrahydrofuran)

The curing agents and molecular structures of the commercial polyurethanes are unspecified, however, the structure of Pellathane is thought to be

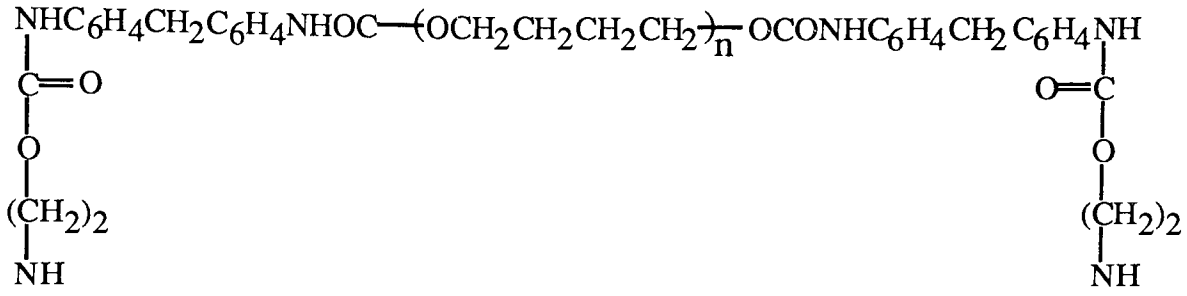

with the value of n being between 2000 and 4000.

2.2 Polymer Synthesis

2.2.1 Preparation of Hydrogel Membranes

Membranes were produced by the polymerisation of the monomer mixture in a glass mould. Two glass plates (15cm x 10cm) were each covered by a Melinex (polyethylene terephthalate) sheet to permit easy separation of the plates. The plates were placed together with two polyethylene gaskets (each 0.2mm thick) separating the Melinex sheets. Spring clips were used to hold the mould together leaving sufficient space for the insertion of a G22 syringe needle for the injection of monomer mixture into the mould cavity (Figure 2.4).

In a typical copolymer composition the monomers were mixed together with ethylene glycol dimethacrylate 1.0% (w/w) and azo-bis-isobutyronitrile 0.5 % (w/w) , while for IPN membranes the linear polymer was dissolved in the monomer, ethylene glycol dimethacrylate 1.0% (w/w) and azo-bis-isobutyronitrile 0.5 % (w/w), until a homogeneous solution was obtained. For the synthesis of both types of polymer the mixture was outgassed with nitrogen before injection into the mould. The mould was then placed in an oven at 60°C for three days followed by two hours postcure at 90°C.

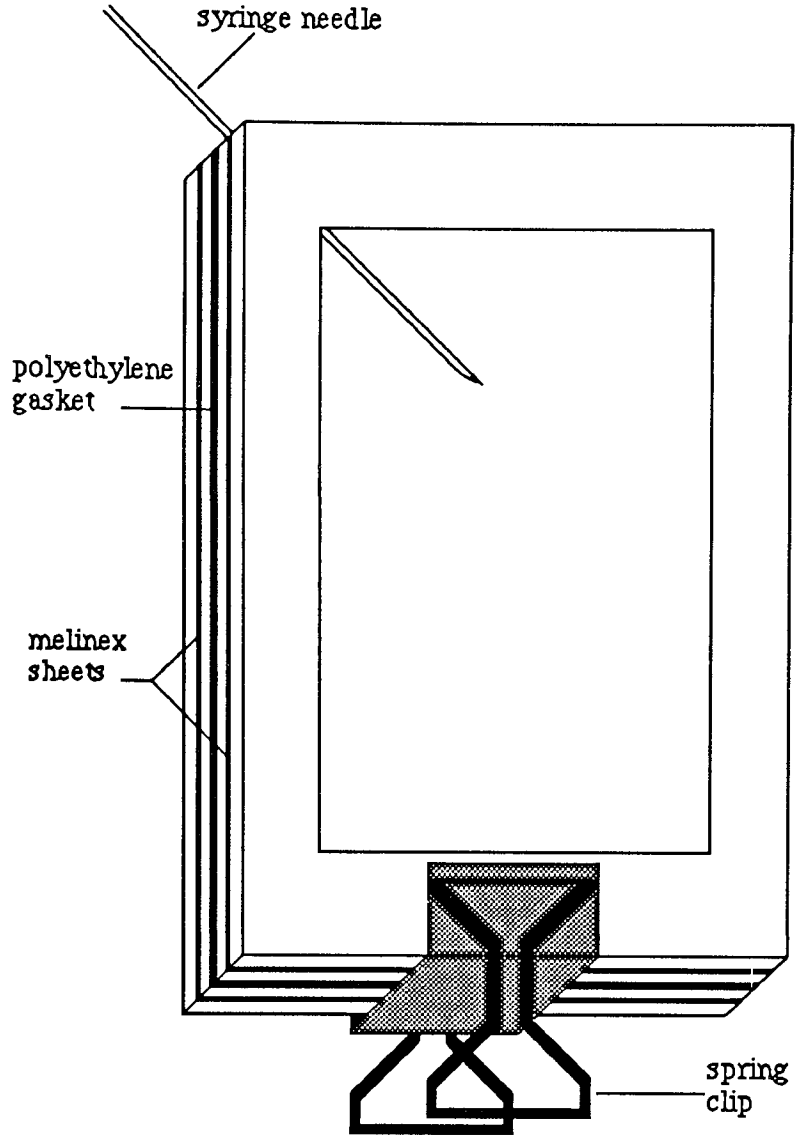

Figure 2.4 Membrane Mould

The spring clips were removed and after opening the mould the membrane was separated from the Melinex sheets, then placed in distilled water to hydrate for at least a week. Studies with a variety of monomer combinations showed that, provided the hydration medium was changed daily, constant values of equilibrium water content were obtained in four or five days. This period of time was sufficient both to reach equilibrium hydration and to extract any of the water soluble residuals (as detected by the appropriate G.L.C. technique used in initial assessments of monomer purity).

2.2.2 Solution Polymerisation

Free radical polymerisations were carried out using conventional techniques on a 0.5 litre scale. The polymerisation was carried out in a five necked 500ml flask which was equipped with a stirrer, condenser, thermometer, pressure equalised dropping funnel, and nitrogen bleed, in a water bath at 65°C for 8 hours. In a typical reaction 200mls of methanol were added to the reaction flask and the temperature was raised to 65°C. 25 gms. of the monomers (e.g. HEMA and NVP) and 0.5% initiator (AZBN), dissolved in 50mls of methanol, were added dropwise to the flask and the mixture was refluxed for 12 hours. The contents of the flask were allowed to cool and then added dropwise into 1.0 litre of ether, cooled with solid CO_2, to give a fine white precipitate. The precipitate was filtered and after three washings with ether, dried in a vacuum oven at 60°C.

2.3 Equilibrium Water Content

The EWC was measured by weight difference as follows. Samples were cut from a hydrated sheet of the hydrogel with a size seven cork borer. Any surface water was removed with filter paper before the samples were transferred to a preweighed sample bottle. The number of samples used (5-10) was varied according to the expected water content in order to give a reasonable total hydrated weight (ca. 0.2g). Thus, even in the case of lower (ca. 5%) water content polymers this produced a difference between hydrated and dehydrated weights of 0.01g.

The samples were weighed, then dehydrated overnight under vacuum at 60°C to achieve constant weight. The EWC was calculated using equation (2.1) and the final value is an average of the results from at least three determinations.

$$EWC = \frac{\text{Weight of water in the gel}}{\text{Total weight of hydrated gel}} \times 100\ \% \qquad (2.1)$$

Some attempt to obtain an objective view of the precision of the measurement was taken with the important hydrogel, poly HEMA. A statistical analysis on 100 samples of the hydrogel was found to give a mean EWC of 37.6% with $\Sigma_{n-1}= 0.42$.

The accuracy of this technique depends on the assumption that the sample of constant weight, obtained by vacuum dehydration, contains no water. This has been a source of some debate in the field of hydrogel chemistry. A more sensitive method for detecting water (independent of its binding state) in hydrogels is the Karl Fischer titration. This may be used as a rapid method of EWC determination. In this context, however, it is particularly valuable in confirming the validity of the vacuum dehydration technique for the removal of water. This confirms the validity of the assumption in the gravimetric method for EWC determination.

2.4 Differential Scanning Calorimetry

Thermograms were obtained using a Perkin Elmer differential scanning calorimeter, DSC-2, fitted with a liquid nitrogen subambient accessory. 1-4 mg. samples were cut from a hydrated sheet of the gel and the surface water was carefully removed with filter paper. The samples were sealed in preweighed aluminium sample pans and the weight of each sample noted.

The samples were cooled to 223K to ensure that any supercooled water was frozen and then allowed to reach equilibrium. The samples were then heated to 253K and subsequently heated at the rate of 5K/min. to ambient temperature. The thermogram was recorded on a Servoscribe 1S 524-20 potentiometric recorder, fitted with a temperature event monitor and a DISC integrator.

A calibration graph was obtained by measuring areas under the peaks produced by weighed samples of distilled water under identical conditions. The area under the melting peaks of the hydrogel sample was measured and the amount of freezing water present in the hydrogel was calculated from the calibration graph.

2.5 Surface Properties

The surface properties of hydrogels are important, principally because of their use in wide range of biomedical applications. The experimental techniques used to measure contact angles will be discussed in this Chapter, however, the theory used to determine surface energies from contact angle measurements is presented in Chapter 5, which also includes a discussion of the predictive techniques available for the estimation of surface energies from molecular constitution.

The surface energies of the hydrogels studied were determined, in the hydrated state, using Hamiltons method and captive air bubble techniques and by using the conventional sessile drop technique for the dehydrated hydrogels. Prior to contact angle measurements the polymer surfaces were thoroughly cleaned by washing with a Tween 20 detergent solution and then rinsing thoroughly in distilled water. For all the techniques used the drop / bubble was photographed using a Cannon AV-1 fitted with 13mm, 21mm, and 31mm extension tubes, a Cannon 70 - 210 macro zoom lens and Sun Nos. 1, 2 and 3 close up filters. After developing the film, with the aid of a Rank Aldis Tutor 2 projector fitted with a short, 5cm, focal length lens an enlarged image of the sessile drop was projected onto a back projection screen. The contact angle was measured by drawing a tangent to the drop / bubble surface at the three phase interface and measuring the angle with a protractor. Each measurement was the average of the contact angles on either side of the drop / bubble. The results were calculated using Makintosh Works™ which was programmed with the relevant equations.

2.5.1 Hamiltons Method[147]

Surface water was wiped from one side of the sample, which was then glued to a glass cover slip. The sample was then suspended inverted in an optical cell, which was then filled with distilled water saturated with n-octane. A small drop of n-octane was placed on the sample surface through a G25 syringe needle; the needle point had been removed by grinding in order that the drop was formed symmetrically on the sample surface.

The drop was photographed as described above and this was repeated for at least 4 different octane droplets. Hamilton showed that as both n-octane and water have the same dispersive component to their surface free energies, 21.8 mN/m, the dispersive component of the surface free energy of the sample cancels out of the mathematics of the system. This leaves only the polar component of the sample as an unknown, so this can now be evaluated.

2.5.2 Captive Air Bubble Technique

For this technique the sample is mounted underwater in exactly the same way as the Hamilton method, however, instead of n-octane droplets air bubbles are released onto the sample surface. A specially curved G35 needle (2.032×10^{-4}m diameter) was obtained from Aston Needles Inc. for this work. Using this needle enables an air bubble to be delivered onto the sample surface, from a microsyringe, in such a way that the needle can be inserted into the air bubble so that its volume can be precisely controlled. The air bubble was enlarged to a diameter of approximately 5-6mm and then reduced down to a size of 2mm and the needle retracted. The air bubbles were again photographed as previously described and this was repeated for at least 4 different bubbles.

2.5.3 Sessile Drop Technique

The hydrogel samples were dried overnight in a vacuum oven and the the dehydrated hydrogel was attached to a microscope slide. This was then placed on a stainless steel support in a glass cell with optically perfect sides. In this way the hydrogel was exposed to an atmosphere saturated with the wetting liquid, thus eliminating evaporation. The sessile drop of the wetting liquid was formed on the surface of the polymer through a G25 hypodermic needle and the drop was photographed as previously described. A minimum of four drops of each wetting liquid were photographed on each polymer sample and the results were calculated using an average of these values and the Owens and Wendt equation[148].

2.6 Mechanical Properties

The mechanical properties of the hydrogels were investigated using a Testometric Micro 500 tensometer (with 100N load cell), interfaced with an Apple IIe computer and an Iiwatso SR6602 personal plotter. Samples of width 6.25mm were cut from the hydrogel under test and these were held between the rubberised jaws of the tensometer. The tests were carried out using a crosshead speed of 10mm/min and a gage length of 10mm. The primary forms of the experimental results (stress / strain and load / extension curves) are shown in Figure 2.1. The ultimate tensile strength (σ_b), elongation to break (ε_b), and Youngs modulus can be calculated from the experimental results using the following equations:

$$\text{Tensile strength } (\sigma_b) = \frac{\text{Load at break}}{\text{Cross-sectional area}} \qquad (2.2)$$

$$\text{Elongation to break } (\varepsilon_b) = \frac{\text{Extension of gage length}}{\text{Original gage length}} \times 100\ (\%) \qquad (2.3)$$

$$\text{Youngs modulus } (E) = \frac{\text{Stress}}{\text{Strain}} \qquad (2.4)$$

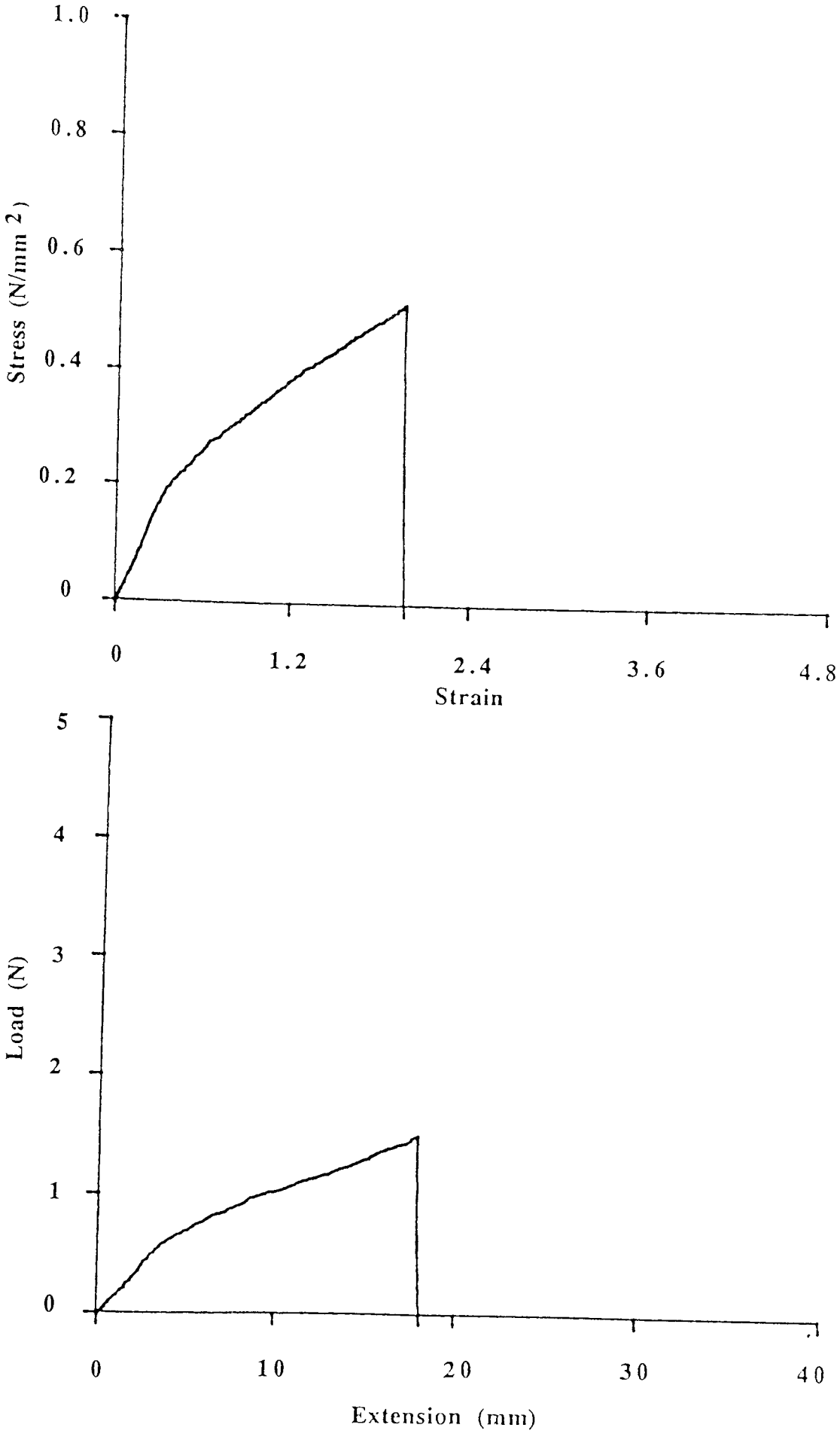

Figure 2.5 **Typical stress / strain and load / elongation tensile curves**

where:-

Stress = Load / Cross sectional area

Strain = Extension of gage length / Original gage length

A BASIC computer program calculated the tensile strength, elongation to break and Youngs modulus of the sample under test. The program plotted stress / strain and load / elongation curves and, in addition, performed a statistical analysis of the five tests run on each sample.

CHAPTER 3

Water Binding Studies on Copolymer Hydrogels

3.1 Introduction

The single most important property of a hydrogel is its equilibrium water content. However, the various states of water present in the gel also influence the properties of the gel. The water binding properties of some simple copolymer systems have been investigated, in an attempt to correlate differences in structure with the water binding properties of the hydrogel. A range of polymers and copolymers were prepared, with water contents varying from 10%-98%. As the water imbibed by the polymers plays a crucial role in determining the properties of these polymers, both the equilibrium water contents and the freezing water contents, as determined by differential scanning calorimetry, were measured. The results obtained are presented in this Chapter in graphical form, to illustrate clearly the trends in behaviour with changes in composition. However the results are tabulated in Appendix 1 to enable the reader to determine the precise values of equilibrium, freezing and non-freezing water contents.

The copolymers synthesised were based on 2-hydroxyethyl methacrylate (HEMA), N-vinyl pyrrolidone (NVP), and N,N-dimethyl acrylamide (NNDMA) copolymerised with methyl methacrylate (MMA), with styrene (St) and with lauryl methacrylate (LMA). Reported values for the monomer reactivity ratios for the copolymerisation of these monomers with various hydroxyalkyl and alkyl acrylates are listed overleaf in Table 3.1. If no literature values have been reported for the system r1 and r2 have been estimated from Q-e values[149]. It has been shown, however, that although these values may be used as a general guide to the relative reactivity ratios, they may differ substantially from the experimental values[150]. In all these systems, there is substantially complete conversion with only traces of hydroxy alkyl acrylates or methacrylates being eluted when the polymers are hydrated. The composition of the copolymers is substantially as predicted, the exception being systems which contain NVP, this being confirmed by elemental analysis and density measurements

on hydrated and dehydrated polymers. However, in systems containing NVP the large disparities in relative reactivity ratios produces marked deviation from random behaviour, which will be discussed in more detail in Section 3.3.

Monomer 1	Monomer 2	r1	r2	Reference
HEMA	MMA	1.054	0.296	150
HEMA	St	0.65	0.57	151
HEMA	NVP	3.12 ± 0.38	0.05 ± 0.09	152
HEMA	NVP	4.43 ± 0.24	0.04 ± 0.14	153
HEMA	NNDMA	1.56*	0.34*	149
NNDMA	LMA	0.54*	0.74*	149
NNDMA	MMA	0.42 ± 0.1	2.30 ± 0.24	154
NNDMA	MMA	0.45 ± 0.08	1.80 ± 0.18	155
NVP	LMA	0.061*	1.78*	149
NVP	MMA	0.02 ± 0.02	4.60 ± 0.4	156
NVP	MMA	0.005± 0.05	4.70 ± 0.5	157

Table 3.1 Relative reactivity ratios for the copolymer hydrogel systems studied (*values calculated from the Q-e scheme)

3.2 Effect of Temperature on Equilibrium Water Content

The effect of temperature on the water binding properties of hydrogels is important, principally because of the wide range of biomedical applications for which these materials have been used[7-23]. It is necessary to know how the water contents, and therefore, the dimensions, of the hydrogels vary from room temperature to body temperature and also at the higher temperatures that are often involved in sterilisation procedures. The effect of temperature on EWC has been examined for poly HEMA and poly NVP with varying levels

of ethylene glycol dimethacrylate crosslinking agent. These results together with those for HEMA-St copolymers, HEMA-MMA copolymers and NVP-MMA copolymers all at a nominal crosslink density of 1% are presented. The results for poly HEMA and HEMA copolymers with St and MMA, shown in Figures 3.1 and 3.2, indicate that the EWC is fairly insensitive to temperature, in the region 22°C to 70°C. There is in fact a slight difference between the effect of increasing the crosslink density and the effect of introduction of hydrophobic styrene monomer. Starting at similar EWCs, as the temperature is increased, the EWC of the more highly crosslinked HEMA decreases at a greater rate than the EWC of any of the HEMA-St copolymers. The increased retractive force in poly HEMA with the higher crosslink density acts to reduce the EWC more rapidly than in the HEMA-St copolymer, where only the hydrophobic group concentration is a factor.

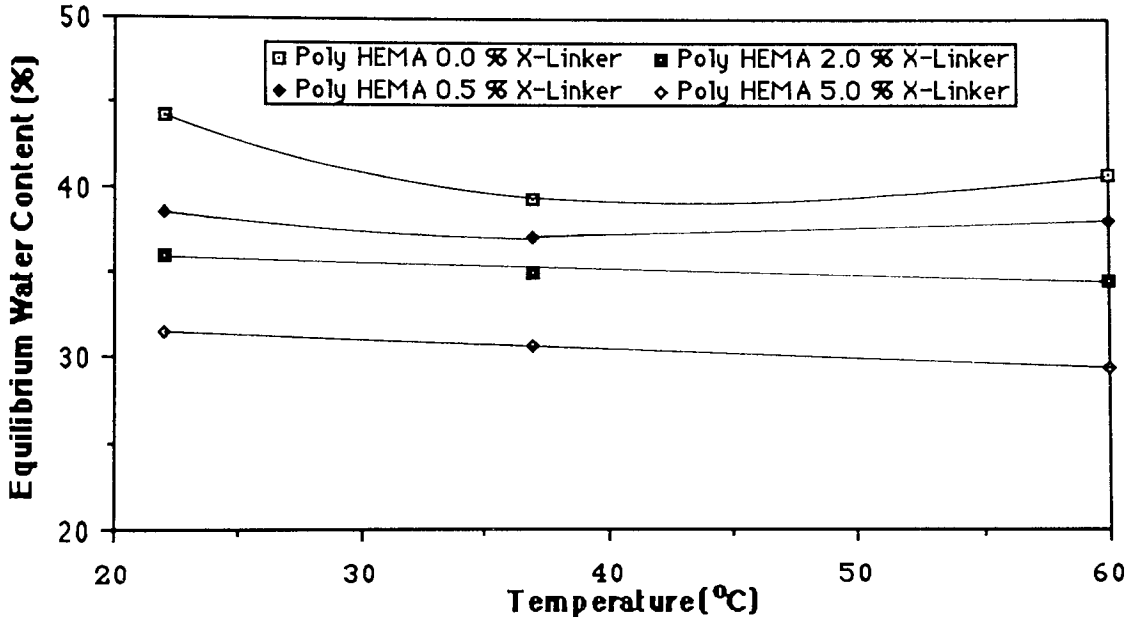

Figure 3.1 **Effect of temperature on the equilibrium water content of poly HEMA containing varying amounts of EGDM crosslinking agent**

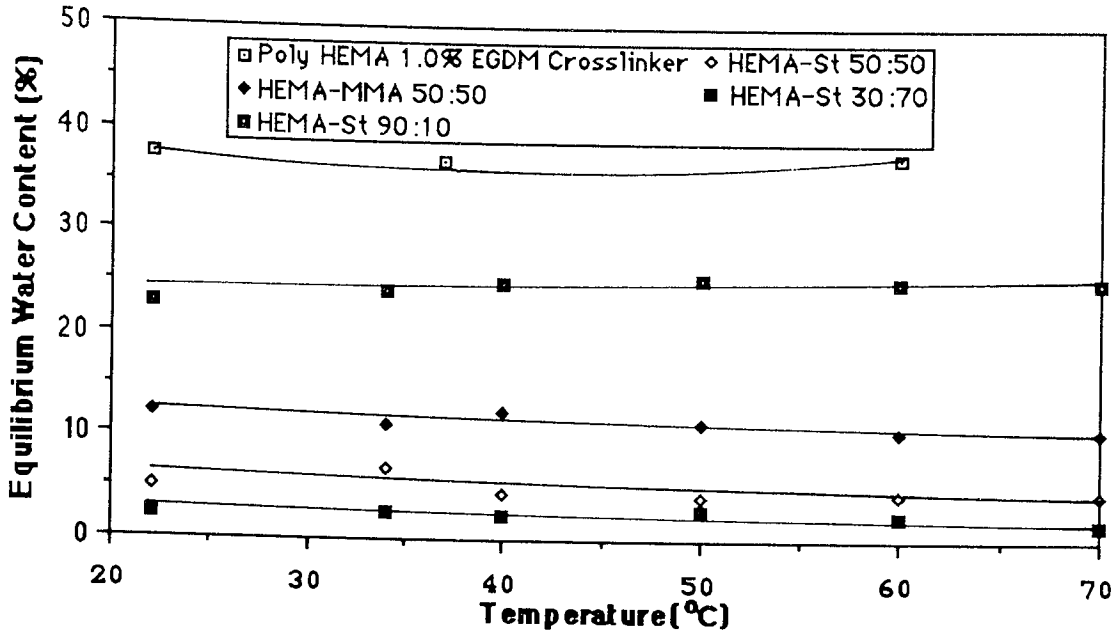

Figure 3.2 **Effect of temperature on the equilibrium water content of poly HEMA, HEMA-MMA copolymers and HEMA-St copolymers**

Refojo[87] has postulated that hydrophobic bonding is important in poly HEMA and that the formation of these bonds is an endothermic process. Similar views of the balance of hydrophobic bonding and macromolecular hydration have been applied to the behaviour of natural polymers for many years[158]. In principle this broad rationale can be applied to any hydrogel system. Okano[159] has used fluorimetric analysis to demonstrate the existence of hydrophobic interactions between the α -methyl groups of oligo-HEMA in a mixed water-dioxane solvent, containing more than 70% water by volume. This technique has also been used to examine hydrophobic interactions in a HEMA-ethylene oxide block copolymer[160]. Hydrophobic bonds are van der Waals interactions between non-polar groups. These result from the driving force that the solubility of a non-polar group in water, hydrophobic hydration, is entropically unfavourable because the water is capable of structuring in the vicinity of a non-polar compound. These hydrophobic bonds act as crosslinks and reduce the EWC of the hydrogel. An increase in the temperature reduces the hydrophobic hydration

and increases the formation of hydrophobic bonds. On the other hand, water forms hydrogen bonds with the polar groups of the polymer and this hydrophilic hydration will increase with increasing temperature. The polymer network should also expand entropically with increasing temperature, causing an increase in the capacity for water absorption.

The competition between these processes will determine the shape of the equilibrium water content-hydration temperature curve. Both the magnitude and position of occurrence of any minimum, in the hydration-temperature profile, will be determined by the nature of the constituent monomers. In the case of crosslinked poly HEMA and HEMA copolymers with styrene and methyl methacrylate (Figures 3.1 and 3.2) virtually no deviation from linearity is observed. Previous work[87,89,158-161] has indicated that minima do occur both for poly HEMA and for HEMA-MMA 80:20 copolymers in the region from 50°C to 80°C. However, these minima are indistinct and although the primary experimental data points of the various workers may be successfully overlayed, the major disagreement lies in the extent to which minima can be successfully discerned. This is in part due to the difficulty in obtaining accurate and reproducible measurements of EWCs at high temperatures. Warren and Prins[89], however, have calculated the partial molar heat of dilution, $\overline{\Delta H}_{dil}$, for poly HEMA and found it to be negative below 55°C. This is indicative of a hydrophobic interaction leading to increased water structuring. Above 55°C, $\overline{\Delta H}_{dil}$, is positive as the normal dispersion forces overcome the water structuring effect. Therefore a minimum might be expected in the hydration - temperature profile at this temperature.

If the hydration - temperature profiles of poly NVP and NVP-MMA copolymers (Figure 3.3) are examined, marked differences are observed in the behaviour of these systems in the temperature range investigated. While little deviation from linearity is observed for poly NVP crosslinked with 5% EGDM crosslinking agent, the other copolymers show a decrease

in EWC with increasing temperature; this decrease being most pronounced in the HEMA-NVP 70:30 and 50:50 copolymers.

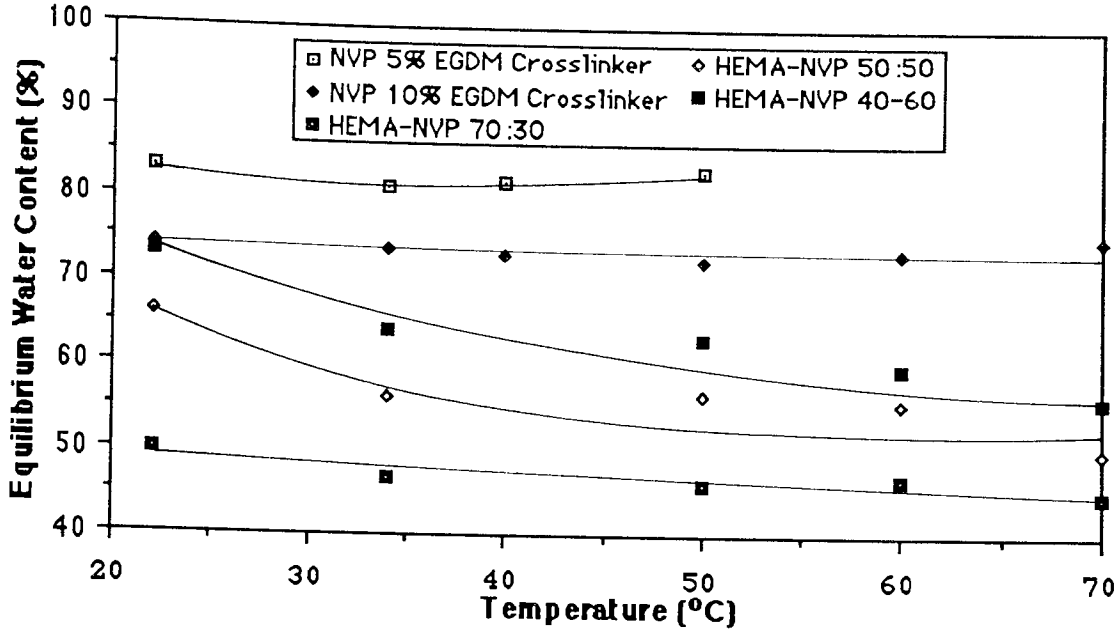

Figure 3.3 **Effect of temperature on the equilibrium water content of poly NVP containing varying amounts of EGDM crosslinking agent and HEMA-NVP copolymers**

Previously it has been reported that the EWC of NVP-MMA copolymers falls in the region 0°C to 90°C[162,163], however, no hypothesis has been forwarded to explain this phenomenon. This reduction in EWC may be due to hydrophobic bonding but in most systems the maximum strength of hydrophobic bonds occurs at around 60°C[164]. However, no work on the thermodynamics of this system has been published and it is possible that the hydrophobic bond strength reaches is maximum value at a higher temperature, in this system.

3.3 Water Binding Studies

Of the techniques available for the study of water binding: nuclear magnetic resonance spectroscopy, differential scanning calorimetry (D.S.C.), dilatometry and specific

conductivity, D.S.C. is in many ways the most convenient. The reasons for this include: the ease of preparation of the small samples, which are sealed in aluminium sample pans to minimise any loss of water from the sample. Additionally, the ease with which measurements on the sample can be made enable the water binding data to be elucidated far more quickly than would be possible, for example, by using NMR relaxation measurements. Furthermore melt / freeze recycling can be carried out rapidly and easily, enabling more detailed crystallisation and water structuring information to be obtained[82].

3.3.1 HEMA Copolymers: Structure and Hydration Properties

The effect of composition on the water binding properties of HEMA copolymers is illustrated in Figures 3.4-3.11. The effect of crosslink density on the equilibrium, freezing and non-freezing water contents of poly HEMA (Figure 3.4) generally follows the expected trend, showing a decrease in both EWC and freezing water content as the crosslink density increases. An increase in the crosslink concentration causes a slight decrease in the non-freezing water content, but a large decrease in the freezing water content since increasing the crosslink density decreases both mobility and hydrophilicity within the network.

The percentage of non-freezing water in the polymer appears to remain fairly constant at around 24%. There has, however, been some disagreement over the amount of non-freezing water present in poly HEMA and values of between 18% and 30% have been reported[48,50,63,82]. Although expressing the water contents as percentages generally clearly illustrates the changes in EWC and freezing water content, sometimes, especially in hydrogels with high water contents, the trend in non-freezing water content is obscured. Expressing the water content in grams of water / gram of polymer or moles of water / mole of repeat unit overcomes this problem and gives an indication of the water binding potential of a single isolated monomer unit.

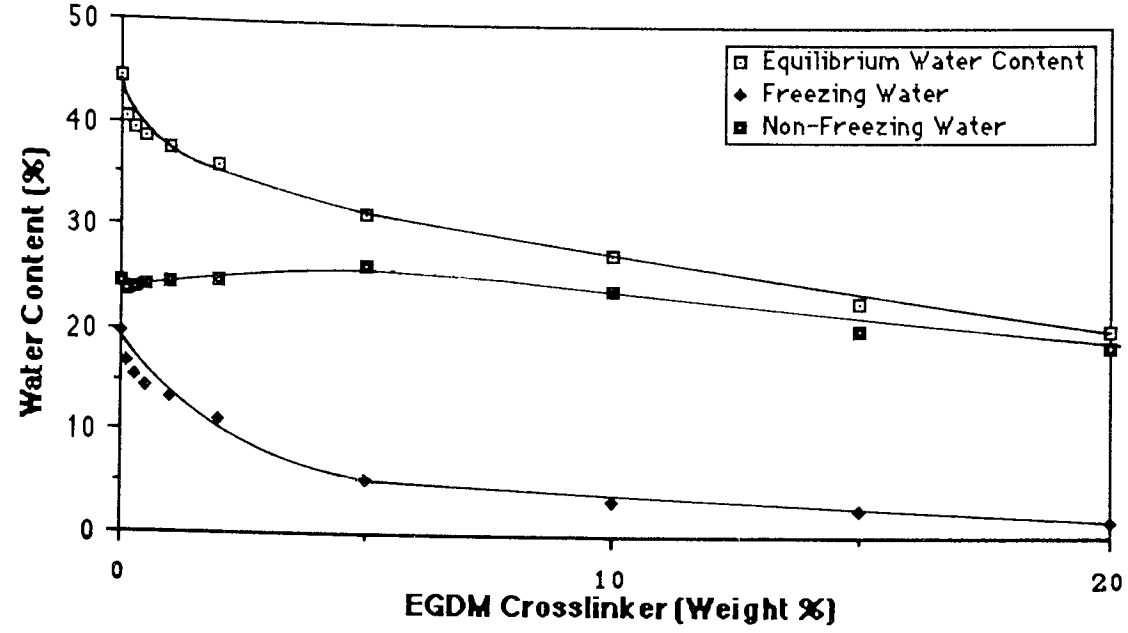

Figure 3.4 Effect of EGDM crosslinking agent incorporation on the water content of poly HEMA

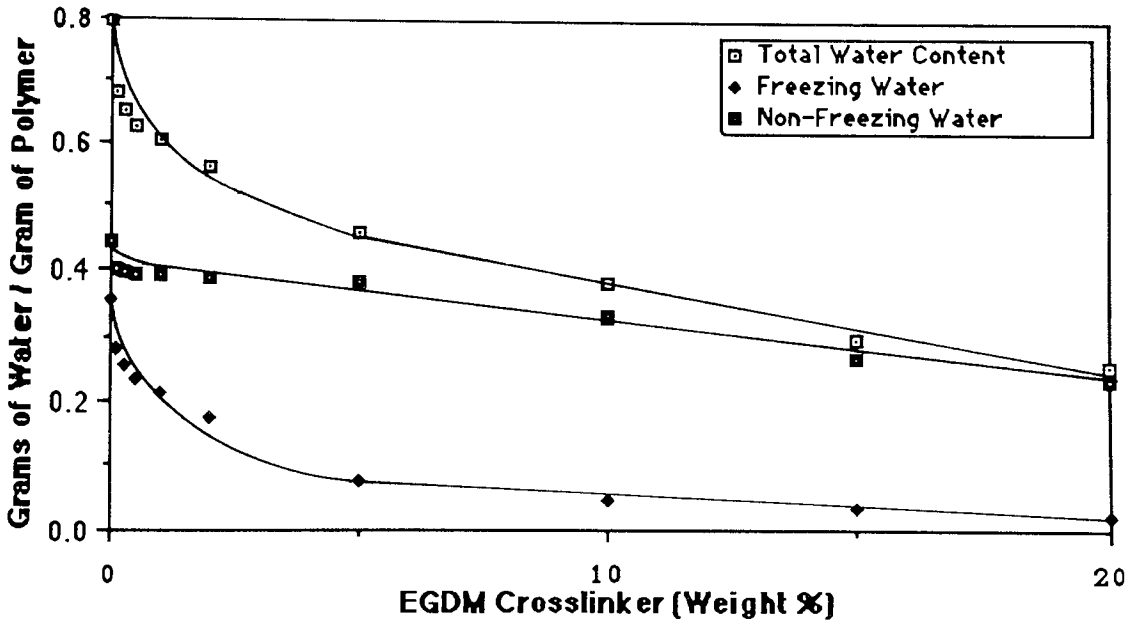

Figure 3.5 Effect of EGDM crosslinking agent incorporation on the water binding of poly HEMA

This is illustrated for poly HEMA in Figure 3.5. As the total water content of the system decreases, the number of moles of non-freezing water per mole of HEMA repeat unit in the polymer decreases (from 3.2 for poly HEMA with no crosslinker to 2.8 for poly HEMA with 5% crosslinker). This small change in non-freezing water is a result of the decreasing availability of hydrophilic binding sites, due to increased steric occlusion.

The effect of addition of EGDM crosslinking agent is especially marked at low levels of incorporation, when the linear crosslinked polymer suffers a more dramatic *pro rata* decrease in network expansibility than is the case at progressively higher crosslink densities. A simplistic view of the water binding process suggests that in non-freezing water the water molecules are hydrogen bonded to hydrophilic groups on the polymer chain, while freezing water molecules are hydrogen bound to both freezing and non-freezing water molecules. Using the concept of hydration shells, it is possible to envisage the non-freezing water hydrogen bonded to the hydrophilic sites (in this case hydroxyl groups) on the polymer chain, with other hydration shells of freezing water molecules surrounding the inner hydration shell. As the number of monomer units between crosslinks decreases, the network becomes more tightly bound and there is a marked decrease in freezing water content with increasing crosslink concentration, together with a small decrease in the ratio of moles of non-freezing water per mole of hydrophilic repeat unit.

Although increased crosslink density in poly HEMA hydrogels produces marked changes in water binding behaviour, similar effects arise from the introduction of hydrophobic and especially sterically hindering monomers such as methyl methacrylate and styrene. The effect of composition on the equilibrium, freezing and non-freezing water contents of HEMA-MMA and HEMA-St copolymers is shown in Figures 3.6 and 3.7.

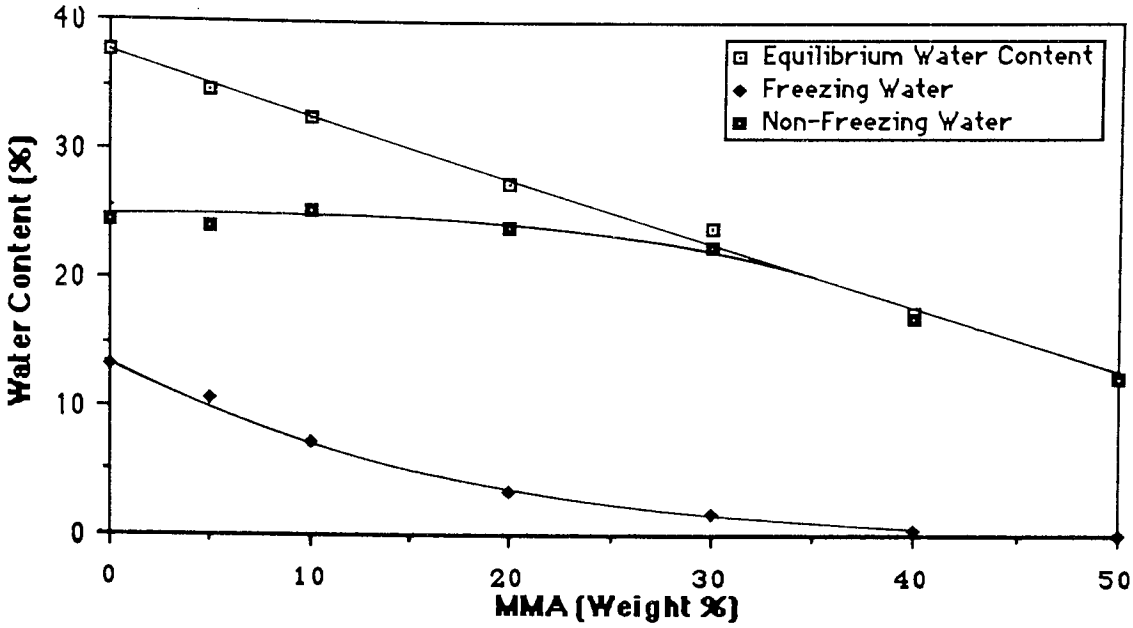

Figure 3.6 Effect of composition on the water content of HEMA-MMA copolymers

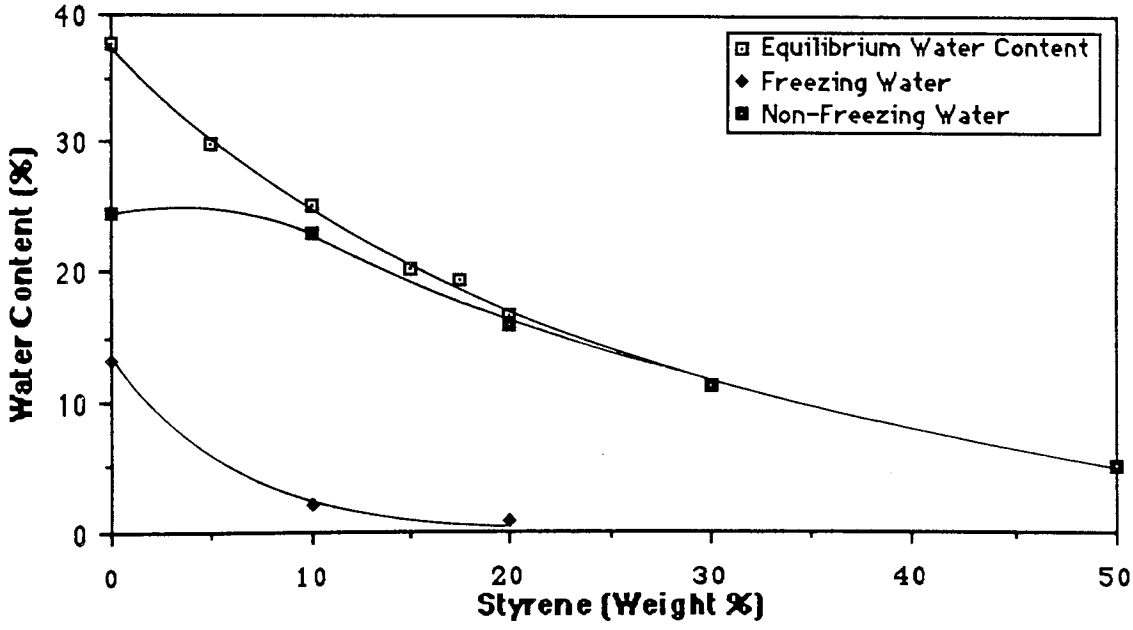

Figure 3.7 Effect of composition on the water content of HEMA-St copolymers

As the percentage of hydrophobic monomer increases the EWC falls and the copolymers become more rigid. This decrease in flexibility can be attributed to the reduction of freezing water in the copolymer (13.2% in poly HEMA but only 0.5% in the 60:40 HEMA-MMA copolymer) and is a demonstration of the plasticising effect of freezing water. The number of moles of non-freezing water per repeat unit in the methacrylate copolymer series decreases from 2.8 for poly HEMA to 1.4 for the HEMA-MMA 60:40 copolymer. Comparing the 80:20 HEMA-MMA and HEMA-St copolymers the number of moles of non-freezing water per repeat unit are 2.2 and 1.6 respectively, reflecting the greater hydrophobicity of styrene compared to methyl methacrylate. This behaviour, which is an extension of that discussed for the effect of the somewhat smaller levels of crosslinking agent in poly HEMA, reflects not only the decreasing hydrophilicity but also the importance of steric effects and resultant restricted mobility and availability of water binding sites within the polymer.

Figures 3.8-3.11 show the effect of incorporation of the hydrophilic comonomers NVP and NNDMA on the water binding of HEMA copolymers. The EWC and freezing water contents show a steady rise, as expected, with progressive incorporation of the hydrophilic monomer. The amount of non-freezing water in both the HEMA-NVP and HEMA-NNDMA copolymers (Figures 3.8 and 3.9) appears to fall with incorporation of hydrophilic monomer, when this value is expressed as a percentage. However, if the non-freezing water is expressed in terms of either grams of water / gram of polymer (Figures 3.10 and 3.11) or moles of non-freezing water / mole of repeat unit the expected trend, an increase in non-freezing water with progressive hydrophilic monomer incorporation, is observed. Thus, the number of moles of non-freezing water / mole of repeat unit increases from 2.82 for poly HEMA to 3.52 for the HEMA-NNDMA 60:40 copolymer and 3.38 for the HEMA-NVP 60:40 copolymer.

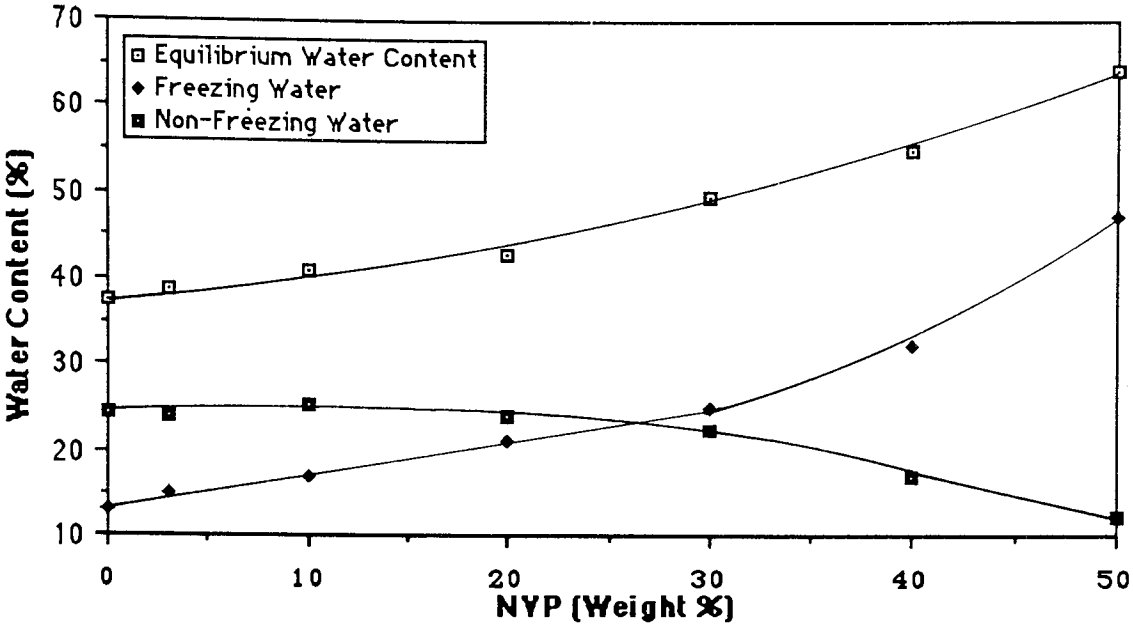

Figure 3.8 Effect of composition on the water content of HEMA-NVP copolymers

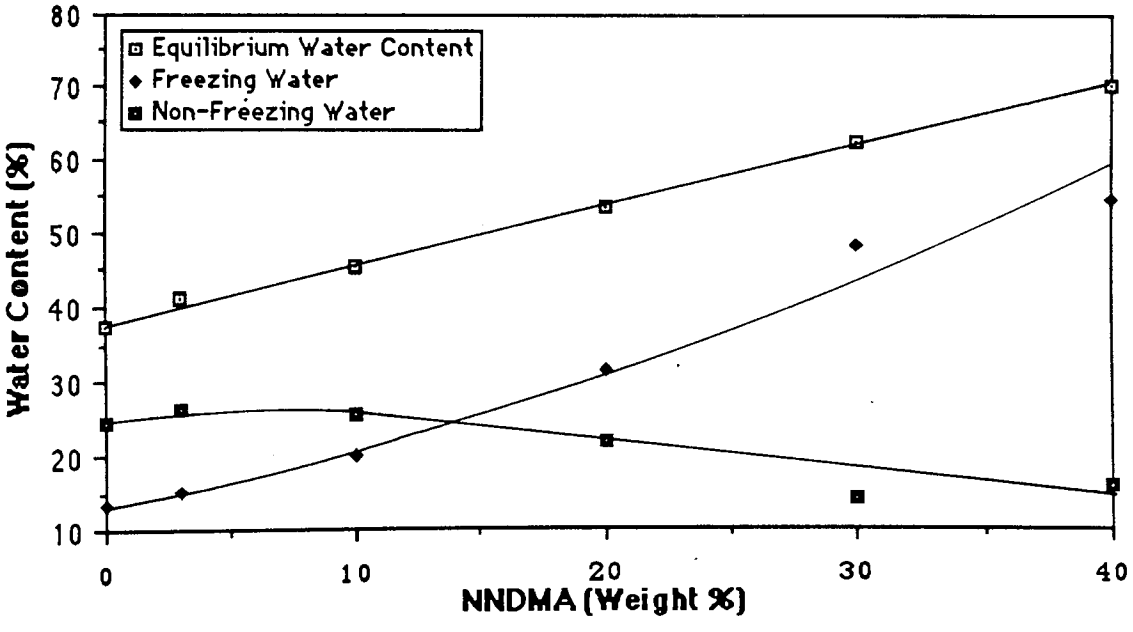

Figure 3.9 Effect of composition on the water content of HEMA-NNDMA copolymers

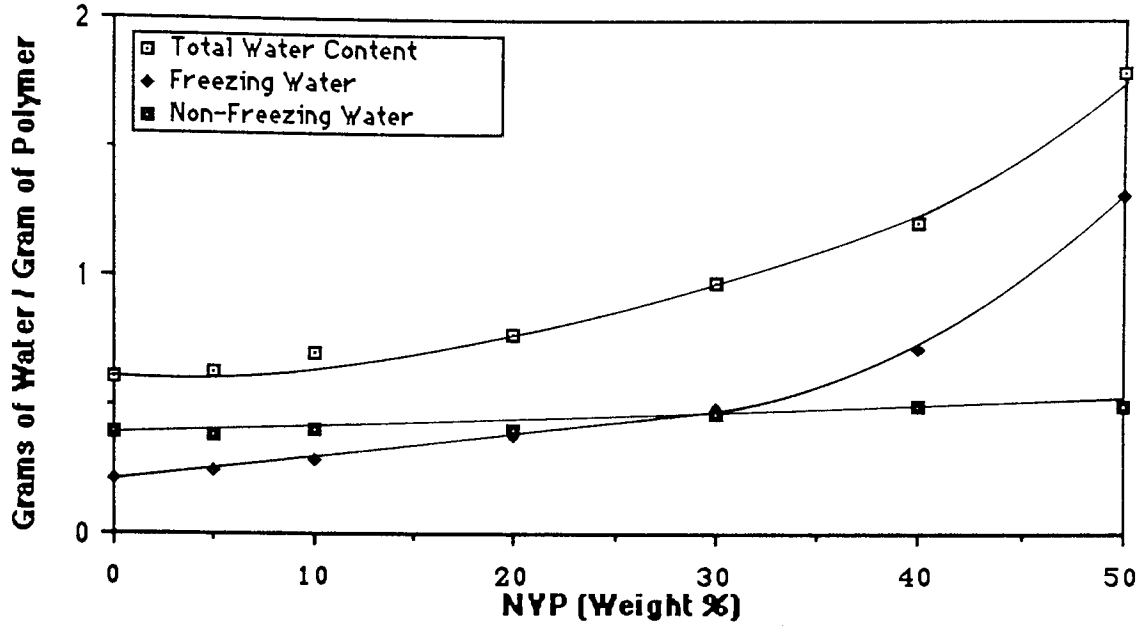

Figure 3.10 Effect of composition on the water binding of HEMA-NVP copolymers

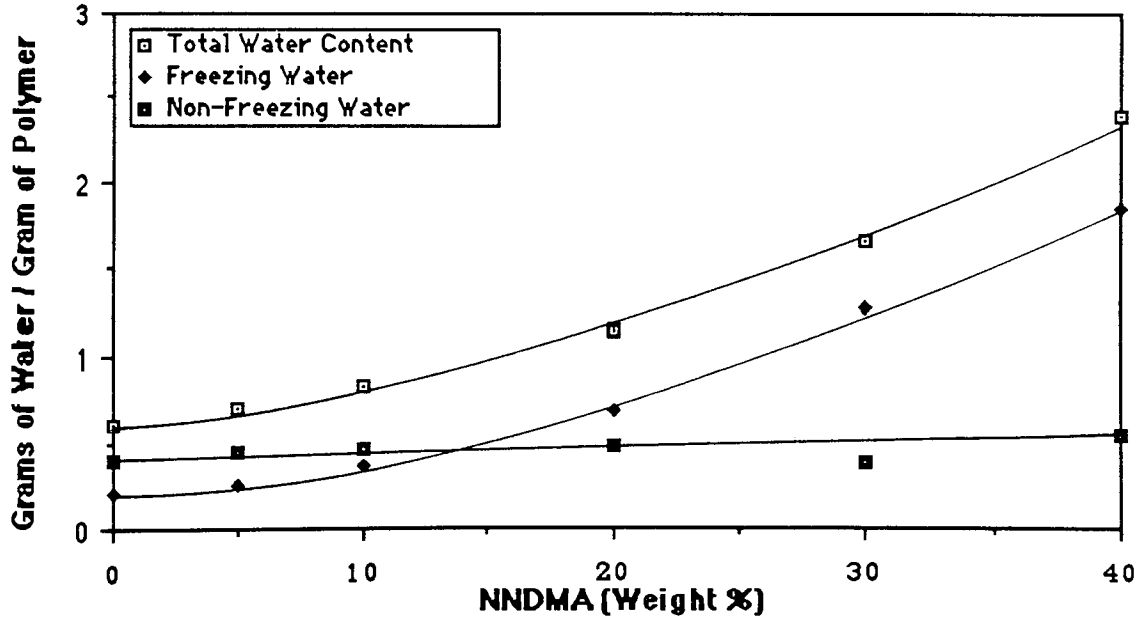

Figure 3.11 Effect of composition on the water binding of HEMA-NNDMA copolymers

The compositions shown on these graphs are based on feed ratios and for most copolymers described here the feed and matrix incorporated ratios will agree to within a few percent. However, for copolymers containing NVP, there can be a large disparity between the feed ratio and copolymer composition and these figures reflect the more efficient incorporation of the NNDMA into the system[38]. Therefore, direct comparisons cannot be made about the relative hydrophilicities of NNDMA and NVP by comparing the water binding properties at the same feed compositions. The differences between NVP and NNDMA will be discussed in section 3.3.2, however, both monomers provide a means of producing hydrogels with much higher water contents than poly HEMA.

3.3.2 NVP and NNDMA Copolymers: Structure and Hydration Properties

Figures 3.12-3.15 show the effects of incorporation of EGDM crosslinking agent on the equilibrium, freezing and non-freezing water contents of poly NVP and poly NNDMA.

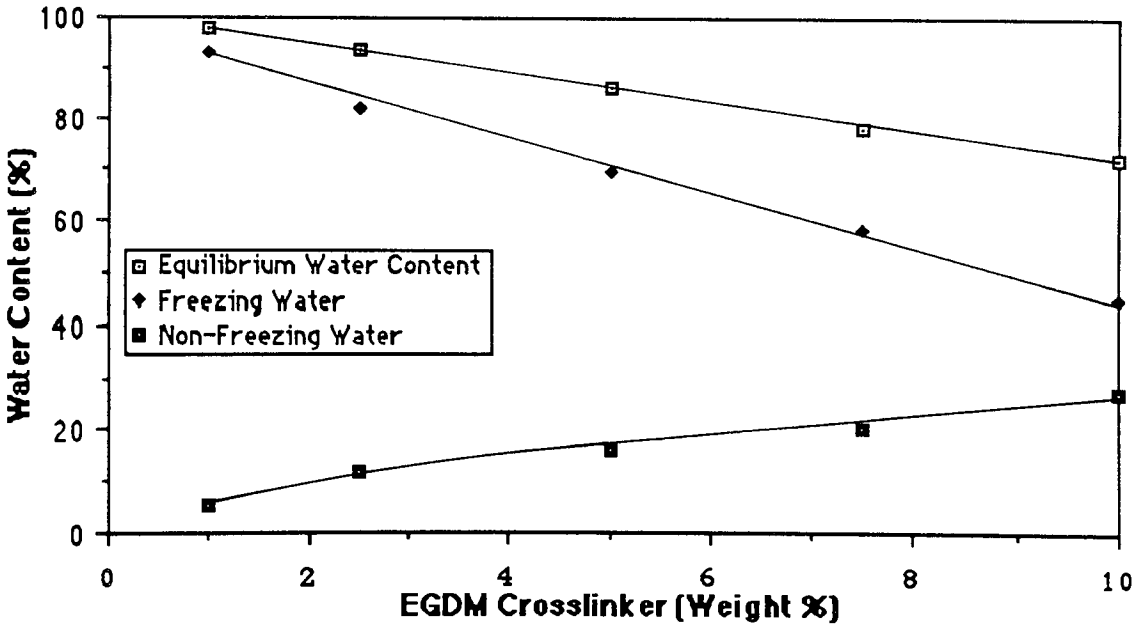

Figure 3.12 Effect of EGDM crosslinking agent incorporation on the water content of poly NVP

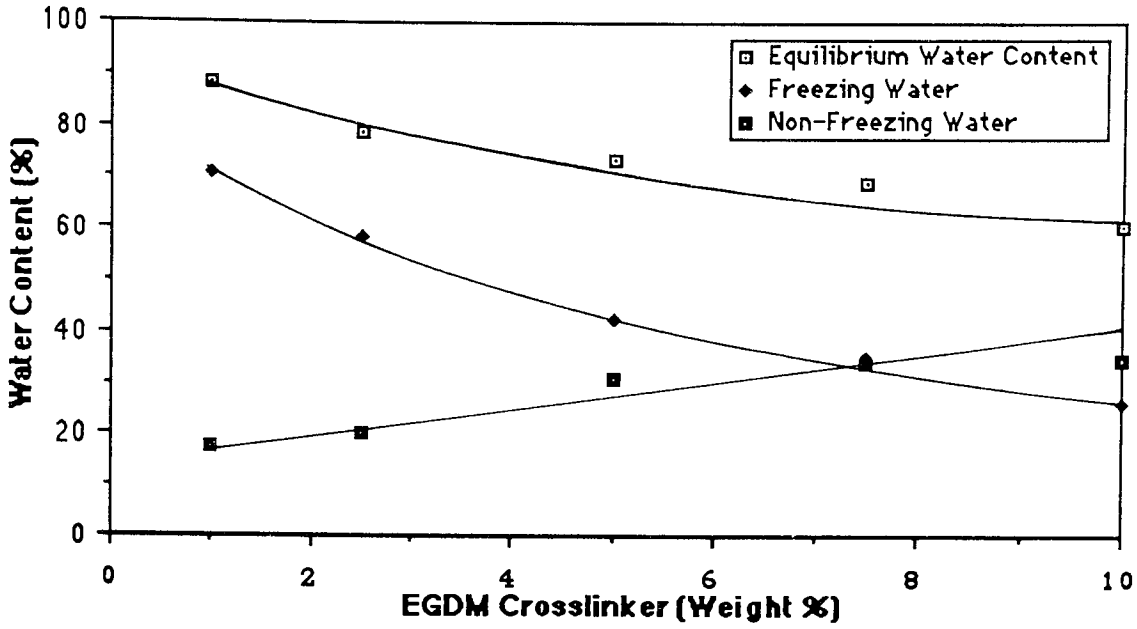

Figure 3.13 Effect of EGDM crosslinking agent incorporation on the water content of poly NNDMA

The water contents of both poly NVP and poly NNDMA fall steadily as increasing amounts of hydrophobic EGDM are added to the system, reducing the hydrophilicity of the network. The most interesting difference between these two polymers lies in the large variation in water binding ability of the polymers containing low percentages of EGDM crosslinking agent. When 1% EGDM is incorporated into the chain poly NVP has over 7 times as much water (including 1.75 times as much non-freezing water) associated with each gram of polymer (Figures 3.14 and 3.15). Once 5% EGDM has been incorporated, however, the amount of non-freezing water / gram of polymer is the same for both systems, although poly NVP still has twice as much water associated with each gram of polymer. One possible reason for the enhanced water binding of poly NVP at low levels of crosslinking agent is its structure. To minimise the interactions between the lactam rings poly NVP may coil in a helical conformation. Thus, in this conformation there is "space" between the rings for water

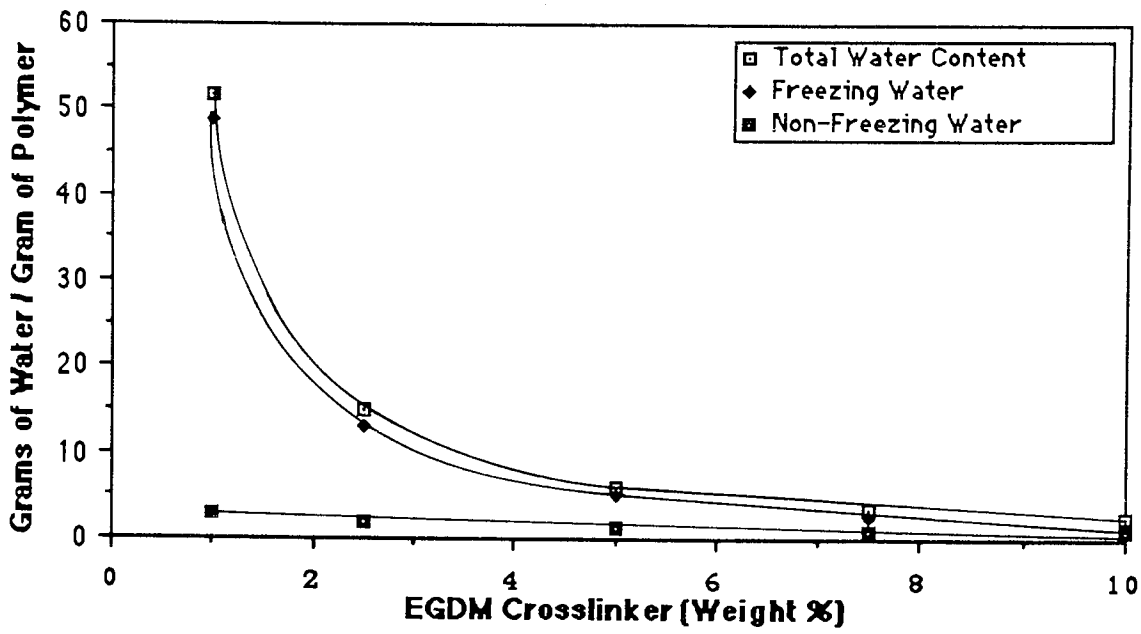

Figure 3.14 Effect of EGDM crosslinking agent incorporation on the water binding of poly NVP

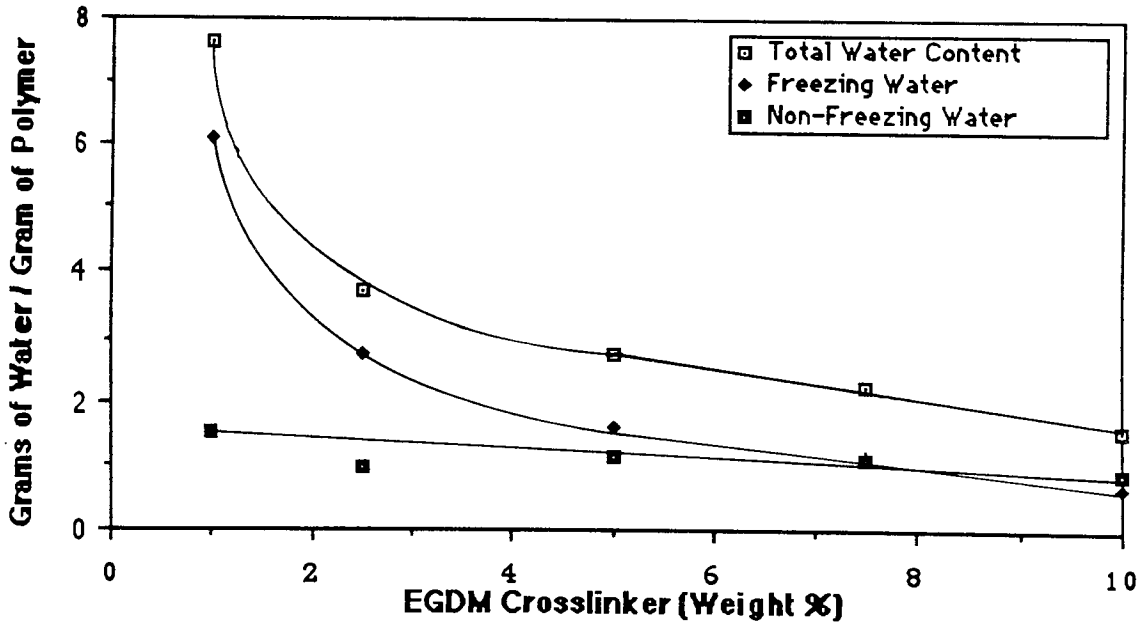

Figure 3.15 Effect of EGDM crosslinking agent incorporation on the water binding of poly NNDMA

molecules which can form a "bridge" between the polar groups on adjacent rings. However, the addition of EGDM crosslinker, or any other monomer, will disrupt the packing arrangement as the polar groups on NVP will interact with the polar groups on the comonomer. The helical conformation of NVP and its interaction with comonomers also has an effect on the surface properties of poly NVP and NVP copolymers. This will be discussed more fully in Chapter 5. It could also be argued that the incorporation of another monomer into poly NVP restricts the access of water to the water binding sites on the molecules. However, a similar effect would also be seen with NNDMA and this does not explain the marked difference in water binding ability between these two monomers. Figures 3.14 and 3.15 demonstrate that the incorporation of EGDM crosslinking agent has a more dramatic effect on NVP than on NNDMA.

Copolymers of both NVP and NNDMA with the hydrophobic monomers methyl methacrylate and lauryl methacrylate have also been synthesised (Figures 3.16-3.23). The equilibrium, freezing and non-freezing water contents follow the expected trend, with progressive incorporation of hydrophobic monomer. For the copolymers with LMA (Figures 3.16-3.19) the water binding behaviour of NVP and NNDMA copolymers containing between 10% and 40% LMA is almost identical, expressed both as grams of water / gram of polymer and as a percentage. The more pronounced initial effect of hydrophobic monomers on NVP is again apparent, with the incorporation of 10% LMA reducing the grams of non-freezing water / gram of polymer by 60% for NVP but by only 35% for NNDMA. The nature of the calculation involved in determining the grams of non-freezing water / gram of polymer means that the error in this value increases with increasing water content. However, even after making allowances for this there is still a more significant reduction of this value in NVP copolymers than in NNDMA copolymers.

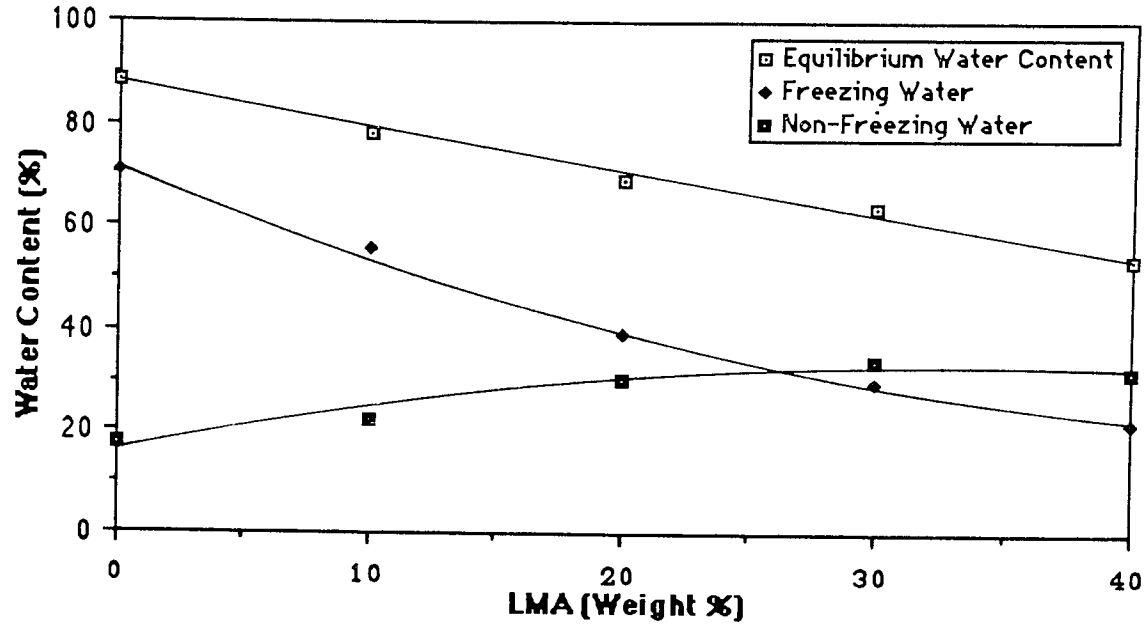

Figure 3.16 Effect of composition on the water content of NNDMA-LMA copolymers

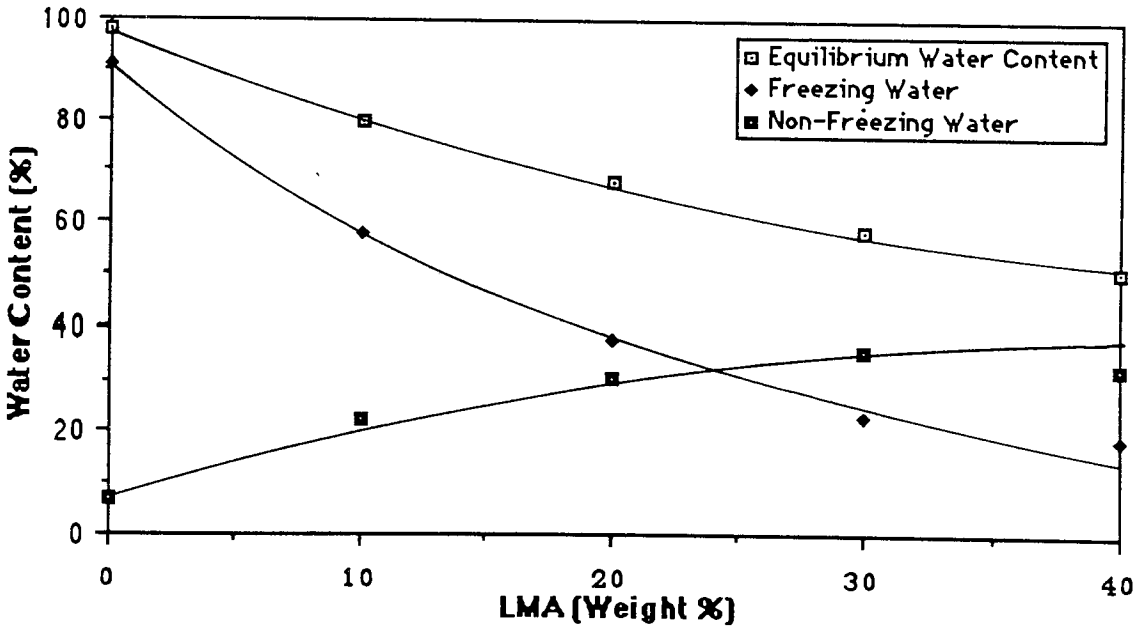

Figure 3.17 Effect of composition on the water content of NVP-LMA copolymers

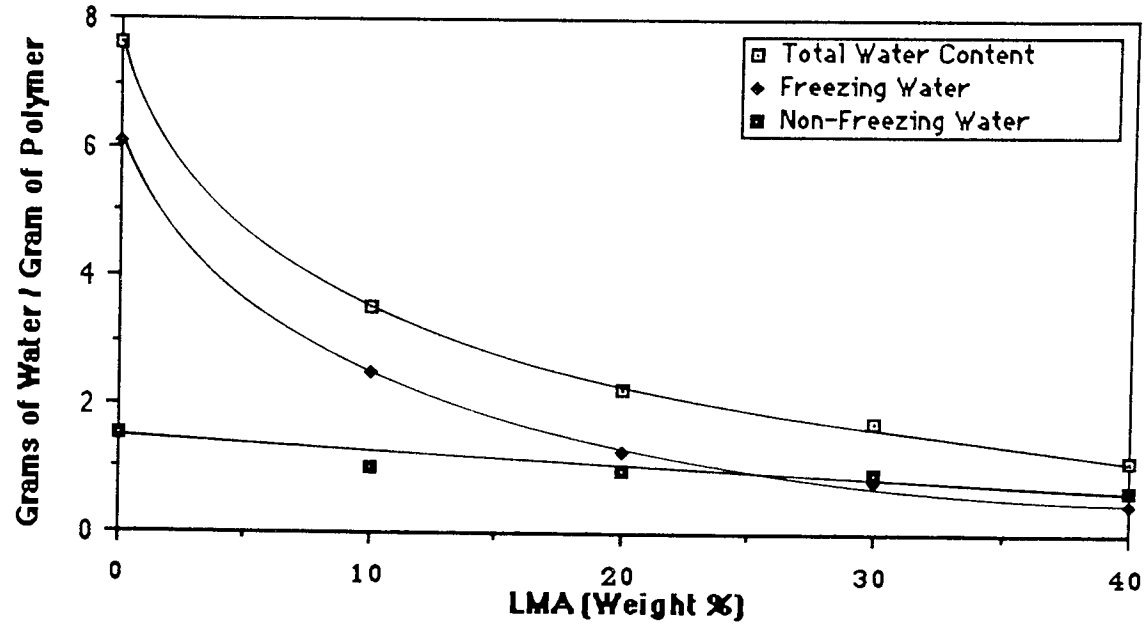

Figure 3.18 Effect of composition on the water binding of NNDMA-LMA copolymers

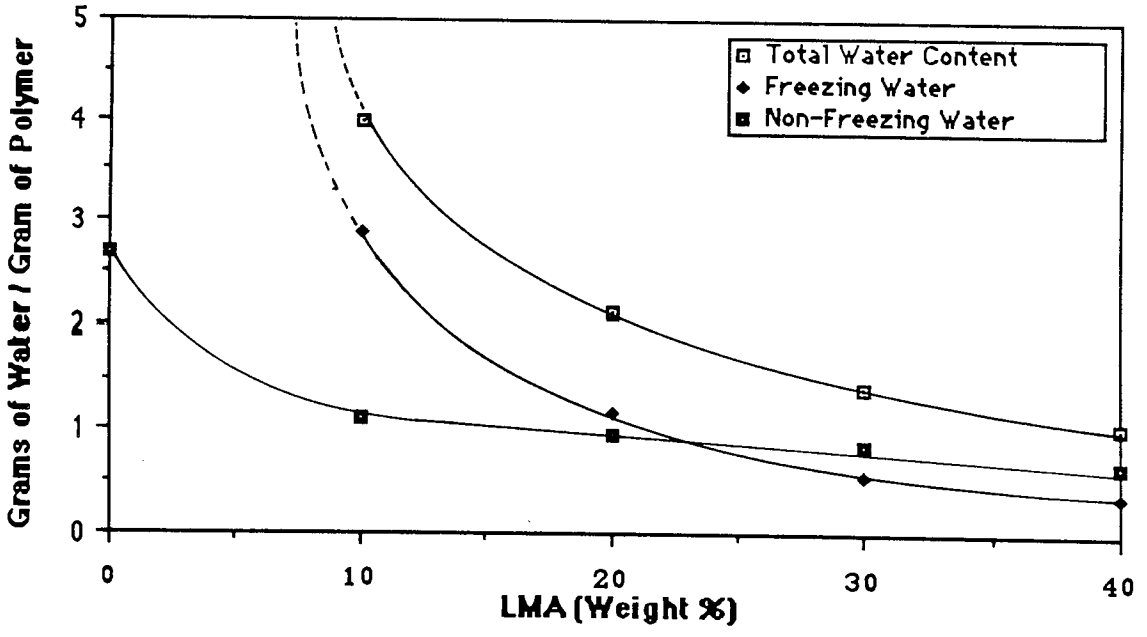

Figure 3.19 Effect of composition on the water binding of NVP-LMA copolymers

This is consistent with view expressed earlier that incorporation of small amounts of comonomer disrupt the helical packing in NVP. Thus, in NVP copolymers there is a greater initial fall in water content than is the case with NNDMA based copolymers. However, at higher levels of comonomer incorporation the water contents of the NVP and NNDMA copolymers are similar. This might be expected due to the similarity of the the water binding groups in both monomers.

NNDMA and NVP also show differences in water binding behaviour when they are copolymerised with MMA (Figures 3.20-3.23). The incorporation of 20% MMA reduces the equilibrium water content of NVP by 30% but the EWC of NNDMA by only 7%; MMA is also much less effective than LMA in reducing the EWC of NNDMA. The same trend is apparent if the figures are expressed in grams of water / gram of polymer (Figures 3.22 and 3.23).

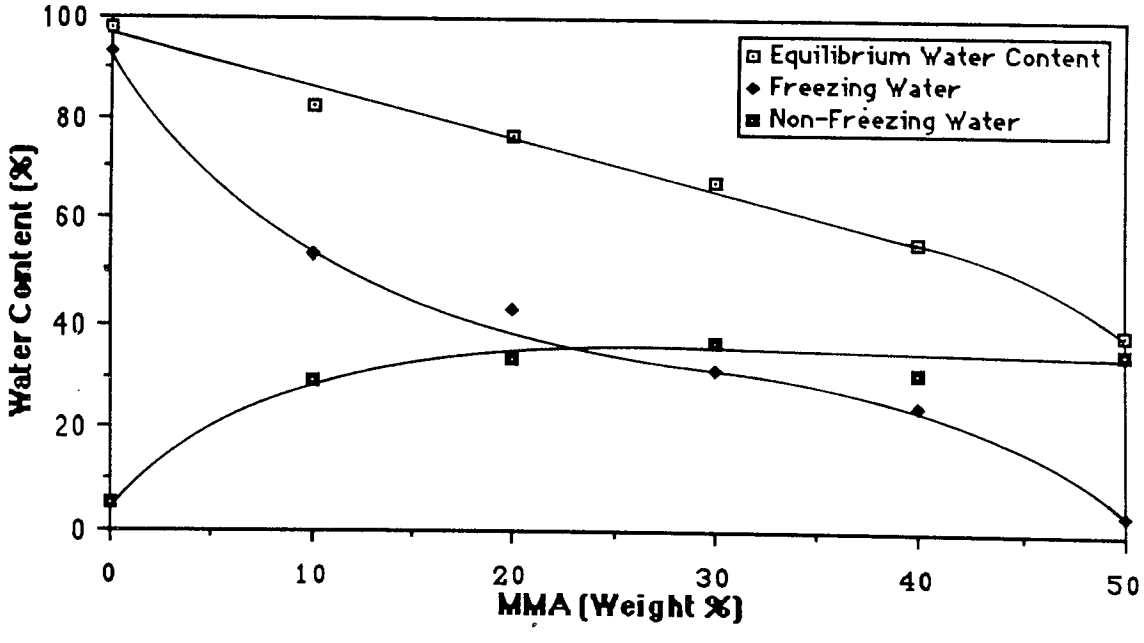

Figure 3.20 Effect of composition on the water content of NVP-MMA copolymers

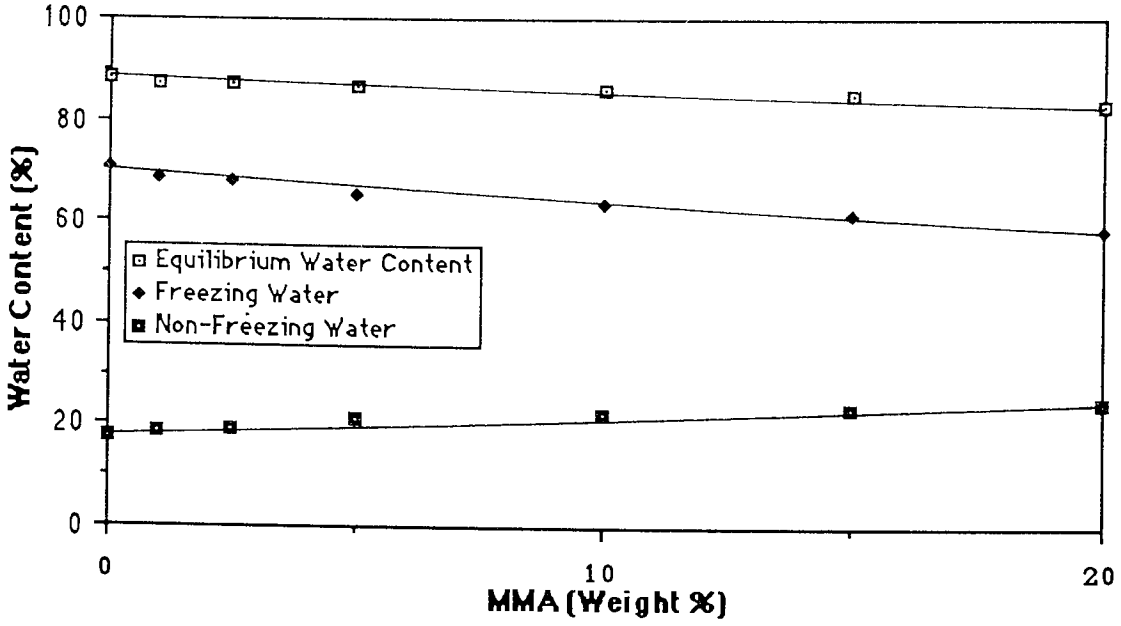

Figure 3.21 Effect of composition on the water content of NNDMA-MMA copolymers

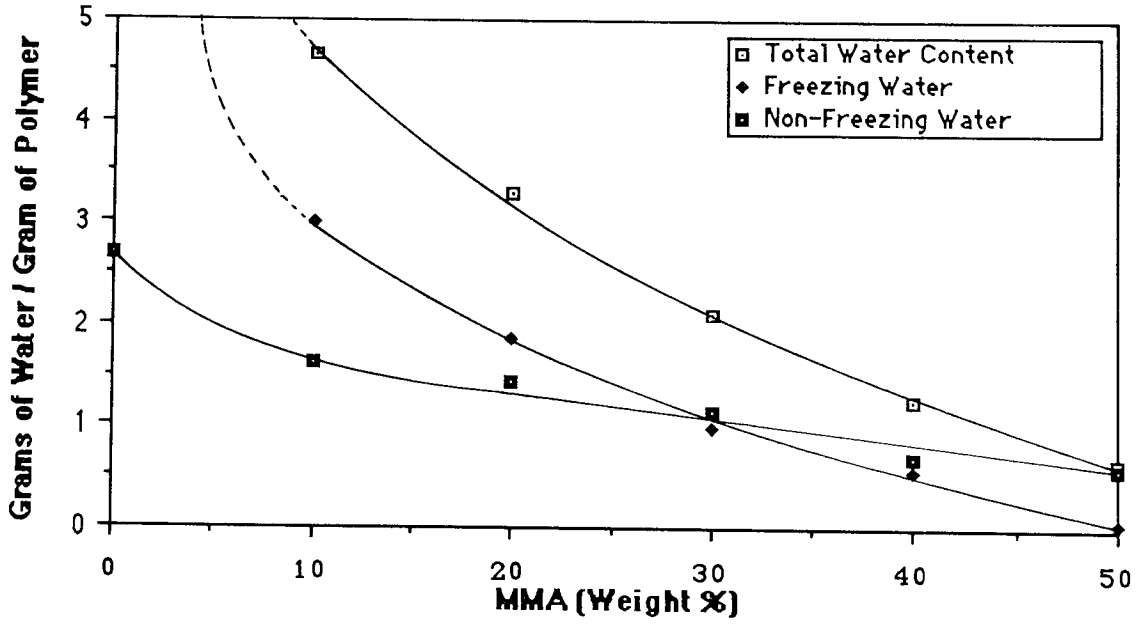

Figure 3.22 Effect of composition on the water binding of NVP-MMA copolymers

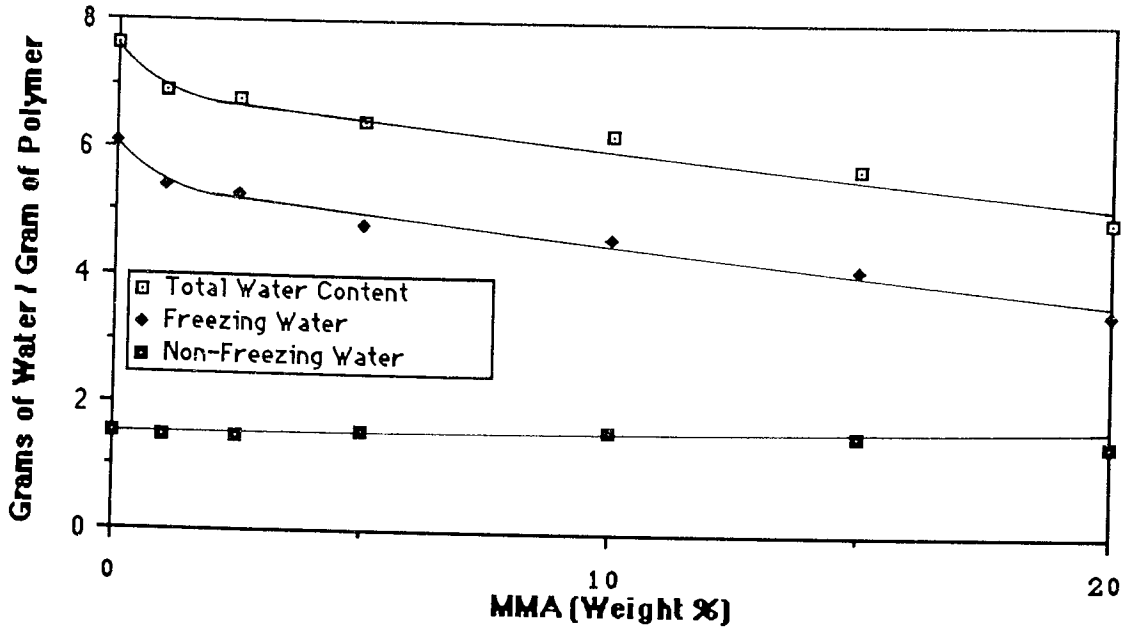

Figure 3.23 Effect of composition on the water binding of NNDMA-MMA copolymers

The incorporation of 20% MMA into NNDMA has less effect on the water content than the addition of 20% MMA to HEMA. There are two possible explanations for this phenomenon. It is possible that packing in NNDMA-MMA copolymers favours the formation of water clusters and, therefore, that the water content of NNDMA-MMA copolymers is influenced less than that of NVP-MMA by the addition of MMA. MMA incorporation will restrict access to the water binding sites on NNDMA, however, this may be compensated for, in part, by the formation of hydration clusters. Another possible reason for the fact that the effect of MMA on NVP is more marked is the helical conformation of poly NVP. This has been previously discussed in more detail.

3.4 Effect of Composition on the Structure of the Melting Endotherm.

The total amount of freezing water in a hydrogel can be obtained from the area under the D.S.C. melting endotherm but it is possible to derive more information from the fine structure of the D.S.C. curves. Throughout this work water has been classified into two

states, freezing water and non-freezing water. However, Figures 3.24-3.26 which show some typical melting endotherms, obtained from D.S.C. studies, illustrate that the freezing water in the hydrogel can be further classified into two or more states. As temperature cycling causes a redistribution of the freezing water present in the hydrogel[82], only two states of water have been discussed.

Figure 3.24 shows the melting endotherms of poly HEMA and two HEMA copolymers. This illustrates that in poly HEMA (crosslinked with 1% EGDM) a significant proportion of the freezing water has a melting temperature lower than that of pure water. This water has been referred to as interfacial water by some workers[63]. This water although not strongly hydrogen bonded to the hydrophilic groups polymer chain obviously does interact, either with the polymer chain or the water strongly bound to the polymer chain. Increasing the amount of hydrophobic monomer, in this case represented by EGDM crosslinking agent, (Figure 3.24b) reduces the weak interactions with the polymer chain and the peak shape moves towards the monolithic melting peak for pure water. In contrast, incorporation of a more hydrophilic monomer (NVP) leads to more complex water structuring in the system (Figure 3.24c). Figure 3.25 shows the melting endotherms of a) poly NVP, b) a NVP-LMA 60:40 copolymer and c) a NNDMA-LMA 70:30 copolymer. The melting endotherm of poly NVP is a relatively simple, ill resolved doublet. Lowering the water content by the introduction of LMA gives better resolution of the doublet and introduces a water structuring peak at a lower temperature (264K). Similar behaviour is seen with the NNDMA-LMA system. Figure 3.26 shows the melting endotherms of poly NNDMA and two NNDMA copolymers. The melting endotherm of poly NNDMA is similar to that of poly NVP and characteristic for high water content polymers, showing a broad peak with a shoulder just below 273K. The introduction of 15% MMA, which only reduces the EWC by 3%, has very little effect on the shape of the melting endotherm. The NNDMA-HEMA

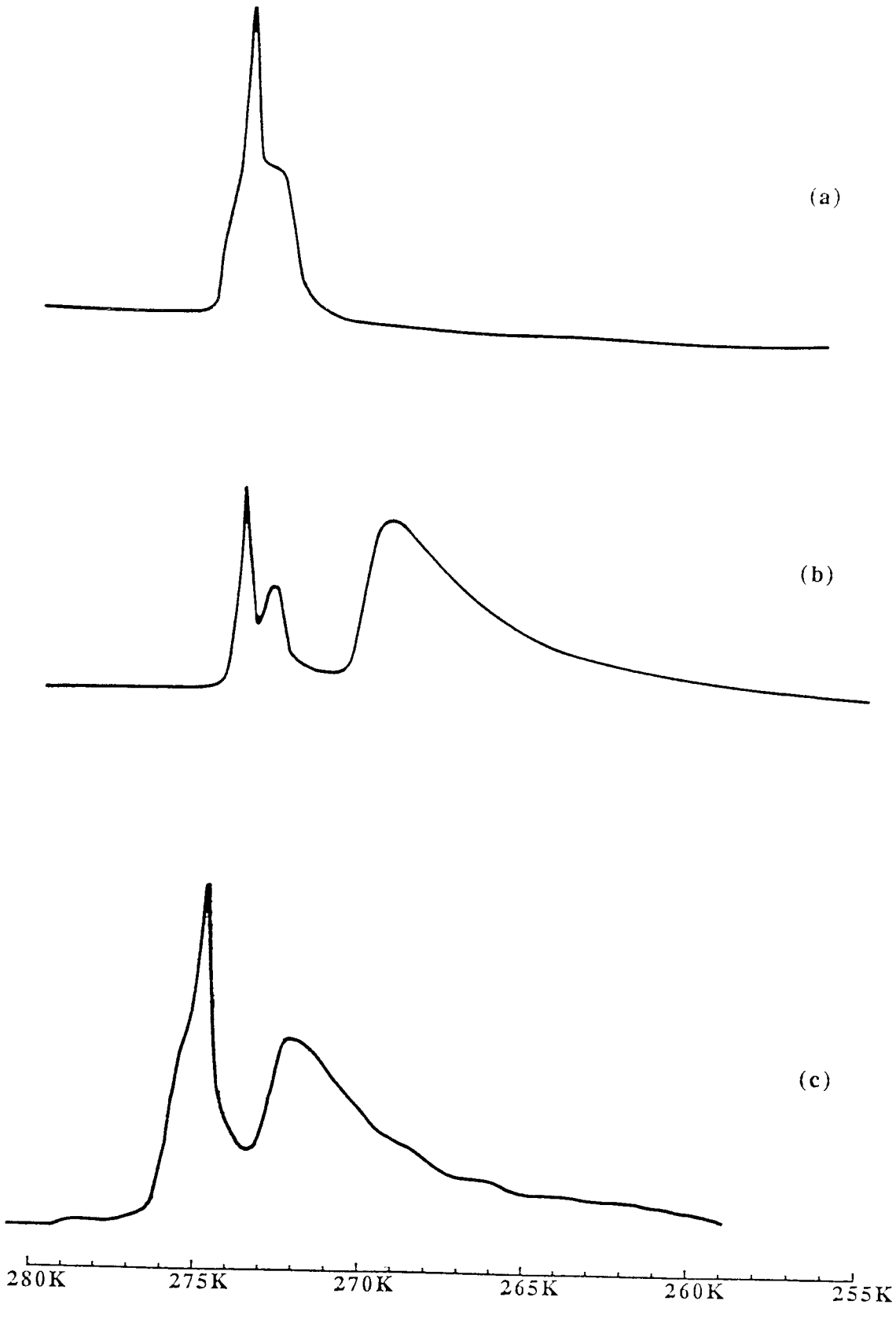

Figure 3.24 Typical melting endotherms for a) poly HEMA with 1.0% EGDM crosslinking agent b) poly HEMA with 5.0% crosslinking agent and c) a HEMA-NVP 60:40 copolymer

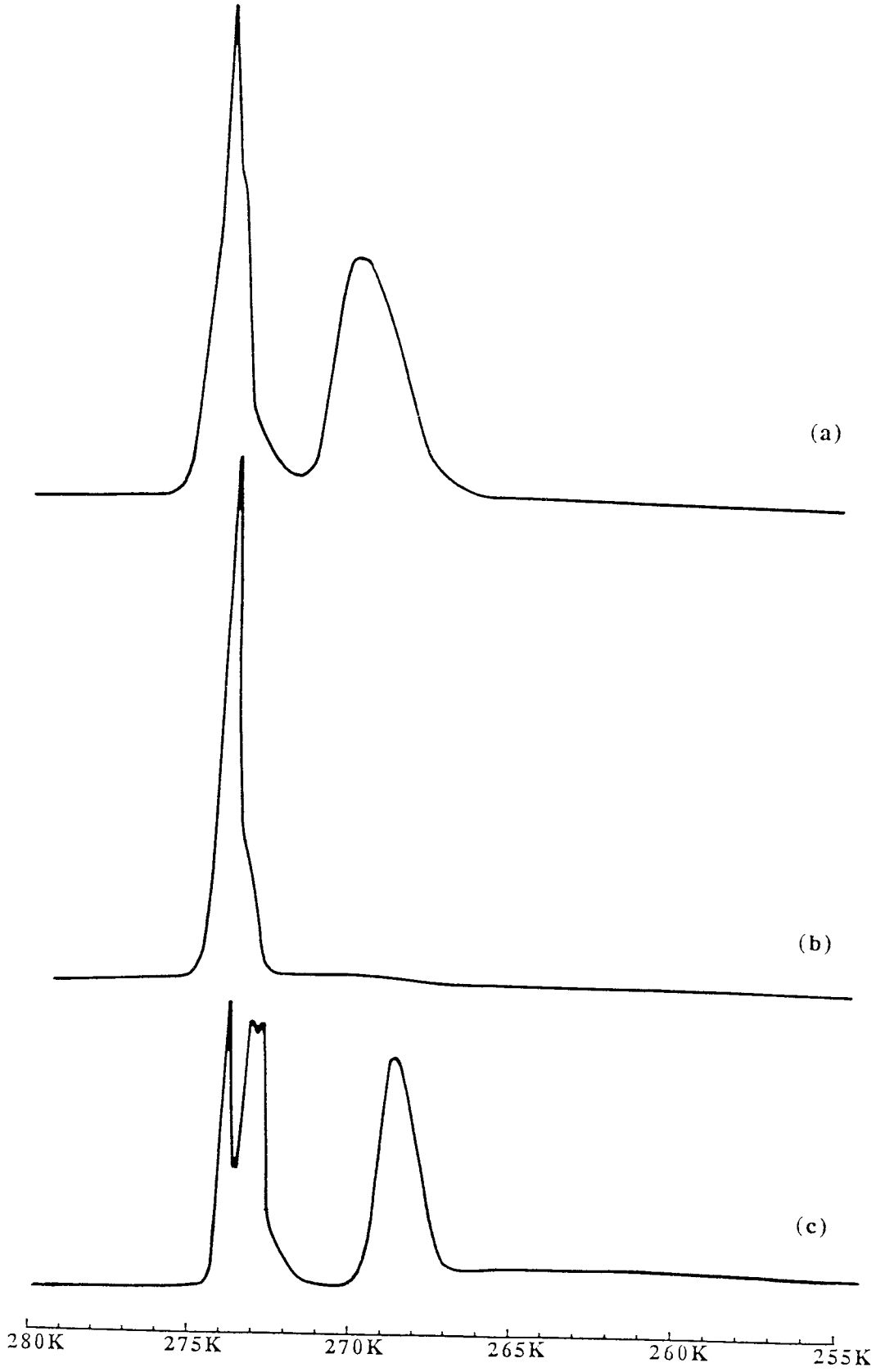

Figure 3.25 Typical melting endotherms of a) poly NVP with 1% EGDM crosslinking agent b) a NVP-LMA 60:40 copolymer and c) a NNDMA-LMA 70:30 copolymer

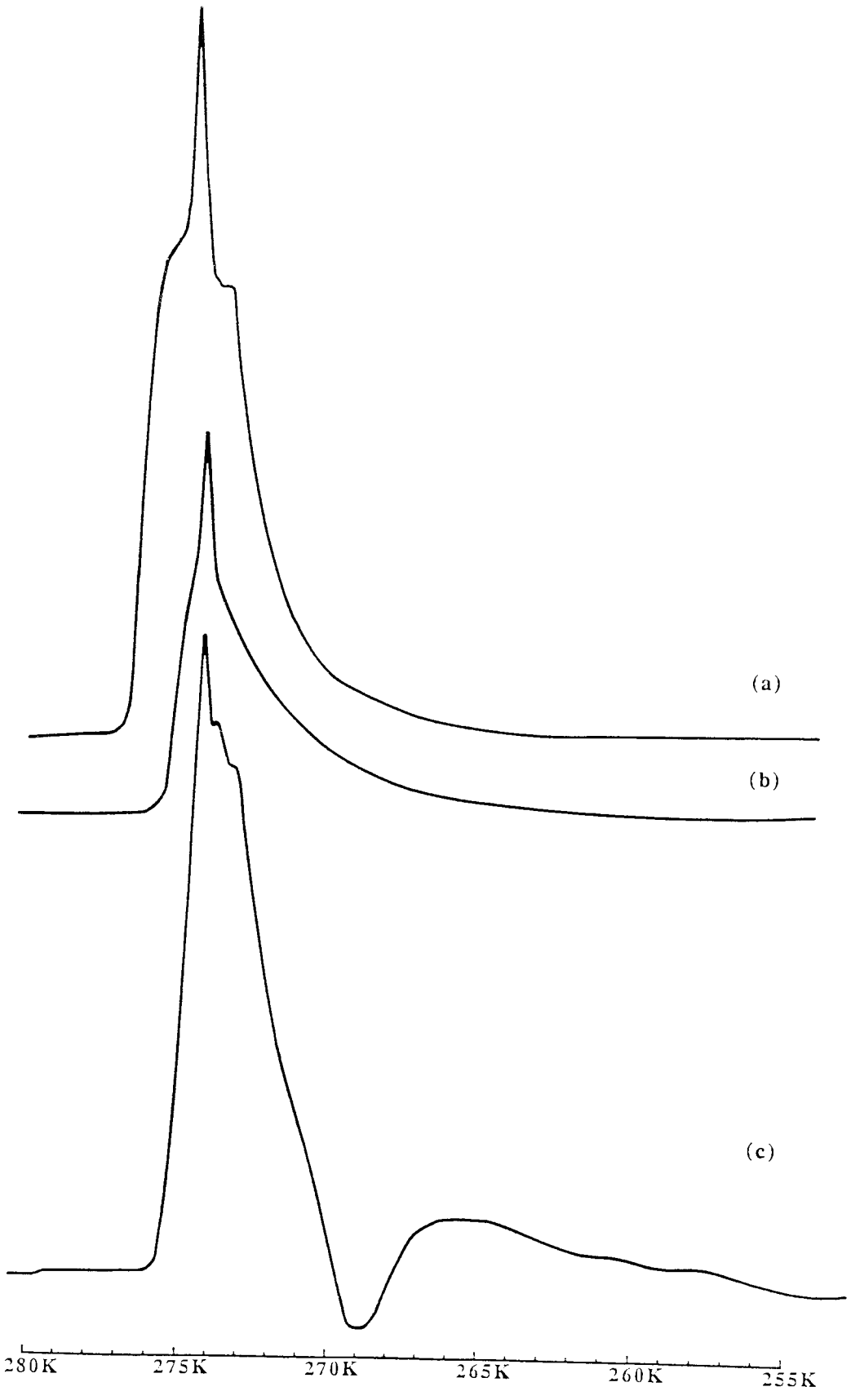

Figure 3.26 Typical melting endotherms of a) poly NNDMA with 1% EGDM crosslinking agent b) a NNDMA-MMA 85:15 copolymer and c) a NNDMA-HEMA 40:60 copolymer

40:60 copolymer (Figure 3.26c) has a melting endotherm beginning at 260K, with two distinct peaks; similar melting endotherms are also produced by polymers containing methacrylic acid.

These results demonstrate that not all the freezing water is completely unaffected by the polymeric environment. A significant percentage of the freezing water crystallises and remelts at a lower temperature than that of pure water. This supports the idea that the water present in a hydrogel exists in a continuum of states between the extreme non-freezing and freezing forms. The structure of water in hydrogels is affected not only by the composition of the hydrogel but also by the nature of the hydrating medium.

3.5 Effect of Hydrating Medium on the Shape of the Melting Endotherm

The structure of water in polymers is also affected by the nature of the hydrating medium. Preliminary studies have, therefore, been undertaken on the effect of anions on the water structuring in poly HEMA. The structure of water around electrolytes in solution has been discussed in terms of a three phase model[29].

i) A primary phase around the electrolyte which is strongly associated with and ordered by the electrolyte

ii) A secondary phase, which is less ordered than the primary phase but still influenced by the electrolyte

iii) A tertiary phase, not influenced by the electrolyte and which is, therefore, bulk water

Ions can be classified as either structure makers or structure breakers, by observing the effect of the ion on the surrounding water molecules. Small or multivalent ions (e.g. F^- and SO_4^{2-}) are normally referred to as structure making ions as they increase the size of the

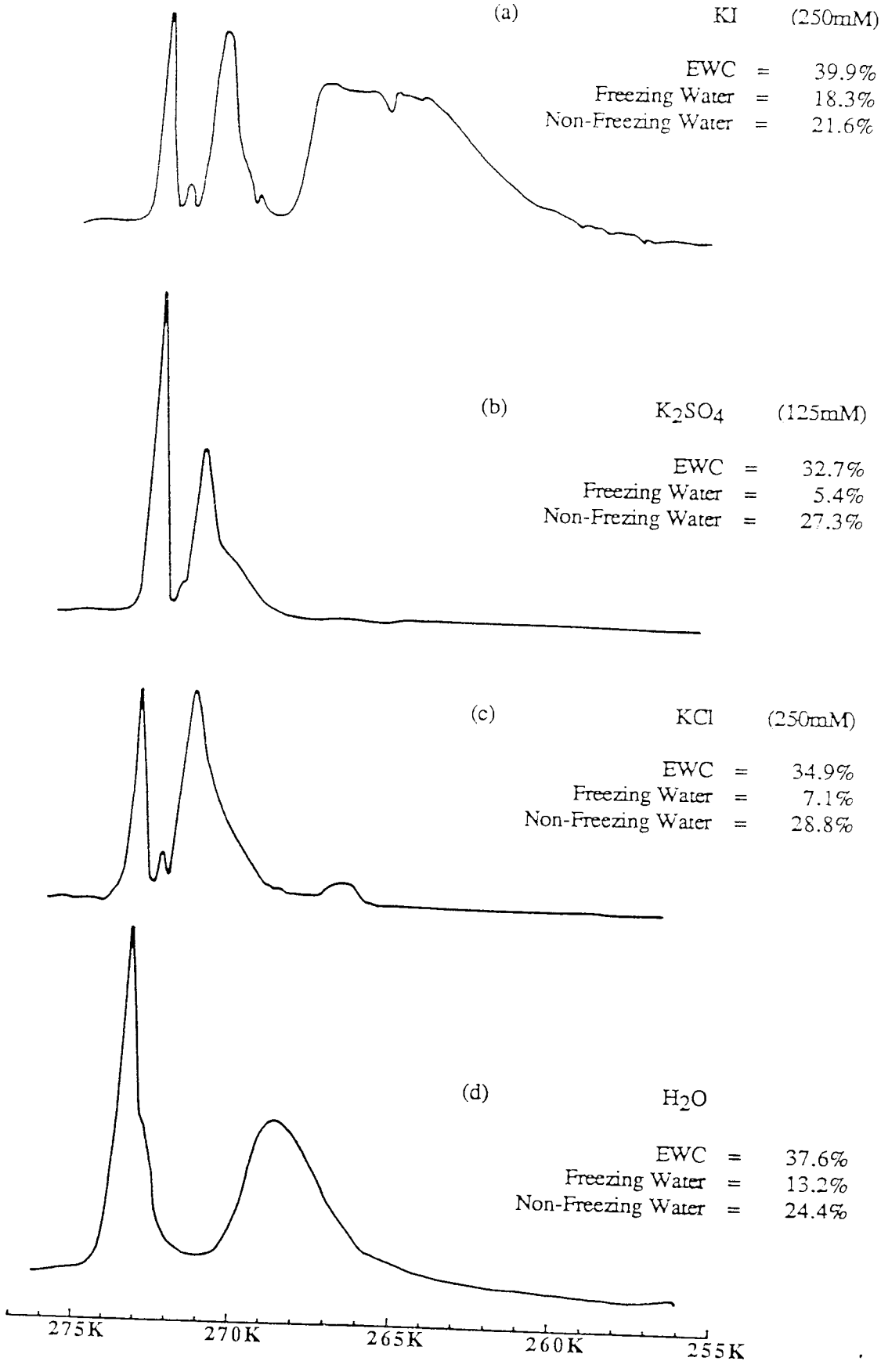

Figure 3.27 Effect of hydrating medium on water structuring in poly HEMA

ordered, primary phase, around them. Large monovalent ions (e.g. I^- and Br^-) however, are normally referred to as structure breaking ions as they are incapable of producing a large ordered phase around them. These ions do, however, produce a large secondary phase around them[165]. This behaviour is shown clearly in Figure 3.27 which shows the effect of various anions (iodide, sulphate and chloride) on the water structuring in poly HEMA. Hydrating poly HEMA in potassium sulphate (a strong structure maker) reduces the equilibrium water content of the hydrogel and increases the proportion of the non-freezing water (i.e. water in the primary phase around an electrolyte). However, when potassium iodide (a strong structure breaker) is used as the hydrating medium the equilibrium water content of the poly HEMA is increased. The D.S.C. melting endotherm also demonstrates the dramatic increase in water in the secondary disordered phase, present in the polymer. Potassium chloride behaves in some respects as a structure maker, and in others as a structure breaker. Hydrating poly HEMA in KCl causes an increase in the proportion of non-freezing water present in the polymer, however, the presence of some water with a melting point of 267K indicates that KCl is also acting as a structure breaker.

3.6 Conclusions

The water binding properties of a range of polymers and copolymers, with a wide range of EWCs have been examined. The observations relating to the total amount of water in the hydrogel are clearly related to the balance of hydrophilicity / hydrophobicity in the copolymer and, in particular, the steric and polar contributions of backbone substituents. Values for the equilibrium, freezing and non-freezing water contents of poly HEMA (37.6%, 13.2% and 24.4% respectively) have been determined. Many workers agree on the value for the EWC of poly HEMA, however, there has often been disagreement about the amount of freezing and non-freezing water present in the gel. This may be due to the wide range of methods used to determine EWC or varying interpretations of the results obtained.

Although discrepancies between values for freezing and non-freezing water arise due to differences in techniques, further experimental variation can result from the the well known difficulty of the purification of HEMA, which contains as major impurities, ethylene glycol dimethacrylate (EGDM) and methacrylic acid. In addition to this, polymerisation conditions can lead to disproportionation of monomer and generation of further EGDM. As a result two extreme situations may be envisaged, one resulting from the influence of excess crosslinking agent and the other from the influence of adventitious carboxyl groups in the polymer chain. At physiological and slightly acidic pH the influence of the carboxyl group is small, but at high pH the influence of the carboxylate anion has a dramatic effect, leading to a marked increase in the ratio of freezing to non-freezing water. Unless the hydrating solution is deliberately buffered, adventitious carbon dioxide normally results in acidic hydration conditions and the effect of addition of crosslinking agent dominates that of the carboxyl groups.

The EWCs of HEMA-St and HEMA-MMA copolymers are insensitive to changes in temperature in the range 22°C to 70°C. The effect of temperature on water binding has been discussed in terms of the balance between, hydrophobic bonding between substituent groups in the polymer chain and the hydrophilic interactions, which are normally dominant. However, it is interesting to compare the behaviour of the isomeric monomers HPA and HEMA. Previous work in our laboratories[145] has shown that HPA copolymers show pronounced minima in the EWC temperature profile in marked contrast to the behaviour of the HEMA-St and HEMA-MMA systems (Figures 3.1 and 3.2). The differences between acrylate and methacrylate copolymers can be rationalised in terms of the effect of the hydrophilic / hydrophobic balance in the backbone on the ease of phase separation within the hydrated gel. It is one of the potential values of the types of polymer described here, that the water binding properties can be modulated to produce a range of hydrogels which show

a remarkable temperature independence of water binding behaviour. Although in hydrogels containing NVP the EWC is temperature dependent, this effect is not too pronounced and it does not preclude their use in biomedical applications.

The behaviour of HEMA copolymers with hydrophilic monomers and copolymers based on the hydrophilic monomers NVP and NNDMA can also be explained in terms of copolymer structure. However, in systems containing both NNDMA and NVP both the structure and composition of the final copolymer may vary from those expected. In systems based on NVP the disparity in radical reactivity ratios may lead to the formation of a polymer with some degree of block copolymer character, rather than the expected random, alternating copolymer. The other problem encountered with NVP copolymers is the difference between feed ratios and composition of the final polymer, also due to disparities in reactivity ratios. Despite this, by careful selection of comonomers a range of copolymers, based on NVP, with water contents varying from that of poly HEMA to in excess of 90% can be synthesised.

One interesting series in this respect are the copolymers based on NVP and MMA, incorporation of increasing quantities of MMA in copolymers with NVP has the effect of 'titrating out' freezing water. Therefore, the NVP-MMA 50:50 copolymer, which has an EWC similar to that of poly HEMA has a very low freezing water content. Polymers of this type may be useful in reverse osmosis applications as the water binding behaviour has a marked effect on the permselectivity and permeability of the hydrogels.

In copolymers containing NNDMA chain transfer has proved to be a problem. The readily abstractable hydrogens (Figure 2.1) promote chain transfer reactions which increase the effective crosslink density. This may be one reason why the the EWC of poly NNDMA

with varying levels of EGDM crosslinking agent is consistently lower than that of poly NVP. The problem of chain transfer and its effect on mechanical properties will be discussed in Chapter 4.

The fine structure of the D.S.C. melting endotherms provide valuable information on the water structuring in hydrogels. The structure of the melting endotherm is dependent not only on the hydrophilic-hydrophobic interactions in the copolymer system but also on the water structuring ability of the hydrating medium. Hydrophilic or relatively hydrophobic copolymers produce relatively simple melting endotherms. However, there is less uniform water structuring in systems where there are interactions between two monomers of varying hydrophilicity. It is interesting to note that the amphiphilic poly HEMA has a melting endotherm similar to that of copolymers where there is a balance of hydrophilic and hydrophobic interactions. One further point which can be noted is that the complexity of the melting endotherms supports the hypothesis that the water in hydrogels exists in a continuum of states.

CHAPTER 4

Mechanical Properties of Copolymer Hydrogels

4.1 Introduction

The mechanical properties of many hydrogel systems are poor and this has proved to be a limiting factor in several biomedical applications. However, in many respects, this is not surprising as hydrogels often contain more than 50% water. In many applications a combination of high water content and mechanical strength is necessary. Therefore, attempts have been made to synthesise high water content hydrogels with improved mechanical properties. In addition, before investigating the mechanical properties of more complex systems, several simple copolymer hydrogels have been examined to determine the factors controlling mechanical properties. The effects of monomer structure and equilibrium water content on the mechanical properties of a series of hydrogels have been studied and the results are presented graphically below and listed in Appendix 2. The primary forms of the experimental data (stress / strain and load / elongation) curves and the equations used to calculate tensile strength (σ_b), elongation to break (ε_b) and Youngs modulus (E) have been discussed previously in Section 2.6.

4.2 Effect of Hydrogel Composition on Mechanical Properties

The effect of EGDM incorporation on the mechanical properties of poly HEMA and poly NNDMA is illustrated in Figures 4.1-4.3. Both polymers show an increase in tensile strength and a reduction in elongation to break as increasing amounts of crosslinking agent are added. This can be explained by a decrease in the chain length between crosslinks which leads to an increased retractive force in the polymers. Similar behaviour has previously been reported for poly HEMA by Raab and Janacek[166]. They also noted that the measured value of the tensile strength of water swollen hydrogels is very sensitive to changes in temperature and crosshead speed. The value for the tensile strength of poly HEMA obtained in this work was 0.495MPa ; several other workers have also measured the tensile strength of poly HEMA and a range of values (0.402MPa[166], 0.318MPa[167], 1.19MPa[168] and 1.09MPa[168]) have been reported. Values of elongation to break of 208% and 210%, in

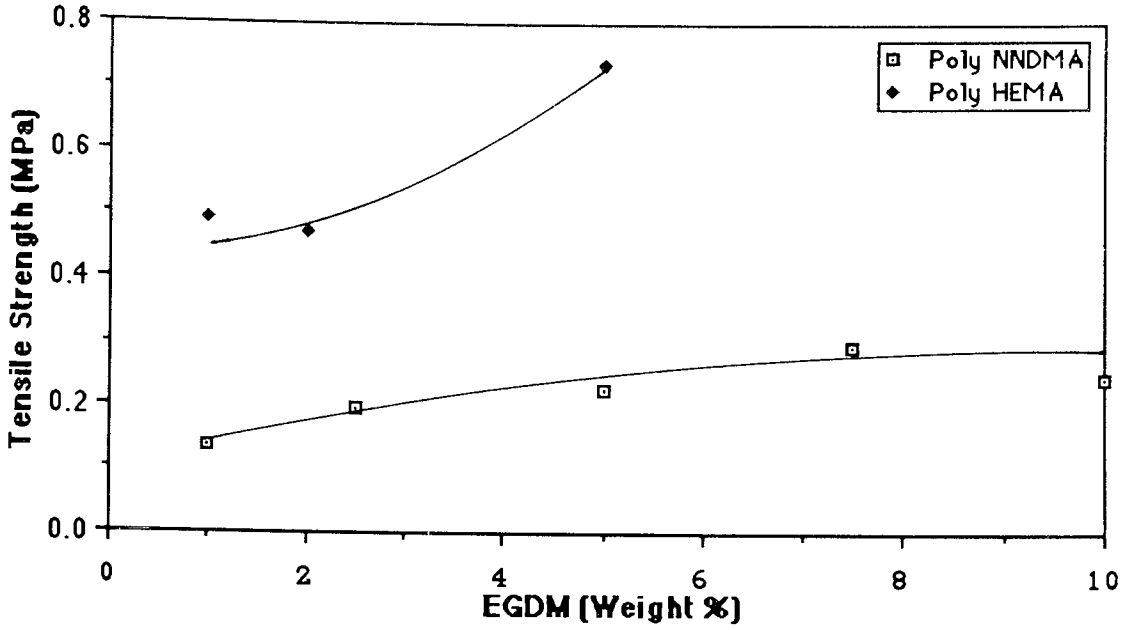

Figure 4.1 Effect of EGDM incorporation on the tensile strength of poly HEMA and poly NNDMA

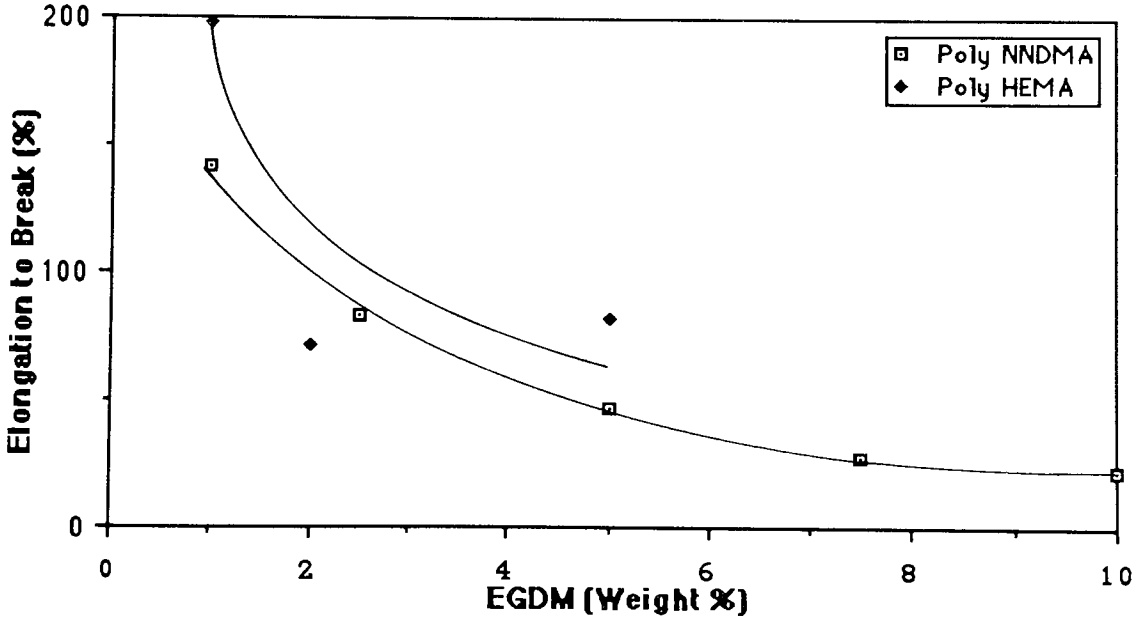

Figure 4.2 Effect of EGDM incorporation on the elongation to break of poly HEMA and poly NNDMA

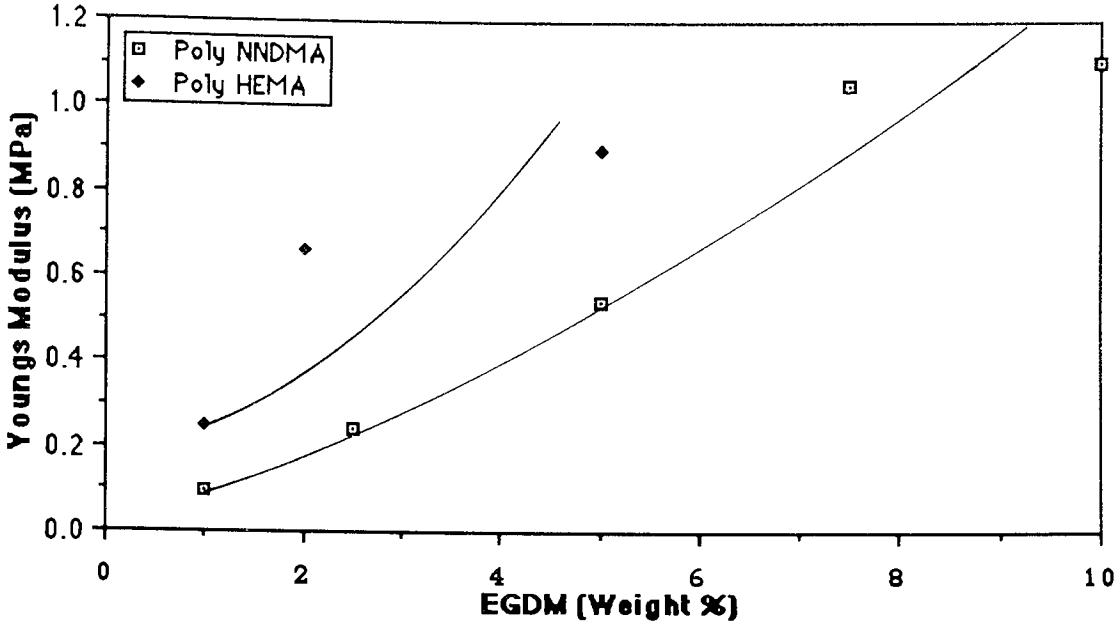

Figure 4.3 Effect of EGDM incorporation on the Youngs modulus of poly HEMA and Poly NNDMA

good agreement with the 198% measured here have also been reported[168]. The Youngs modulus of both poly HEMA and poly NNDMA increase as expected in systems where the σ_b is increasing while ε_b is being reduced.

The effect of incorporation of the hydrophobic monomers methyl methacrylate and styrene into poly HEMA is illustrated in Figures 4.4 and 4.8. The values of σ_b and ε_b for HEMA-MMA and HEMA-St copolymers derived from the primary data are shown in Figures 4.5-4.7 which additionally illustrate the results obtained from NVP-MMA copolymers. The effect of MMA incorporation on the mechanical properties of poly HEMA is demonstrated in Figure 4.4. The load to break increases with the addition of increasing amounts of hydrophobic MMA. However, after the addition of 40% MMA (Figure 4.4d) an obvious transition in the mechanical properties occurs.This transition can also be seen clearly graphically as there is a large increase in σ_b and E with a accompanying reduction in ε_b. It is interesting to note that this transition from flexible to rigid behaviour takes place at a point

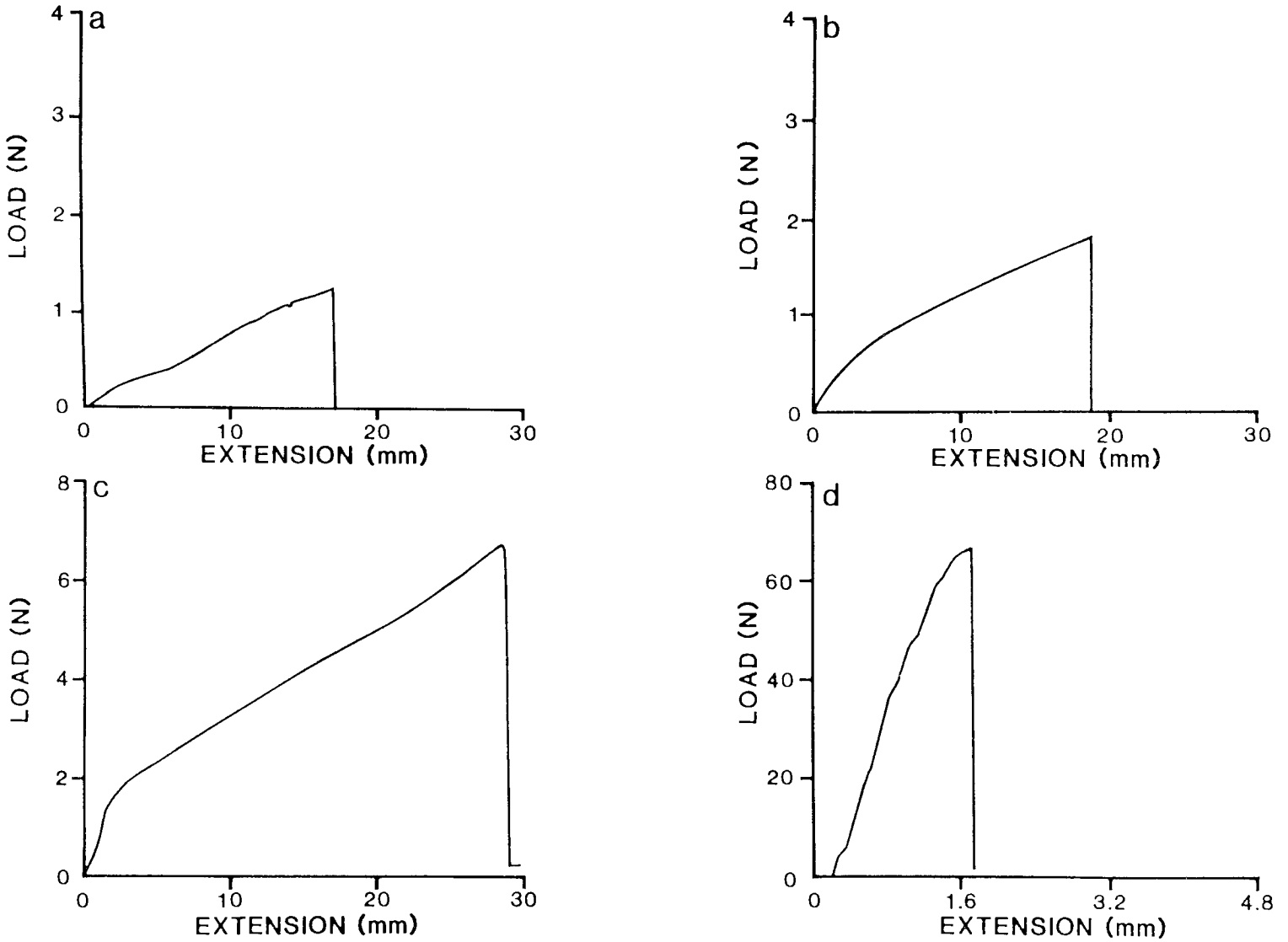

Figure 4.4 Load-extension curves for (a) poly HEMA (b) a HEMA-MMA 90:10 copolymer (c) a HEMA-MMA 70:30 copolymer and (d) a HEMA-MMA 60:40 copolymer

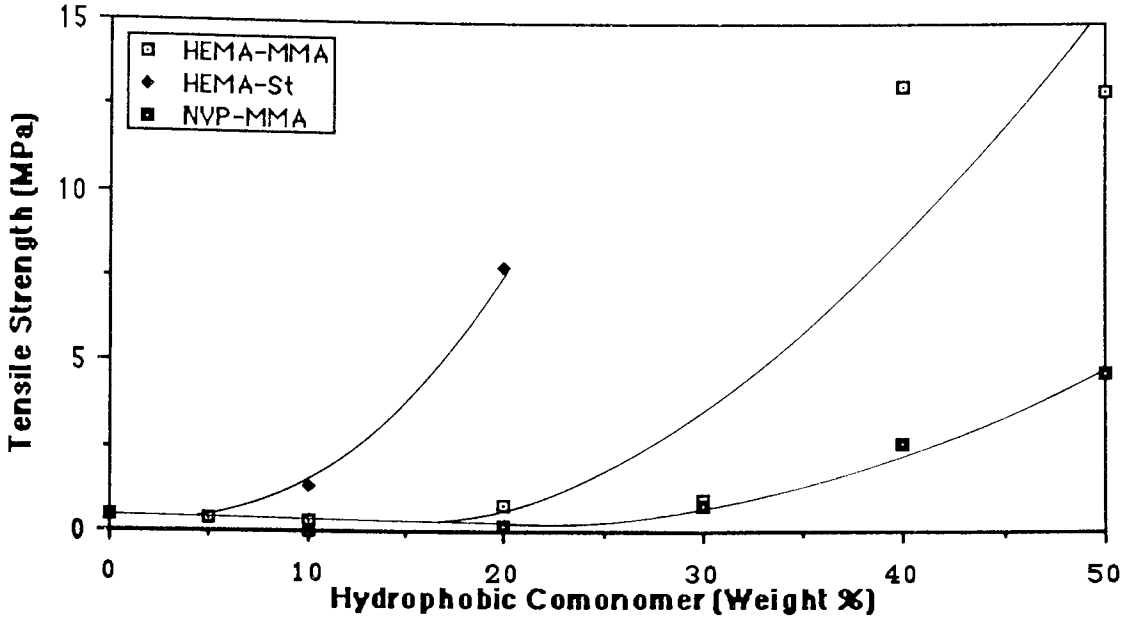

Figure 4.5 Variation in tensile strength with composition for copolymers of HEMA-St, HEMA-MMA and NVP-MMA

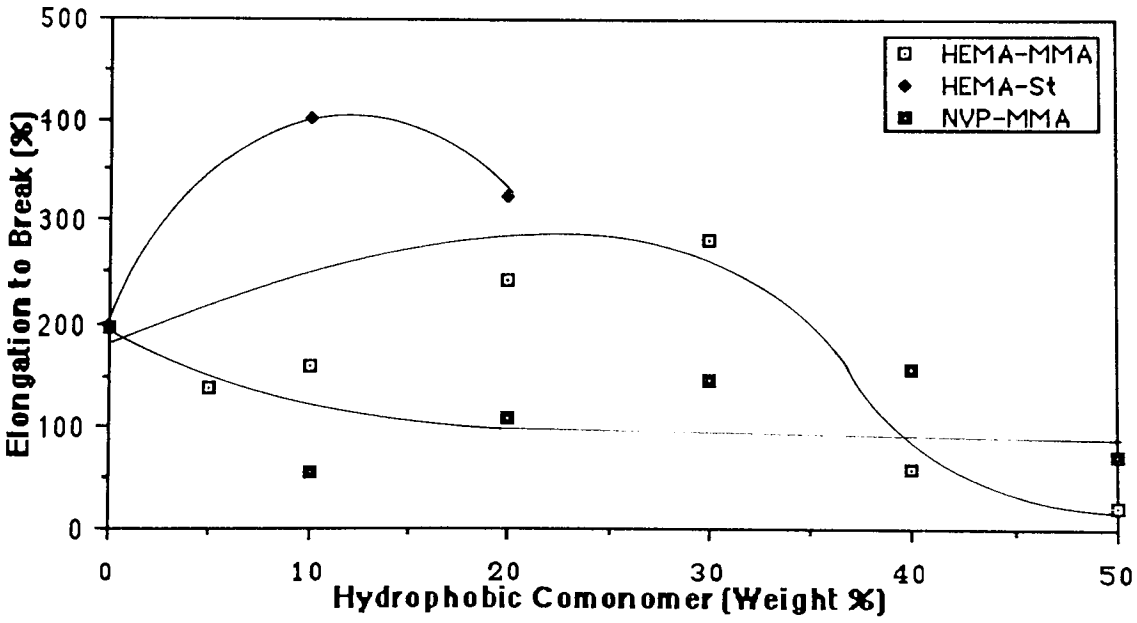

Figure 4.6 Variation in elongation to break with composition for copolymers of HEMA-St, HEMA-MMA and NVP-MMA

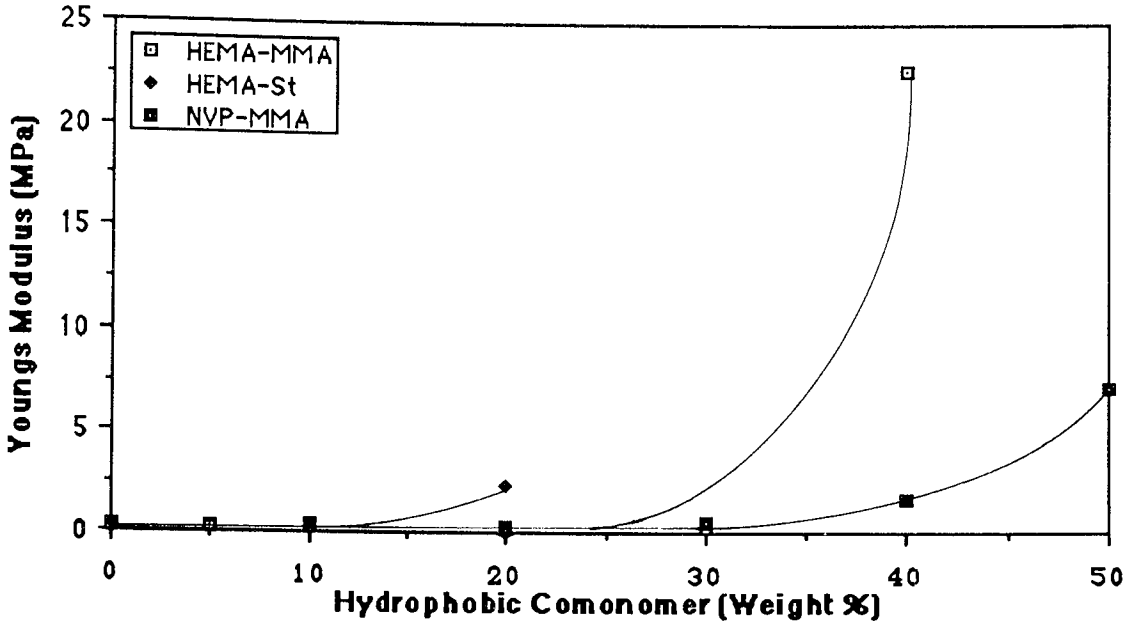

Figure 4.7 Variation in Youngs modulus with composition for HEMA-St, HEMA-MMA and NVP-MMA copolymers

corresponding to the disappearance of freezing water in the copolymer series. Freezing water can also be regarded as plasticising water, in view of its greater relative effect on chain mobility and this is a demonstration of the plasticising effect of freezing water. The NVP-MMA system, on the other hand, displays a gradual increase in σ_b and E values with increasing MMA incorporation enabling a 70:30 NVP-MMA copolymer (with a water content of 68%) to have a higher tensile strength but lower elongation to break than poly HEMA. Hosaka[168] has again reported higher values of σ_b and ε_b in this system. One interesting point is the reduction in ε_b in the NVP-MMA 50:50 copolymer which demonstrates the effect of reducing the freezing water content from 24.6% in the NVP-MMA 60:40 copolymer to 3.5% in this system. Similar behaviour is also seen in the HEMA -MMA 60:40 and 50:50 copolymers which also contain only trace amounts of freezing water.

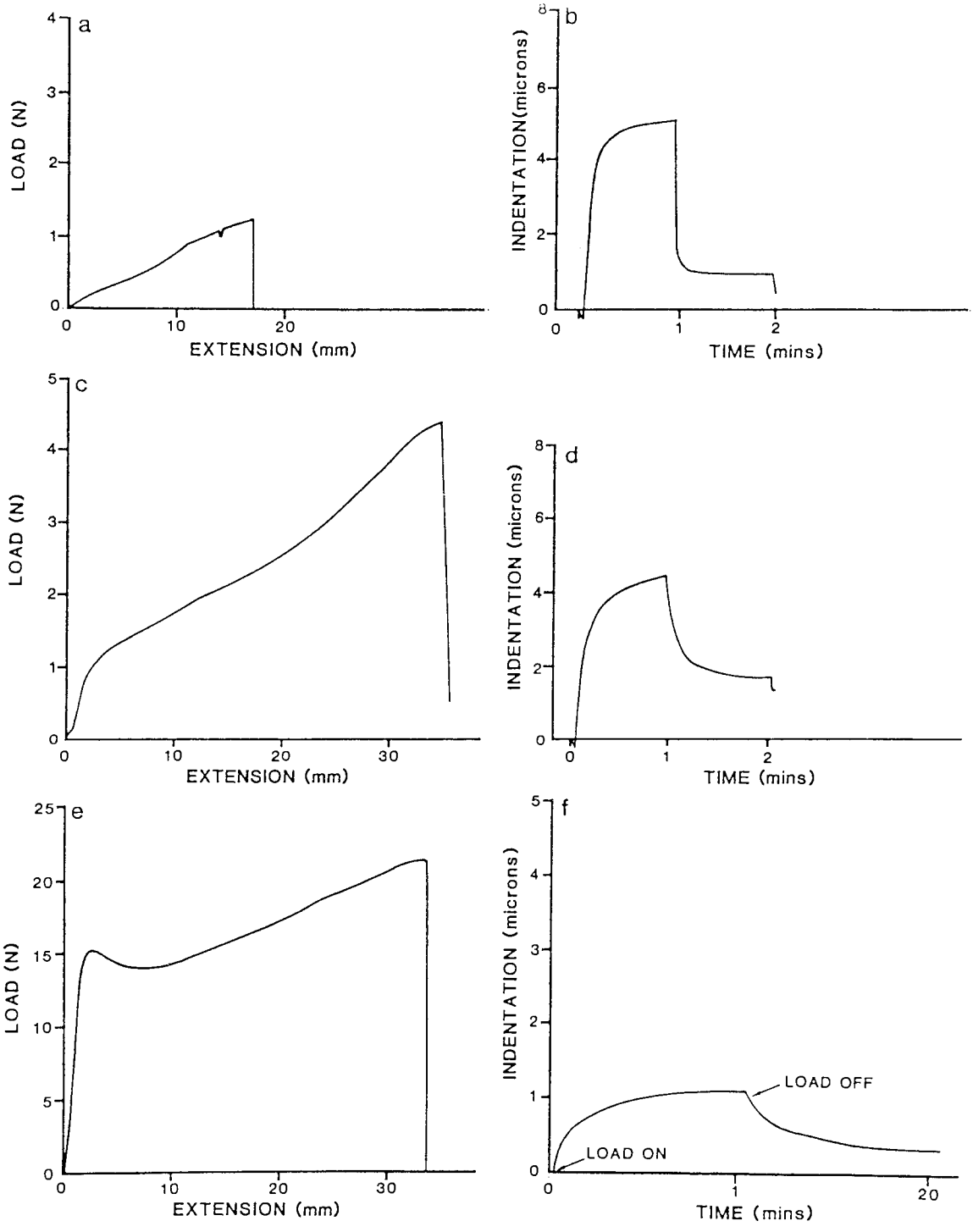

Figure 4.8 **Load-extension and indentation-recovery curves for (a & b) poly HEMA (c & d) a HEMA-St 90:10 copolymer and (e & f) a HEMA-St 80:20 copolymer**

Another useful technique for examining the mechanical behaviour of hydrogels is microindentation. This technique has been used to study the compression behaviour of hydrogels and especially as an *in vitro* technique to study the response of potential contact lens materials to the eyelid load. The technique enables relatively small samples, which may be immersed in a liquid to prevent dehydration, to be used. The temperature of the sample can be also controlled between -50 and 90°C and the choice of a spherical indentor of an appropriate size, together with a range of loads enables determination of equilibrium deformation / recovery values and the mechanical properties of the material to be well characterised. Figure 4.8 compares the indentation / recovery curves (microindentor) with the corresponding load / extension curves (tensometer) for poly HEMA and two HEMA / St copolymers. This illustrates the marked change in elastic behaviour accompanying the drop in equilibrium water content, from 38% to 17%, in these three materials. The stress-strain curves are of the same form as the load-extension curves and the HEMA-St 80:20 copolymer shows strain softening normally associated with amorphous glassy polymers e.g. polystyrene and poly methyl methacrylate[169]. The stress increases rapidly to the yield point and then falls (strain softening) due to the disruption of non-binding interactions between segments which permits flow at a lower stress. There is then an increase in stress to break (strain hardening) due to the orientation of the polymer chains in the sample. The HEMA-St 80:20 copolymer also shows a reduction in ε_b associated with the removal of freezing water from the system.

Figures 4.9-4.11 demonstrate the effect of NVP and NNDMA incorporation into poly HEMA. In both systems there is a steady fall in tensile strength with increasing concentrations of the more hydrophilic monomer and while the elongation to break also decreases, Youngs modulus appears to go through a maximum. As the tensile strengths of both poly NNDMA and poly NVP are much lower than the σ_b of poly HEMA this

behaviour is not unexpected.

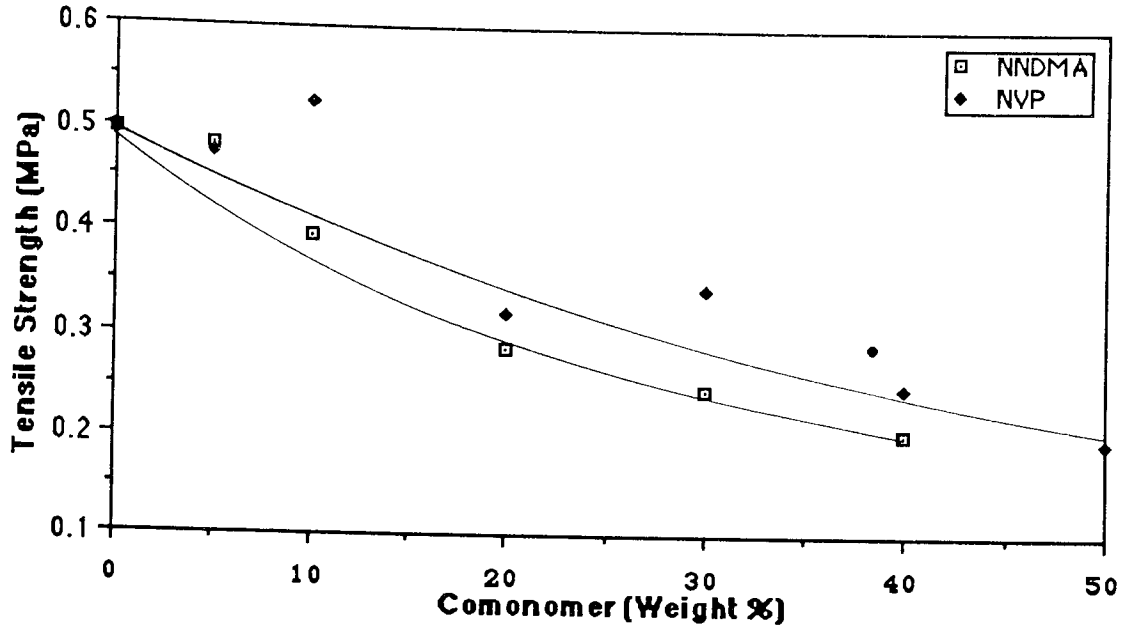

Figure 4.9 Variation in tensile strength with composition for copolymers of HEMA with NNDMA and with NVP

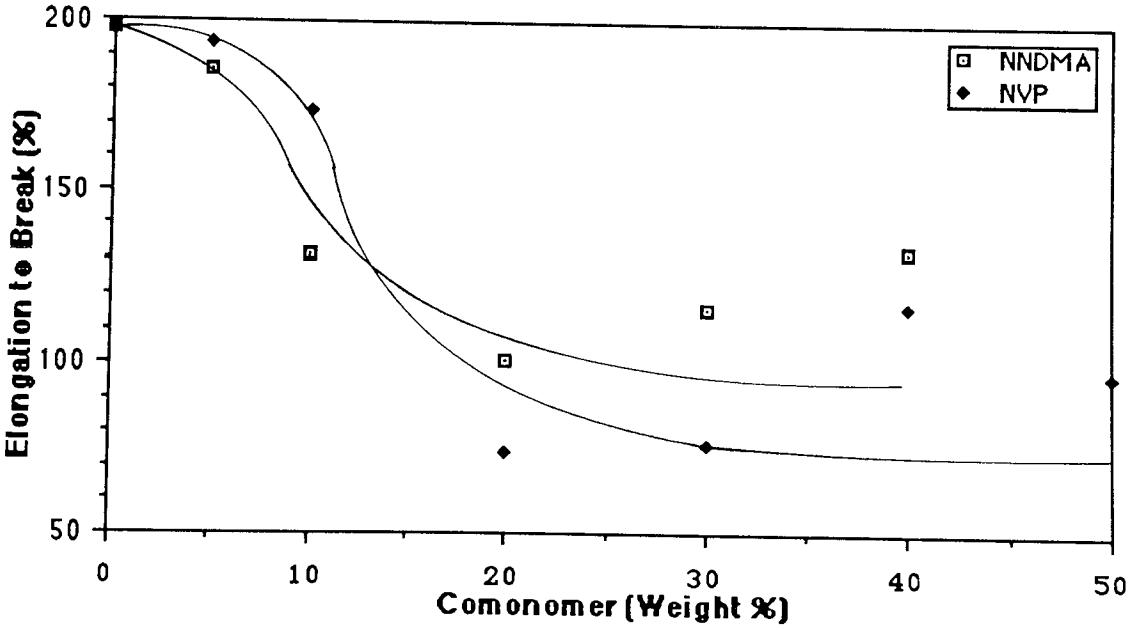

Figure 4.10 Variation in elongation to break with composition for copolymers of HEMA with NNDMA and with NVP

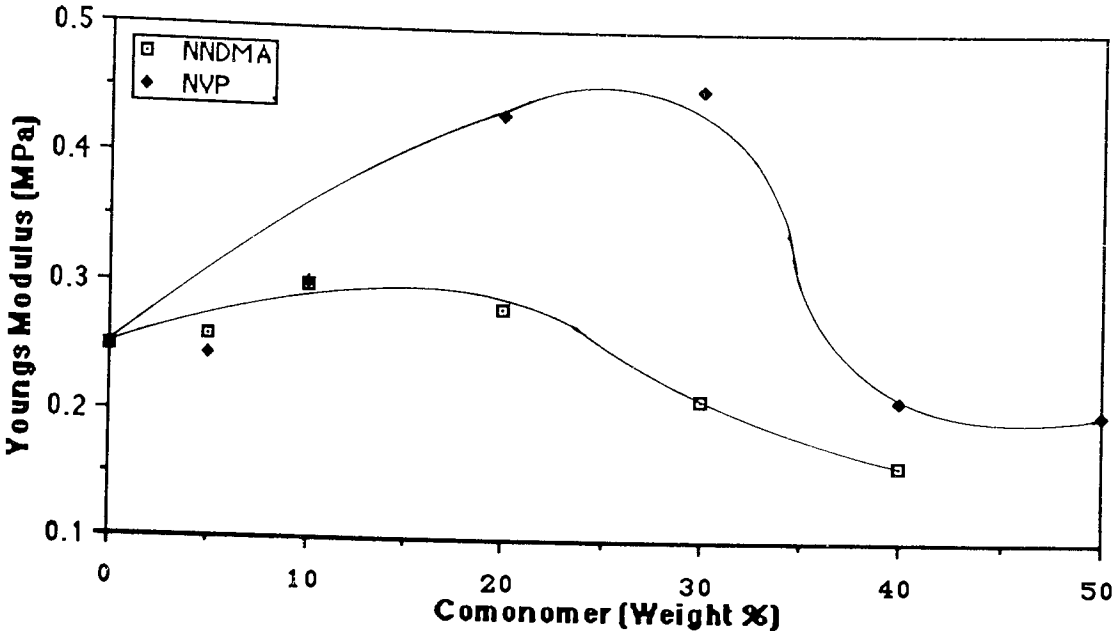

Figure 4.11 Variation in Youngs modulus with composition for copolymers of HEMA with NVP and with NNDMA

One problem encountered with NNDMA incorporation, however, is the readily abstractable hydrogens on the methyl groups which cause chain transfer during polymerisation, producing polymers with a low tear strength. This does not appear to be a factor in determining the mechanical properties in the HEMA-NNDMA copolymers. In fact, in both these systems the mechanical properties appear to be controlled by EWC, as both copolymers have very similar mechanical properties at equivalent EWCs. However, the mechanical properties of these systems in the dehydrated state have not been examined and it is likely that the mechanical properties of dehydrated HEMA-NVP and HEMA-NNDMA copolymers will be similar. Therefore, in the hydrated state water may act as a filler and lower the already poor tensile strengths in these systems.

In an attempt to overcome the problems of chain transfer associated with NNDMA, copolymers of NNDMA with monomers which contained long, flexible chains were

synthesised. The results obtained with ethoxyethyl methacrylate and methoxy PEG_{350} methacrylate were disappointing, however, promising results were obtained from the NNDMA-LMA system. Figures 4.12-4.14 show σ_b, ε_b and E for both NNDMA-LMA and NVP-LMA copolymers. Generally, in both copolymer series there is an increase in tensile strength as increasing amounts of LMA are added. LMA acts as an internal plasticiser, this is demonstrated in NNDMA-LMA copolymers where LMA addition reduces the problems caused by chain transfer, increasing the tear strength of the polymers. This enables high water content polymers with mechanical properties similar to those of poly HEMA to be synthesised. This effect can be attributed to the long, flexible LMA chain which helps to counteract the chain shortening effect of chain transfer in these polymers.

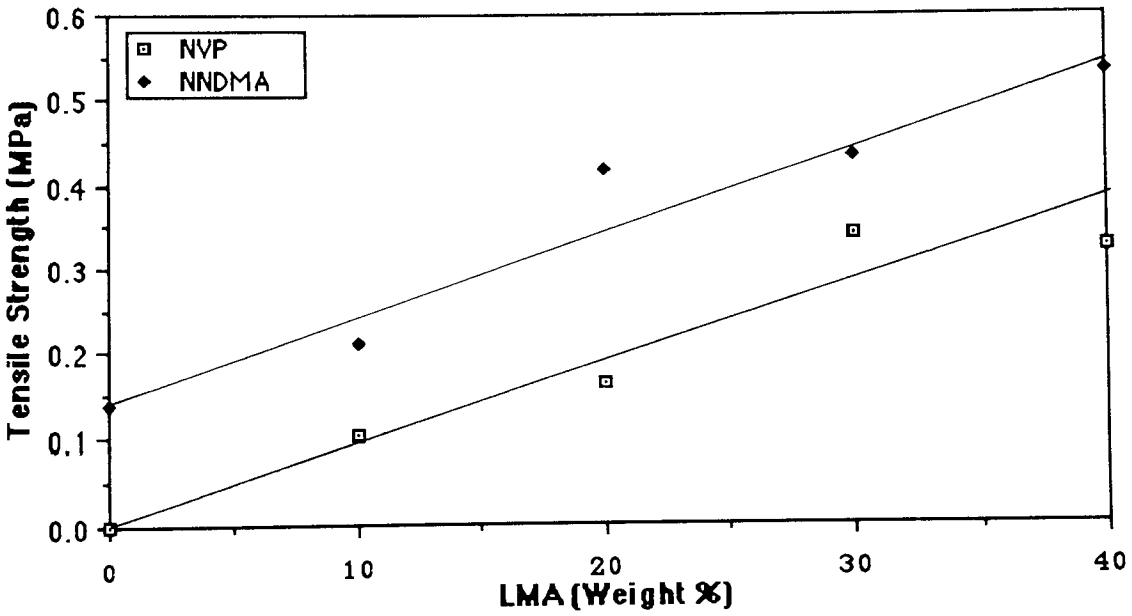

Figure 4.12 Effect of LMA incorporation on the tensile strength of NNDMA-LMA and NVP-LMA copolymers

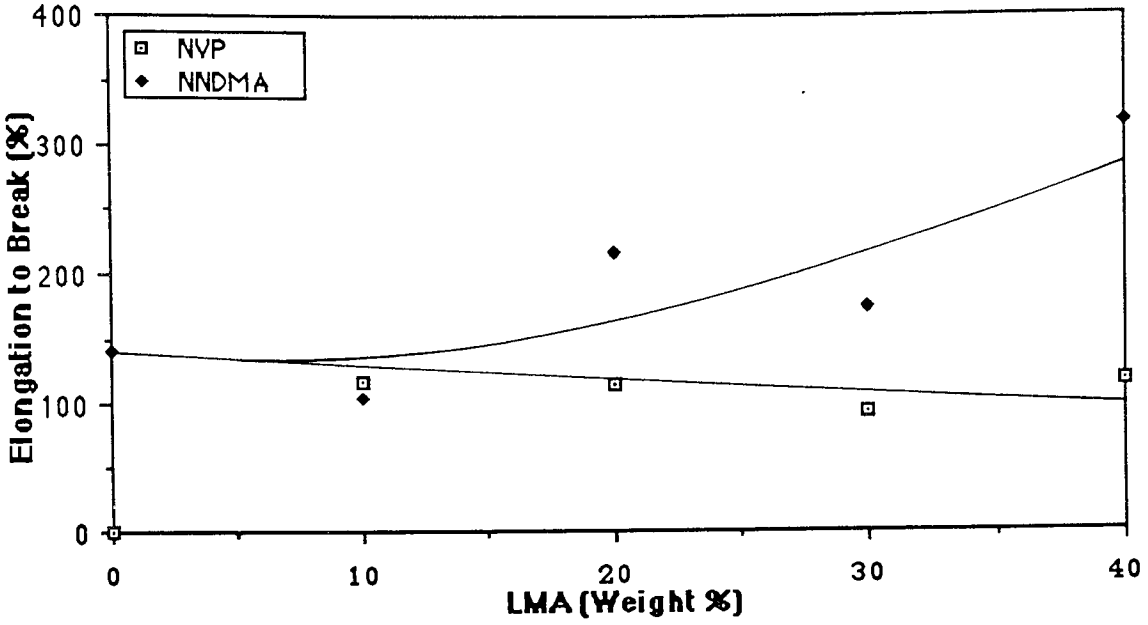

Figure 4.13 Effect of LMA incorporation on the elongation to break of NNDMA-LMA and NVP-LMA copolymers

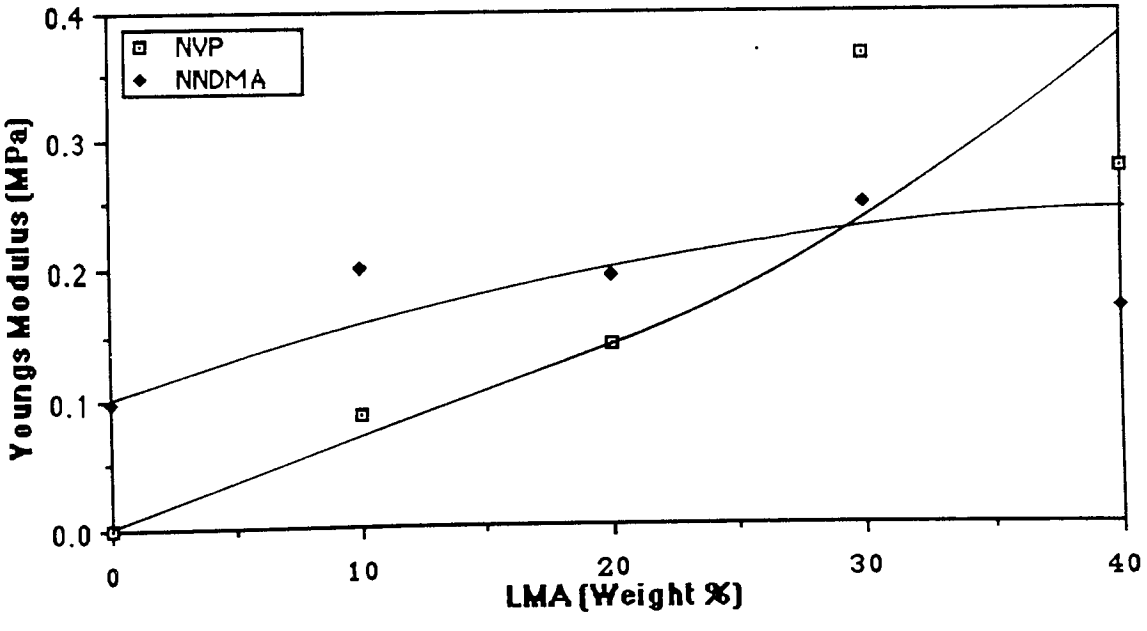

Figure 4.14 Effect of LMA incorporation on the Youngs modulus of NNDMA-LMA and NVP-LMA copolymers

4.3 Effect of EWC on Mechanical Properties

The effect of EWC on the tensile properties of the hydrogel copolymers studied is shown in Figures 4.15-4.17. The general trend shown is a fall in tensile strength with increasing equilibrium water content (Figure 4.15). However, copolymer structure also has an important part to play in determining tensile strengths and those copolymers containing MMA and St have much higher tensile strengths than would be expected from their EWCs (three HEMA-MMA and HEMA-St copolymers with EWCs of 17.5%, 16.7% and 12.3% and tensile strengths of 13.173 MPa, 7.840 MPa and 13. 259 MPa respectively have been omitted from the graph for clarity). Therefore, the incorporation of even small amounts of a comonomer with a superior tensile strength can cause a dramatic increase in the tensile strengths of a copolymer. Copolymer structure is the major factor in determining the elongation to break as in some of the hydrogels studied (e.g. HEMA-NVP copolymers) ε_b falls with increasing EWC, while in others (e.g. NNDMA polymers with varying amounts of EGDM crosslinking agent) the opposite trend is observed.

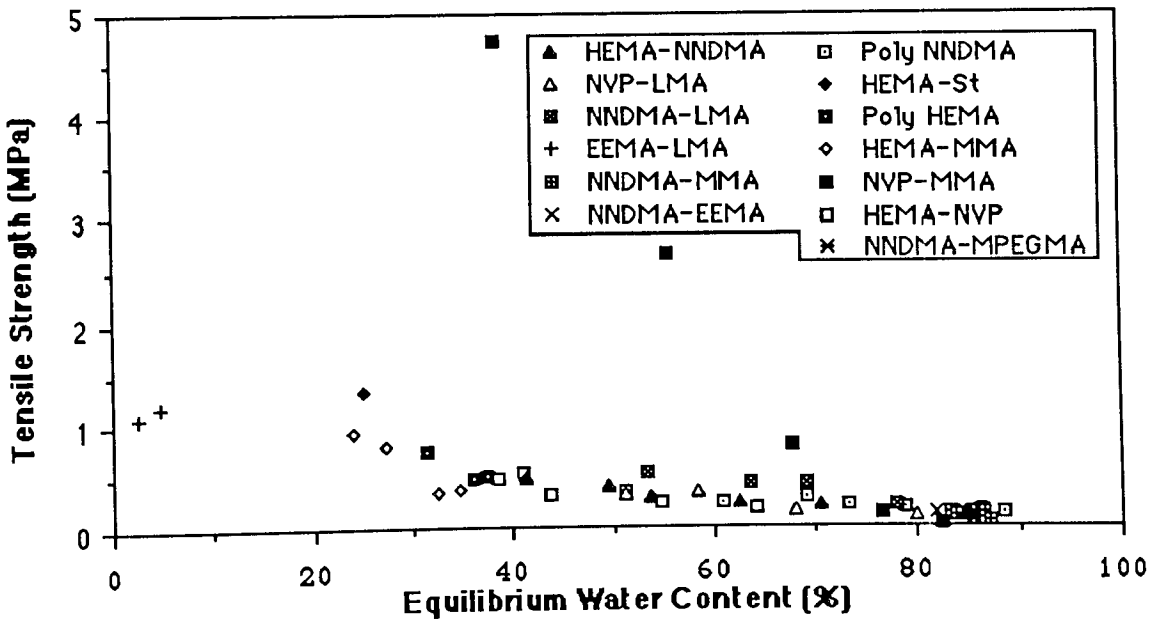

Figure 4.15 **Variation in tensile strength with equilibrium water content for copolymer hydrogels**

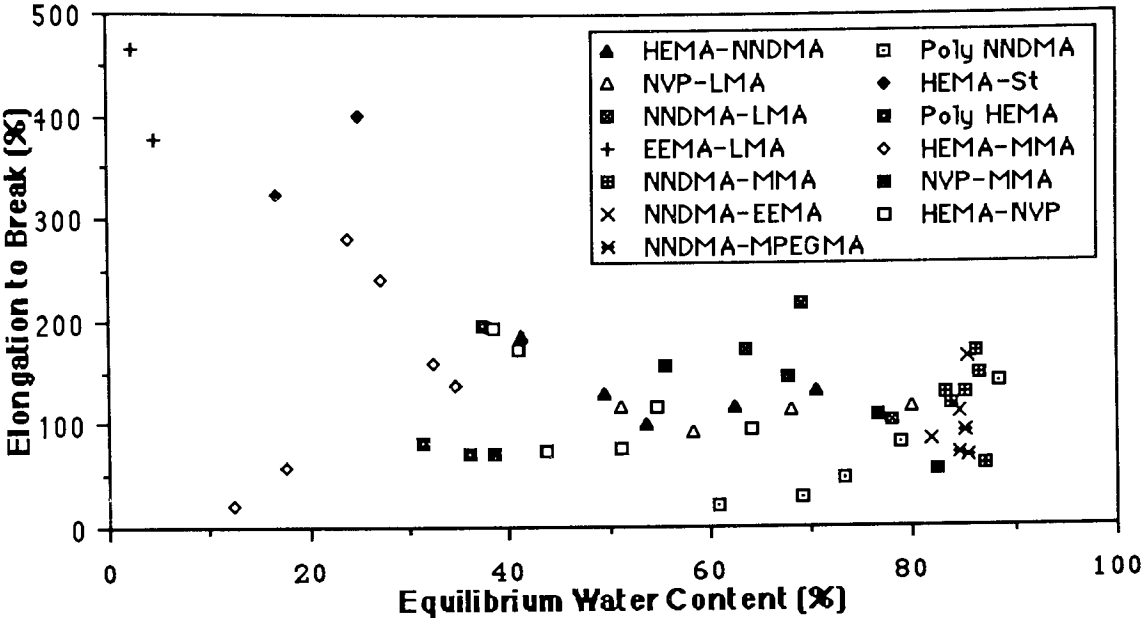

Figure 4.16 Variation in elongation to break with equilibrium water content for copolymer hydrogels

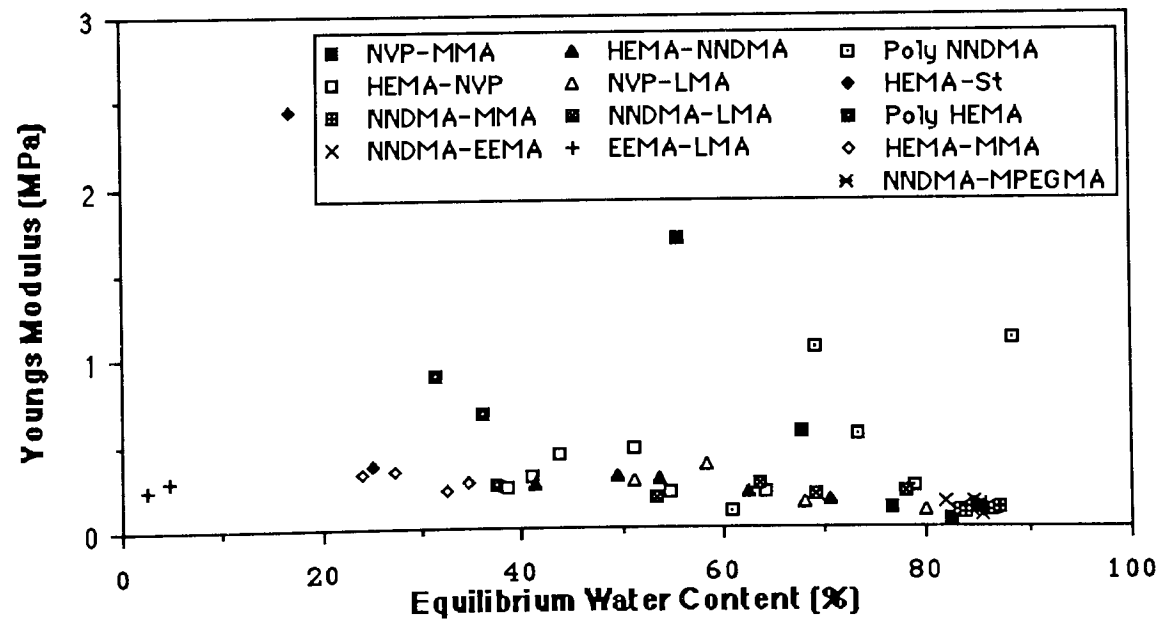

Figure 4.17 Variation in Youngs modulus with equilibrium water content for copolymer hydrogels

The effect of EWC on the Youngs modulus of the copolymer hydrogels is illustrated in Figure 4.16. In general there is a slight increase in E with a decrease in EWC. However, once again copolymer structure overrides the effect of EWC in several systems.

4.4 Conclusions

The mechanical properties of a series of hydrogel copolymers with a range of mechanical properties have been investigated. The values of σ_b, ε_b and E obtained in this work are not, however, absolute values as the measured values are very sensitive to changes in crosshead speed and temperature. As all the values were obtained under the same conditions they provide a useful means of comparing the mechanical properties of these hydrogels. As poly HEMA is, arguably, the most important hydrogel for use in biomedical applications the measured values of σ_b, ε_b and E (0.495 MPa, 198% and 0.250 MPa respectively) have been used as a yardstick throughout this work.

The effect of crosslink density on mechanical properties was investigated for poly HEMA and poly NNDMA. Both σ_b and E increased, while there was a fall in ε_b with an increase in crosslink density. Similar behaviour has been observed previously in poly HEMA and in NVP-butyl acrylate copolymers[170]. Incorporation of increasing amounts of of hydrophobic monomer (e.g. St and MMA) in poly HEMA provides another means of increasing the tensile strength and Youngs modulus of the system to over twenty times that achievable by poly HEMA alone. Styrene or MMA addition also has the effect of "titrating out" the freezing water producing stiff, inflexible polymers with a very low elongation to break. However, although these copolymers (e.g. HEMA-St 70:30) have a low water content they have unusual surface properties, with a high polar component of the surface free energy. This will be discussed in more detail in Chapter 5.

Although high water content hydrogels may be synthesised by the incorporation of the hydrophilic monomers NVP and NNDMA into poly HEMA the mechanical properties of these systems are poor. Additionally, another problem encountered with NNDMA incorporation is chain transfer which leads to a reduction in ε_b and tear strength of the polymers. Copolymerisation of NNDMA with LMA, a monomer with a long, flexible sidechain and a low T_g improves the poor mechanical properties associated with NNDMA. It is interesting to note that a similar effect is seen in HEMA-LMA copolymers[167]. Hydrated poly LMA has a similar σ_b and lower ε_b than poly HEMA, however, incorporation of 30% LMA doubles the ε_b (of poly HEMA), increases σ_b by a factor of ten and E by a factor of thirty. A similar, but less pronounced, synergistic effect is also apparent in the NNDMA-LMA copolymers. Thus, it is possible to synthesise a NNDMA-LMA copolymer with an EWC of 60% but with mechanical properties similar to those of poly HEMA.

Another copolymer system which produces high water content hydrogels with good mechanical properties is based on the monomers NVP and MMA. By varying the molar ratios of the copolymers a wide range of mechanical properties can be obtained (e.g. tensile strengths from 0.05 to 10 times those of poly HEMA). In addition, the interesting water binding behaviour described previously in Section 3.3.2 and its effect on mechanical properties, illustrated in Figures 4.5-4.7, enhances the promising properties of these copolymers. As there is a large disparity in reactivity ratios between NVP and MMA, the copolymers synthesised will have structures similar to those of semi-interpenetrating polymer networks (IPNs) i.e. large blocks of PMMA in poly NVP matrix. IPNs display unusual properties which will be discussed in Chapters 6-8 but they are known to have good mechanical properties. However, it is more by accident than design that several extended wear contact lenses based on this combination of monomers e.g. Duragel have achieved commercial significance. These lenses were not synthesied with a prior knowledge

of the likely properties of this system but have ben used as they are strong for their EWC. The tensile properties of some of these commercial lenses have been previously reported[168]. In this work values of σ_b, ε_b and E for the NVP-MMA 70:30 copolymer (with an EWC approaching 70%) of 0.807 MPa, 145 and 0.557 MPa respectively were obtained, which compare favourably with the values obtained for poly HEMA.

The most important conclusions which can be drawn from this work on a range of hydrogel systems concerns the factors controlling the tensile properties of these materials. It appears that copolymer structure is the major factor controlling the mechanical properties in these systems. Although σ_b, ε_b and E of these copolymers have not been determined in the dehydrated state, it is known that the mechanical properties of HEMA, NVP and NNDMA are poor. Therefore, σ_b and E of the majority of copolymers synthesised are low and the incorporation of increasing amounts of water tends to mask the small differences between them and reduce the values of σ_b and E down to the same level. However, in Figures 4.15 - 4.17 some points lie outside the narrow band which encompasses the expected variation in mechanical properties if the EWC was the only controlling factor. These copolymers include the NVP-MMA and NNDMA-LMA copolymers described earlier and those copolymers which are tough in the dehydrated state. Thus, the HEMA-St and HEMA-MMA copolymers have a high tensile strength and Youngs modulus as σ_b, and E for polystyrene and PMMA are much higher than for poly HEMA. In the some of the HEMA-St and HEMA-MMA copolymers there is little freezing water due to their low EWC. Therefore, in these polymers the mechanical properties in the hydrated and dehydrated states are similar. Previous work in these laboratories on the behaviour of hydrogels under compression has also demonstrated that mechanical properties are not solely related to EWC[39]. Therefore, it can be seen that although the EWC does influence the mechanical properties, copolymer structure and composition is usually the dominant factor.

CHAPTER 5

Surface Properties of Hydrogel Copolymers

5.1 Introduction

As the major use of hydrogels is in the field of biomaterials, hydrogel surfaces are often in intimate contact with body fluids or tissue. Several workers[85,104,106] have suggested that the surface free energy of a polymer is an important parameter in determining the biocompatibility or biotolerance of the material. In this Chapter the measured surface energies of several hydrogel copolymers in both their hydrated and dehydrated states are presented, in an attempt to correlate molecular structure with surface free energy. The experimentally determined results are also compared with values for surface energy derived from predictive techniques based on molecular constitution. The results are presented graphically in this Chapter and are listed in Appendices 3, 4 and 5. However, before presenting the experimental results the theory behind both surface energy measurements, in the hydrated and dehydrated states, and the predictive methods used in this work will be discussed.

5.2 Determination of the Structure of Solid Surfaces from Contact Angles

The first equation to represent the equilibrium which defines the boundary of a liquid in contact with a solid was presented in 1805 by Young[171]. By resolving the forces at the point of contact of a sessile drop and a solid (Figure 5.1) he derived the equation

$$\gamma_{sv} = \gamma_{sl} + \gamma_{lv} \text{ Cos } \theta \qquad (5.1)$$

Some sixty years later Dupre[172] demonstrated that the reversible work of adhesion of a liquid and a solid, Wa, could be expressed

$$Wa = \gamma_s + \gamma_{lv} - \gamma_{sl} \qquad (5.2)$$

Combining equations (5.1) and (5.2) leads to the well known Young - Dupre equation (5.3).

$$Wa = (\gamma_s - \gamma_{sv}) + \gamma_{lv} (1 + \text{Cos } \theta) \qquad (5.3)$$

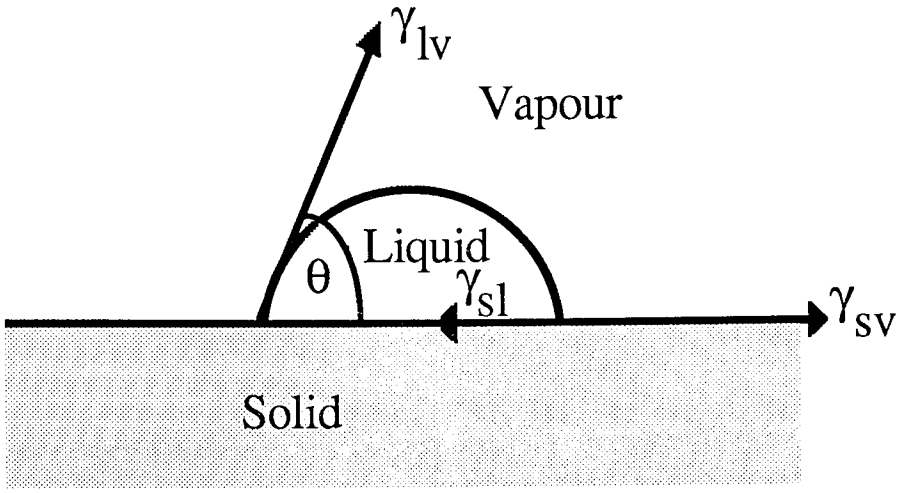

γ_{lv} = liquid - vapour interfacial free energy

γ_{sl} = solid - liquid interfacial free energy

γ_{sv} = solid - vapour interfacial free energy $\approx \gamma_s$ = solid surface free energy

Figure 5.1 Components of solid surface free energy

When the solid surface comes into contact with the saturated vapour of the wetting liquid there will be some adsorption of the liquid onto the surface and the surface free energy of the solid will be reduced. This difference between γ_s (the solid surface free energy) and γ_{sv} (the solid / vapour interfacial free energy) is known as the spreading pressure π_e[173].

$$\pi_e = \gamma_s - \gamma_{sv} \qquad (5.4)$$

However, when the liquid forms a finite contact angle with the solid it has been shown that, for low energy solids, the spreading pressure is negligible[174].

5.3 Critical Surface Tension

In a series of papers on the spreading of liquids on solid surfaces Zisman and his co-workers[175-179] plotted the cosine of the contact angle (θ) of the wetting liquid on the solid, against the surface tension of the wetting liquid. This graph was then extrapolated back to Cos θ = 1 to give the value for the surface tension of a hypothetical liquid which would completely wet the solid surface. This value is called the critical surface tension, γ_c, and in calculating this value it is assumed that $\pi_e = 0$. The value of the critical surface tension will depend, to some extent, on the wetting liquid used. Using non-polar wetting liquids yields the maximum value of γ_c while polar liquids give the minimum γ_c value. It has been suggested that the wetting liquids used to determine critical surface tension be classified into three groups[180]; group one comprising the non-polar solvents (eg the n-alkanes), group two containing the polar liquids (eg esters and halogenated solvents) and group three containing the hydrogen bonding liquids (eg formamide). Using wetting liquids from these groups would give three values of critical surface tension A, B and C.

5.4 Work of Adhesion

For many years the reversible work of adhesion had been expressed in terms of the Dupre equation

$$Wa = \gamma_s + \gamma_{lv} - \gamma_{sl} = 2(\gamma_{lv}\,\gamma_s)^{0.5} \qquad (5.2)$$

However, when polar force interactions across the interface were considered this equation was found to be inadequate and therefore it had to be modified. Good *et. al.*[181-183], using molecular force interaction parameters, developed a molecular theory for the work of adhesion.

$$Wa = 2\Phi_v\Phi_a\,(\gamma_1\gamma_2)^{0.5} \qquad (5.5)$$

γ_1 and γ_2 are the surface tensions of the two pure phases adjacent to the interface (ie for a liquid / solid interface γ_{lv} and γ_s) and Φ_v accounts for the difference in molar volume

between the two phases. However, as the molar volumes of the two phases are usually similar this tends towards unity.

Φ_a may be expressed as

$$\Phi_a = a_{12} / [(a_1 a_2)^{0.5}] \qquad (5.6)$$

a_1, a_2 and a_{12} are molecular attraction constants which may be defined in terms of the equations covering basic molecular interactions (eg London dispersion and Keesom dipole forces). Using the geometric means of the polar and dispersive fractions of the energy density of the adjacent phases Φ_a can be redefined

$$\Phi_a = (d_1 d_2)^{0.5} + (p_1 p_2)^{0.5} \qquad (5.7)$$

where p and d are the polar and dispersive components, respectively, of a. It is, therefore, possible to rewrite equation (5.5)

$$W_a = 2 (\gamma_1 \gamma_2)^{0.5} [(d_1 d_2)^{0.5} + (p_1 p_2)^{0.5}] \qquad (5.8)$$

The dispersion force part W_a^d of the total work of adhesion has been previously defined by Fowkes as

$$W_a d = 2 (\gamma_1 {}^d \gamma_2 {}^d)0.5 \qquad (5.9)$$

Therefore equation (5.8) can be rewritten to correlate the expressions of Good and Fowkes

$$W_a = 2[(\gamma_1 {}^d \gamma_2 {}^d)^{0.5} + (\gamma_1 {}^p \gamma_2 {}^p)^{0.5}] \qquad (5.10)$$

For a liquid-solid interface the work of adhesion will have a polar and dispersive component, this can be expressed as[147,148,186,187]

$$W_a = \gamma_{lv} + \gamma_s - \gamma_{sl} = 2[(\gamma_{lv} {}^d \gamma_s {}^d)^{0.5} + (\gamma_{lv} {}^p \gamma_s {}^p)^{0.5}] \qquad (5.11)$$

This equation can be combined with the Young equation (5.1) to give the expression

$$1 + \cos\theta = (2 / \gamma_{lv})[(\gamma_{lv} {}^d \gamma_s {}^d)^{0.5} + (\gamma_{lv} {}^p \gamma_s {}^p)^{0.5}] \qquad (5.12)$$

This expression is often referred to as the Owens and Wendt equation[148] and it may be used to determine the surface free energies of polymers in the dehydrated state. Two wetting

liquids which have been fully characterised for polar and dispersive components are used. By measuring the contact angles of the liquids on the polymer surface and solving the equations simultaneously, γ_s^p and γ_s^d, the polar and dispersive components of the surface free energy of the polymer may be determined. Several liquids have been characterised into polar and dispersive components and these are shown in Table 5.1[148,186,187]. The two most widely used wetting liquids are water and diiodomethane (methylene iodide) because of their high total surface free energies and their balance of polar and dispersive forces.

Table 5.1 **Polar and dispersive components of some wetting liquids commonly used for contact angle studies**

Liquid	γd mN/m	γp mN/m	γt mN/m
Water	21.8	51.0	72.8
Glycerol	37.0	26.4	63.4
Formamide	39.5	18.7	58.2
Diiodomethane	48.5	2.3	50.8
n-Hexadecane	27.6	0.0	27.6
n-Octane	21.8	0.0	21.8

5.5 Hydrated Surfaces

When attempting to measure contact angles on hydrated polymers in air two major problems are encountered. The first, is that there is no efficient and reproducible method to remove the surface water from the sample and the second is the dehydration of the polymer surface. Two techniques (Hamiltons method[147,188] and the captive air bubble technique[34,189]) have been developed to overcome these problems, which arise when trying to measure contact angles on hydrated polymers in air, as they enable the surface energy of the

hydrogel to be measured in the fully hydrated state.

5.5.1 Hamiltons Method

A technique to characterise hydrated solid surfaces has been developed by Hamilton[147,188]. By measuring the contact angles of small n-octane droplets on solid surfaces under water and assuming that the effect of gravity is negligible for such droplets, the polar component of the surface free energy may be determined (Fig. 5.2).

An equation for the work of adhesion at a solid liquid interface was developed by Fowkes[190] assuming that there was no polar interaction across the interface.

$$\gamma_{sl} = \gamma_s + \gamma_{lv} - 2(\gamma_{lv}{}^d\gamma_s{}^d)0.5 \qquad (5.13)$$

Although this equation contains a term $[2(\gamma_{lv}{}^d\gamma_s{}^d)0.5]$ which accounts for the stabilisation from dispersion forces, there is no term to account for stabilisation by non-dispersion forces (eg dipole interactions and hydrogen bonding). A modified form of this expression was developed by Tamai *et al* [191] which accounted for stabilisation by polar forces

$$\gamma_{sl} = \gamma_s + \gamma_{lv} - 2(\gamma_{lv}{}^d\gamma_s{}^d)0.5 - I_{sl} \qquad (5.14)$$

where

$$I_{sl} = 2(\gamma_{lv}{}^p\gamma_s{}^p)0.5 \qquad (5.15)$$

As n-octane has no polar component and the dispersive components for n-octane and water ($\gamma_{lv}{}^d$) are identical, combining equations (5.1) and (5.14) (and using the subscripts o for n-octane and w for water) leads to the following expression for I_{sw}, the polar stabilisation energy between water and the solid.

$$I_{sw} = \gamma_{w'v} - \gamma_{ov} - \gamma_{ow}.\text{Cos}\ \theta \qquad (5.16)$$

$\gamma_{w'v}$ is the surface tension of n-octane saturated water and as γ_{ov} and γ_{ow} can be determined experimentally, solving the equation enables I_{sw} to be determined. Therefore, γ_s, the polar component of the surface free energy may be calculated from equation (5.15).

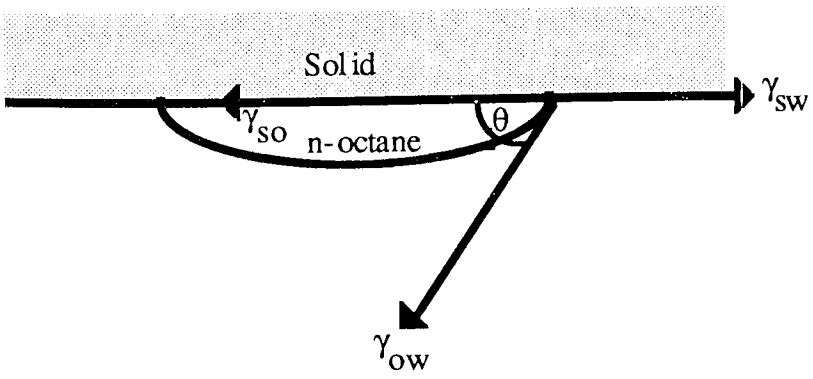

γ_{sw} = solid - water interfacial free energy

γ_{so} = solid - octane interfacial free energy

γ_{ow}= octane - water interfacial free energy

Figure 5.2 Components of surface free energy for Hamiltons method

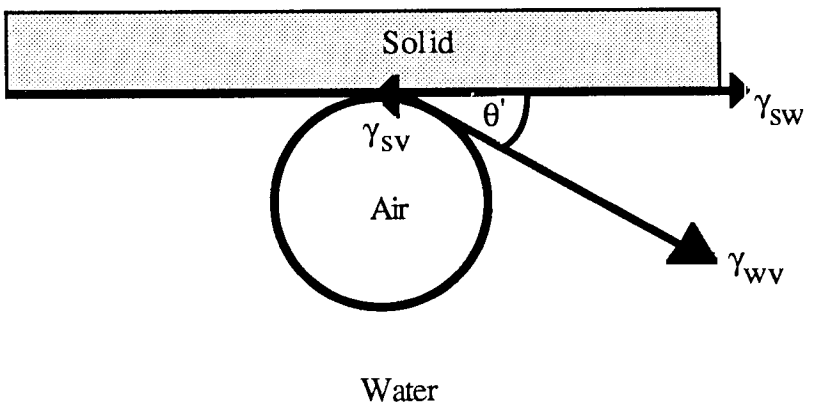

γ_{sw} = solid - water interfacial free energy

γ_{wv}= water - vapour interfacial free energy (ie surface tension of water)

γ_{sv} = solid - vapour interfacial free energy $\approx \gamma_S$ = solid surface free energy

Figure 5.3 Components of surface free energy for captive air bubble technique

Hamilton initially assigned the value of 51.6 mN/m to $\gamma_{w'v}$, the surface tension of n-octane saturated water. However, as the solubility of n-octane in water is negligible <1ppm, it has been suggested[192-194] that the value should be close to that of pure water, 72.8mN/m. A calibration curve has been constructed (Figure 5.4) showing the relationship between Hamilton contact angle and the polar component of the surface free energy; it can be seen that as the contact angle becomes larger (i.e. moves toward 180°), γ_s^p also increases.

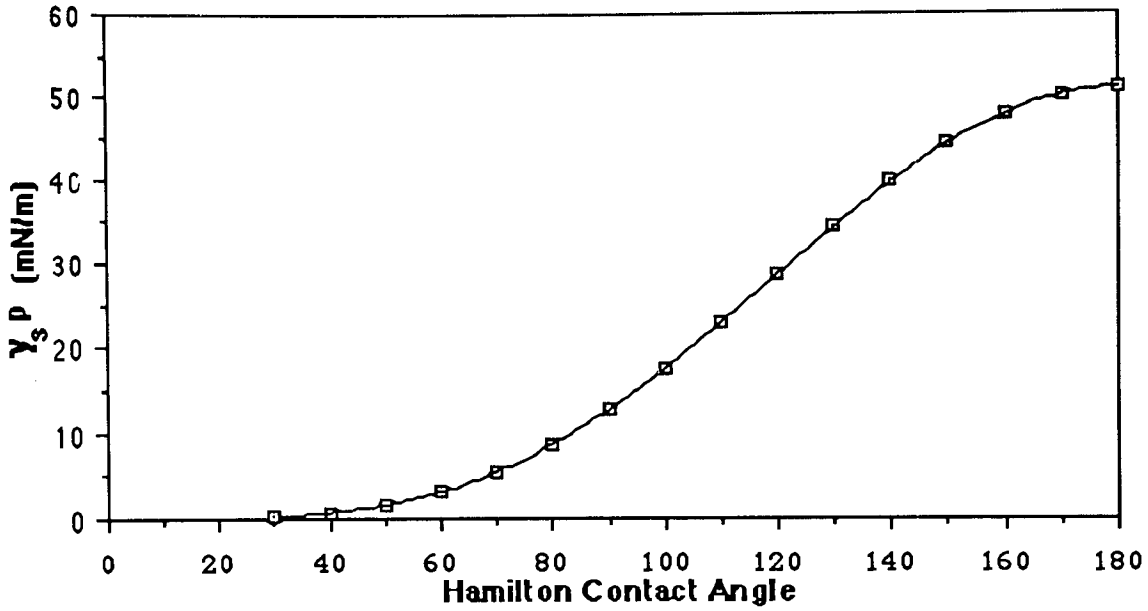

Figure 5.4 Relationship between Hamilton contact angle and the polar component of surface free energy

5.5.2 Captive Air Bubble Technique[34,189]

Andrade *et. al.*[35] have shown that by using data obtained from both the Hamilton and captive air bubble techniques it is possible to obtain values for γ_{sv}, γ_{sv}^p, γ_{sv}^d and γ_{sw} for the hydrogel water interface. Applying Youngs equation to the situation, with water as the liquid phase gives:

$$\gamma_{sv} - \gamma_{sw} = \gamma_{wv}\text{Cos}\theta' \qquad (5.17)$$

As γ_{wv} is known (72.8 mN/m) and θ' is the captive air bubble contact angle the adhesion tension ($\gamma_{sv} - \gamma_{sw}$) can be elucidated. An equation for the polar stabilisation parameter (I_{sw}) has previously been derived (5.16).

$$I_{sw} = \gamma_{wv} - \gamma_{ov} - \gamma_{ow}.\text{Cos}\,\theta' \qquad (5.16)$$

As γ_{wv} = 72.8 mN/m, γ_{ov} = 21.8 mN/m and γ_{ow} = 51.0 mN/m this equation can be rewritten

$$I_{sw} = 51.0\,(1 - \text{Cos}\,\theta') \qquad (5.18)$$

Therefore, I_{sw} can also be calculated. Combining equations (5.14) and (5.17) gives

$$(\gamma_{sv} - \gamma_{sw}) = 2(\gamma_{wv}^{d}\gamma_{sv}^{d})0.5 + I_{sw} - \gamma_{wv} \qquad (5.19)$$

This equation may be rearranged to give an expression for the dispersive component (γ_{sv}^{d}) of the hydrogel

$$\gamma_{sv}^{d} = \left[\{(\gamma_{sv} - \gamma_{sw}) - I_{sw} + \gamma_{wv}\} / 2\,(\gamma_{wv}^{d})0.5\right]^2 \qquad (5.20)$$

γ_{sv}^{p} can also be derived be rearranging equation (5.15) to give

$$\gamma_{sv}^{p} = I_{sw}^{2} / (4\gamma_{wv}^{p}) \qquad (5.21)$$

($\gamma_{sv} - \gamma_{sw}$), I_{sw}, γ_{sv}^{d}, γ_{sv}^{p}, γ_{sv}, and γ_{sw} were calculated using Makintosh Works™ and the results for all the hydrogels studied are listed in Appendix 5.

An alternative method of calculating the dispersive component of the surface free energy of hydrated gels based on the Owens and Wendt equation (5.12) was also used in this work. After calculating the polar component using Hamiltons method (Section 5.5.1) the insertion of this value, together with the measured water / air contact angle, into the Owens and Wendt equation enables the dispersive component to be calculated. The results obtained for the dispersive components of the surface free energy from both these methods agree to within 0.2 mN/m and the trends shown by both methods are identical. The values presented graphically in this Chapter are based on calculations using the Owens and Wendt equation

but both sets of results are listed in Appendices 4 and 5.

5.6 Predictive Techniques-Dehydrated Surfaces

The correlation of the structure of polymers with their chemical and physical properties is one of the important aspects of polymer science. The determination of surface properties, by the measurement of surface free energies, for example, is often difficult and tedious. However, the surface properties of hydrogels are of utmost importance because of their use in biomedical applications. Therefore, if surface properties could be predicted from polymer structure it would assist in the selection of materials for specific applications. In this work two predictive techniques, the parachor and cohesive energy density, have been used to estimate the surface free energies of the dehydrated polymers studied and these values have been compared with experimentally determined values.

5.6.1 Parachor

A relationship between the surface free energy of a liquid and its density was derived by Macleod[195] in 1923

$$\gamma = C(D-d)^4 \qquad (5.22)$$

where D and d are the densities of the liquid and its vapour and C is a constant, characteristic of the liquid. This expression was revised by Sugden[196] who expressed the constant in molar proportions and called it the parachor. Sugdens revised form of the equation has the following form

$$\gamma = [P(D-d)/M]^4 \qquad (5.23)$$

where M is the molecular weight and P is the parachor. When the vapour density is small in relation to the density of the liquid this equation becomes

$$\gamma = [PD/M]^4 \qquad (5.24)$$

or

$$\gamma = [P/V_m]^4 \qquad (5.25)$$

where V_m is the molar volume of the liquid.

This equation has been modified for application to copolymers by Rastogi and St. Pierre[197]

$$\gamma_{co} = x_1[P_1D_1 / M_1]^4 + x_2[P_2D_2 / M_2]^4 \qquad (5.26)$$

where x_i is the mole fraction of component i and γ_{co} the surface free energy of the copolymer. This equation assumes that there is a gradual transition in surface properties with incorporation of the comonomer. However, this is not always the case and in this work the following equation has also been used to calculate parachor predicted values of surface free energy

$$\gamma_{co} = [(x_1P_1 + x_2P_2)^4 + (x_1D_1 + x_2D_2)^4] / (x_1M_1 + x_2M_2)^4 \qquad (5.27)$$

This equation takes into account surface excess behaviour which may occur when there is a large disparity between the surface energies of the two homopolymers.

Atomic constants were calculated, assuming that the parachor was an additive function. Therefore, for organic compounds the most important value is the value for the methylene unit (CH_2). The first value proposed for the parachor of the methylene unit, by Sugden, was 39. This value was derived from examination of the surface free energies of several homologous series. Values for double bonds, rings and other constitutive features were then assigned on the basis that the parachor was additive. However, after examining anomalies in the parachors of fatty acids, reported by Hunten and Maass[198], Mumford and Phillips[199] concluded that the incorrect value had been assigned to the methylene unit. They assigned a mean value of 40 to the methylene unit after realising that Sugden had failed to take into account chain branching and isomers and also proposed assigning values to branches present in the the molecule to allow for the "strain" introduced. Quayle[200] has produced an extensive review of parachor values, assigned to constituent parts of various molecules and produced a table of values for a large number of elemental units. These

values have been used in this work.

5.6.2 Cohesive Energy Density

The cohesive energy density (δ^2) has been defined as[201]

$$\delta^2 = - (u / v) \qquad (5.28)$$

where u is the molar internal energy and v is the molar volume. A more useful definition is

$$\delta^2 = (\Delta H_{vap} - RT) / v \qquad (5.29)$$

An equation connecting surface free energy with molar volume and cohesive energy density was produced by Hildebrand and Scott[201]

$$\delta^2 = k^2 (\gamma / v^{0.33})^{0.86} \qquad (5.30)$$

where k is a constant, dependent on temperature. Although this is fairly accurate for non-polar liquids, when applied to polar liquids and polymers the limitations of the equation are revealed. A review of this work by Wu[202], with respect to polymers, found that the relationship between molar volume and cross sectional area were not as simple as supposed due to their chainlike properties. He replaced the molar cross sectional area by a term called the effective molar cross sectional area given by

$$A = kN^{0.5} n_s (V_m / n_s)^{0.33} \qquad (5.31)$$

where n_s is the number of atoms in a segment, V_m is the molar volume of a segment, N is Avagadros number and k is a parameter determined by the structure and the packing geometry of the polymer molecule. This equation assumes that each polymer molecule can be thought of a series of equivalent spheres, each sphere being an interacting unit of volume V_m / n_s. Wu's final equation arrived at by considering only dispersive contributions is

$$\gamma = 0.327 \left[(\Sigma F)_s / n_s\right]^{1.85} \left[n_s / v_s\right]^{1.52} \qquad (5.32)$$

where n_s is the number of atoms, $(\Sigma F)_s$ is the summation of the Smalls[203] force constants for the segments and v_s is the molar volume of the repeat unit.

The appropriate parameters for use in both the parachor based and cohesive energy density based calculations of surface free energy are presented in Table 5.2.

5.7 Predictive Techniques-Hydrated Surfaces

As the measurement of hydrated surface free energies is often difficult in this work two techniques have been used to predict values for γ^t in the hydrated state. The first technique is not totally theoretical but is dependent on the knowledge of an accurate value for the polar and dispersive components of surface free energy for the dehydrated polymer and its EWC. The hydrated copolymer is considered to have only two phases polymer and water and the surface energy is assumed to be an additive function of the volume fraction of these two components. Therefore, in a polymer with a 40% volume fraction of water, for example, the hydrated surface free energy is considered to be 60% of γ^p and γ^d for the polymer plus 40% of γ^p and γ^d for water. As this technique is dependent on the knowledge of the EWC of the polymer it has been referred to throughout this work as the water content predictive technique.

The second predictive method is dependent on the parachor predicted surface energies (Section 5.6.2) and a knowledge of the water binding states in the polymer as determined by differential scanning calorimetry (Chapter 3). With this method the water in the polymer is classified into two types, as described previously, freezing and non-freezing water (i.e water which interacts strongly with the polymer chains). A knowledge of these values enables the number of moles of water "bound" to each mole of repeat unit to be calculated and this combination of polymer and water can be considered as the new repeat unit. A parachor value is then assigned to this repeat unit and its density and molecular mass are calculated. The hydrated surface energy of a hydrophilic polymer can then be determined by summing the contribution form this new repeat unit and the contribution from freezing

Monomer	Molecular Weight (gm/mole)	Density (gm/cm^3)	Parachor	ΣF	No of Atoms in Repeat Unit (n_s)
Hydroxyethyl Methacrylate	130	1.28	270.7	1000	19
Hydroxypropyl Methacrylate	144	1.24	310.7	1109	22
Hydroxyethyl Acrylate	116	1.36	234.4	907	16
Hydroxypropyl Acrylate	130	1.24	274.4	1016	19
Methyl Methacrylate	100	1.19	216.4	778	15
Lauryl Methacrylate	254	1.02	656.4	2241	48
Styrene	104	1.07	245.4	896	16
N-Vinyl Pyrrolidone	111	1.21	245.3	910	17
N'N' Dimethyl Acrylamide	99	1.16	230.2	829	16

Table 5.2 **Parameters used for the prediction of surface free energy using both the parachor and cohesive energy density methods**

water. This predictive method was also extended to both hydrophilic-hydrophobic and hydrophilic-hydrophilic copolymers. In the hydrophilic-hydrophobic copolymers it was assumed that water was only associated with the hydrophilic segments of the copolymer, while in the hydrophilic-hydrophilic copolymers it was assumed that the water binding ability of the two polymers was identical. As this is obviously not the case some discrepancies might be expected in the predicted values for hydrophilic-hydrophilic copolymers. Another problem encountered in using a parachor based technique for hydrated polymers is in determining a value for the parachor of water. As the majority of tabulated parachor values have been calculated from covalently bonded liquids, no provision has been made for the unusual properties of water. Barnes[204] has previously suggested values of 39.8 and 25.5 for the parachor of water but in this work a value of 54.2 has been utilised.

5.8 Results and Discussion

5.8.1 Surface Properties of Dehydrated Polymers

Before detailed discussion of individual copolymer series some general observations can be made. The first point of interest is that the total surface energies of the copolymers studied are not dissimilar from those of conventional vinyl and acrylic polymers, such as polystyrene and poly methyl methacrylate, all falling in the range 42 - 51 mN/m. A marked difference does arise, however, when polar and dispersive components are taken into account, since there is a large disparity between the two groups of materials. Even within the copolymers studied here there is a wide variation in the polar and dispersive fractions of the surface free energy. Thus, in poly HEMA the polar fraction of the surface free energy is 0.43, whereas, in the NVP-MMA 50:50 copolymer it is 0.1. The measured surface energies will be a function of both the interactions within the bulk polymer and at the surface. In amphiphilic copolymers such as poly HEMA, for example, the orientation of the surface groups may be dependent on the polarity of the adjacent phase which will cause variations

in the measured surface free energy.

The surface energies of the HEMA-MMA copolymers, illustrated in Figure 5.5, show a gradual transition moving from the MMA-HEMA 50:50 copolymer to poly HEMA. Although the total surface free energy of the copolymer increases with increasing incorporation of poly HEMA, the most dramatic change is seen in the polar and dispersive fractions of the surface free energy. Thus, the polar fraction increases from 0.20 for the MMA-HEMA 50:50 copolymer to 0.43 for poly HEMA.

The parachor predicted values of surface free energy are in excellent agreement with the experimentally determined values in this system. However, the predicted values obtained using the C.E.D. show large variations from the measured values. This disparity between C.E.D. predicted surface energy and measured surface energy is not unexpected as the

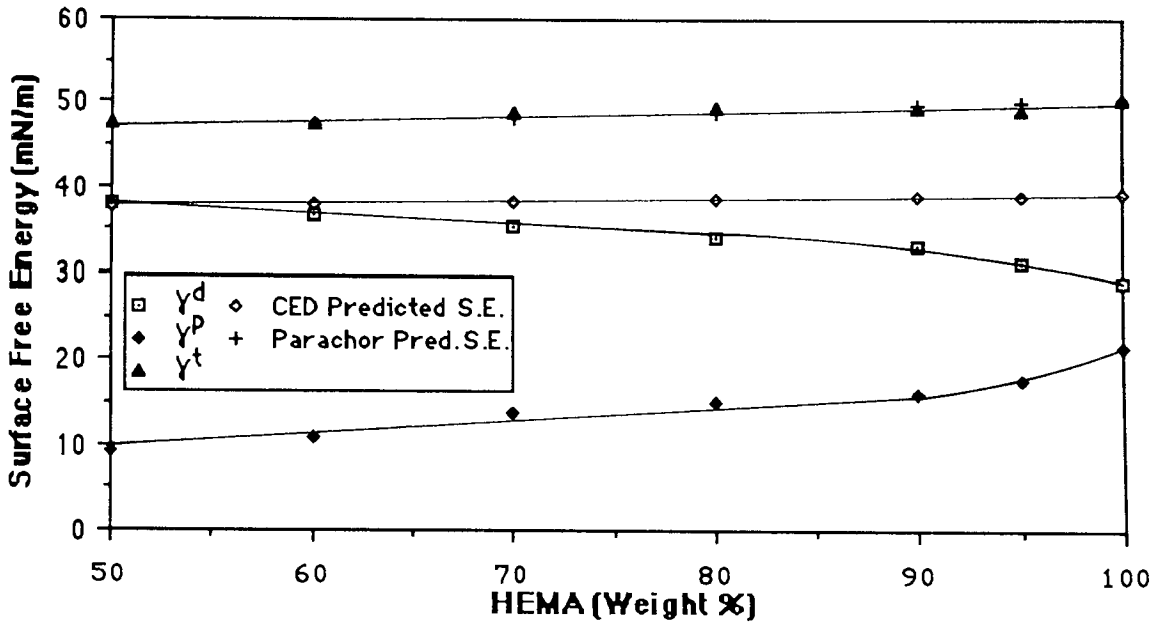

Figure 5.5 **Effect of composition on the measured (γ^t, γ^p and γ^d) and predicted surface free energy of dehydrated HEMA-MMA copolymers**

measured surface energy values show that there is a large polar contribution to the surface energy in these HEMA copolymers. The C.E.D. predicted values do approximate to the dispersive component of the total surface free energy at low levels of HEMA incorporation but there is increasing deviation as the amount of HEMA in the copolymer increases.

The effect of structural variation on the surface free energy of copolymers of styrene with hydroxyalkyl acrylates and methacrylates is illustrated in Figures 5.6 and 5.7 in which γ^t, γ^p and γ^d are plotted as a function of composition. The total surface free energy of all the copolymers increases in moving from styrene to the hydroxyalkyl acrylate or methacrylate (Figure 5.6). With the St-hydroxyalkyl methacrylate copolymers there is a gradual change in surface energy throughout the composition range. However, with the hydroxyalkyl acrylate copolymers there is a dramatic increase at low levels of hydroxyalkyl acrylate incorporation, this effect being more marked in the St-HPA copolymers. The total surface free energy of the copolymers with styrene decreases in the order HPA>HEA>HEMA>HPMA while γ^p decreases in the order HEA>HPA>HEMA>HPMA (Figure 5.7). The hydroxyalkyl acrylates are, therefore, more polar than the hydroxyalkyl methacrylates as the sterically hindering α-methyl group on the backbone restricts chain rotation, in the hydroxyalkyl methacrylates and reduces polar group expression at the polymer surface. The α-methyl group also influences the water binding properties of these polymers, and this effect has been discussed previously[145]. The dispersive component of all the copolymers falls dramatically with the incorporation of even 10% of hydroxyalkyl acrylate or hydroxyalkyl methacrylate into styrene and then continues falling gradually moving towards the hydroxyalkyl acrylate or methacrylate homopolymer.

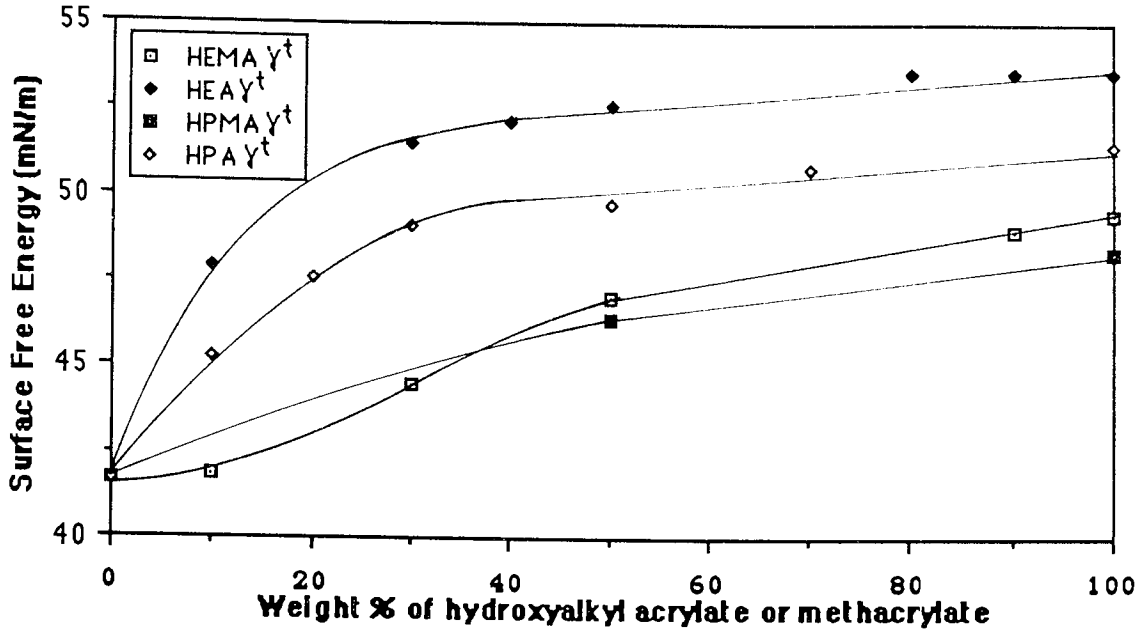

Figure 5.6 Effect of composition on the surface free energy of styrene hydroxyalkyl acrylate and styrene-hydroxyalkyl methacrylate copolymers

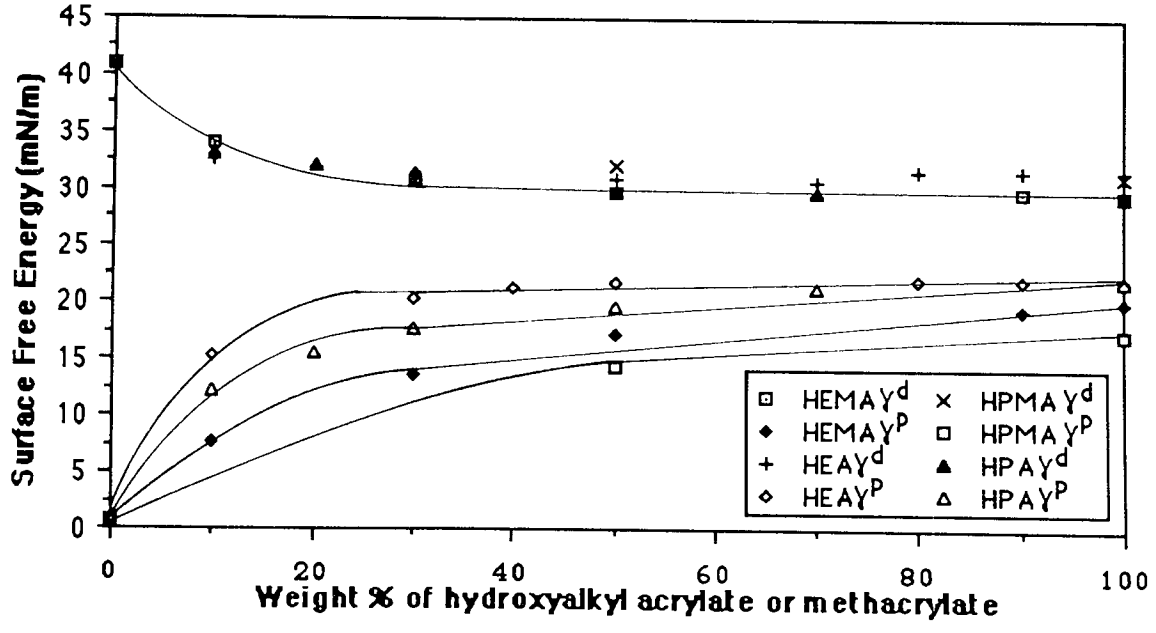

Figure 5.7 Effect of composition on the polar and dispersive components of surface free energy of styrene-hydroxyalkyl acrylate and styrene-hydroxyalkyl methacrylate copolymers

The parachor predicted surface free energies are in excellent agreement with the experimentally determined values in the HEMA-St copolymer series. However, in the hydroxyalkyl acrylate-St copolymers the parachor predicts a steady change in properties between the two homopolymers, in contrast to the behaviour described above. The C.E.D. predicted surface free energy gives a poor approximation to both γ^t and γ^d in these systems.

Although good agreement between predicted and measured surface free energies is found in the hydrophilic-hydrophobic HEMA copolymers studied, the same is not true in the hydrophilic-hydrophilic HEMA copolymers. The effect of composition on the surface energies of the the two hydrophilic-hydrophilic copolymer systems studied is shown in Figures 5.8 and 5.9. Incorporation of even 5% of NVP into HEMA reduces the polar component of the copolymer to a level below that of both poly HEMA and poly NVP (Figure 5.8).

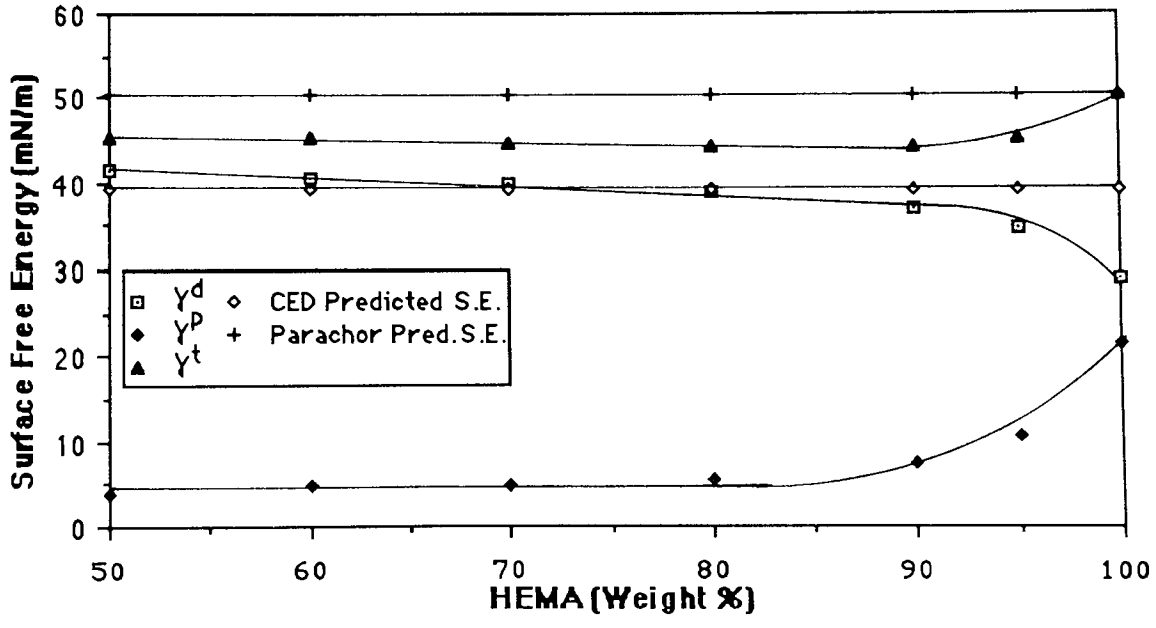

Figure 5.8 **Effect of composition on the measured (γ^t, γ^p and γ^d) and predicted surface free energy of dehydrated HEMA-NVP copolymers**

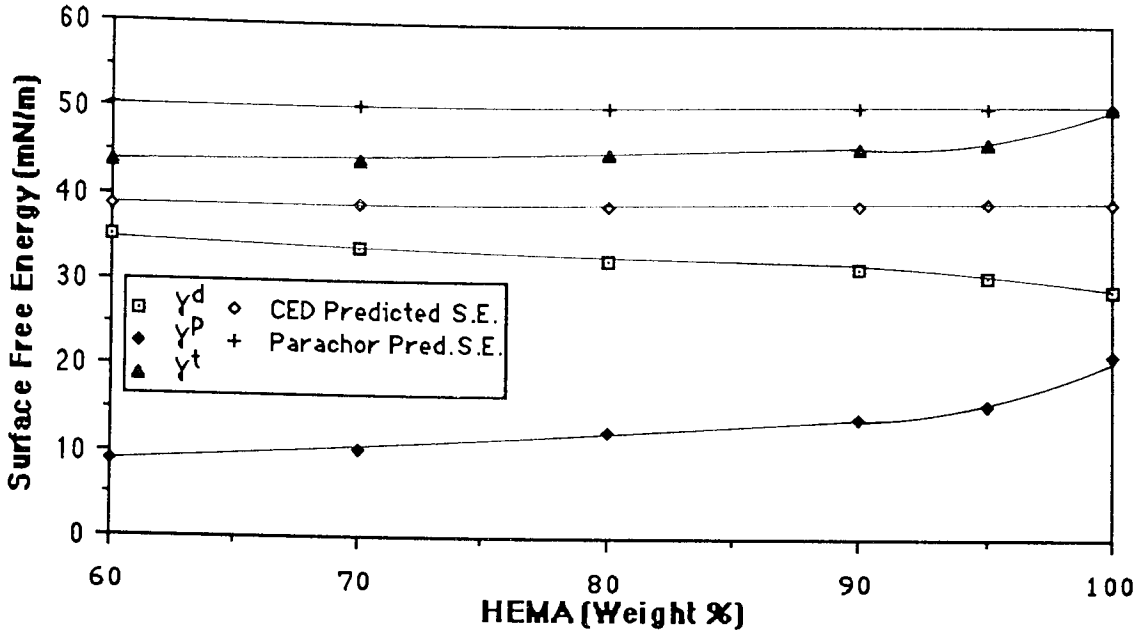

Figure 5.9 **Effect of composition on the measured (γ^t, γ^p and γ^d) and predicted surface free energy of dehydrated HEMA-NNDMA copolymers**

Incorporation of further NVP causes a steady reduction in the polar component until, in the HEMA-NVP 50:50 copolymer, it comprises only 8% of the total surface free energy. Therefore, the polar component must pass through a minimum before increasing at higher levels of NVP incorporation until it reaches the value for poly NVP. A minimum is also observed in the total surface free energy and this minimum is caused by the same phenomenon that produces a reduction in polar component in these copolymers. A molecular complex is formed and the orientation of the polymers in the complex leads to the more hydrophobic sites in the molecules being expressed at the surface. Thus, complex formation cause the specific orientation of polar groups within the bulk of the polymer and therefore, the surface is rendered less polar. This is shown by the increase in the dispersive component, while the polar component is falling in these copolymers. After further NVP incorporation the packing in the system will change and more polar groups will be

expressed at the polymer surface. The surface will then become more polar until the polar component of poly NVP (12.6 mN/m) is achieved.

The parachor predicted values of the surface free energy are higher than the measured values and although this technique also predicts little variation in γ^t, it cannot account for the dipole-dipole interactions and steric occlusion which cause the minima observed in this system. The C.E.D. predicted values are once again in better agreement with the dispersive component of the surface free energy.

The HEMA-NNDMA copolymers display similar behaviour to that observed in the HEMA-NVP system, with NNDMA incorporation causing a fall in both γ^p and γ^t (Figure 5.9). The polar component of the surface energy in the copolymer falls to a level below that of either of the homopolymers and it is obvious that the γ^t must also pass through a minimum, as γ^t for poly NNDMA is 50.7 mN/m while for the 60:40 HEMA-NNDMA copolymer the value is 43.8 mN/m. These results suggest that an intramolecular complex is also formed in this system, which causes orientation of the polymers and reduces polar group expression at the polymer surface. The parachor predicts little change in surface properties in the composition range studied and obviously cannot cope with the polymer-polymer interactions in systems of this type.

Poly NNDMA has a similar total surface free energy to poly HEMA, however, the polar contribution to the surface energy is much less in this nitrogen containing monomer. This reflects the greater polarity of the hydroxyl group in poly HEMA. Incorporation of hydrophobic EGDM crosslinking agent (Figure 5.10) causes a reduction in both γ^p and γ^t.The behaviour of this system is unusual in that the reduction in polar component is accompanied by a reduction in the dispersive component of the surface free energy. This

behaviour is anomalous and unlike that found in poly HEMA, where increasing the crosslinker concentration causes a decrease in the polar component but an increase in the dispersive component of the surface free energy.

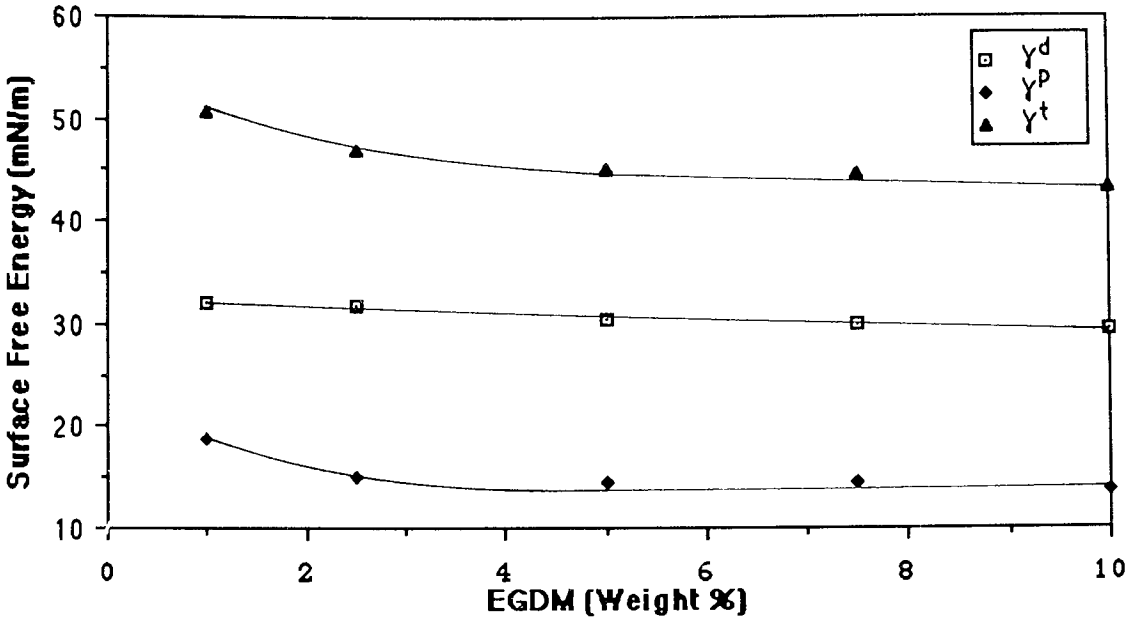

Figure 5.10 Effect of EGDM incorporation on the measured surface free energy of dehydrated poly NNDMA

Copolymerisation of poly NNDMA with the hydrophobic monomers LMA and MMA (Figures 5.11 and 5.12 respectively) gives rise to systems which conform to the expected patterns of behaviour. As the amount of hydrophobic monomer in the system is increased both γ^p and γ^t fall with the γ^d increasing. It is apparent from these results that MMA incorporation has a more pronounced effect on surface properties (i.e. is more hydrophobic) than LMA. It is, therefore, surprising that greater hydrophobicity of the NNDMA-MMA copolymers in the dehydrated state does not manifest itself, for example in terms of EWC, when the polymers are hydrated.

In both systems the the C.E.D. predicted surface free energies correspond more closely to γ^d with good agreement being observed in copolymers containing a higher concentration of

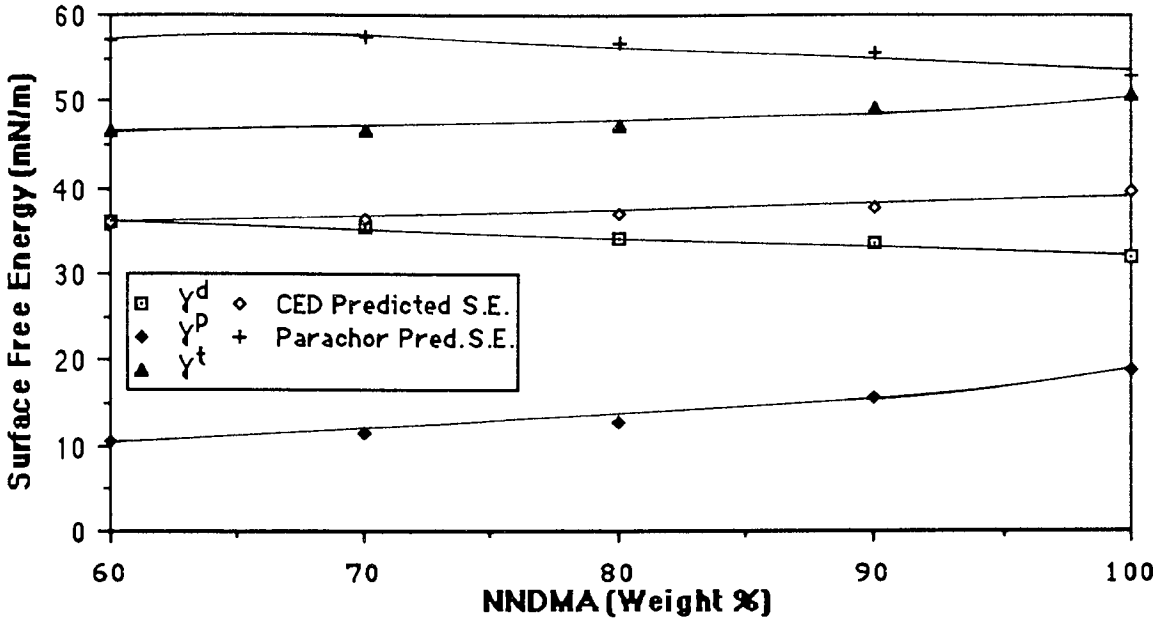

Figure 5.11 Effect of composition on the measured (γ^t, γ^p and γ^d)and predicted surface free energy of dehydrated NNDMA-LMA copolymers

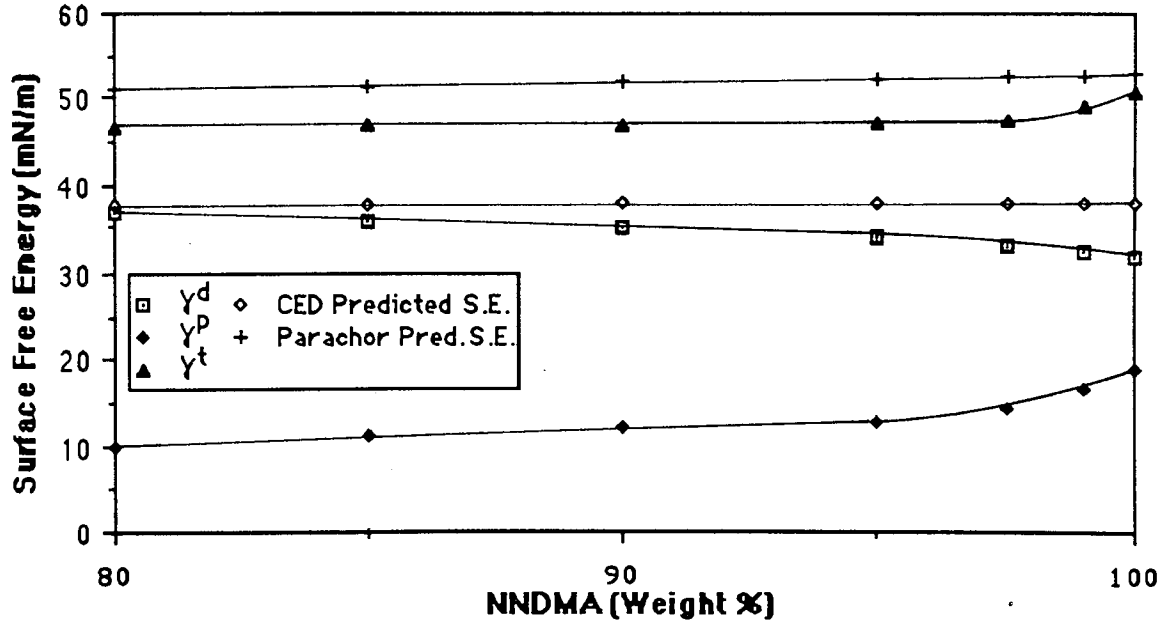

Figure 5.12 Effect of composition on the measured (γ^t, γ^p and γ^d) and predicted surface free energy of dehydrated NNDMA-MMA copolymers

hydrophobic monomer in both systems. Moving towards poly NNDMA the C.E.D. technique predicts consistently higher values for γ^d than are measured experimentally and an increase in γ^d, rather than the decrease which is observed. This difference between predicted and observed behaviour can be explained by the increased contribution of polar forces to the surface free energy when large amounts of NNDMA are present in the copolymer. For the NNDMA-MMA system the parachor technique predicts the correct trend, a decrease in the total surface free energy. However, the parachor predicted values are higher than the measured values and the extent of the decrease is larger than predicted. In the NNDMA-LMA system although the surface energies obtained using the equation of Rastogi and St. Pierre (Eqn 5.26) predict a fall in the surface energy, those calculated from the equation allowing for surface excess behaviour (Eqn. 5.27) predict a maximum. This is caused, in part, by the large disparities in both the parachors and molecular weights of poly NNDMA and poly LMA. A further reason which may explain any discrepancies in the predicted surface energies of copolymers containing LMA is the difficulty of obtaining an accurate value for the density of poly LMA. This is due to the low T_g of the polymer which causes particular difficulties in measuring the density of the polymer using a density gradient column.

Poly NVP also has a similar total surface energy to both poly NNDMA and poly HEMA but the polar component of the surface energy of poly NVP is much lower. Previously, to explain the unusual water binding properties of poly NVP, it has been postulated that the lactam rings in poly NVP pack in a helical arrangement (Section 3.3.2). The low polar component of the surface free energy could also be explained by helical packing as the hydrophobic CH_2 groups on the lactam ring are at the surface of the helix, while the polar groups in the centre of the helix are shielded.

Copolymerisation of NVP with both LMA and MMA (Figures 5.13 and 5.14 respectively) produces copolymers with similar surface behaviour to that observed in the NNDMA-LMA and NNDMA-MMA systems. Increasing the amount of LMA or MMA in the copolymer causes a reduction in the polar component and increases the dispersive component of the surface free energy. While the total surface energy of the NVP-LMA copolymers falls with increasing LMA incorporation, in the NVP-MMA system it remains almost constant at a level just below that of poly MMA. Once again the C.E.D. predicted surface energy is in better agreement with γ^d than γ^t. The parachor predicted surface energies are higher than the measured values in both systems. However, although the values for the NVP-MMA system are a reasonable estimate of the surface energy, in the NVP-LMA system the parachor predicted values show the opposite trend to that observed experimentally and in some cases, are over 10 mN/m too high.

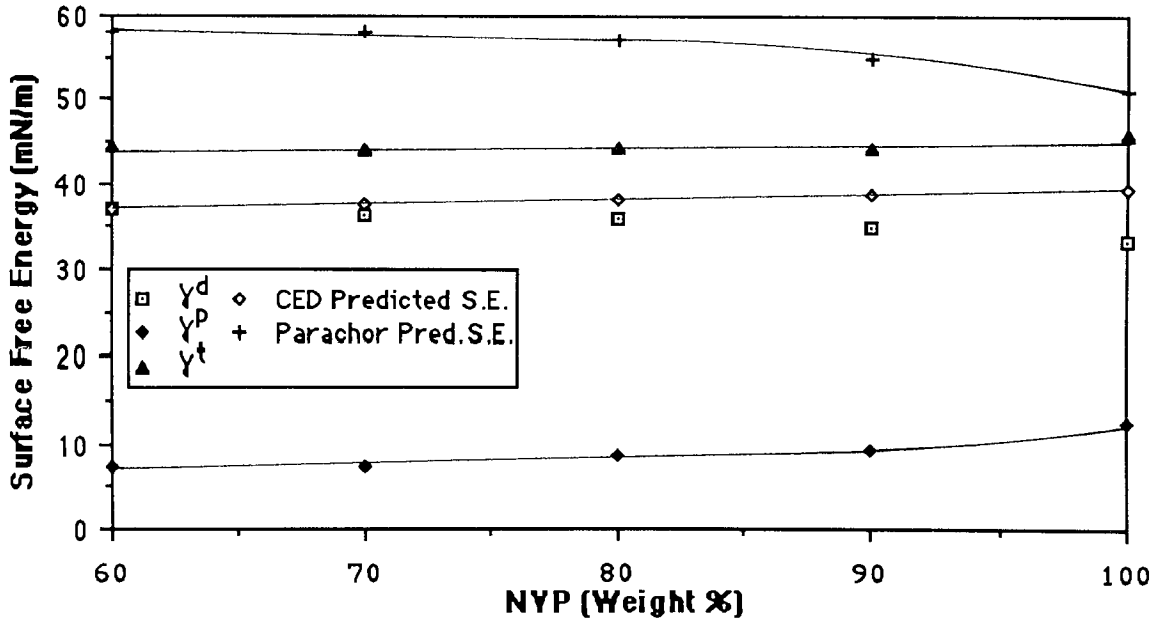

Figure 5.13 Effect of composition on the measured (γ^t, γ^p and γ^d)and predicted surface free energy of dehydrated NVP-LMA copolymers

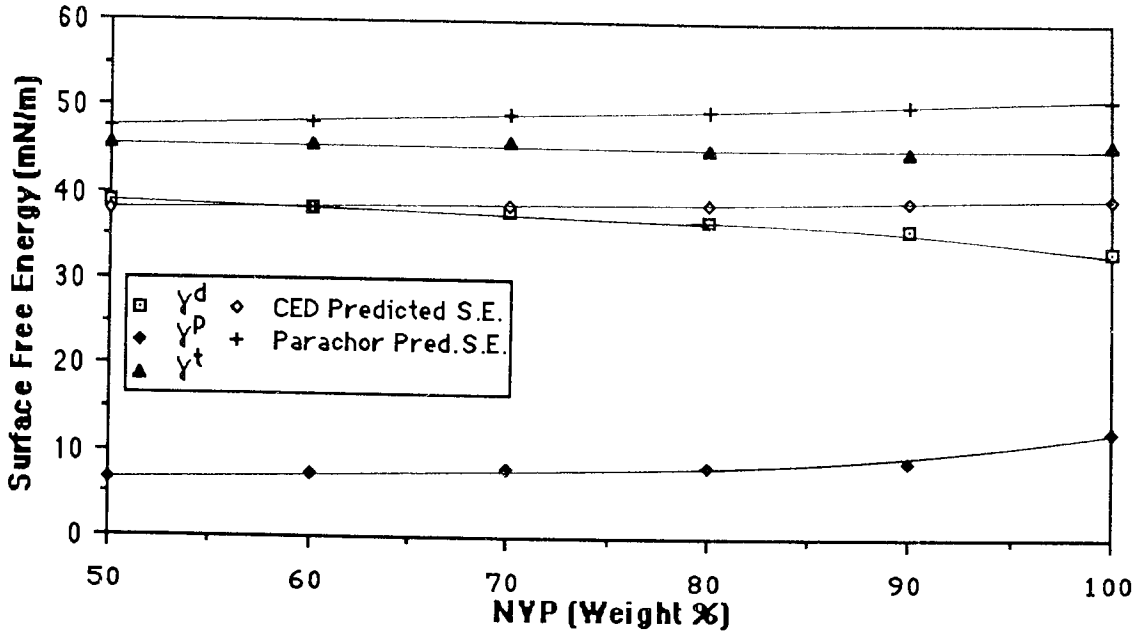

Figure 5.14 **Effect of composition on the measured (γ^t, γ^p and γ^d) and predicted surface free energy of dehydrated NVP-MMA copolymers**

The reasons for this disparity have been discussed previously for NNDMA-LMA copolymers (i.e. the difficulty of obtaining an accurate density for LMA and the large differences in parachor and molecular weight between the two polymers)

5.8.2 Surface Properties of Hydrated Polymers

Although the study of the variation in surface properties with composition in the dehydrated state is interesting and enables the effect of monomer structure to be observed, the hydrogels described in this work are for the most part of high water content and extremely hydrophilic, even in the dehydrated state. This produces problems in the accurate measurement of surface energies of the dehydrated materials, both because of rapid hydration in air and the rapid interaction with water, when this is used as a wetting liquid in sessile drop measurements. In principle, the most successful method of overcoming the problems associated with surface energy measurements on hydrogels is to use the inverted

octane droplet method due to Hamilton[147], in conjunction with the captive air bubble method. The surface properties of the the polymers in their hydrated state have been investigated using the aforementioned techniques in an attempt to determine the factors controlling the surface properties of the polymers.

Although these inverted droplet methods solve the problem of dealing with hydrated materials in principle, they are not without shortcomings in practice. Thus, interfacial angles are difficult to measure with precision, deformation of the air bubble leads to variation in values produced by different workers, and the whole principle of the technique produces the suspicion that interfacial adsorbed water layers dominate the measurements that are made. However, some useful information can be derived from measurements of the surface energies of hydrated materials. The surface energies of the hydrogels in the hydrated state have been calculated by the methods described in Section 5.5.

The first point that can be made about the measured surface free energies of the hydrogels in the hydrated state is that they are all higher than those observed in the dehydrated state, as the surface energy of water is much higher than the surface energy of the polymers. The absorption of small amounts of water can have a dramatic effect in increasing the surface energy of the copolymer, a factor which be discussed in detail subsequently in this Chapter. In addition, the importance of the polar component of surface free energy becomes even more marked in the hydrated gels. This is shown in Figures 5.15 and 5.16 which illustrate that in this series of HEMA-St hydrogels, the polar fraction rises from a vanishingly small value in polystyrene to the point where it dominates the surface energy in poly HEMA hydrogel. Taking the dehydrated values as a baseline, this reflects the inevitable consequence of incorporating increasing quantities of a liquid (water) having a polar component of 51mN/m and dispersive component of 21.8mN/m. It illustrates the particular

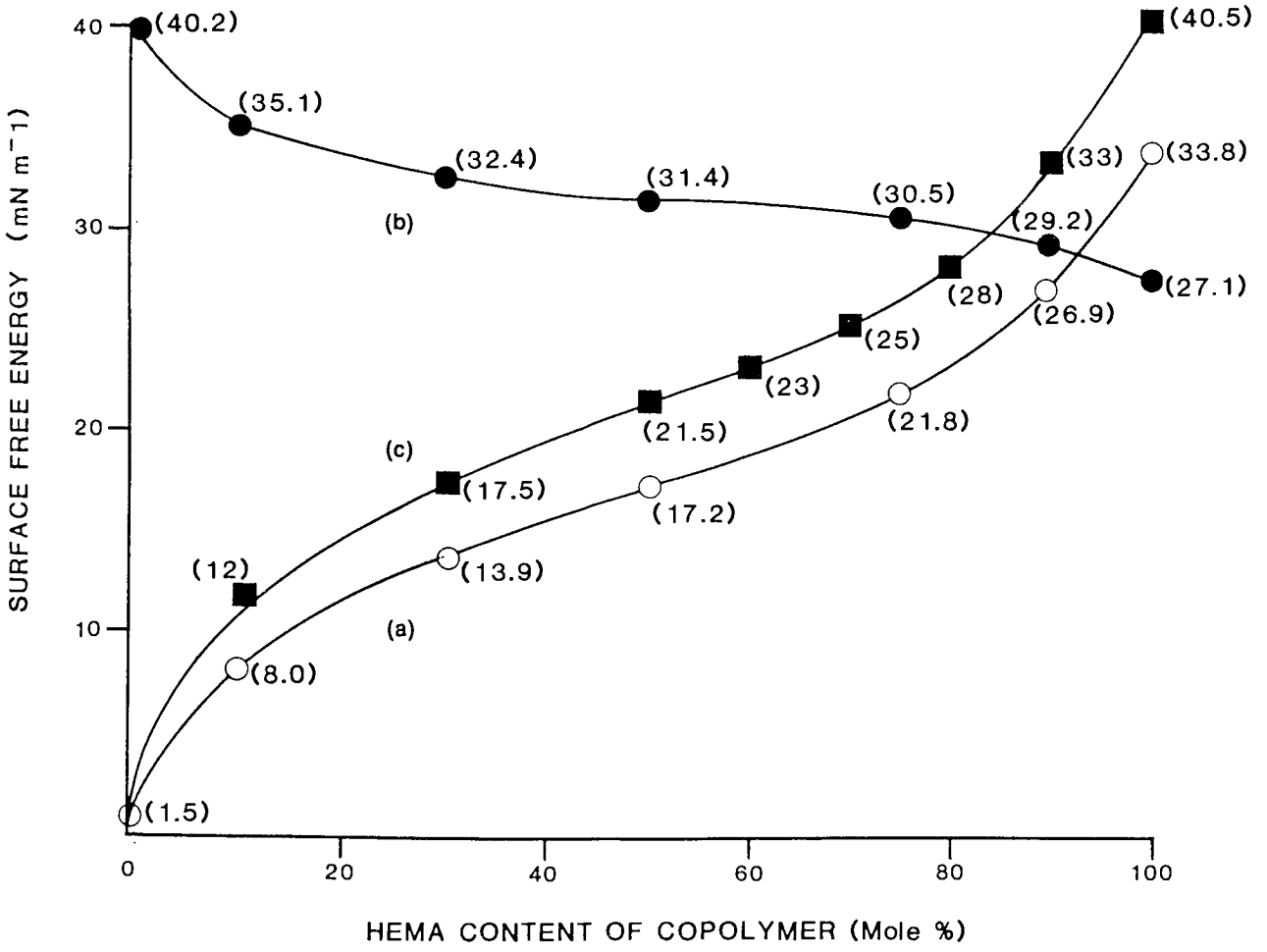

Figure 5.15 Calculated polar (a) and dispersive (b) components of the surface free energy of HEMA-St copolymers. Values of the polar component (c) measured by the Hamilton technique shown for comparison.

interest in these families of hydrogels in which the transition from a dispersive dominated to a polar dominated surface occurs. The values shown have been obtained by a combination of techniques. Lines (a) and (b) show the polar and dispersive components derived from the water content predictive techniques. A similar calculation predicts the difference in surface energies between alkyl methacrylates and hydroxyalkyl methacrylates to within 5% of the measured values. The polar components of the St-HEMA based hydrogels measured directly by the Hamilton technique are shown in line (c). Figure 5.16 presents further information as a function of changing water content in the gel. These results which are based on a wide range of hydroxyalkyl acrylates and methacrylates show the measured polar component (Hamilton technique, line a) together with the measured dispersive component (line b). Because of the uncertainties inherent in the Hamilton method, line (a) illustrates the spread of measurements, made by several workers, on some 50 gels, in these laboratories.

Several problems exist in the measurement of surface properties of hydrogels that are not encountered in determining values for non water-containing polymers. These problems are associated with the fact that water plays an integral part in the establishment of the surface properties of the system and yet it is its very presence that makes direct droplet means used at the surface difficult. The use of water immersion (captive air bubble and octane droplet) techniques maintains the surface in a hydrated state but makes it difficult for the droplet probes to displace the adsorbed water layers. For this reason the results are modified by this water layer. In other studies on adsorbed species on polymer surfaces it has been shown that the values of the surface energy components of such systems are a function of both adsorbed and substrate layers[205]. The difference between the the derived (Figure 5.15 (a)) and directly measured (Figure 5.15 (c)) polar components of the St-HEMA based hydrogels may reflect a similar phenomenon. Additionally, the contact angle values produced by such

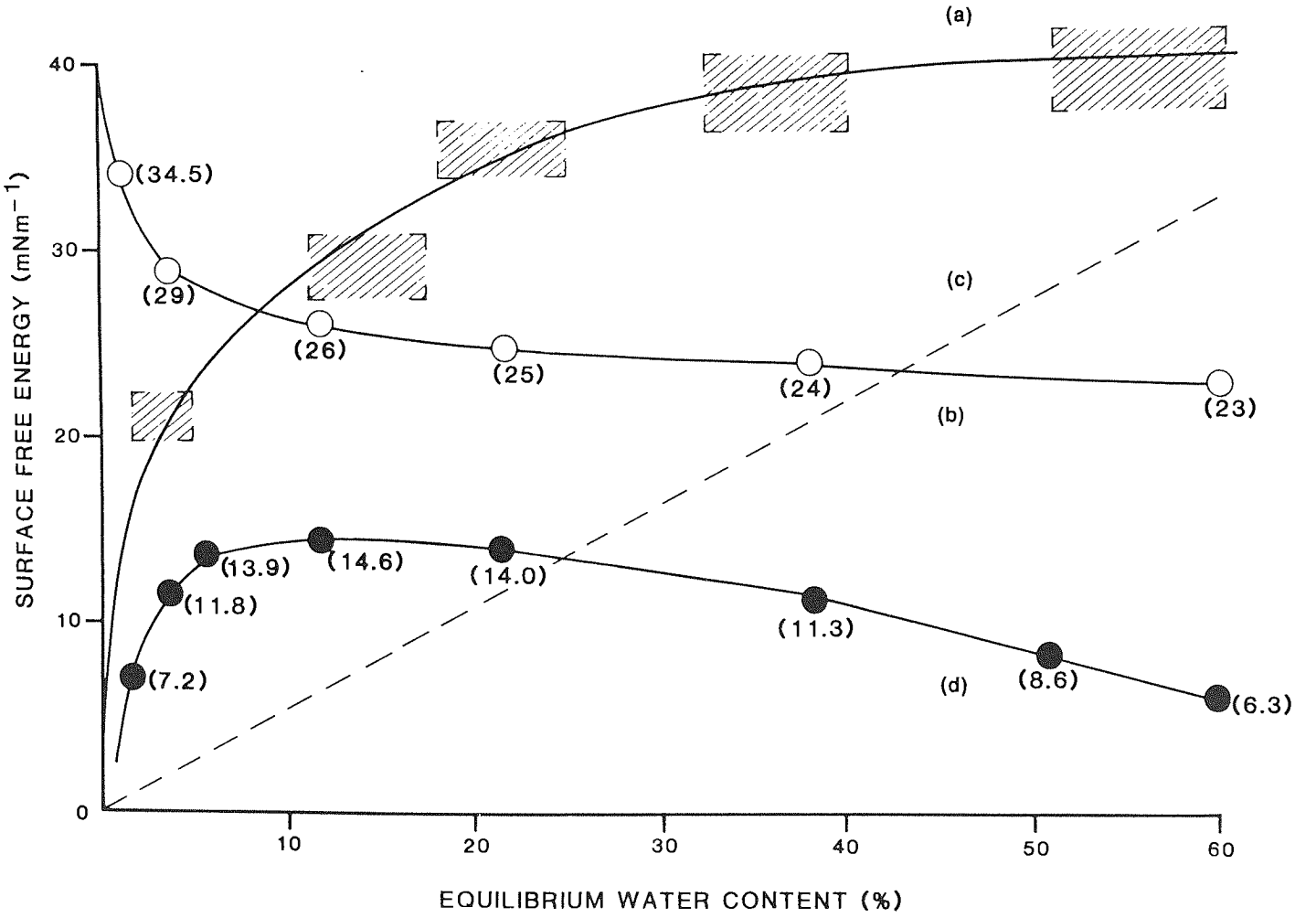

Figure 5.16 Measured polar (a) and dispersive (b) components of the surface free energy of hydroxyalkyl acrylate and methacrylate copolymers shown as a function of EWC. The separate calculated contributions of water (c) and polymer (d) to the polar component are also shown.

hydrophilic surfaces are difficult to measure accurately and reproducibly. Conventional sessile drop in air techniques, on the other hand, present related problems. The use of measurements involving water droplets on freshly blotted gel surfaces suffer from the disadvantage that the surface layer dehydrates rapidly and becomes relatively hydrophobic. If a residual aqueous film is left intact before the water droplet is applied the surface is unrepresentatively hydrophilic. The essence of the problem lies in the fact that the interface between a hydrogel surface and water is much more diffuse than between conventional hydrophobic polymers than water. Some studies have been carried out by Andrade and his group on copolymers of HEMA with methoxyethyl methacrylate using air bubble and octane droplet techniques[35]. This work with styrene copolymers and using other hydroxyalkyl acrylates and methacrylates produces the same trends, although with small but significant differences in detailed values. Andrades results suggest that virtually no measurable changes occur in gels containing more than 20% water by weight and that the interfacial tension is already zero at this point. These results indicate a continuous variation between 20% and 60% EWC, a trend continued in a series of hydrogels having water contents of ~ 85%[38]. The interfacial tension falls as the EWC of the polymer is increased. Values for the interfacial tension of the polymers studied are listed in Appendix 5. The small but real values of interfacial tension measured accords with the fact that the water contact angle does not fall to zero within this range of polymers.These results suggest that polymer structure is capable of influencing the detailed surface energy components throughout this range and the relative contribution of water and polymer to the polar component of the surface energy is shown in Figure 5.16 (c) and (d). The use in this way of measurements on dehydrated surfaces illustrates the way in which the surface energy parameters of hydrogels should be affected by polymer structure. They support the view that currently available direct measurement techniques for hydrated surfaces produce the impression of a surface layer of water that dominates the measured values. Molecular processes at hydrogel surfaces (eg biological

interaction and protein deposition) indicate that surface changes, inadequately detected by macroscopic droplet techniques, take place as the nature of the polymer matrix and the volume fraction of water are varied. Calculations of the type shown in Figure 5.16 (c and d) reflect the nature of such changes.

It is instructive to calculate the interfacial tension (γ_{WH}) between water (W) and the hydrogel (H) surface using, for example, the geometric mean technique:

$$\gamma_{WH} = \gamma_W + \gamma_H - 2(\gamma_W^p \gamma_H^p)^{0.5} - 2(\gamma_W^d \gamma_H^d)^{0.5} \qquad (5.33)$$

A direct correlation can be made with the magnitude of the water sessile drop contact angle obtained in air on a hydrogel surface from which excess water has been previously removed. There is general agreement that this value is around 20° for poly HEMA hydrogel and will rise with HEMA-styrene copolymers to a value of around 90° for polystyrene.

The interfacial tension obviously plays an important part in governing biointeractions at hydrogel surfaces. This is a complex area because biological fluids contain naturally occurring wetting agents whose size generally precludes them from entering the hydrogel matrix. Their surface tensions (typically around 50 mN/m) are initially lower than that of the water swollen matrix, a situation that is modified by subsequent biological deposition. In the case of hydrogels for biomedical applications, therefore, a low interfacial tension with water is not necessarily a relevant guide to compatibility.

The measured surface free energies of hydrated HEMA-MMA copolymers are illustrated in Figure 5.17. As with all the graphs in this section γ^p, γ^d and γ^t are shown together with estimates of the surface free energy based on two techniques; a modified form of the parachor and a technique based on the measured dehydrated surface energy and the water content of the hydrated polymer. As increasing amounts of MMA are incorporated into

HEMA, reducing the water content, the polar component of the surface free energy is reduced and the dispersive component increases. This behaviour is similar to that observed in the dehydrated copolymers but the effect in the hydrated copolymers is more pronounced. As the total surface free energy of water 72.8mN/m is much larger than that of the homopolymers and the polar and dispersive components (51.0mN/m and 21.8mN/m respectively) are also vastly different, a marked effect is seen when the amount of water in these copolymers is reduced by the addition of a hydrophobic monomer.

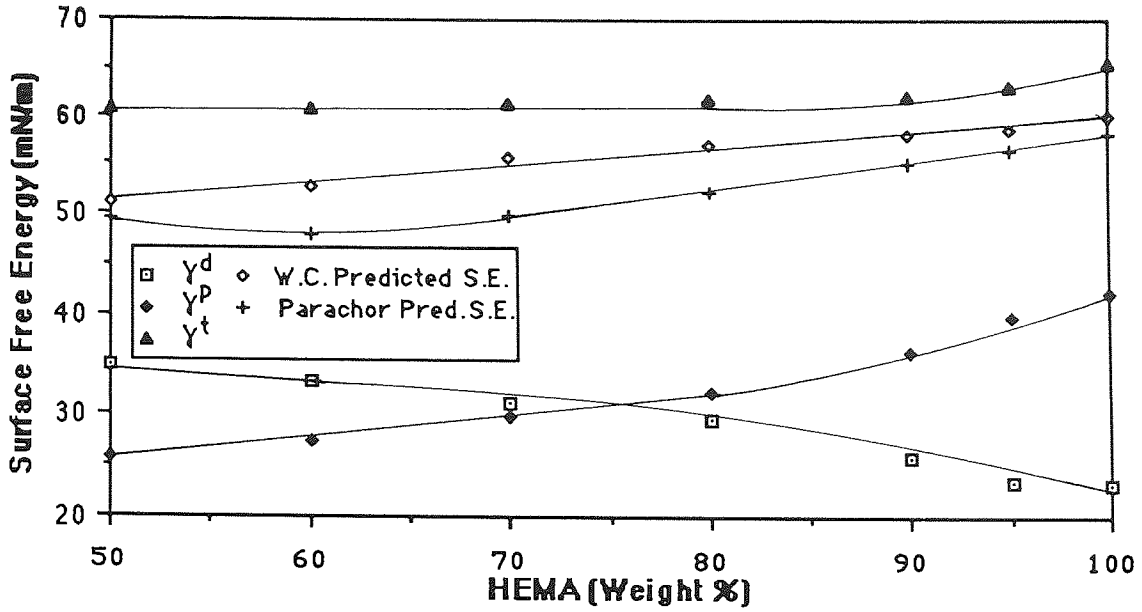

Figure 5.17 Effect of composition on the measured (γ^t, γ^p and γ^d) and predicted surface free energy of hydrated HEMA-MMA copolymers

The measured surface free energy is, however, in excess of that predicted by both the parachor and water content techniques which both predict values that are in close agreement. The surface energy of hydrated poly HEMA is much greater than would be expected for a polymer with its EWC.

The hydrophilic-hydrophilic HEMA copolymers investigated display interesting surface properties in the hydrated state. The surface free energy of the copolymer increases as increasing amounts of NVP are incorporated into the copolymer and γ^p also increases as would be expected from a copolymer series where the EWC is increasing (Figure 5.18). The minima observed in the surface energies of the dehydrated copolymers are not seen in the hydrated system as it is energetically more favourable for the polymers to interact with water, rather than with each other. Thus, the HEMA-NVP system displays the behaviour that might be expected from such a system.

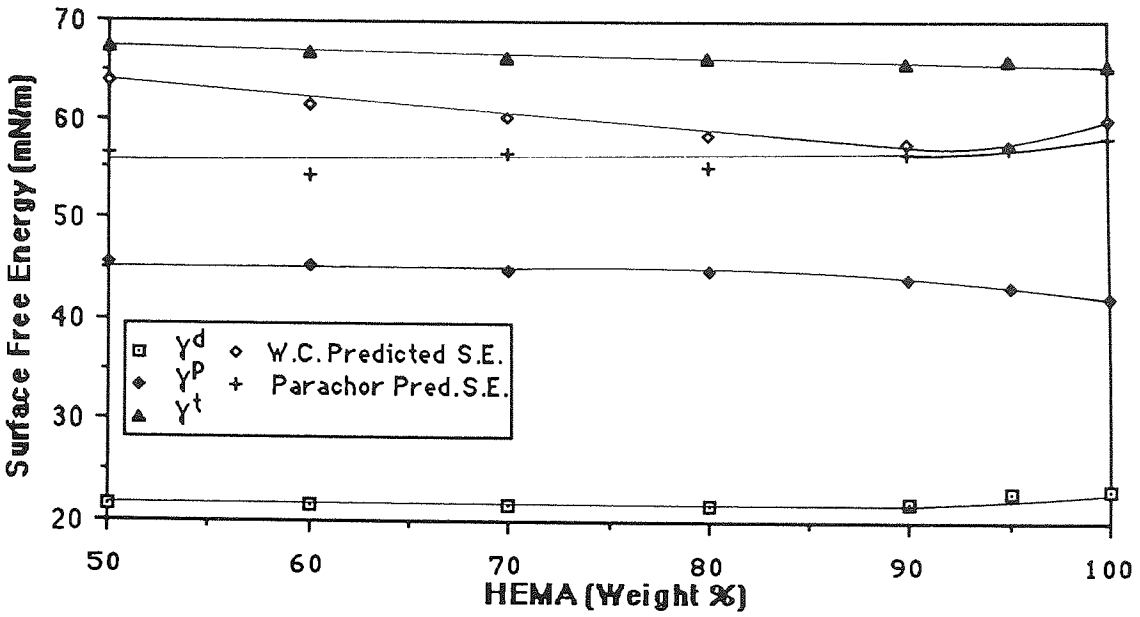

Figure 5.18 Effect of composition on the measured (γ^t, γ^p and γ^d) and predicted surface free energy of hydrated HEMA-NVP copolymers

The water content predicted surface free energy is once again lower than the measured γ^t but shows the correct trend, an increase in surface free energy with increasing NVP incorporation. The parachor predicted surface energy values are scattered but the general trend is a decrease in γ^t with increasing NVP incorporation.

The results obtained from the HEMA-NVP copolymer series can be easily explained, however, those obtained from the HEMA-NNDMA system present more difficulties. Increasing the amount of hydrophilic NNDMA in the copolymer increases the EWC but also causes a reduction in the polar component and an increase in the dispersive component of the surface free energy (Figure 5.19). These results are concomitant with the formation of an intramolecular complex, with orientation of the polar groups within the bulk of the polymer reducing their expression at the surface. Although this behaviour is observed in the dehydrated copolymer, it is surprising that similar behaviour is seen in the hydrated state as interaction with water would usually be energetically more favourable than polymer-polymer interaction. The total surface free energy also increases slightly with NNDMA incorporation as γ^d increases at a greater rate than γ^p falls.

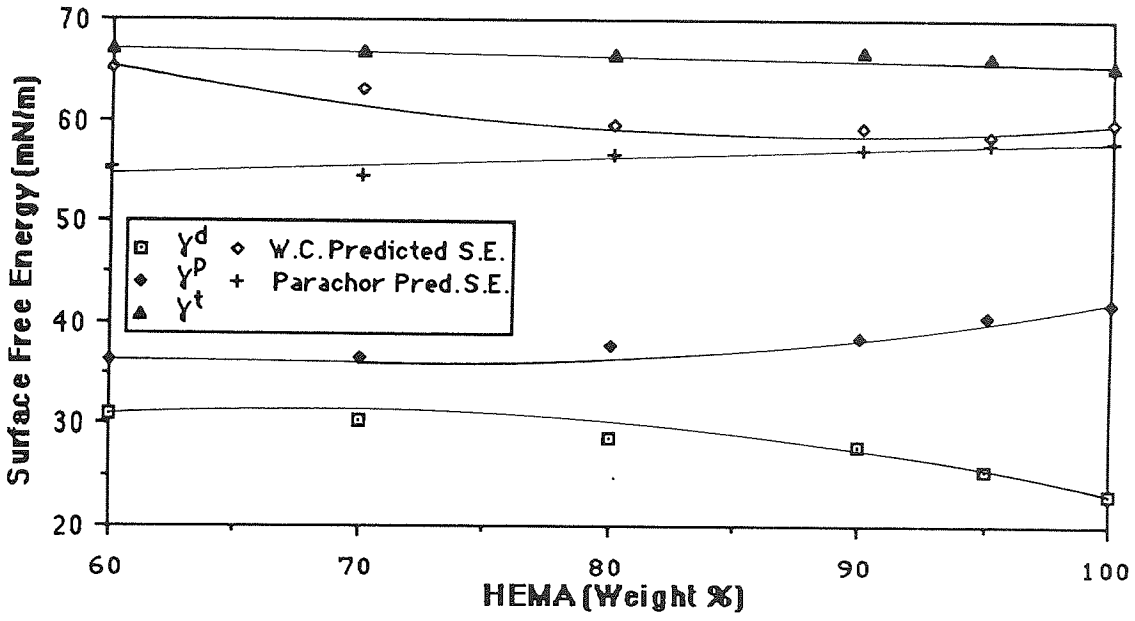

Figure 5.19 **Effect of composition on the measured (γ^t, γ^p and γ^d) and predicted surface free energy of hydrated HEMA-NNDMA copolymers**

The water content predicted surface free energy goes through a minimum before predicting a rise in γ^t. However, if this is resolved into polar and dispersive components, an increase in γ^p and a decrease in γ^d is predicted, the opposite of the experimentally observed behavior. The parachor, on the other hand, predicts a fall in γ^t.

Hydrated poly NNDMA has very similar surface energy parameters to poly HEMA in the hydrated state, even though there is a great difference in EWC. Although NNDMA might be expected to be more polar because of its increased water content, the greater polarity of poly HEMA observed in the dehydrated state makes a significant contribution to the surface energy, even when the polymer is hydrated. Increasing the amount of hydrophobic EGDM crosslinking agent causes a reduction in γ^p but this is accompanied by a similar increase in γ^d so there is little change in the total surface free energy. This behaviour parallels that observed in the dehydrated state.

When NNDMA is copolymerised with the hydrophobic monomers LMA (Figure 5.20) and MMA (Figure 5.21) the anomalous behaviour seen in the HEMA-NNDMA copolymers is not observed. Increasing the amount of hydrophobic monomer causes a decrease in γ^p and a concurrent increase in γ^d. It is interesting to note that even in the hydrated state, where water would be expected to make a significant contribution to the surface free energy, the polar component of the NNDMA-MMA copolymers falls rapidly with only a small decrease in water content. Therefore, the 80:20 NNDMA-MMA copolymer (EWC 83.1%) has a polar component of 9.8 mN/m while the 90:10 NNDMA-LMA copolymer (EWC 78.0%) has a polar component of 15.6 mN/m. Once again it appears that MMA behaves as a more hydrophobic monomer than LMA. This illustrates the fact the structural features do have an important part to play in determining the surface free energy in the hydrated state and that γ^t is not dominated solely by water content.

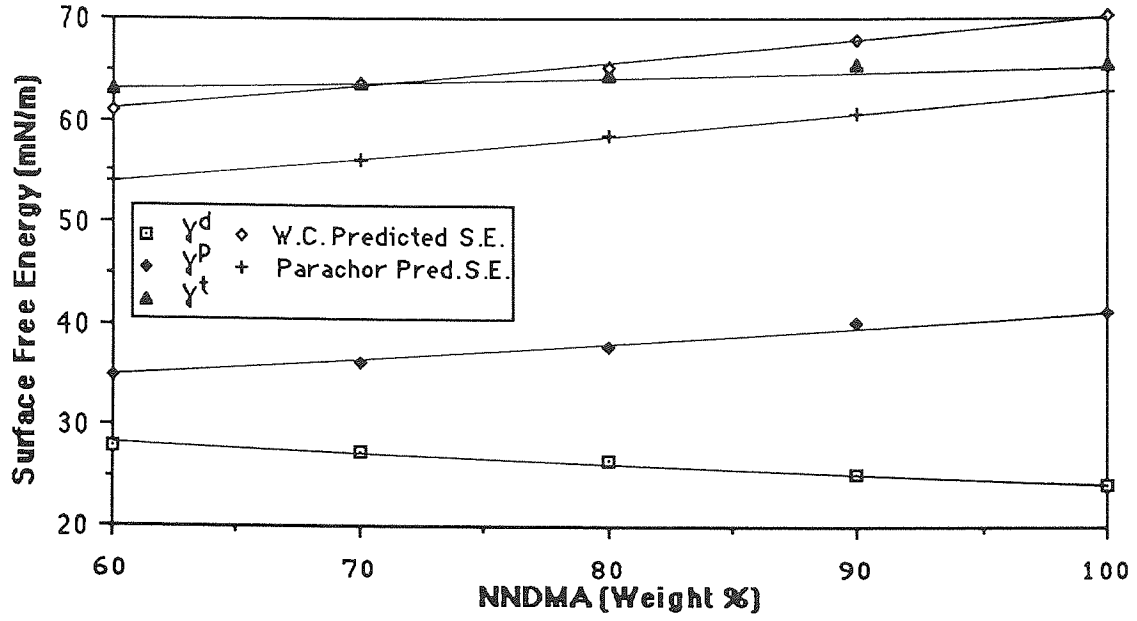

Figure 5.20 Effect of composition on the measured (γ^t, γ^p and γ^d) and predicted surface free energy of hydrated NNDMA-LMA copolymers

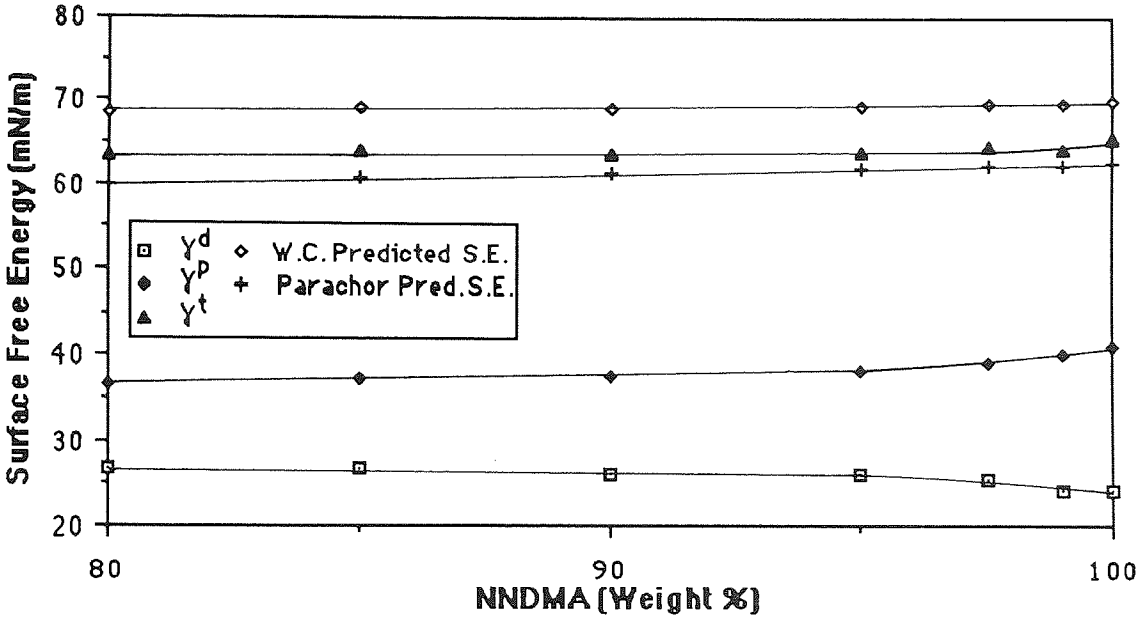

Figure 5.21 Effect of composition on the measured (γ^t, γ^p and γ^d) and predicted surface free energy of hydrated NNDMA-MMA copolymers

increasing amounts of hydrophobic monomer but there is again some disparity between the measured and predicted values and the rate of decrease of γ^t.

Although in the dehydrated state poly NVP has the lowest surface free energy of all the homopolymers studied, the opposite is true when it is hydrated. It is apparent that, at such high EWCs, water is the dominant feature in determining the surface energy and both γ^p and γ^d approach the values of water. As γ^d for poly NVP is so low and γ^p is so high, the effect of copolymerisation with hydrophobic monomers is more dramatic than in the other copolymer systems examined. This is illustrated in Figures 5.22 and 5.23 which show the effect of composition on the surface free energy of NVP-LMA and NVP-MMA copolymers respectively.

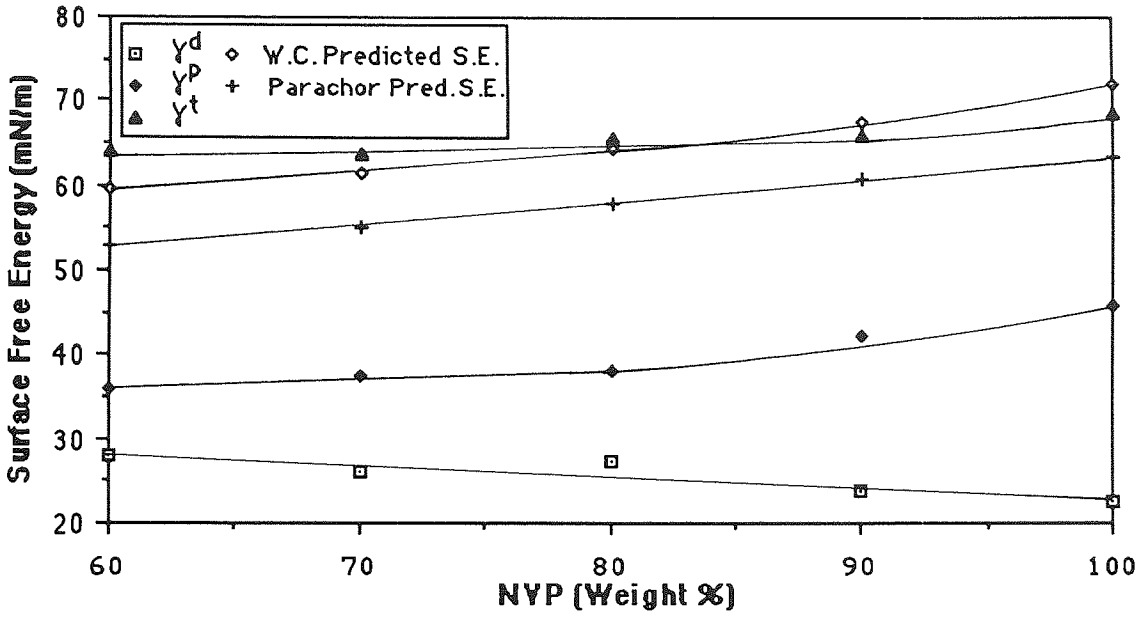

Figure 5.22 **Effect of composition on the measured (γ^t, γ^p and γ^d) and predicted surface free energy of hydrated NVP-LMA copolymers**

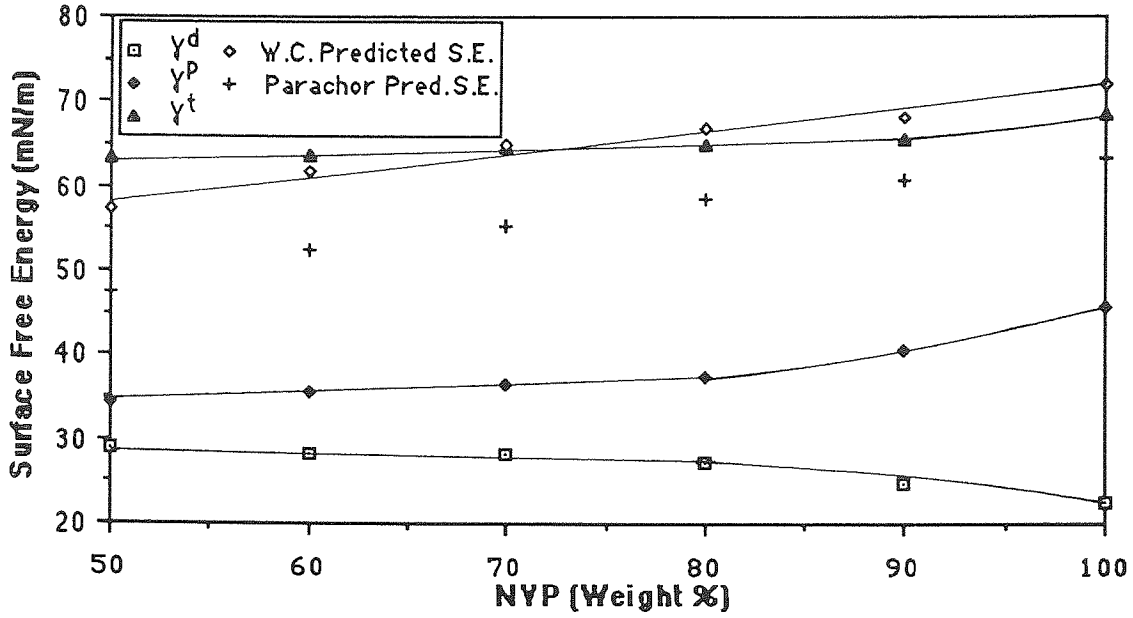

Figure 5.23 **Effect of composition on the measured (γ^t, γ^p and γ^d) and predicted surface free energy of hydrated NVP-MMA copolymers**

The fall in γ^p and increase in γ^d which normally accompanies the increase in hydrophobic monomer concentration is seen in this system. One feature which is again apparent in these systems is the greater effect of MMA at reducing γ^p at similar water contents. The parachor and water content predicted surface free energies again predict the correct trend, a decrease in γ^t with increasing amounts of hydrophobic component. However, they predict a more dramatic change in surface energy than is observed experimentally. Another point which can be made is the striking similarity of the surface energies of the NNDMA and NVP copolymers in the hydrated state. In the dehydrated state significant differences between the copolymers based on these two polymers can be seen; this behaviour demonstrates the homogonising effect that water can have on surface energy.

The fact that variations in polymer structure produce effective differences in surface properties at a given water content is demonstrated in Figure 5.24 in which Hamilton

contact angle is plotted as a function of equilibrium water content. The points which lie outside the 10° band, which illustrates the reasonable limits of experimental error, are those in which polymer structure plays a major role in determining surface properties. Although relatively few of the copolymers investigated in this work lie outside this range, previous work in these laboatories[38] has indicated that significant variations can occur, particularly in copolymers where both monomers have appreciable hydrogen bonding capability.

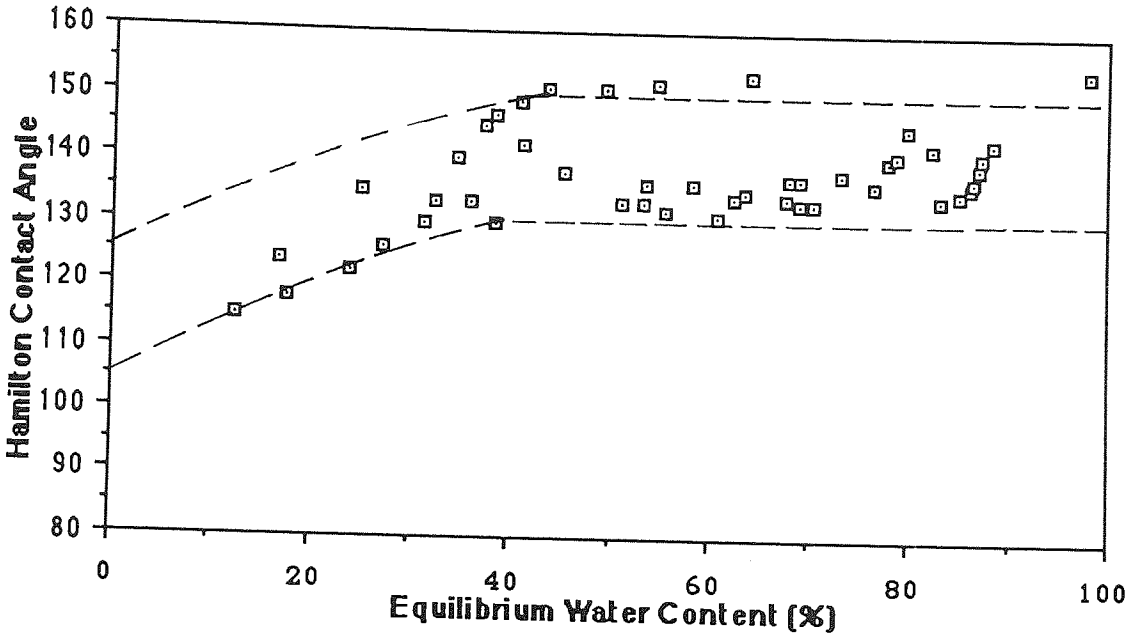

Figure 5.24 Variation in Hamilton contact angle with EWC

Previously, it has been suggested that it is only in low water content hydrogels that water makes direct contribution to the surface energy[204]. At higher EWCs the main effect of water is thought to be the effect it has on the ease of chain rotation.

5.8 Conclusions

The surface properties of hydrogels are unique as even in the dehydrated state they have a higher polar component of surface free energy than conventional polymers. However, it is in the hydrated state where the most interesting changes in surface properties occur in these

systems. In the same copolymer series it is possible to move (by the incorporation of a greater percentage of hydrophilic monomer and therefore, more water) from compositions where the surface free energy is dominated by γd, through compositions where there is a balance of γd and γp, to compositions where γp is the major component of γt. The wide range of surface properties displayed from simple combinations of monomers is one of the reasons for the great potential of hydrogels in biomedical applications.

Despite the difficulties encountered in the measurement of surface free energies of polymers in both the dehydrated and hydrated states, it is clear that valuable information can be elucidated from measurements of this type. In the majority of copolymer systems examined in this work the changes in surface energy with composition can be explained in terms of structural changes in the polymer. In the dehydrated state, for example, the incorporation of increasing amounts of hydrophobic monomer into a hydrophilic system decreases γ^p and increases γ^d. In the styrene copolymers with hydroxyalkyl acrylates and methacrylates changes in γ^p, γ^d and γ^t can be related to steric occlusion and changes in hydrophobicity in the hydroxyalkyl acrylates and hydroxyalkyl methacrylates. Even when the surface free energy appears to show unusual behaviour (e.g. HEMA-NVP and HEMA-NNDMA copolymers) this can be attributed to polymer-polymer interactions i.e the formation of intramolecular complexes.

The parachor has proved to be a more accurate predictive method than the C.E.D. for all the copolymer systems studied with excellent agreement between the predicted and measured values being observed in the HEMA-St and HEMA-MMA systems. However, parachor predicted values of surface free energy are less accurate in systems where there are strong polymer-polymer interactions, causing steric occlusion. The C.E.D. predicted values of surface free energy are in poor agreement with the measured values as they do not take into

account any polar contribution to the surface free energy. In systems based on hydrophilic monomers the polar contribution accounts for a significant proportion of γ^t. Therefore, one might expect that the C.E.D. predicted value of γ^t to be a closer approximation to γ^d and this is found in the majority of systems studied.

The surface behaviour of polymers in the hydrated state is more complex as the surface energy is a function of both polymer-polymer and polymer-water interactions. Although as a general observation it could be stated that γ^p decreases and γ^d increases as the EWC falls, i.e. as the amount of hydrophobic monomer in the copolymer increases, structural variations do override water content considerations to produce differences in surface properties at a given EWC. The variations in water binding behaviour (described in Chapter 3), which are a function of the water structuring groups present in the hydrogels, might be expected to produce differences in the surface properties of the hydrated polymers. However, no marked differences are detected on a macroscopic scale using droplet techniques. The surface properties of some of the copolymer hydrogels described here have also been investigated using a more sensitive biological probe technique, which employs anchorage dependent fibroblast cells. The results from this study are presented in Chapter 8.

The predictive techniques for hydrated surface are less accurate than those for dehydrated surfaces and generally predict lower values for γ^t than the experimentally determined values. The low values predicted by the parachor based method are a reflection of both the inability of the technique to cope the interactions between the polymer and water and the difficulty in assigning an accurate parachor value for water. However, the parachor value assigned to water in this work (52.8) gives a value of 71.8mN/m for the surface free energy of water, in good agreement with the experimentally determined value of 72.8mN/m. The values predicted by the water content method are, in general, lower than the measured values of γ^t.

These results are concordant with the idea that there is an adsorbed layer of water on the surface of hydrated polymers, which gives rise to higher than predicted surface energies.

CHAPTER 6

Interpenetrating Polymer Network Hydrogels: Water Binding Studies

CHAPTER 6

Interpenetrating Polymer Network Hydrogels: Water Binding Studies

6.1 Introduction

In the past two decades much research has been carried out on polymer blends and composites, principally because of the enhanced mechanical properties which these materials often possess. However, there has been relatively little work on hydrogel blends and composites and there is still some confusion about the precise definition of blends and composites when applied to polymers. Although "a mix of components which are inseparable and indistinguishable" has been defined as a blend while a composite has been defined as "a material made of constituents which remain recognisable", problems arise when trying to use these terms on a molecular level. Mason and Sperling[206], for example, have used the terms polyblend or polymer blend to refer to a system which contains two distinguishable types of polymer molecules. Their definition will be used throughout this work. In the following chapters the water binding, mechanical and surface properties of several types of polymer blends will be discussed. The effect of the filler polymer on all the above properties will be examined in detail and any correlation between composition and these properties will also be noted.

6.2 Interpenetrating Polymer Networks

Interpenetrating polymer networks (IPNs) have been defined as a combination of two polymers, each in network form, at least one of which has been synthesised and / or crosslinked in the presence of the other[207]. This is shown schematically in Figure 6.1, which shows the varying forms which a blend or mixture of two polymers may take. Varying methods are used to synthesise IPNs and this, in turn, determines the class of IPN produced. These methods may be described as follows:

i) Monomer I is polymerised and crosslinked to give a polymer which is then swollen with monomer II plus its own crosslinker and initiator. Polymerisation of monomer II *in situ* produces a SEQUENTIAL IPN.

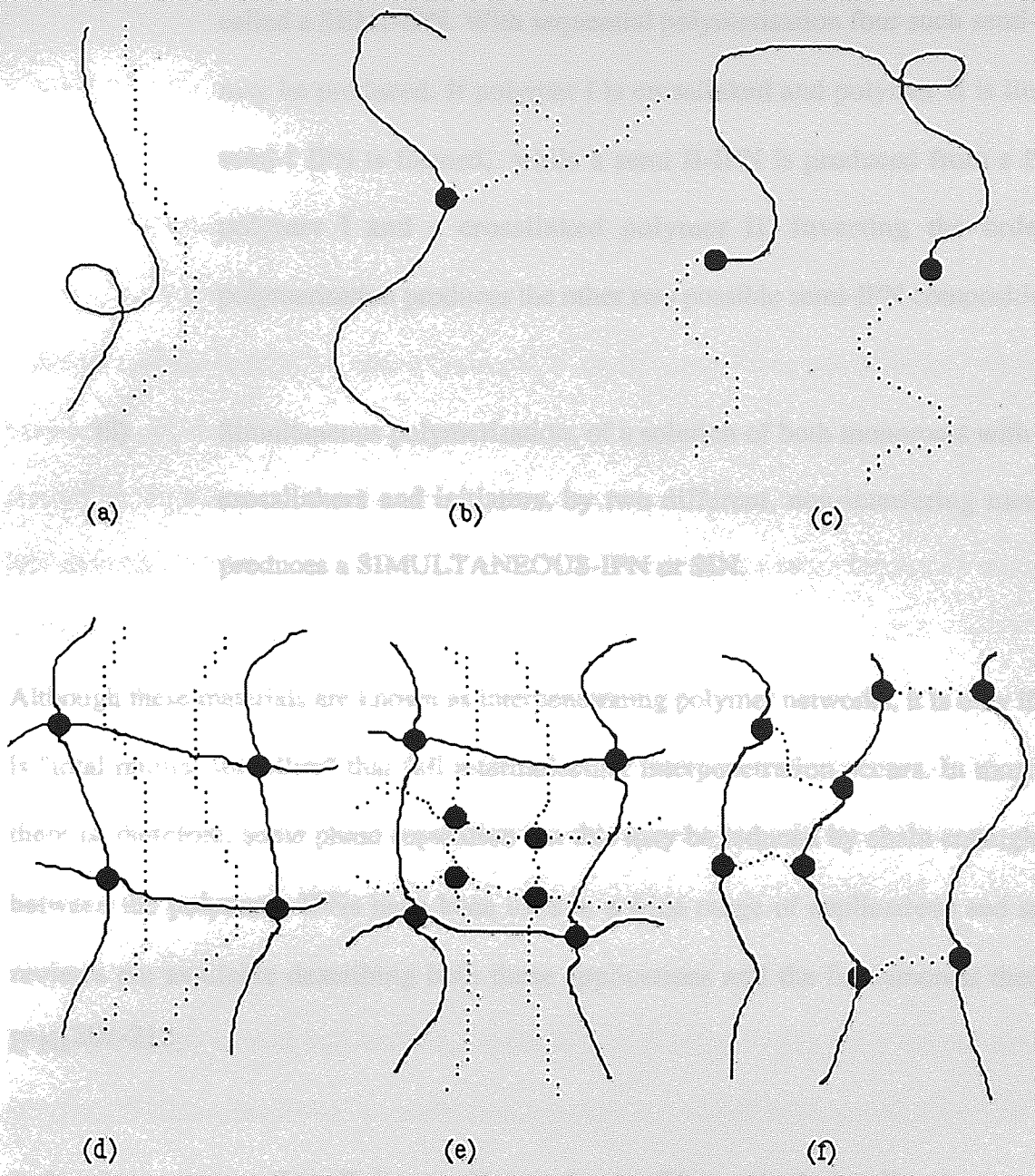

Figure 6.1 Possible simple two polymer combinations: (a) polymer blend (b) graft copolymer (c) block copolymer (d) semi-IPN (e) full IPN and (f) AB crosslinked polymer (redrawn from reference 207)

ii) If only one polymer in the system is crosslinked the network formed is called a SEMI-IPN. With sequential polymerisation four such semi-IPNs may be produced. If polymer I is crosslinked and polymer II is linear a semi-I IPN is formed, while a semi II-IPN is produced from a linear polymer I and a crosslinked polymer II. Inverting the order of polymerisation produces the other two possible semi-IPN compositions.

iii) Simultaneous polymerisation, of a solution of both monomers with their crosslinkers and initiators, by two different, non-interfering methods produces a SIMULTANEOUS-IPN or SIN.

Although these materials are known as interpenetrating polymer networks, it is only if there is "total mutual solubility" that full intermolecular interpenetration occurs. In most IPNs there is, therefore, some phase separation but this may be reduced by chain entanglement between the polymers. IPNs have been used in a wide range of applications and several reviews are available describing both these applications and the fundamental theory of IPNs[207-212].

6.3 Interpenetrating Polymer Networks in Biomedical Applications

The use of IPNs in wound dressing applications has been described previously (Section 1.8.1). There are, however, several other biomedical applications of IPNs. In 1978 Bausch and Lomb were granted a patent for an IPN which was claimed to be useful in contact lens applications[213]. This was based on a crosslinkable siloxane compound in conjunction with HEMA or NVP and ethylene glycol dimethacrylate. The mixture is polymerised and crosslinked to produce a polymer containing interpenetrating hydrophilic and hydrophobic chains, which is oxygen permeable and transparent. No evidence of the clinical or

commercial success of this material has appeared, however.

"Gradient" IPNs have been synthesised and tested for use as drug delivery systems. These IPNs consist of a bead or sheet of polymer which is then swollen at the surface by a monomer. Polymerisation of this monomer leads to the formation of "gradient IPNs". IPNs of this type, based on a HEMA or HEMA-methoxyethoxyethyl methacrylate copolymer hydrogel swollen in EGDM, which is then U.V. irradiated to form a crosslinked outer layer, have been used to release progesterone at a substantially constant rate over a prolonged time period[214]. Squibb and Sons have been granted a patent[215] based on the use of a gradient IPN formed from hydrogel beads and an acrylic swelling monomer for use in controlled release applications.

Recently it has been demonstrated that the rate of diffusion of a water soluble drug from HEMA-NVP hydrogel beads can be controlled by the thickness of the gradient layer, in this case a polyurethane based on a diol or triol and 2,4,4, (2,2,4)-trimethylhexane-1,6,-diisocyanate[216]. By varying the temperature, reaction time and the relative concentrations of the reactants, solvent and catalyst, the depth of IPN formation in the hydrogel bead may be controlled. Studies with a model compound, Oxprenolol.HCl, a water soluble drug, have confirmed the potential of these systems in drug delivery applications. An alternative approach to gradient IPN formation is based on a poly(ether urethane) matrix swollen with poyacrylamide[217,218].It is hoped that these IPNs may be useful as blood contact materials.

6.4 General Observations

The IPNs synthesised in this work are not true sequential IPNs but semi-II-IPNs. They are synthesised by dissolving the filler polymer in a solution of monomer and then crosslinking the monomer. These semi-II-IPNs will be referred to throughout this work as IPNs.

Many high water content hydrogels which could be useful in biomedical applications are rejected because of their poor mechanical properties. The formation of IPN hydrogels may provide a method to overcome this, as previous work has shown that IPNs have unique mechanical and surface properties[137]. The IPNs synthesised in this work were based on N'N' dimethyl acrylamide (NNDMA) which possess very good solvent properties but which usually has poor mechanical properties in copolymer systems due to chain transfer. Therefore, in this work the IPNs were synthesised which incorporated a filler polymer with improved mechanical properties e.g poly methyl methacrylate. As poly NNDMA has been well characterised previously, it forms the basis of a very sensitive system for experimentation on the effect of filler polymers on water binding, surface and mechanical properties. Due to solubility limitations it was only possible to investigate partial molar ranges in all the IPN systems examined. The limits of solubility for all the filler polymers used in this work are illustrated in Figure 6.2.

A IPN based on acrylamide and agar, Geliperm, (Section 1.8) has achieved commercial success as a wound dressing material. It has an ideal combination of properties, high water content, high tensile strength and although it is oxygen permeable it is impermeable to bacteria. Therefore, initially in this work attempts were made to utilise carbohydrates (e.g. agar, hydroxethyl cellulose, chondroitin-6-sulphate etc.) as filler polymers. IPNs based on these materials had a high water content, however, these polymers had limited solubility in NNDMA. The maximum amount of filler polymer which could be incorporated into NNDMA was 15% (20% for CMC in solution) and the mechanical properties of the IPNs were poor, possibly because of their high EWCs. The most promising IPNs with carbohydrate filler polymers were those with cellulose acetate and cellulose acetate butyrate and these will be compared with IPNs incorporating other commercially available vinyl polymers and polyurethanes in this Chapter.

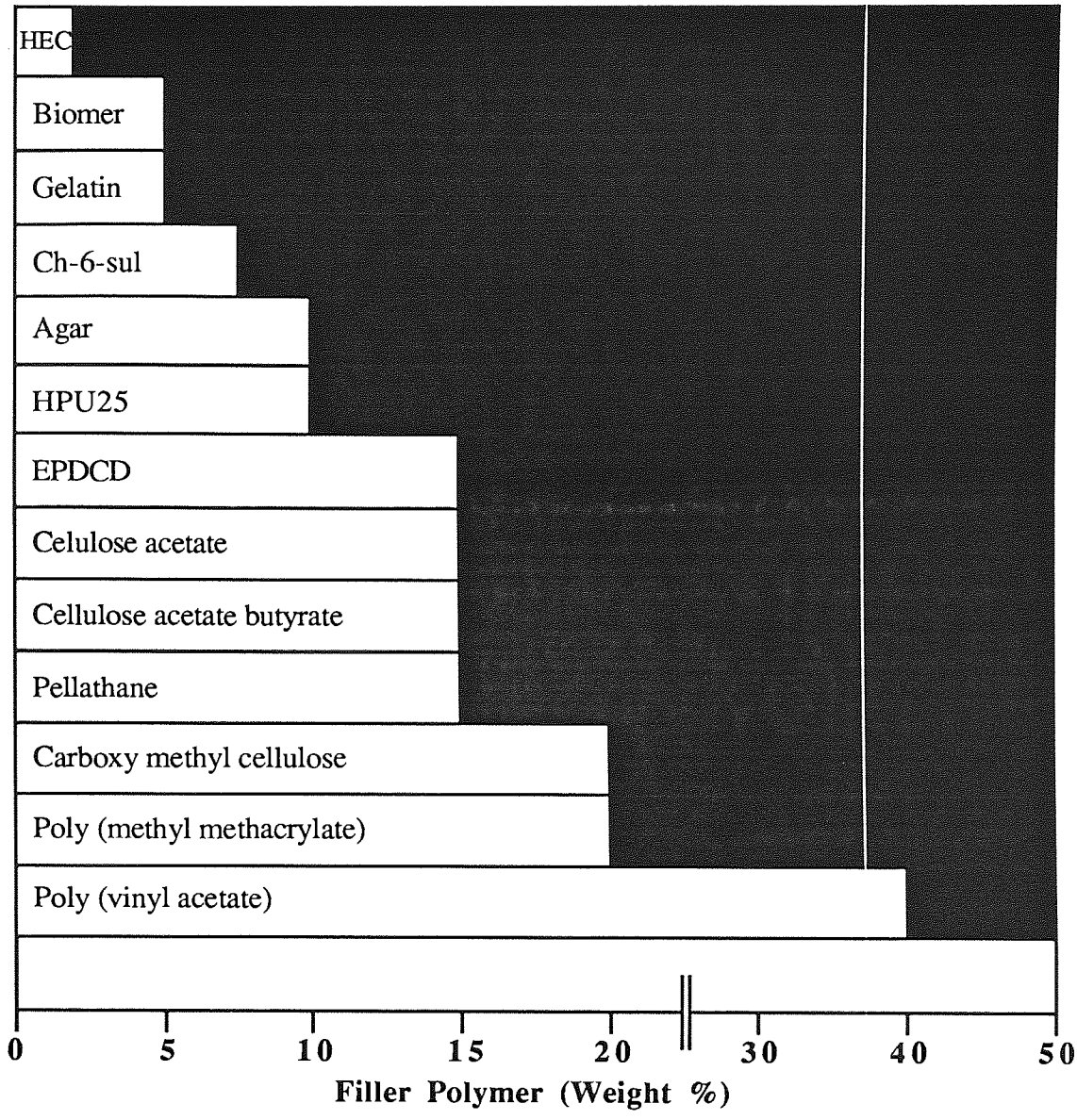

Figure 6.2 Maximum solubility of some filler polymers in NNDMA (black=insoluble)

6.5 IPN Hydrogels: Water Binding Studies

The water binding characteristics the IPN hydrogels sythesised in this work (all with EWCs in excess of 65%) were examined using differential scanning calorimetry. Some typical melting endotherms of these hydrogels are illustrated in Figure 6.3. All the melting endotherms are relatively simple, ill defined doublets characteristic of high water content materials (c.f. Section 3.4) and little information on the detailed water structuring in these

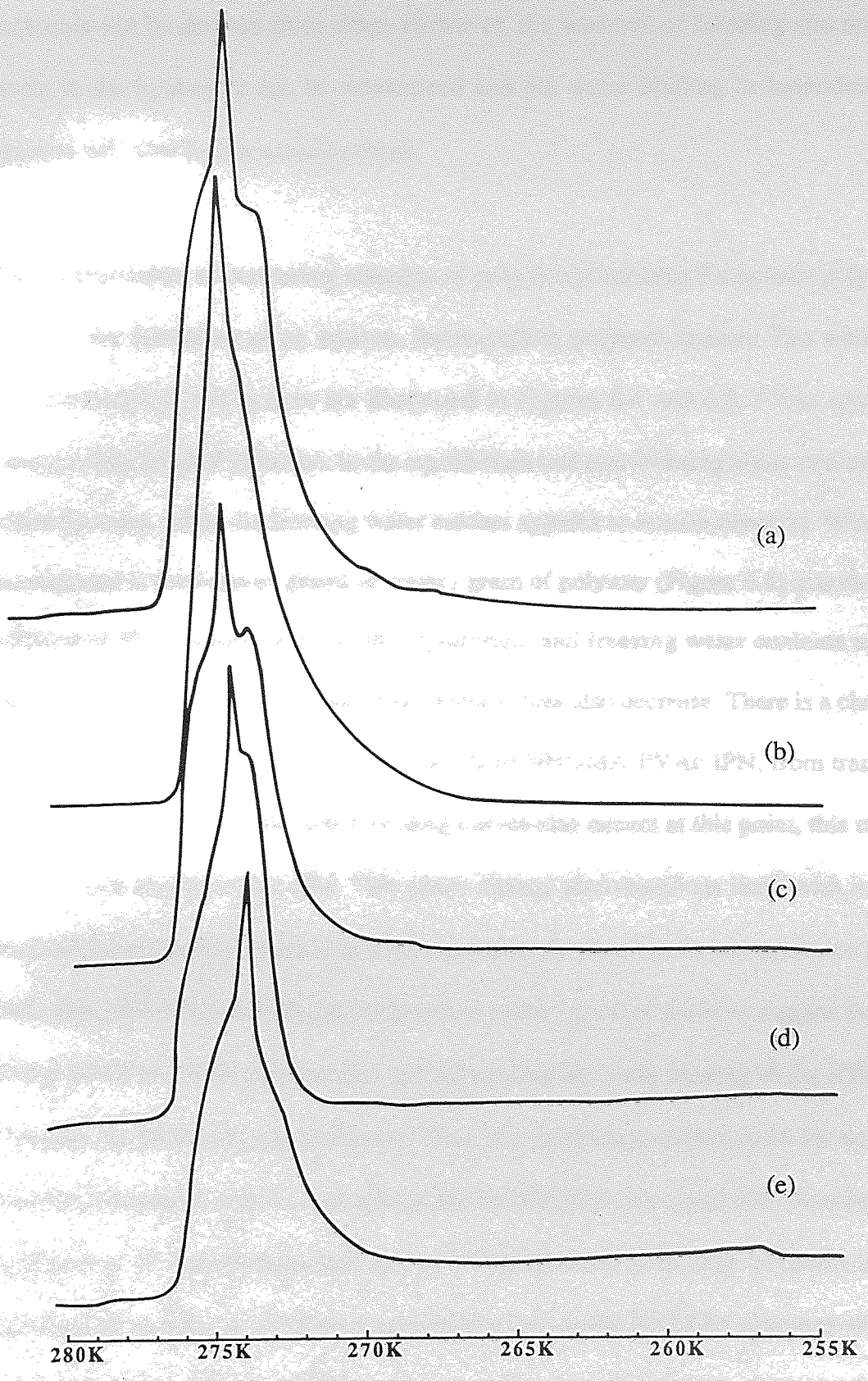

Figure 6.3 Typical melting endotherms of a) a NNDMA-Pellathane 95:5 IPN b) a NNDMA-CA 90:10 IPN c) a NNDMA-HPU25 90:10 IPN d) Geliperm and e) a NVP-CAB 90:10 IPN

materials can be derived from them. However, the amounts of freezing and non-freezing water in the hydrogels can be determined and the water binding in individual polymer systems will now be discussed in detail.

The incorporation of increasing amounts of poly (vinyl acetate) PVAc into poly NNDMA leads to the formation of an opaque, incompatible polymer system. The water binding characteristics of this system are illustrated in Figures 6.4 and 6.5. PVAc incorporation causes a very gradual reduction in the equilibrium and non-freezing water contents after an initial increase, while the freezing water content appears to remain constant. When the data is examined in the form of grams of water / gram of polymer (Figure 6.4) it is clear that the addition of PVAc causes a fall in the equilibrium and freezing water contents and a slight increase in the non-freezing water before these values also decrease. There is a change in the appearance of the IPNs subsequent to the 90:10 NNDMA-PVAc IPN, from translucent to opaque. An inflexion in the water binding curves also occurs at this point, this may be due to the phase change in the IPN. This phase change also manifests itself with its effect on mechanical properties which will be discussed in Section 7.2. In compositions containing more than 10% PVAc the results for grams of water / gram of polymer suggest that PVAc is acting solely as a filler polymer (i.e. not influencing the water binding of the IPN except by reducing the NNDMA concentration). Thus, the percentage reduction in the non-freezing water is consistent with the percentage fall in NNDMA concentration. Another possible explanation of this phenomenon is that PVAc interacts with both NNDMA and water, reducing the number of available water binding sites in the NNDMA segments of the chain, while providing some in the PVAc segments. This could also cause the type of behaviour described above. However, the incompatibility in this system makes the precise water binding characteristics difficult to determine as although PVAc may have an appreciable water binding capacity the distribution of water between the two phases cannot be

determined.

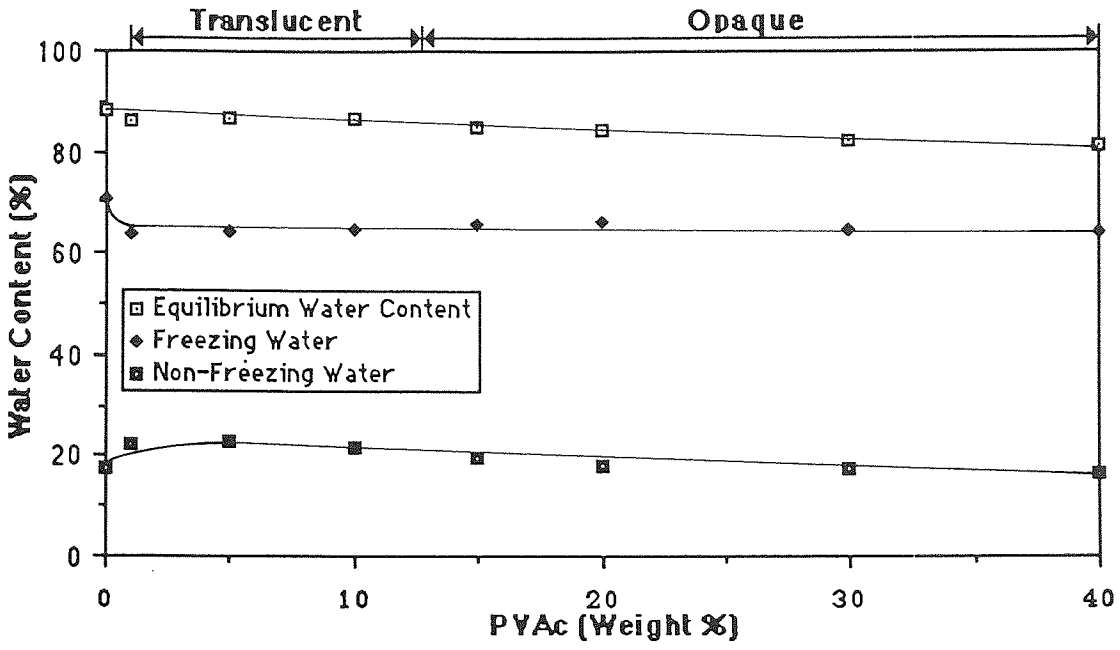

Figure 6.4 Effect of composition on the water content of NNDMA-PVAc IPN hydrogels

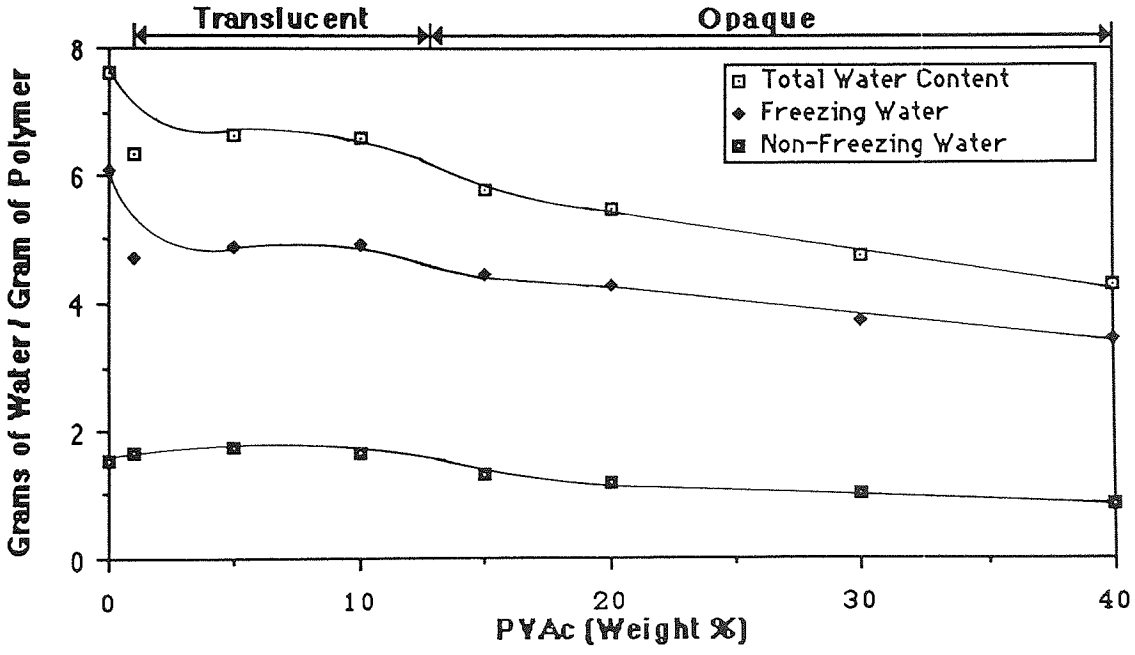

Figure 6.5 Effect of composition on the water binding of NNDMA-PVAc IPN hydrogels

The structures of poly vinyl acetate and poly methyl methacrylate are similar, therefore, it is interesting to compare the difference in water binding behaviour of these two polymers. Figures 6.6 and 6.7 illustrate the water binding characteristics of the NNDMA-PMMA IPNs in contrast with the behaviour of the NNDMA-MMA copolymers. The first point which can be made is that PMMA is less soluble in NNDMA than PVAc and therefore, a reduced composition range has been investigated. PMMA has a much greater effect on the water content than does PVAc, which would be expected as PMMA is a more hydrophobic monomer due to the α-methyl group on the backbone. This causes steric hindrance which reduces the accessibility of the water binding sites on NNDMA. Although it is useful to compare copolymers and IPNs based on the same monomers NNDMA-vinyl acetate copolymers were not synthesised as vinyl acetate is easily hydrolised. However, comparing the NNDMA-MMA copolymers and NNDMA-PMMA IPNs marked differences in behaviour are apparent.

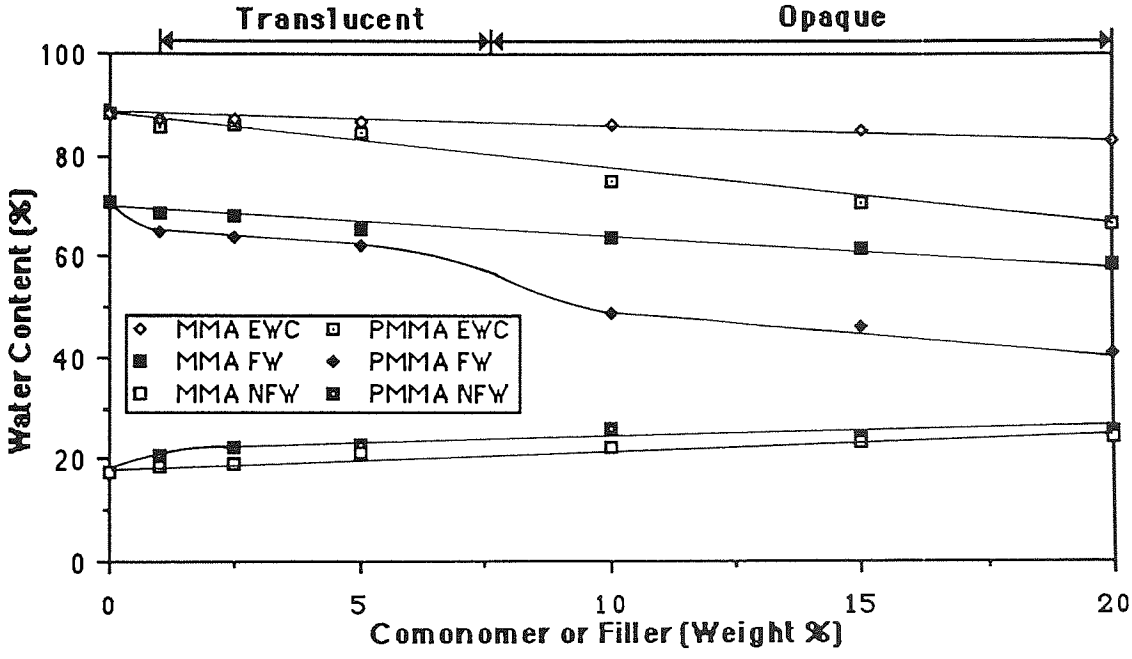

Figure 6.6 Effect of composition on the water contents of NNDMA-MMA copolymers (all clear) and NNDMA-PMMA IPNs

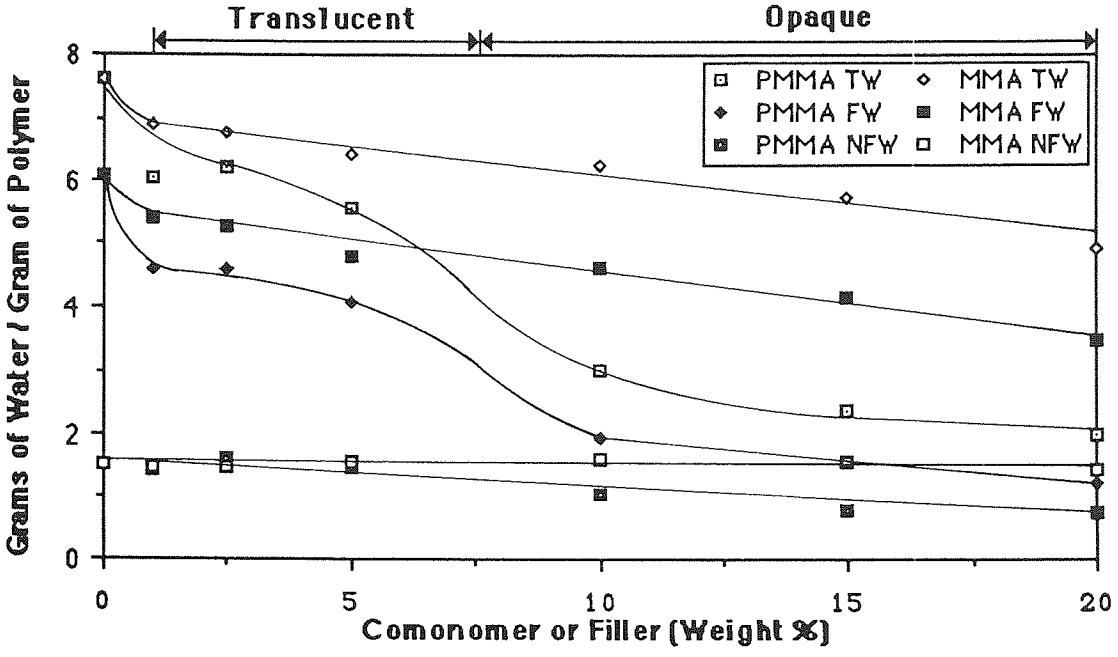

Figure 6.7 **Effect of composition on the water binding of NNDMA-MMA copolymers (all clear) and NNDMA-PMMA IPNs**

It is clear that in both systems the EWC and freezing water contents are reduced, with the effect being more marked in the IPNs than in the copolymers. This difference between the water binding behaviour of the IPNs and copolymers is best explained in terms of the compatibility of the systems. While the copolymer hydrogels are clear and compatible throughout the composition range this is not the case with the IPN hydrogels. There is a transition in these polymers from clear to opaque, as increasing amounts of PMMA are added, with the transition between translucency and opacity taking place between the 95:5 and 90:10 IPNs. This transition occurs in the dehydrated state and is due to incompatibility, not to water structuring in the IPNs. In the copolymers there is a gradual reduction in the total and freezing water with the non-freezing water appearing to pass through a maximum before decreasing. However, two marked transitions are seen in the water binding characteristics of the IPNs as expressed in terms of grams of water / gram of polymer (Figure 6.7). Interestingly, one of these transitions occurs between the same compositions

as the change in appearance from translucent to opaque occurs. Prior to this composition, although the values of total and freezing water contents of the IPNs are lower than those of the copolymers the non-freezing water content is identical, within the limits of experimental error. Between these compositions there is a dramatic fall in all types of water present followed by a steady reduction in water content. These results suggest a phase change between 5% and 10% PMMA incorporation. Subsequent to this composition the access to the water binding sites on NNDMA molecules is more restricted by the bulky α-methyl group on PMMA. There is pronounced reduction in non-freezing water content, with the fall being over twice that expected if PMMA was acting only to reduce the NNDMA concentration. Therefore, the IPN will contain hydrophobic PMMA segments coupled with water containing NNDMA segments. A similar fall in water content is seen with the incorporation of 1% of PMMA into NNDMA. In this case, however, the change in water content can be attributed to the disruption of packing in NNDMA caused by the introduction of PMMA.

IPNs were synthesised from NNDMA and the commercially available polyurethanes Biomer, Pellathane and HPU25. However, because of solubility limitations it was only possible to prepare a series of polymers with the NNDMA-Pellathane IPNs. The water binding characteristics of this system are illustrated in Figures 6.8 and 6.9. It is clear that Pellathane incorporation causes a reduction in EWC and freezing water content, with a slight increase in the non-freezing water content (Figure 6.8). Similar behaviour is shown by the limited number of Biomer and HPU25 containing IPNs examined. Pellathane incorporation reduces the EWC to a level slightly above that of PMMA, at a similar composition. When the water contents are expressed in terms of grams of water / gram of polymer (Figure 6.9) it is apparent that Pellathane incorporation causes a reduction in all types of water present.

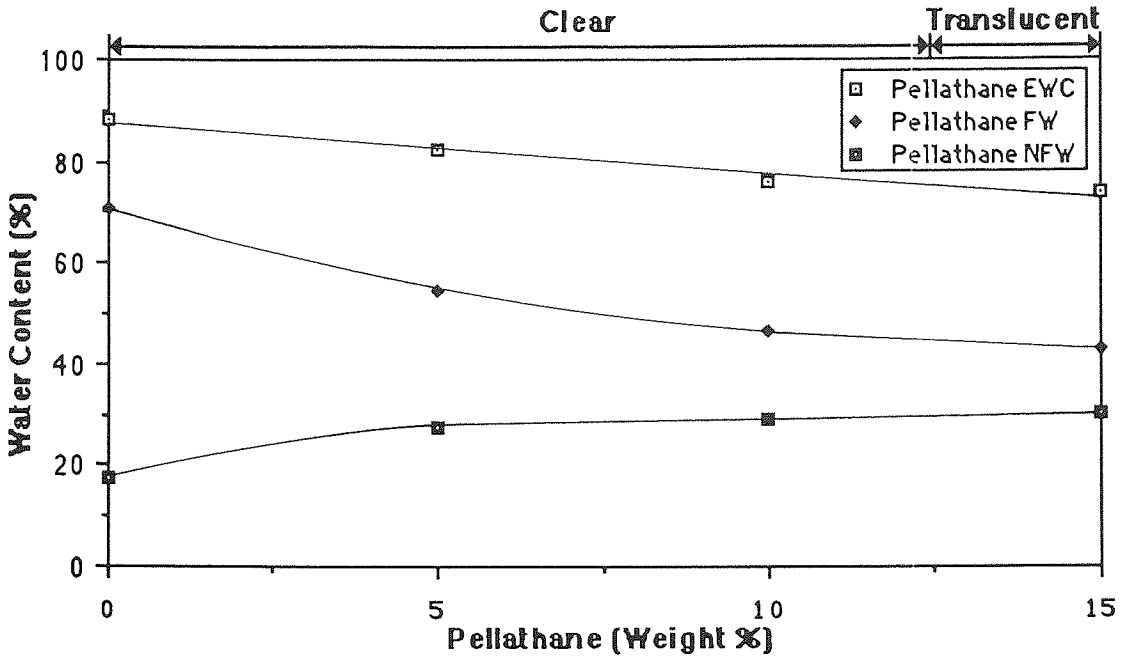

Figure 6.8 Effect of composition on the water content of NNDMA-Pellathane IPN hydrogels

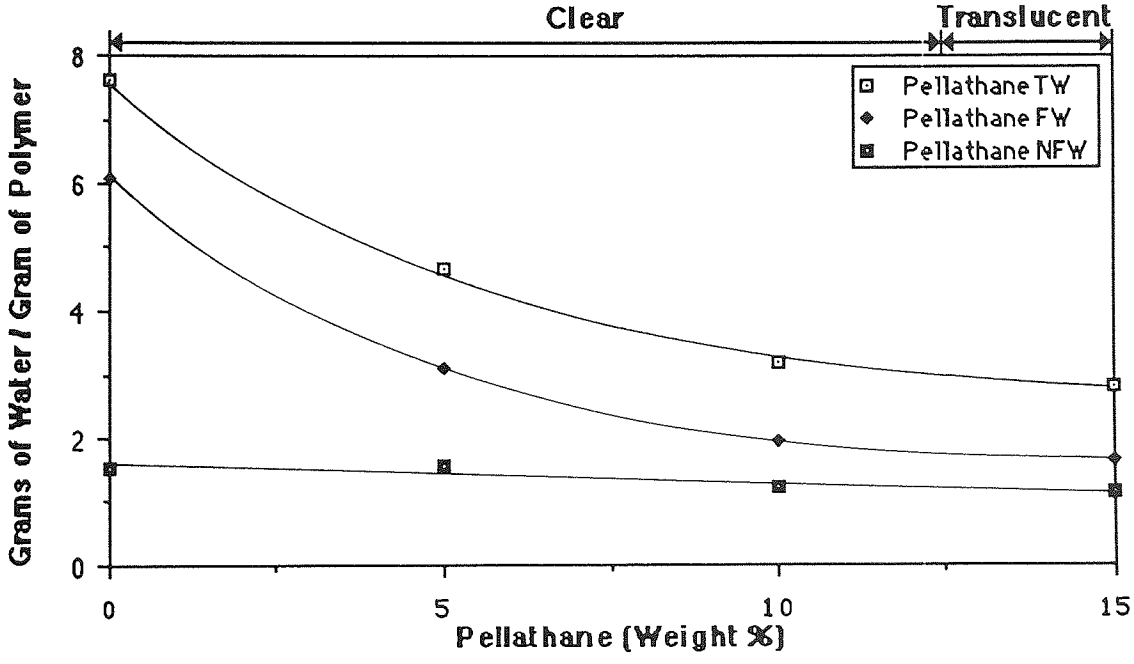

Figure 6.9 Effect of composition on the water binding of NNDMA-Pellathane IPN hydrogels

Comparing the PMMA and Pellathane containing IPNs it can be seen that at similar water contents the NNDMA-Pellathane IPNs have a much higher non-freezing water content. These values are lower than would be expected if Pellathane was acting just as a filler polymer. However, Pellathane has an excess of hydrophilic groups and there will almost certainly be an interaction between these hydrophilic groups and the water binding sites on NNDMA. This will tend to further reduce the water binding ability of the system. This reduction will be compensated for, in part, by water binding to the Pellathane. The effect of the water binding ability of the polyurethane on the water content of NNDMA-polyurethane IPNs can be demonstrated by comparing the EWCS of NNDMA-Pellathane and NNDMA-HPU25 IPNs. HPU25 is a more hydrophilic polyurethane than Pellathane and the EWC of the 90:10 NNDMA-HPU25 IPN is 10% higher than the corresponding NNDMA-Pellathane IPN.

The water binding properties of IPN hydrogels of NNDMA and the epoxide of poly (1, 2, dihydroxy cyclohexa 3, 5, diene dimethyl carbonate) (EPDCD) were examined as this polymer appeared to have a potential for use in IPNs, having a fairly rigid backbone with hydrophilic pendant groups. However, it can be seen that the incorporation of EPDCD into NNDMA leads to a reduction in the EWC and freezing water with an apparent rise in the non-freezing water content (Figure 6.10). The marked effect of EPDCD incorporation is best represented in terms of grams of water / gram of polymer (Figure 6.11). This Figure illustrates that the water binding ability of the IPNs, as expressed in terms of non-freezing water, is marginally reduced by EPDCD incorporation. As in the NNDMA-Pellathane system the major effect of EPDCD incorporation is seen to be in the reduction of the freezing water present in the IPN. In terms of the two state model for the structure of water discussed previously, EPDCD reduces the amount of unassociated (or weakly associated) water present in the hydrogel. Access to the water binding sites on the NNDMA molecules

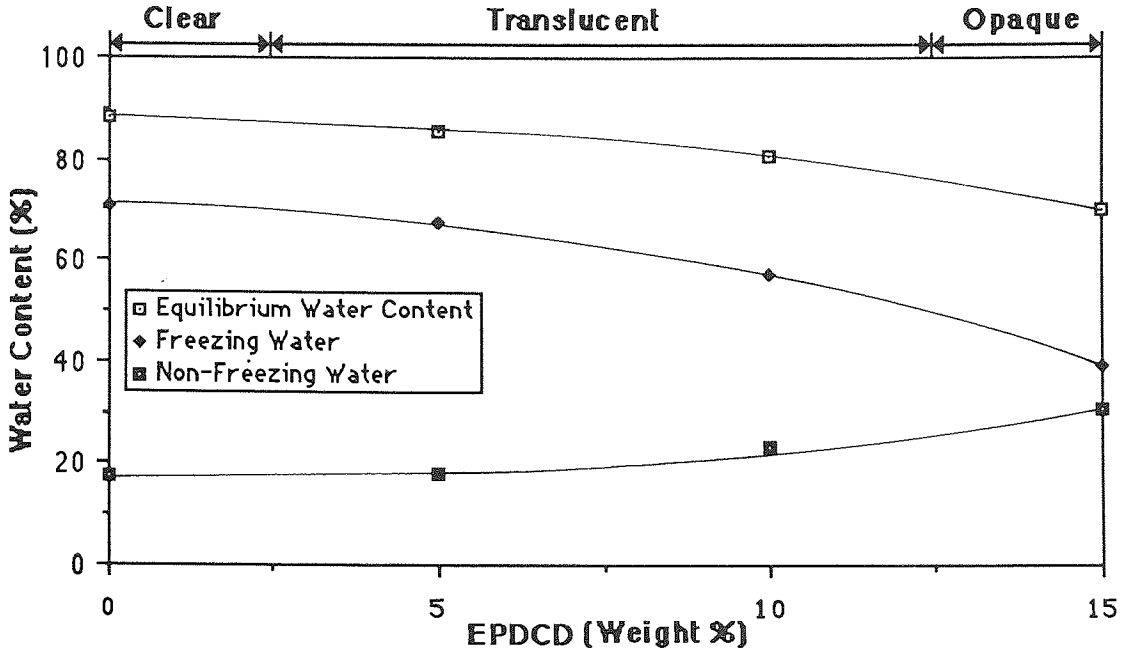

Figure 6.10 Effect of composition on the water content of NNDMA-EPDCD IPN hydrogels

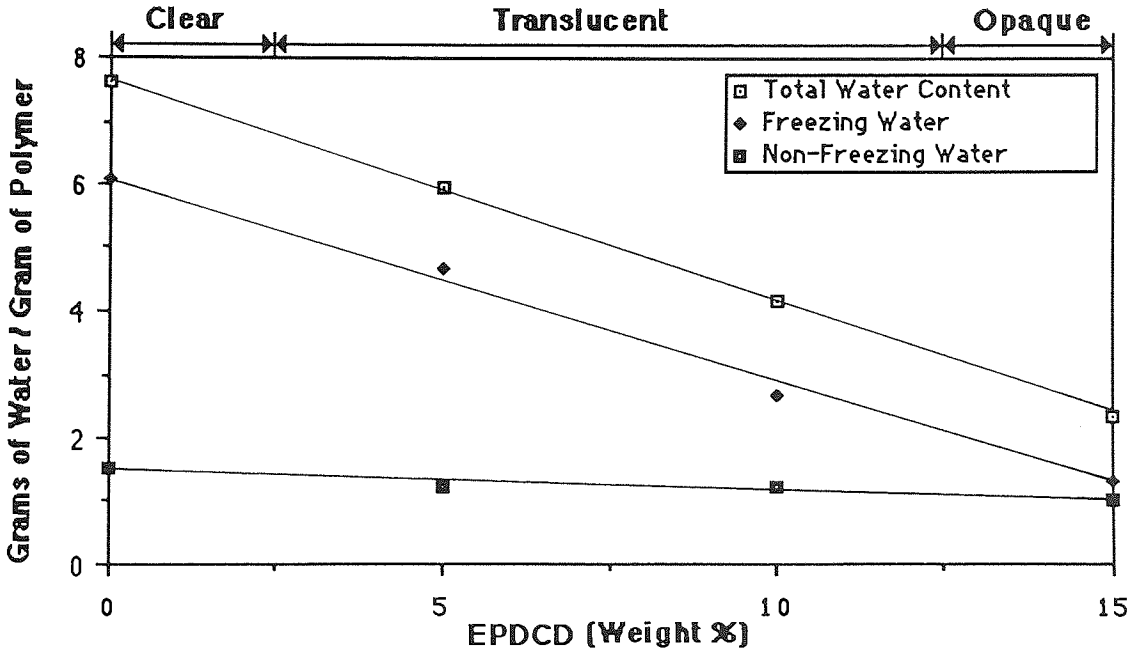

Figure 6.11 Effect of composition on the water binding of NNDMA-EPDCD IPN hydrogels

must also be restricted, as the water binding capacity of the IPNs is lower than would be expected if it was assumed that EPDCD was just acting as a filler and reducing the NNDMA concentration in the IPN. This reduction in water binding ability is characteristic of the introduction of a bulky, relatively hydrophobic monomer which will reduce both the hydrophilicity and the available "space" in the polymer network. In this system, as in the NNDMA-PVAc IPNs, the incorporation of increasing amounts of filler polymer changes the appearance of the membrane. The membranes change from clear (poly NNDMA), through translucence, to opacity in the NNDMA-EPDCD 85:15 IPN. This change in appearance may be caused by either inhomogeneous distribution of water in the system or phase separation due to incompatibility. However, in this system phase separation is the most likely cause of the opacity as domains are clearly visible in the 85:15 NNDMA-EPDCD IPN.

The water binding properties of two further IPN systems containing filler polymers with a backbone based on a ring system, cellulose acetate (CA) and cellulose acetate butyrate (CAB), were also investigated. The behaviour of these systems is illustrated in Figures 6.12 and 6.13. The first point which can be made about these systems is that IPN formation with either CA or CAB causes a reduction in both EWC and freezing water content while the non-freezing water content remains relatively constant. However, when the values are expressed in terms of grams of water / gram of polymer (Figure 6.13) a downward trend in the non-freezing water content is also apparent. There is a small, but real, reduction in water content in the NNDMA-CAB IPNs in comparison with NNDMA-CA IPNs of similar composition. The structural similarities of CA and CAB suggest that only a small difference, if any, should be seen between the water binding of IPNs containing these filler polymers. Although the rings in the backbone are the major factor in determining the hydrophilicity of the molecule the slightly greater hydropobicity of CAB, caused by CH_2 insertion in the pendant sidechain can be detected.

insertion in the pendant sidechain can be detected.

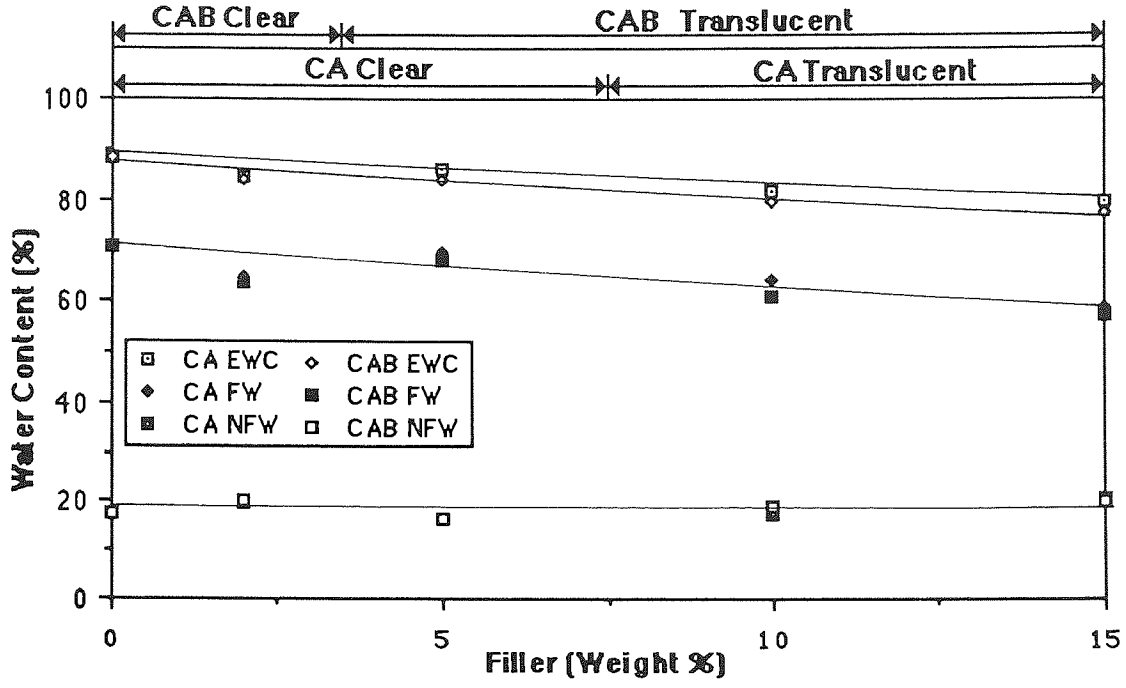

Figure 6.12 Effect of composition on the water content of NNDMA-CA and NNDMA-CAB IPN hydrogels

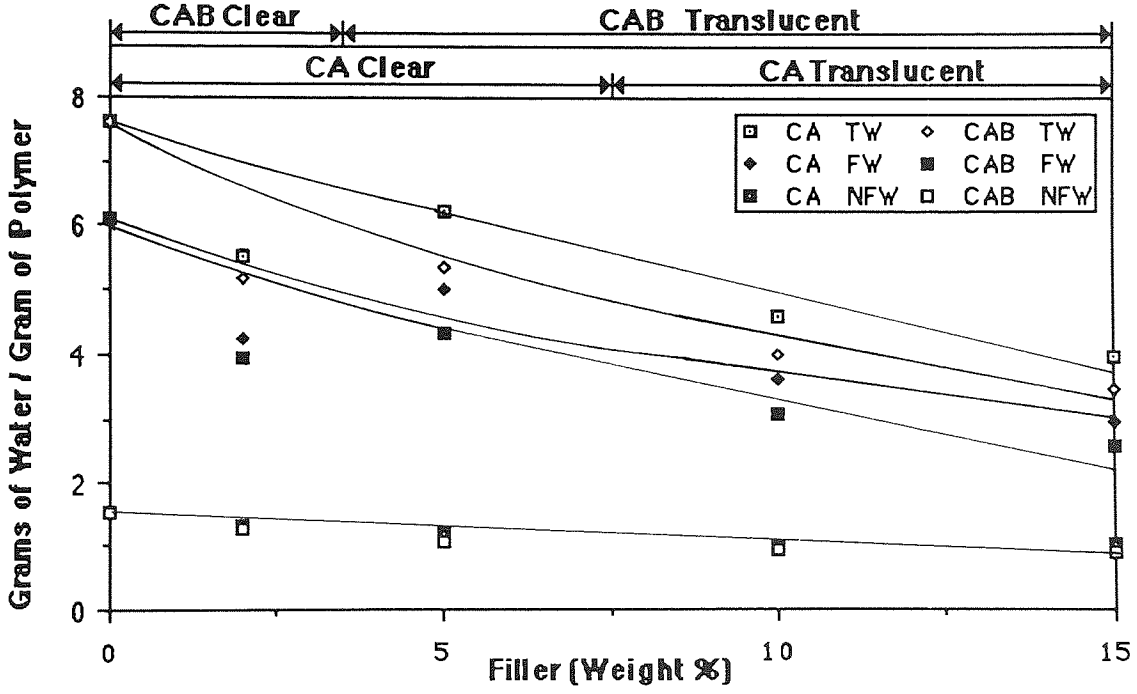

Figure 6.13 Effect of composition on the water binding of NNDMA-CA and NNDMA-CAB IPN hydrogels

In contrast to the NNDMA-EPDCD and NNDMA-Pellathane IPN hydrogels described previously, in the NNDMA-CA and NNDMA-CAB systems there is a more dramatic fall in the non-freezing water content than would be expected, while the freezing water content is proportionately higher. As is the case with NNDMA-Pellathane IPNs there are an excess of hydrophilic sites on the CA and CAB chains. Thus, there are two possible mechanisms by which the water content of the system may be reduced. CA and CAB may restrict access to the water binding sites on NNDMA by steric occlusion. However, the hydrophilic groups on the chain may also interact with the hydrophilic binding sites on NNDMA, reducing its water binding ability. This reduction in water binding ability will be partially offset by the water binding to the remaining hydrophilic sites on the CA and CAB chains.

Having compared the difference in water binding between NVP and NNDMA in copolymers it is interesting to see if these same differences in behaviour are displayed in IPNs based on these monomers. One point which should be made about these families of IPNs is the difference in the synthetic routes to the polymers. NNDMA is a good solvent and can dissolve appreciable amounts of CA or CAB. However, this is not the case with NVP. Therefore, while in those IPNs based on NNDMA the filler polymer was dissolved in the monomer, in those based on NVP 10% of a cosolvent (e.g. toluene, acetone or tetrahydrofuran) was added to the system to aid dissolution. However, after hydration for two weeks, with regular changes of water, no solvent could be detected leaching from the gels. The NVP gels described here were all synthesised using toluene as a cosolvent but studies with varying concentrations of a range of cosolvents demonstrated that the solvent had a negligible effect (i.e <1% change) on the EWCs in these systems.

The poor solubility of filler polymers in NVP would limit the commercial applications of IPNs of this type based on this monomers. However, the structural similarities between the

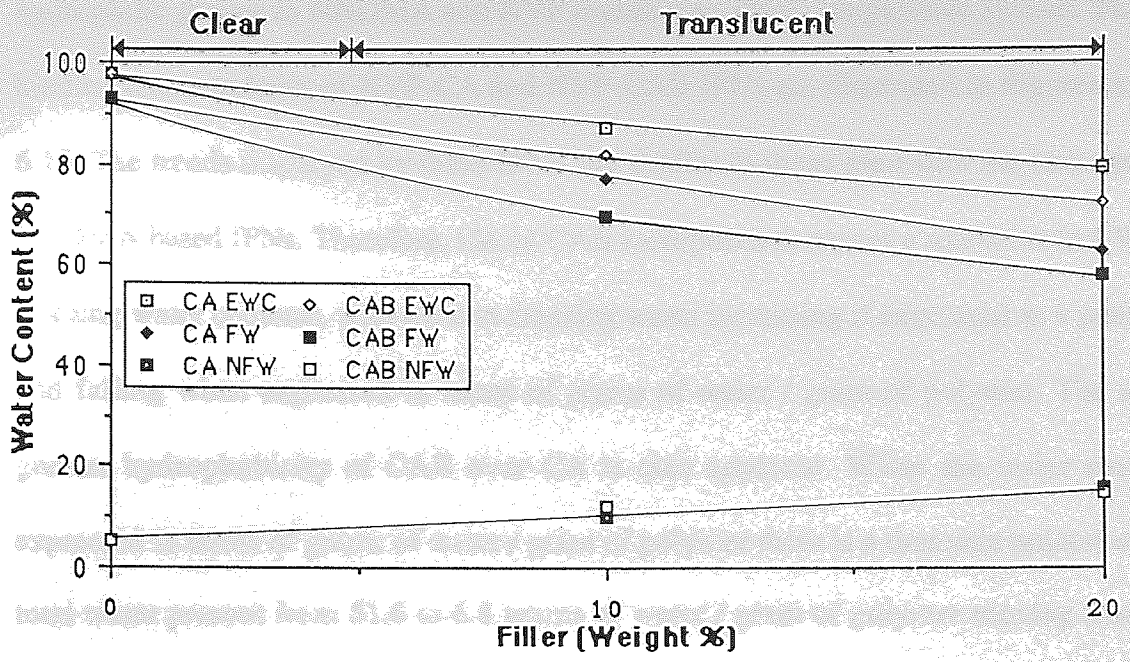

Figure 6.14 Effect of composition on the water content of NVP-CA and NVP-CAB IPN hydrogels

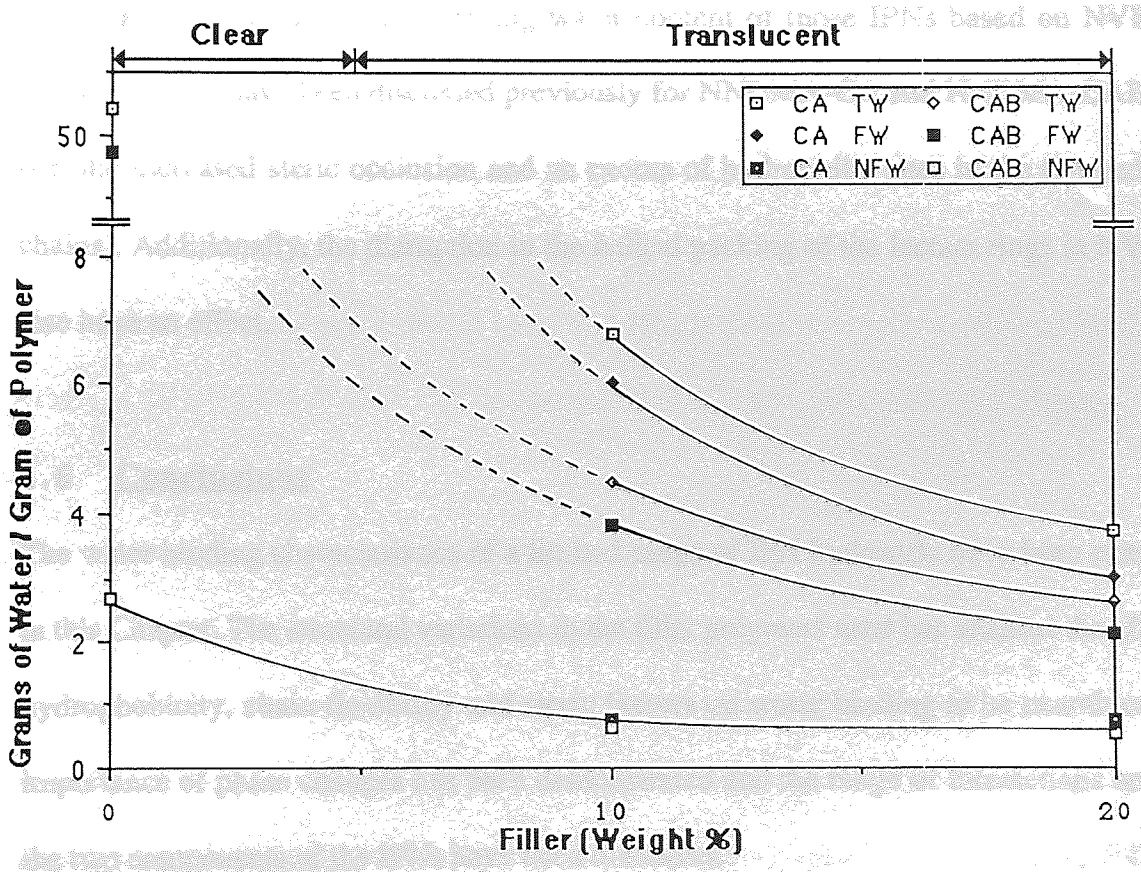

Figure 6.15 Effect of composition on the water binding of NVP-CA and NVP-CAB IPN hydrogels

hydrophilic groups in NNDMA and NVP makes it an ideal comparative system. The water binding characteristics of NVP-CA and NVP-CAB IPNs are illustrated in Figures 6.14 and 6.15. The trends displayed by these IPNS are similar to those seen with the corresponding NNDMA based IPNs. Therefore, CA or CAB incorporation causes a reduction in EWC and freezing water contents, with the non-freezing water increasing if expressed as a percentage and falling when expressed in terms of grams of water / gram of polymer. The slightly greater hydrophobicity of CAB over CA is also apparent. When the water content is expressed in terms of grams of water / gram of polymer there is a dramatic reduction in the total water present from 51.6 to 6.8 grams of water / gram of polymer moving from poly NVP to the NVP-CAB 90:10 IPN. This illustrates the marked change in grams of water / gram of polymer that can be caused by small changes in water content, when dealing with high water content materials. The major difference between the NVP based and NNDMA based IPNs is the lower non-freezing water content of those IPNs based on NVP. The reasons for this have been discussed previously for NNDMA-CA and NNDMA-CAB IPNs (i.e. the increased steric occlusion and an excess of hydrophilic sites in the CA and CAB chains). Additionally, the disruption in the helical packing of the lactam rings in NVP will also have an effect.

6.6 Conclusions

The water binding characteristics of a limited range of IPN hydrogels have been examined in this Chapter. The structural variations in the filler polymers used has enabled the effect of hydrophobicity, chain flexibility and steric factors on water binding to be examined. The importance of phase changes has been demonstrated and the range of interactions between the two components of the IPNs have been discussed.

The NNDMA-PVAc IPNs proved a good "baseline" series to study as the high solubility of

PVAc in NNDMA enabled an extended composition range to be examined. A phase change was also observed in this system, which is characteristic of several IPN systems examined in this work. When the water content of these IPNs is expressed in terms of grams of water / gram of polymer the values suggest that PVAc has no influence on the water structuring in these IPNs and acts solely to reduce the NNDMA concentration.

Despite the structural similarities between PVAc and PMMA the water binding characteristics of NNDMA IPNs with these filler polymers differ significantly. NNDMA-PMMA IPNs are more hydrophobic than those containing PVAc; this is a function of the α-methyl group on the backbone of PMMA which increases steric occlusion and causes a dramatic reduction in both EWC and non-freezing water content. The effect of PMMA is more marked subsequent to the phase change in the IPN signalled by the change in appearance from translucent to opaque. This phase change also marks the point at which the water binding properties of the copolymer and IPN begin to differ significantly. Although the EWC and freezing water contents of the IPNs are lower than those of the copolymer prior to this composition, this variation can be attributed to to the difference in distribution of the MMA in the materials. While in the copolymer there is a random, even distribution of MMA in the IPNs the PMMA will be concentrated in blocks throughout the system.

The NNDMA-polyurethane IPNs synthesised display differences in water binding behaviour to those systems previously described. The excess hydrophilic groups on the polyurethane segments interact with the water binding sites on NNDMA. Therefore, Pellathane incorporation, for example, substantially reduces the EWC. Although the non-freezing water content is reduced by intramolecular interaction the water binding ability of the polyurethane will tend to increase this value. Therefore, the more hydrophilic NNDMA-HPU25 IPN has a greater non-freezing water content than the comparable NNDMA-

Pellathane IPN.

The water binding properties of IPNs with filler polymers which have rings in the backbone are affected not only by the nature of the ring but also by the pendant groups. Therefore, slight differences are observed between CA and CAB containing IPNs with the CAB containing IPNs being more hydrophobic. Interestingly, differences are seen in the distribution of water in the NNDMA-EPDCD and the NNDMA-CA and NNDMA-CAB IPNs. Thus, whilst the NNDMA-EPDCD IPNs have a lower EWC they have a higher non-freezing water content than the IPNs containing CA and CAB. This is a reflection of the excess of hydrophilic groups in CA and CAB which interact with the water binding sites in NNDMA reducing the amount of non-freezing water in the IPNs.

Interpenetrating Polymer Network Hydrogels:
Mechanical Properties

CHAPTER 7

Interpenetrating Polymer Network Hydrogels: Mechanical Properties

7.1 Introduction

In the previous Chapter, the water binding properties of IPN hydrogels were discussed and related to changes in the structure of the filler polymer. In this Chapter the mechanical properties of these IPNs will be examined. By synthesising IPNs it may be possible to produce stiffer and stronger NNDMA based polymers and the effect of structural differences in the filler polymers will be investigated. Full IPNs are known to exhibit unusual mechanical properties[210,212]. Thus, the semi-IPNs synthesised in this work were investigated to see if any anomalies were apparent.

7.2 IPN Hydrogels: Mechanical Properties

The mechanical properties of IPNs have attracted a great deal of interest and it has been shown that syneresis does occur in such systems, particularly if one component is dispersed in a continuous phase of the second component[219]. NNDMA based IPNs prove a particularly sensitive system to study changes in mechanical properties because of the initial fragility of poly NNDMA. The mechanical properties of the IPNs synthesised have been investigated under tension and the results are discussed below.

The NNDMA-PVAc IPNs synthesised had low tensile strengths and Youngs moduli, however, reasonable values were obtained for elongation to break in this system and these are illustrated in Figure 7.1. It can be seen that after an initial rise ε_b begins to fall, subsequent to the 90:10 NNDMA-PVAc IPN. The appearance of the IPNs also changes, from translucent to opaque, subsequent to this composition and a change in the water binding properties is also observed (Figure 6.5). Interestingly, the shape of the composition versus elongation to break curve parallels that of composition versus freezing water. The plasticising effect of freezing water has been demonstrated previously by workers in these laboratories[145]. Therefore, the phase change which occurs at this composition, alters the

morphology of the system, reducing the freezing water content which in turn causes a reduction in ε_b in this system.

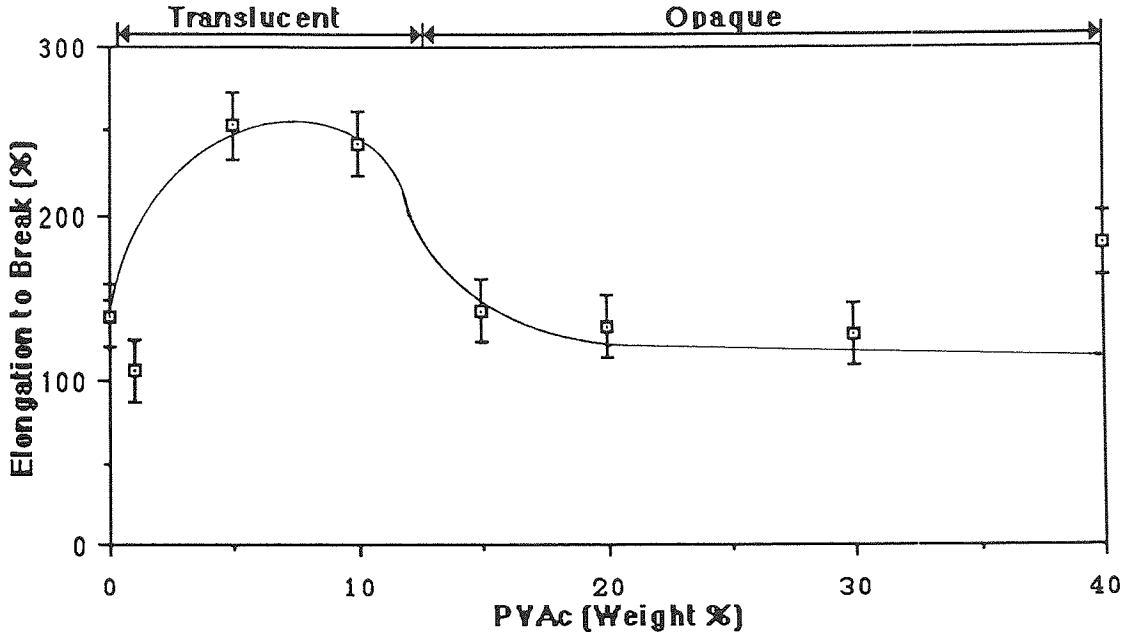

Figure 7.1 Effect of composition on the elongation to break of NNDMA-PVAc IPN hydrogels

The poor mechanical properties shown by this system demonstrate that σ_b is not an additive property as the incorporation of 40% of PVAc, with a σ_b of approximately 30MPa, causes a reduction in tensile strength. Therefore, other factors such as compatibility and EWC must also have a part to play in determining σ_b.

The mechanical properties of NNDMA-PMMA IPNs are illustrated in Figures 7.2-7.4 and contrasted with those of NNDMA-MMA copolymers. The structural changes involved in moving from PVAc to PMMA cause a dramatic increase in E and σ_b of the IPNs. One factor which is common to both systems is the effect of the phase change on mechanical properties; this will subsequently be discussed in more detail. However, it is sufficient to

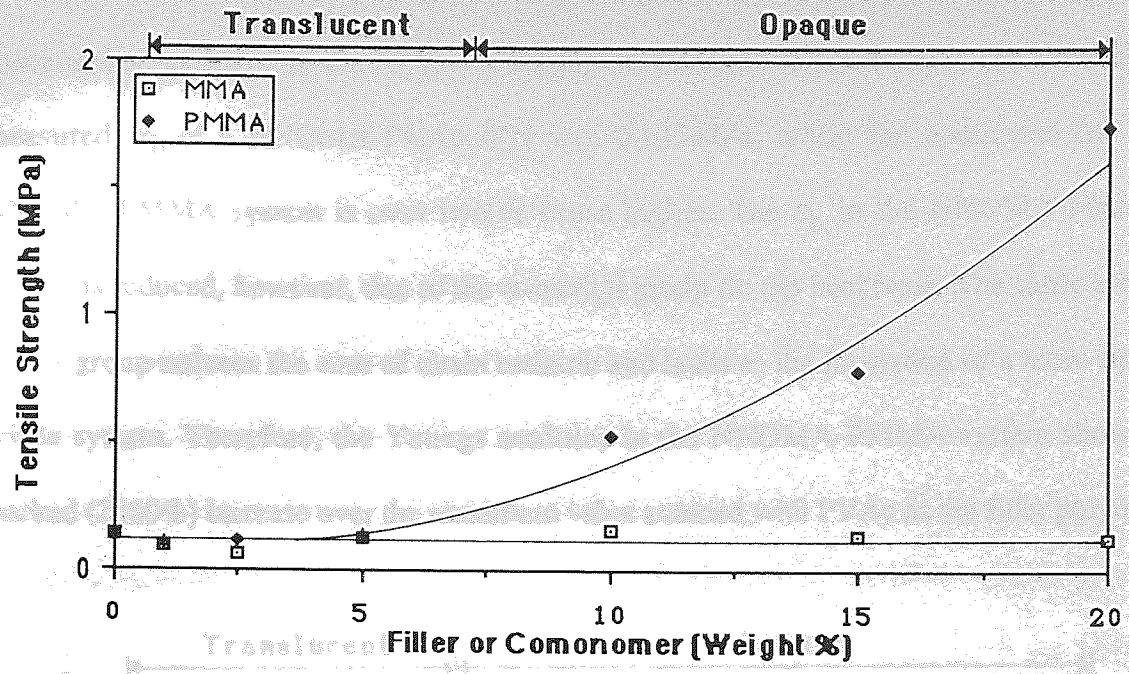

Figure 7.2 Comparison of the tensile strength of NNDMA-MMA copolymer hydrogels (all clear) and NNDMA-PMMA IPN hydrogels

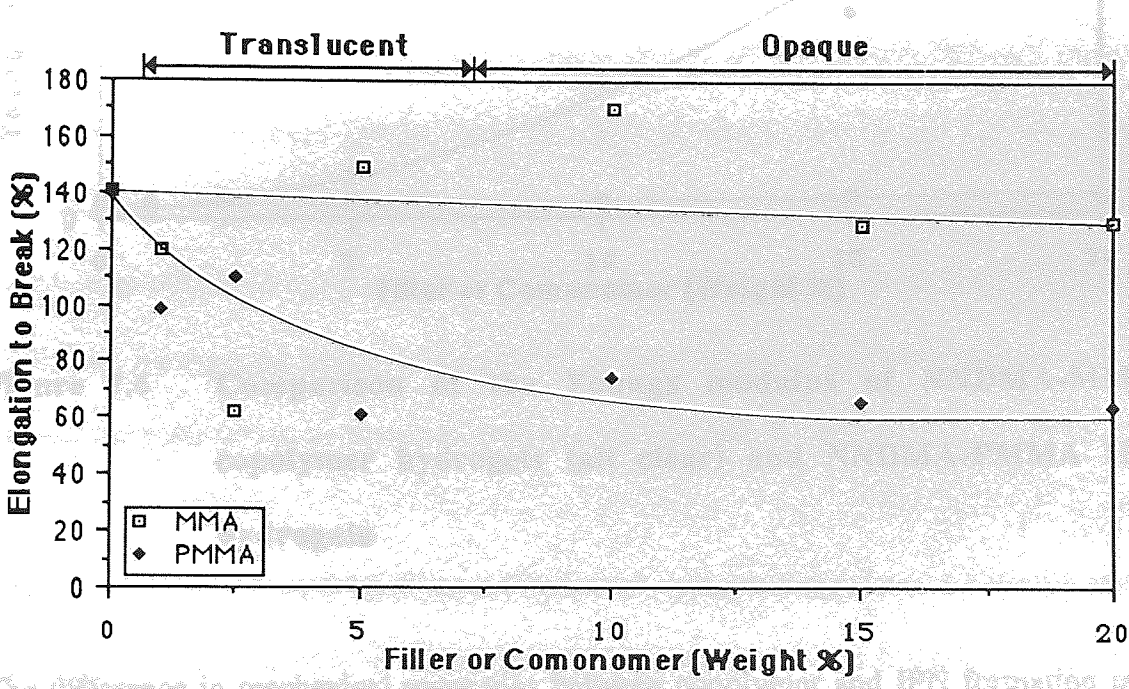

Figure 7.3 Comparison of the elongation to break of NNDMA-MMA copolymer hydrogels (all clear) and NNDMA-PMMA IPN hydrogels

note that there is not a smooth transition in mechanical properties with changes in composition, as found in the NNDMA copolymers examined previously. The maximum measured σ_b of a NNDMA-PVAc IPN was 0.145MPa, while the maximum for the NNDMA-PMMA system is over twelve times higher. The ε_b in the NNDMA-PMMA system is reduced, however, due to the α-methyl group on the backbone. The steric effect of this group reduces the ease of chain rotation and leads to the formation of a more rigid, brittle system. Therefore, the Youngs modulus in the NNDMA-PMMA system shows a marked (2500%) increase over the maximum value attained with PVAc as the filler polymer.

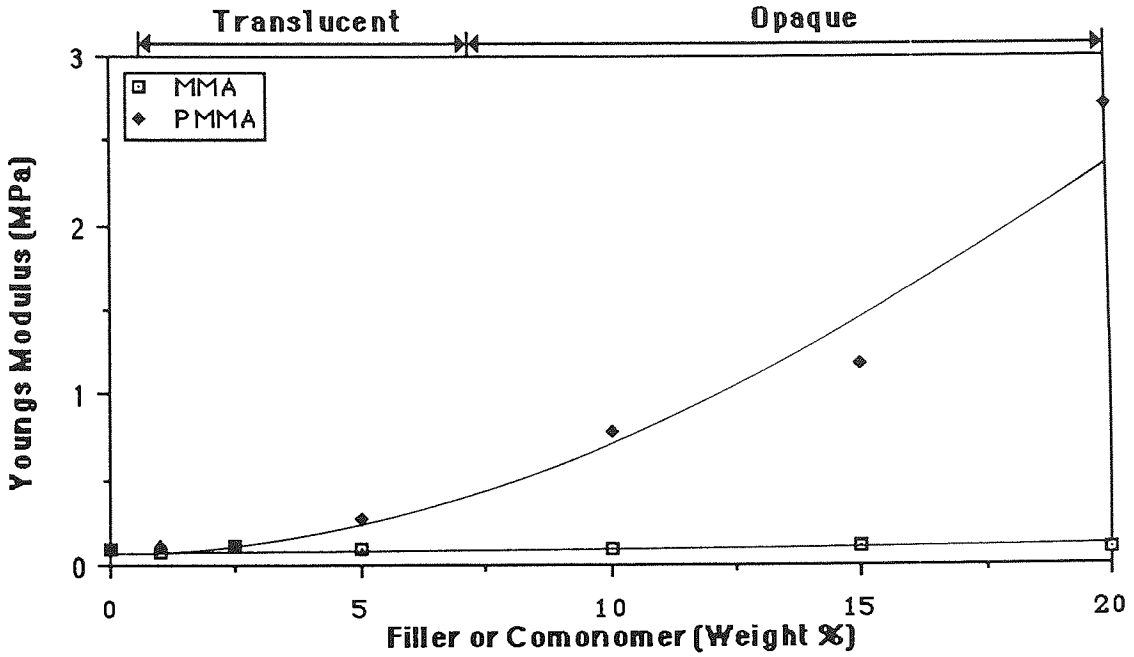

Figure 7.4 **Comparison of the Youngs modulus of NNDMA-MMA copolymer hydrogels (all clear) and NNDMA-PMMA IPN hydrogels**

The difference in mechanical properties between copolymer and IPN formation in the NNDMA-MMA system are also illustrated in Figures 7.2-7.4. Comparing the tensile strengths of both systems (Figure 7.2) it is clear that both the copolymers and IPNs have similar tensile strengths until 5% MMA or PMMA is present in the system. At this point,

however, the behaviour of the two systems diverges. The σ_b of the NNDMA-MMA does not vary significantly, showing only a slight increase, at compositions with a higher MMA concentration. In contrast, the σ_b of the NNDMA-PMMA IPNs increases by a factor of 12 between the 95:5 and 80:20 compositions. It is interesting to note that this divergence of behaviour occurs at the point where the appearance and water binding properties of the IPNs are also changing (Figure 6.7) and it is apparent that the phase change has an equally dramatic effect on the mechanical properties of the copolymer. One reason for the marked difference in mechanical properties between copolymer and IPN formation is the distribution of the MMA in the system. While in the copolymers the MMA will be present in single monomer units or oligomeric chains evenly distributed throughout the NNDMA matrix, this is not the case in the IPNs. After incorporation of 10% PMMA, large blocks of high molecular weight PMMA will be present in the IPN. It is these MMA domains which lead to the improvement of mechanical properties

The elongation to break of the copolymers and IPNs also show different patterns of behaviour. In the copolymers there is much scatter in the ε_b but ε_b does not vary significantly over the composition range, showing a only a slight decrease. In the IPNs there is an initial fall in ε_b until the NNDMA-MMA 95:5 composition is reached, which is followed by a period where no significant change occurs. The phase change once again marks the point where an alteration in properties occurs in this system.

The Youngs moduli of the polymers (Figure 7.4) behave similarly to the tensile strengths with the behaviour of the NNDMA-MMA copolymers and NNDMA-PMMA IPNs diverging subsequent to the 95:5 composition. The reasons for this behaviour have been discussed previously.

Several IPNs based on commercially available, biotolerant, polyurethanes (which have been used extensively as biomaterials) were synthesised. The composition range of the IPNs was once again limited by the solubility of the polyurethanes in NNDMA. Therefore, only the results obtained from NNDMA-Pellathane IPNs, where it was possible to synthesise a series of polymers, are shown in the Figures below. Pellathane incorporation leads to an increase in σ_b and a hydrogel with a higher σ_b than poly HEMA but with twice its EWC can be synthesised using this filler polymer.

The relative flexibility of the polyurethanes can be seen by comparing the ε_b of NNDMA-PMMA and NNDMA-polyurethane IPNs. Although Pellathane incorporation leads to systems with the lowest ε_b among the PUs, the IPNs produced are evidently more flexible than comparable compositions with PMMA as the filler polymer. It is difficult to attribute differences in mechanical properties to changes in the structures of the polyurethanes in all the systems examined as the precise structures are unknown, however, these results suggest

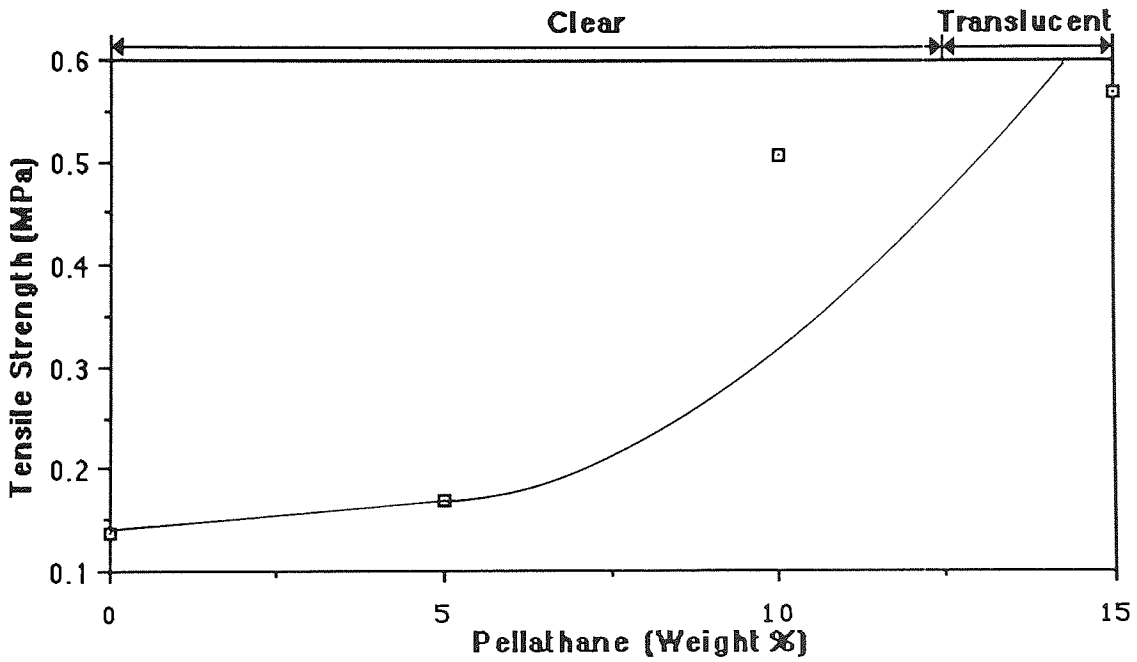

Figure 7.5 **Effect of composition on the tensile strength of NNDMA-Pellathane IPN hydrogels**

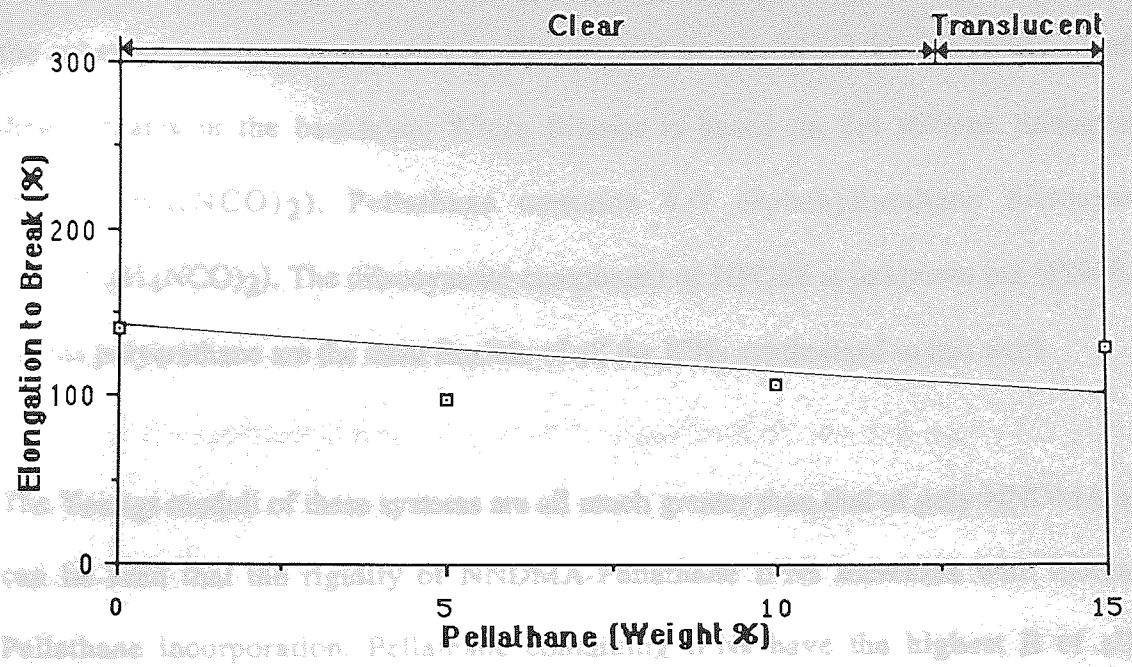

Figure 7.6 Effect of composition on the elongation to break of NNDMA-Pellathane IPN hydrogels

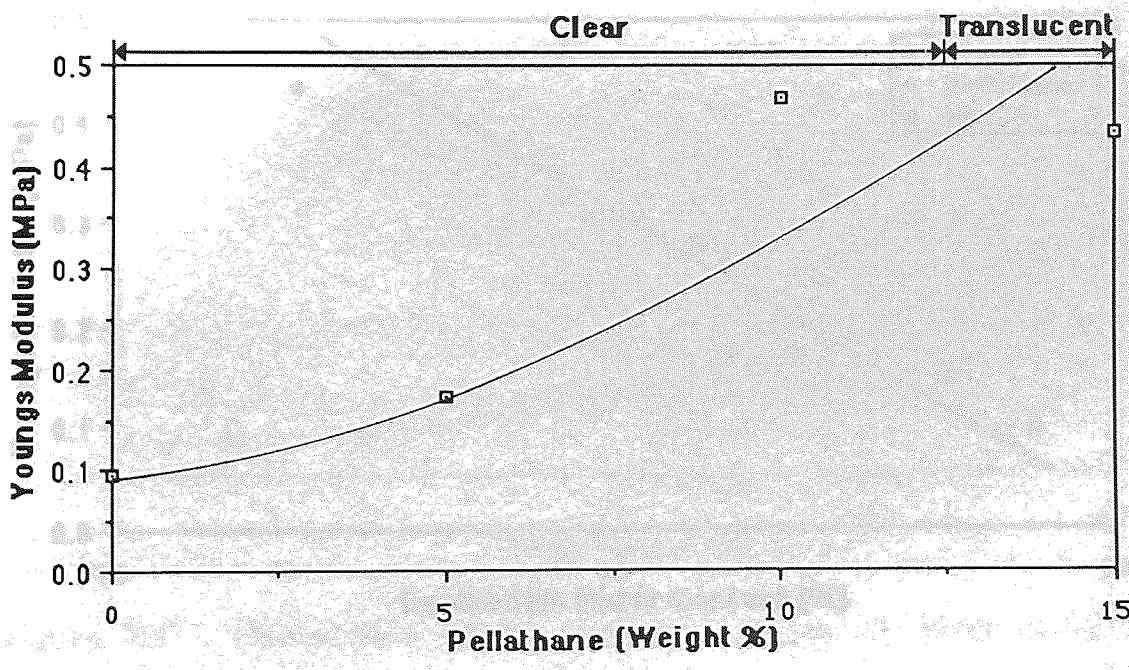

Figure 7.7 Effect of composition on the Youngs modulus of NNDMA-Pellathane IPN hydrogels

that Pellathane is the most rigid of the polyurethanes examined. Its increased rigidity over the other polyurethanes studied e.g. Biomer can be explained by the structure of the diisocyanates in the backbone. While Biomer is based on 2,4 toluene diisocyanate ($CH_3C_6H_3(NCO)_2$), Pellathane contains 4,4' diphenylmethane diisocyanate ($CH_2(C_6H_4NCO)_2$). The diisocyanate component of HPU25 is unknown but IPNs based on this polyurethane are the most flexible of all the IPNs synthesised in this work.

The Youngs moduli of these systems are all much greater than that of poly NNDMA and it can be seen that the rigidity of NNDMA-Pellathane IPNs increases with increasing Pellathane incorporation. Pellathane containing IPNs have the highest E of all the polyurethanes examined. The trend shown in E is similar to that seen in σ_b and the values of E show a significant improvement on those for poly NNDMA reaching nearly double the value for poly HEMA. The values of E obtained for all the polyurethane containing IPNs

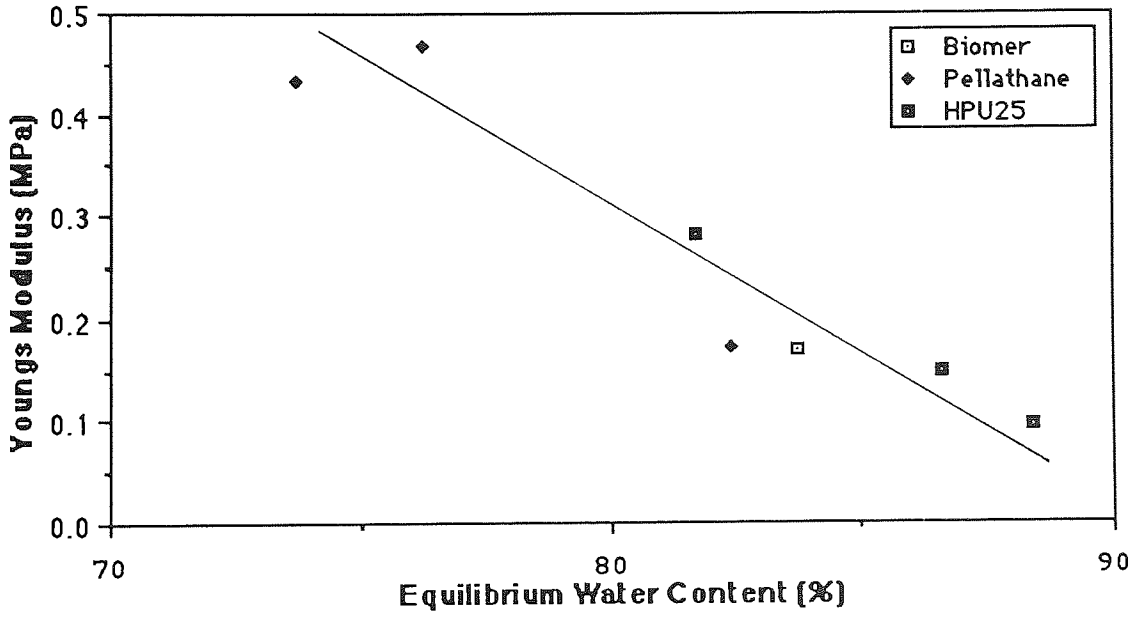

Figure 7.8 **Variation in the Youngs modulus of NNDMA-Biomer, NNDMA-Pellathane and NNDMA-HPU25 IPN hydrogels with equilibrium water content**

can be smoothed if they are presented as a function of water content. This is illustrated in Figure 7.8 and it is apparent that despite the structural differences between the polyurethanes, EWC is the major factor controlling E in these high water content systems.

A range of commercially available filler polymers were examined in this work and PMMA was found to be the polymer which gave the greatest improvement in mechanical properties. However, the mechanical properties of IPNs based on NNDMA and a new ICI polymer, the epoxide of poly (1, 2, dihydroxy cyclohexa 3, 5, diene dimethyl carbonate) (EPDCD), were also examined. Figures 7.9-7.11 illustrate the mechanical properties of the three IPNs synthesised using this monomer in comparison with the NNDMA-PMMA IPNs described previously.

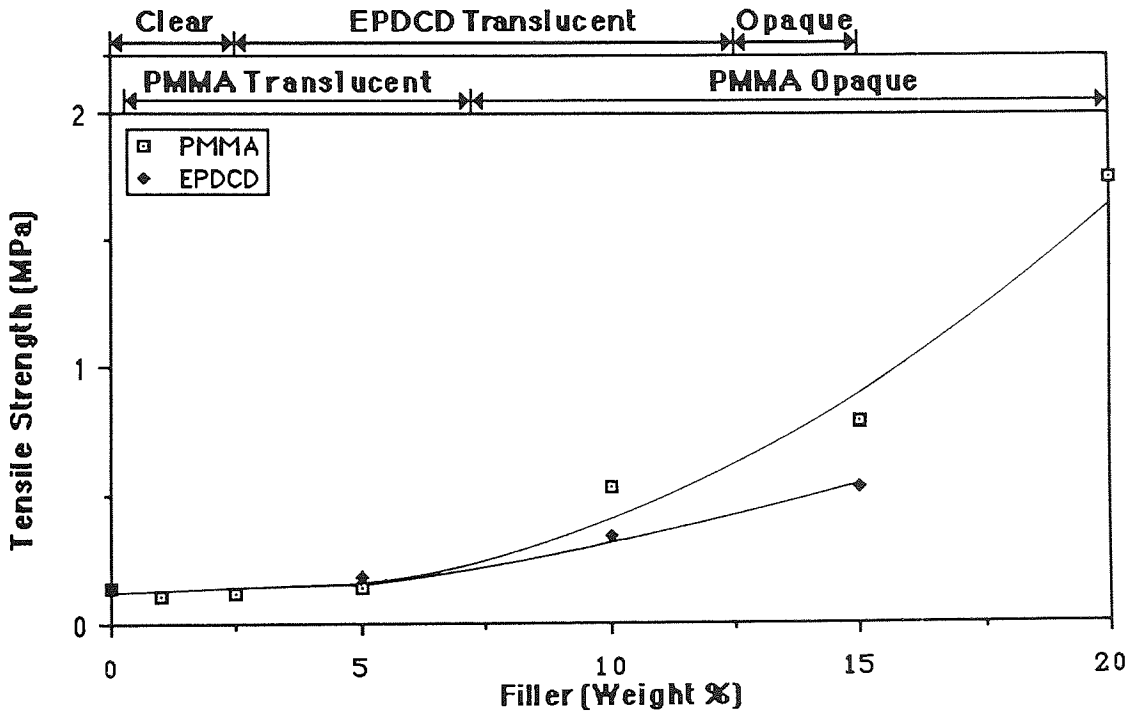

Figure 7.9 **Comparison of the tensile strength of NNDMA-PMMA and NNDMA-EPDCD IPN hydrogels**

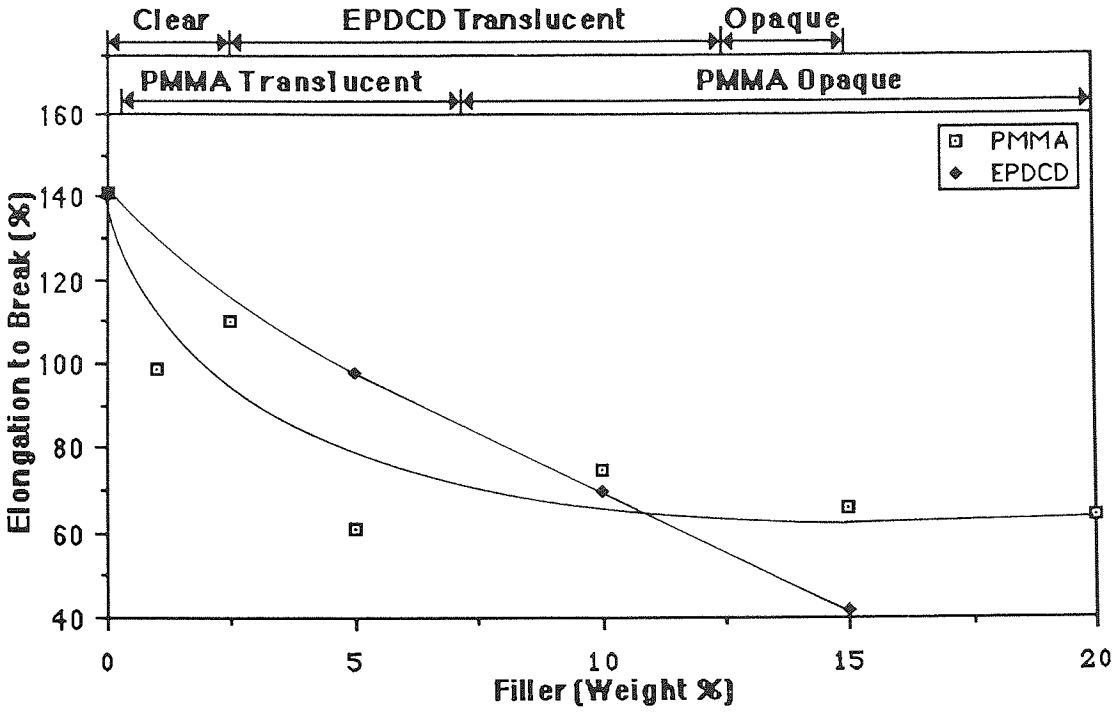

Figure 7.10 Comparison of the elongation to break of NNDMA-PMMA and NNDMA-EPDCD IPN hydrogels

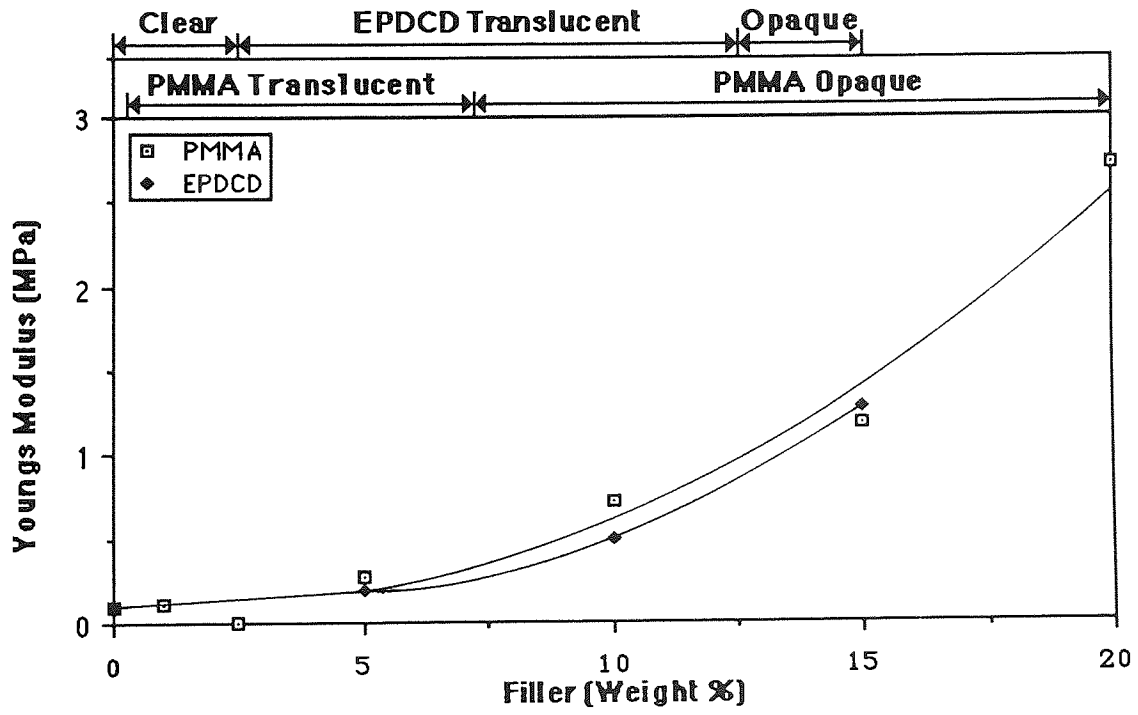

Figure 7.11 Comparison of the Youngs modulus of NNDMA-PMMA and NNDMA-EPDCD IPN hydrogels

It is clear that the NNDMA-EPDCD IPNs have slightly lower tensile strengths than those of NNDMA-PMMA IPNs at similar compositions and EWCs. The relatively high σ_b of NNDMA-EPDCD IPNs can be attributed to the incorporation of a bulky, sterically hindering, stiff polymer into the NNDMA matrix. However, the elongation to break of these materials decreases rapidly with increasing EPDCD incorporation. This IPN series also demonstrates a dramatic reduction in freezing water with increasing EPDCD concentration. Therefore, one of the reasons for the fall in ε_b is the reduction in the amount of plasticising water present in the gels. The Youngs moduli of the IPNs are again similar to those found in the NNDMA-PMMA system and the highest of all the IPNs examined in this work. Although these IPNs have very high tensile strengths and Youngs moduli they are, perhaps, too brittle for use in biomedical applications. A range of polymers based on the same backbone but with a range of sidechains can be synthesised. Thus, it is possible that by incorporating long, flexible side chains or sidechains which increased the freezing water content, an IPN with a high tensile strength and a more acceptable ε_b could be synthesised. However, because of the nature of the backbone it is likely that the IPNs based on polymers of this type will always tend to be stiff.

The mechanical properties of NNDMA-CA and NNDMA-CAB IPNs are illustrated in Figures 7.12-7.14. The filler polymers in these systems also have a ring backbone, therefore, it is interesting to compare the results obtained from this system with those from the NNDMA-EPDCD hydrogels described previously. Additionally, these Figures illustrate the mechanical properties of the NVP-CA and NVP-CAB copolymers. The initial σ_b, ε_b and E for poly NVP are taken as zero as the mechanical properties are so poor that the pressure from the jaws of the tensometer causes a fracture. The changes of appearance in these polymer systems are not illustrated, as they do not appear to have any effect on the mechanical properties.

If the tensile strength is examined as a function of composition several points can be discerned (Figure 7.12). The first is that IPNs based on NNDMA have higher tensile strengths than the comparable NVP based IPNs. This demonstrates that the matrix polymer does have some influence on the tensile strength of these IPNs and it is not determined solely by the σ_b of the filler polymer. Another point illustrated in this graph is the increased σ_b of IPNs where CAB rather than CA is the filler polymer. There are two possible explanations for the greater σ_b of CAB containing IPNs. The first is the structural difference between the two polymers; although the lengthening of the pendant chains on the ring may appear to be only a minor structural change it may alter the conformation of the polymer. The second is a consequence of the structural differences between CA and CAB and is the lower water content of the CAB containing IPNs. However, the NNDMA-CA 85:15 and NNDMA-CAB 90:10 IPNs have similar EWCs but the tensile strength of the CAB containing EWCs is approximately 20% greater.

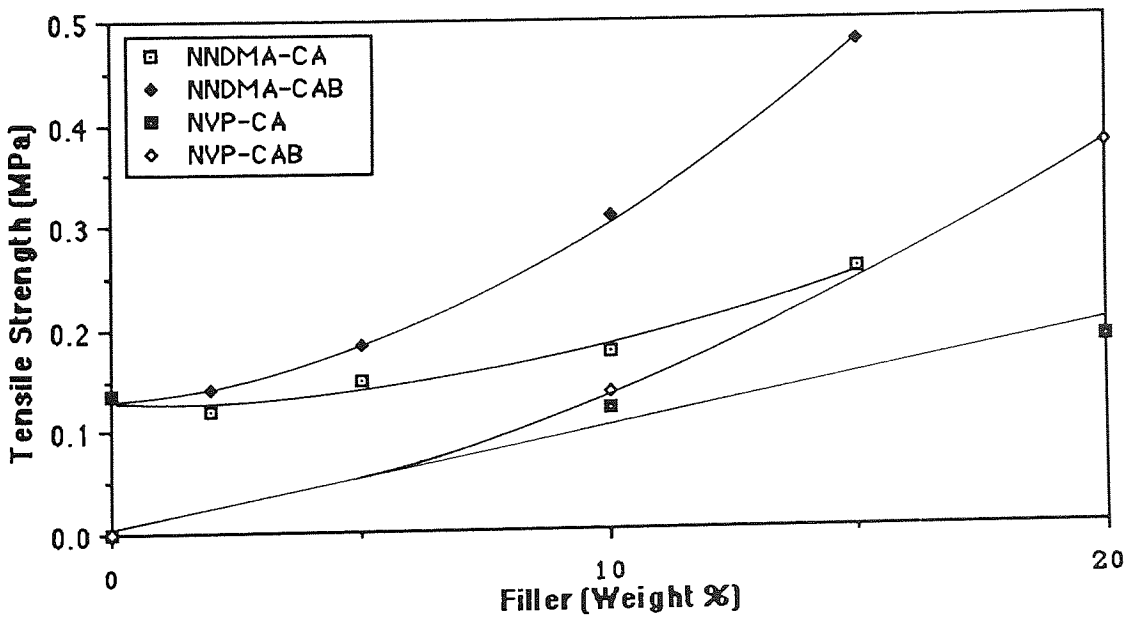

Figure 7.12 **Effect of composition on the tensile strength of NNDMA-CA, NNDMA-CAB, NVP-CA and NVP-CAB IPN hydrogels**

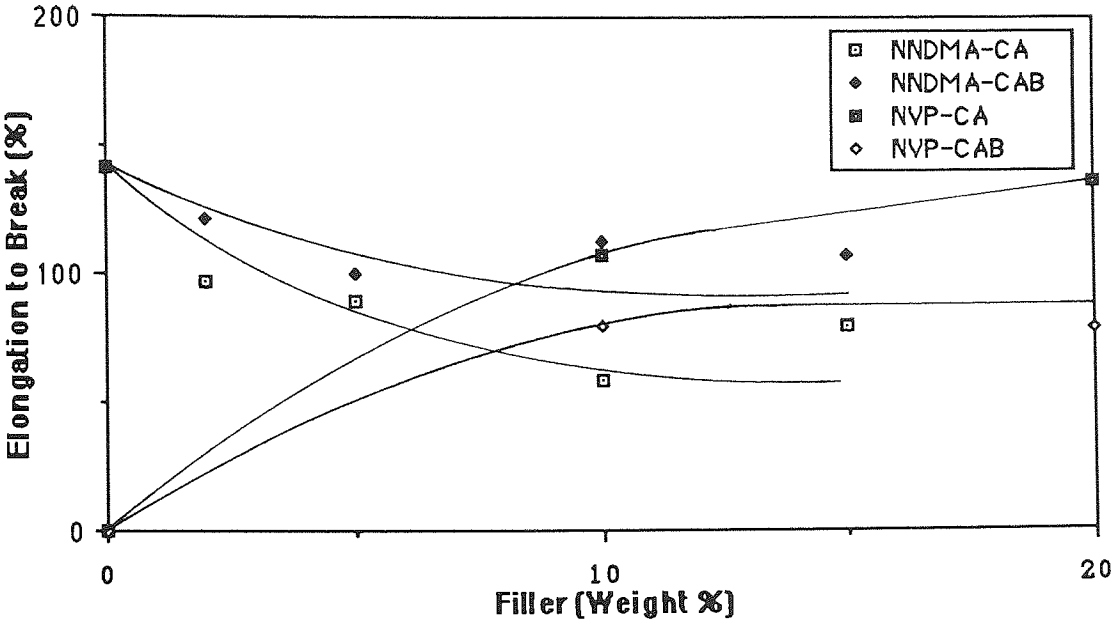

Figure 7.13 Effect of composition on the elongation to break of NNDMA-CA, NNDMA-CAB, NVP-CA and NVP-CAB IPN hydrogels

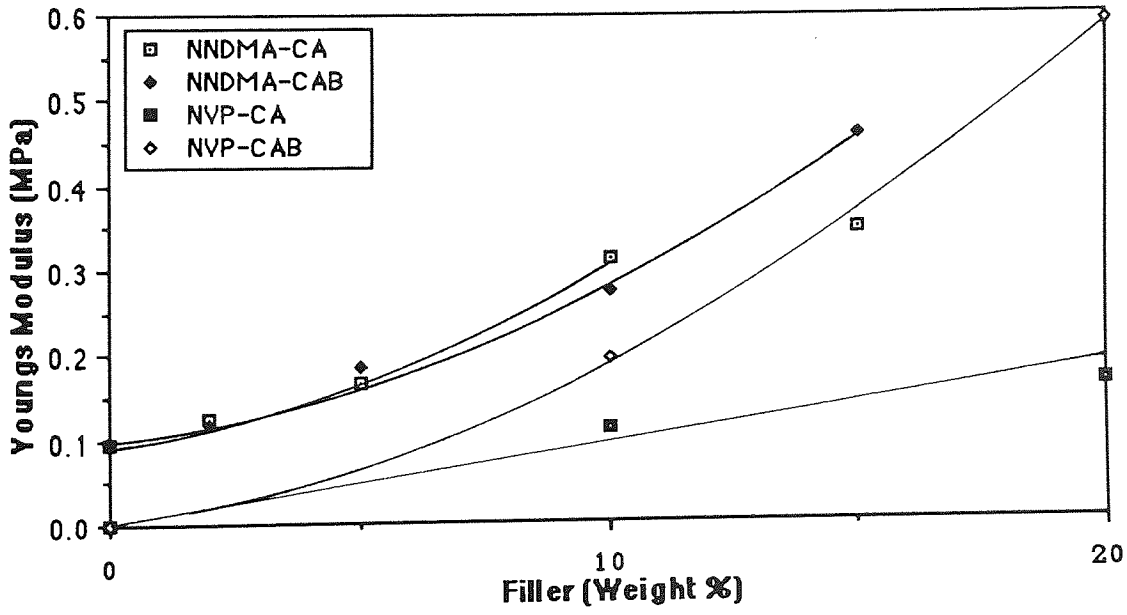

Figure 7.14 Effect of composition on the Youngs modulus of NNDMA-CA, NNDMA-CAB, NVP-CA and NVP-CAB IPN hydrogels

It appears that although the water content will have some effect on the σ_b of these polymers, the structural differences between the polymers is the major factor affecting σ_b. At 15% filler incorporation σ_b for the NNDMA-CAB IPN is less than half that of the σ_b for the NNDMA-EPDCD system. The explanation for this phenomenon lies in the greater stiffness and hydrophobicity of EPDCD which is also reflected in the lower values of ε_b in this system.

Incorporation of either CA or CAB into both NVP and NNDMA leads to the formation of a less flexible system. This is illustrated in Figure 7.13 which shows that ε_b tends to fall with increasing CA or CAB incorporation. The Youngs moduli of the materials show similar behaviour patterns to σ_b, however. E increases with increasing incorporation of CA or CAB into the IPN, the CAB containing IPNs once again giving higher values for E than those in which CA is the filler polymer. Thus, the stiffness of the system is increased by CA or CAB incorporation.

After examining the effect of individual polymers on the tensile properties of poly NNDMA and poly NVP it is interesting to try and correlate both EWC and percentage filler polymer with the mechanical properties of these gels. The following Figures illustrate the effect of both filler polymer and EWC on the tensile strength, elongation to break and Youngs modulus of all the IPN hydrogels synthesised. The best values obtained for copolymers containing NNDMA at a comparable composition are also shown by the line on the Figures. In general, the tensile strength increases with increasing incorporation of filler polymer (the exception being NNDMA-PVAc IPNs). It can be seen that the tensile strengths of the majority of IPNs synthesised are greater than those of the NNDMA copolymers. This might be expected, however, as the tensile strengths of the filler polymers are all greater than that of poly NNDMA. Figure 7.16 illustrates that the EWC also has an effect on the

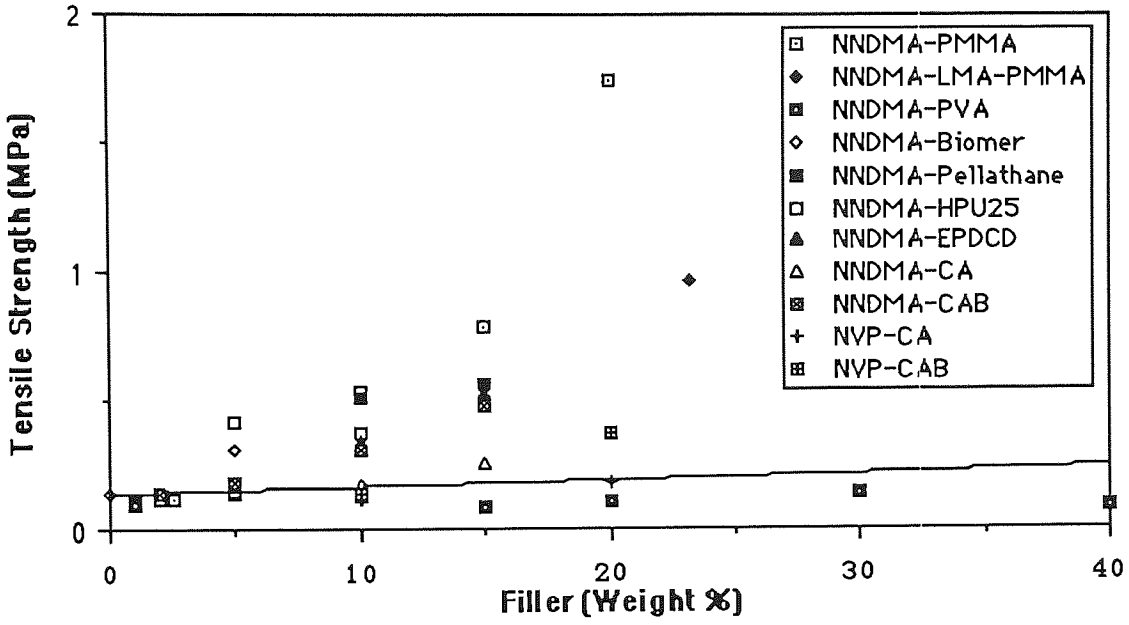

Figure 7.15 Effect of filler incorporation on the tensile strength of NVP and NNDMA IPN hydrogels

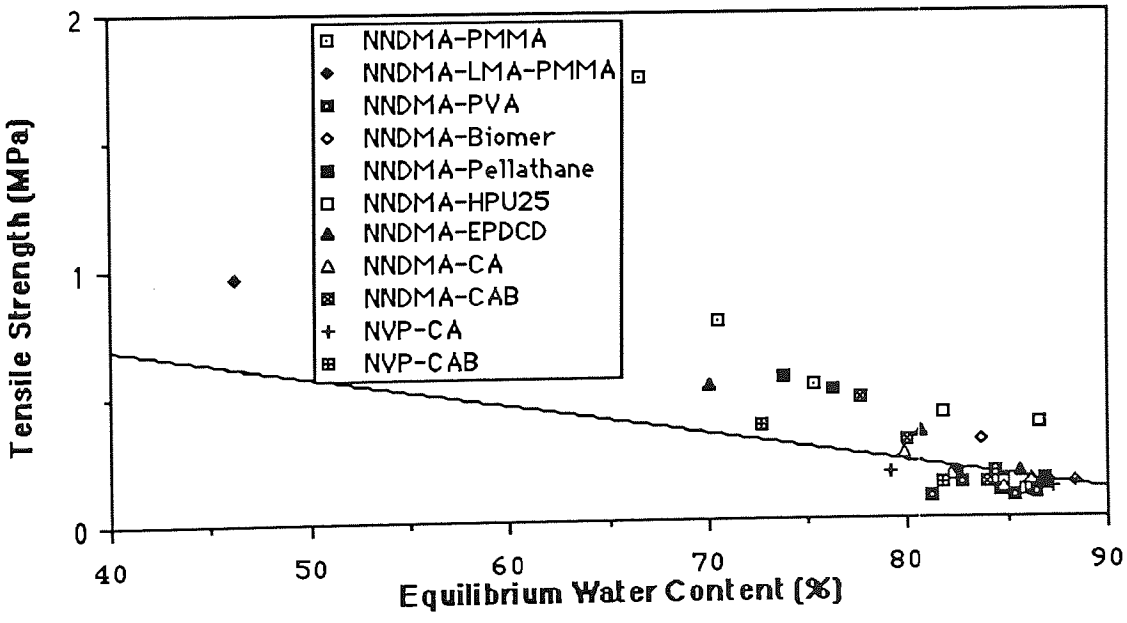

Figure 7.16 Effect of EWC on the tensile strength of NVP and NNDMA IPN hydrogels

tensile strengths of IPN hydrogels. It is apparent that the tensile strengths of the IPNs generally increase as the EWC of the IPNs is reduced. The majority of the results lie in a narrow band but it is not surprising that there is some scatter. Individual polymer structure still has a part to play in determining the σ_b of the IPNs and in polymer systems of this type it is unlikely that there will be equal distribution of the water between the matrix and filler polymer. This would be expected to have a profound effect on the σ_b of these polymers.

No correlation has been found between elongation to break and filler incorporation (Figure 7.17) but the mechanical properties of the filler polymer are again dominant, even after the incorporation of small amounts (<5%) of filler. The majority of the IPN hydrogels have a lower elongation to break than poly NNDMA, however, and in general these materials could be classed as brittle polymers. The NNDMA-PVAc IPNs are again an exception having the best elongation properties of all the hydrogels examined. Only two types of IPNs have an ε_b greater than that of NNDMA-LMA copolymers at similar compositions; these are NNDMA-PVAc IPNs at low levels of PVAc incorporation and NNDMA-polyurethane IPNs with Biomer and HPU25, the most flexible filler polymers examined.

If elongation to break is plotted as a function of EWC (Figure 7.18) there is again no well defined behaviour pattern, however, it could be said that increasing the EWC leads to an increase in ε_b of the polymers. The plasticising effect of freezing water in copolymer hydrogels has been discussed previously [145] (Chapter 3), therefore, it might be expected that increasing the EWC and thus the freezing water content, would increase ε_b.This behaviour can be explained, as the presence of increasing amounts of water will promote chain rotation and chain "disentanglement" under tension. The ε_b of the copolymer system illustrated moves in the opposite direction (i.e. increases with decreasing EWC), this is a consequence of using the NNDMA-LMA copolymer series.

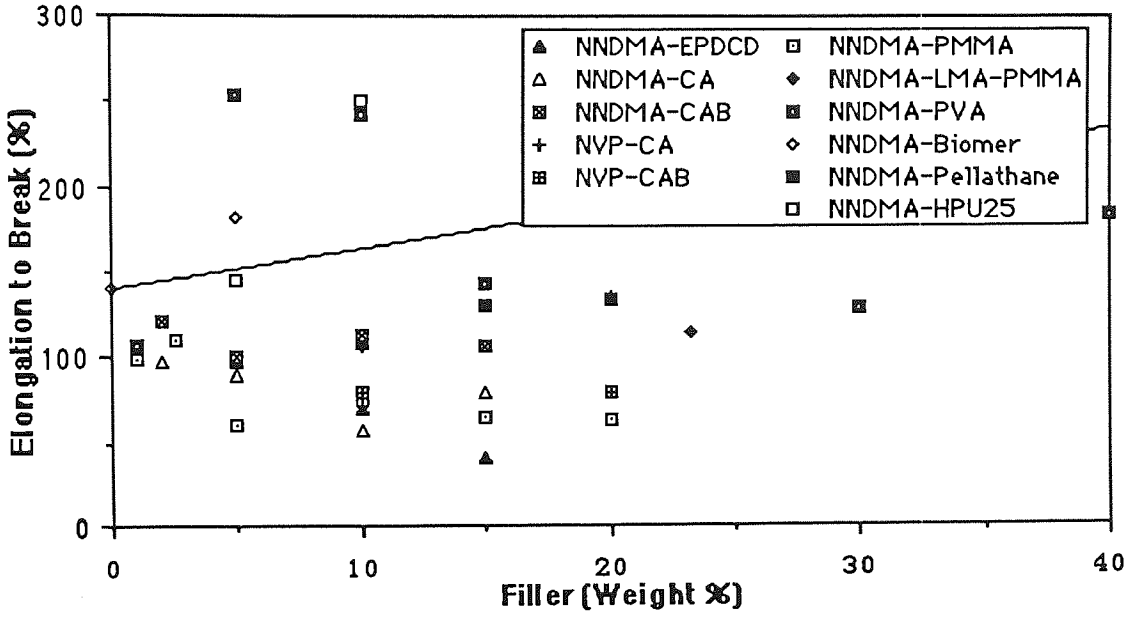

Figure 7.17 Effect of filler incorporation on the elongation to break of NVP and NNDMA IPN hydrogels

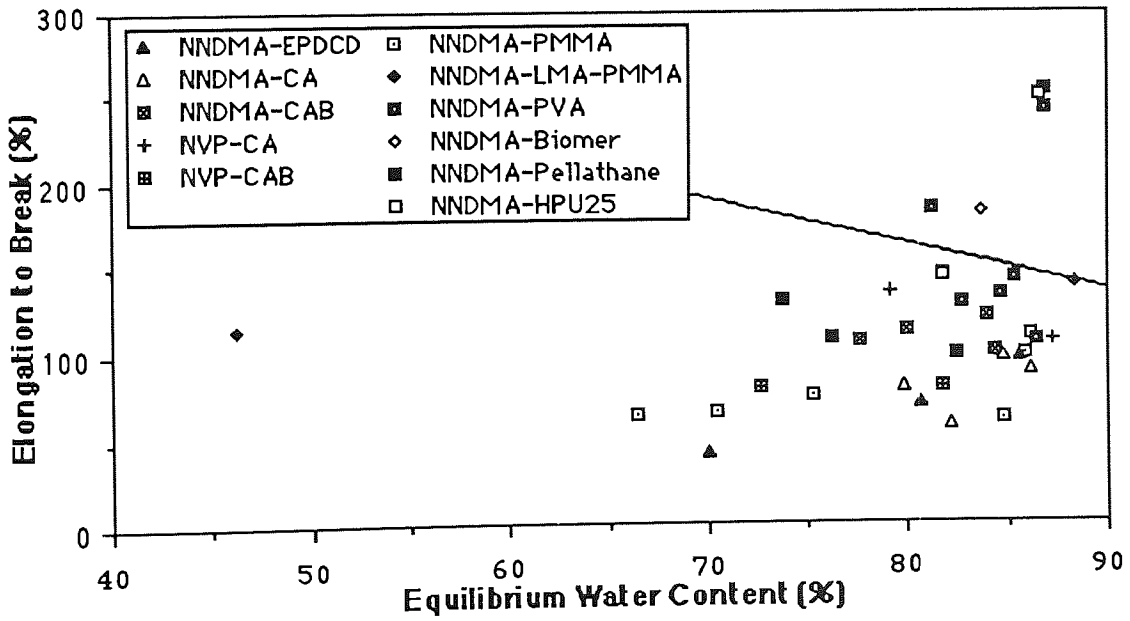

Figure 7.18 Effect of EWC on the elongation to break of NVP and NNDMA IPN hydrogels

Incorporation of increasing amounts of hydrophobic LMA, reduces the EWC but increases ε_b due to the plasticising effect of LMA. If the effect of EWC on the elongation to break of NNDMA-MMA copolymers, for example, is investigated ε_b also decreases with decreasing EWC.

One interesting IPN shown on these graphs is the NNDMA-PMMA-LMA 64:20:16 terpolymer. This was synthesised after examining the mechanical properties of NNDMA-PMMA IPNs and noting that although they possess the necessary tensile strength, they were rather brittle for use in many biomedical applications. It was hoped that the addition of a flexible, long chain, plasticising monomer (e.g. LMA) to the system would improve ε_b, while still retaining the excellent σ_b of the NNDMA-PMMA IPNs. From the above Figures it is apparent that LMA incorporation has reduced the tensile strength, although the σ_b of the IPN is still nearly double that of poly HEMA. Even though ε_b has been increased by LMA incorporation the final IPN still has an ε_b that is low, in comparison with poly HEMA. The rigidity modulus of this system is also higher than E for the majority of IPNs synthesised. Therefore, if a compatible system of this type could be developed it would have potential for use in biomedical applications.

The Youngs moduli of the hydrogels generally show an increase, with increasing concentrations of filler. However, individual polymer structure is still the overriding factor in determining the Youngs moduli of these polymers. The factors controlling σ_b, ε_b and E will be discussed in more detail in Section 7.3. Once again the Youngs modulus of the IPNs is much greater than that of the "best" NNDMA copolymers. Figure 7.20 illustrates E as a function of EWC for all the IPNs synthesised in this work. The Youngs moduli of these IPNs display similar behaviour to the tensile strengths, with the majority of results falling in a narrow band and E increasing as the EWC decreases.

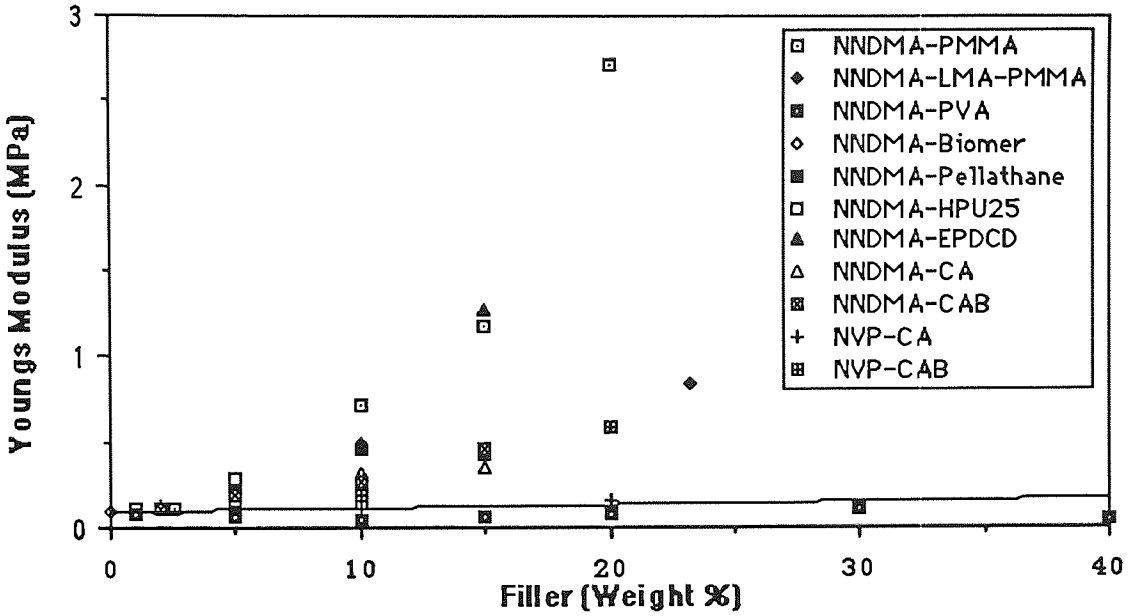

Figure 7.19 Effect of filler incorporation on the Youngs modulus of NVP and NNDMA IPN hydrogels

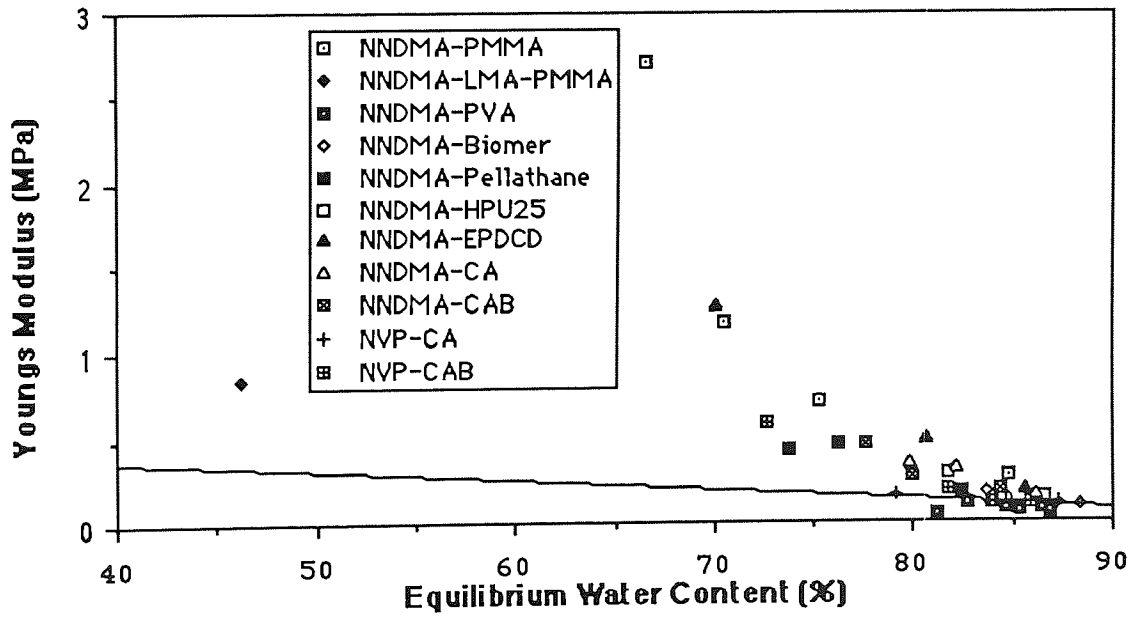

Figure 7.20 Effect of EWC on the Youngs modulus of NVP and NNDMA IPN hydrogels

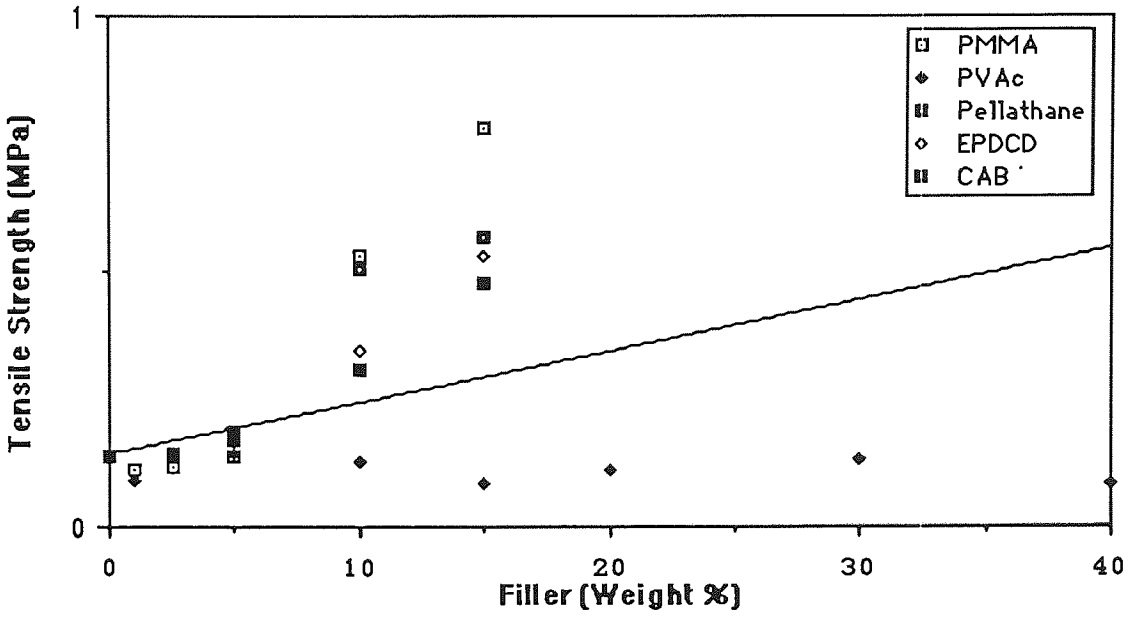

Figure 7.21 Effect of composition on tensile strength for a range of NNDMA IPN hydrogels

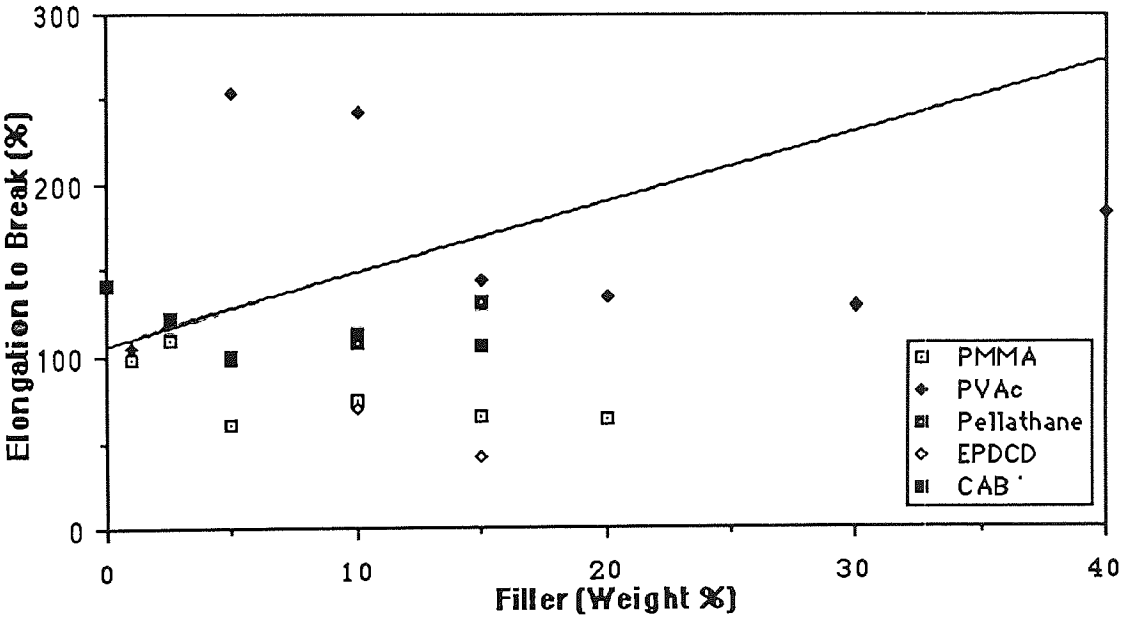

Figure 7.22 Effect of composition on elongation to break for a range of NNDMA IPN hydrogels

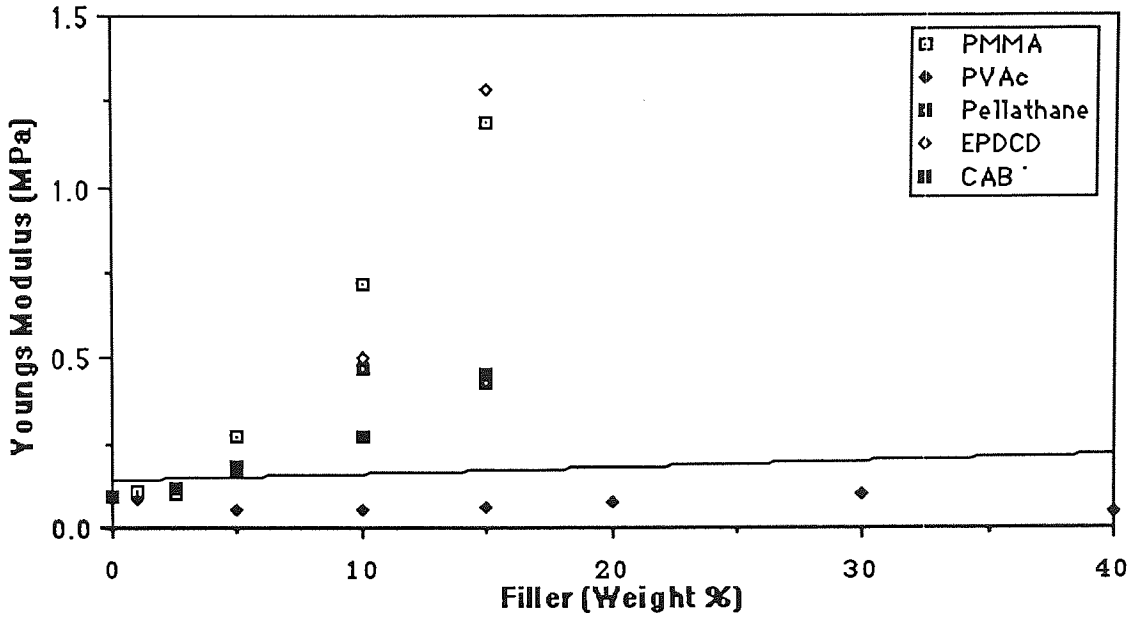

Figure 7.23 Effect of composition on Youngs modulus for a range of NNDMA IPN hydrogels

The results described above could indicate a direct correlation of E with EWC. However, it is more plausible to suggest that E increases as increasing amounts of filler polymer, with superior mechanical properties, are added. This addition of filler polymer also causes a reduction in EWC and therefore, the increase in E with decreasing EWC is a secondary, rather than primary effect. The Youngs moduli of the IPNs are, however, once again far superior to those obtained for NNDMA copolymers.

The effect of filler polymer structure on mechanical properties is summarised in Figures 7.21-7.23 in which σ_b, ε_b and E are illustrated as a function of composition for a range of NNDMA IPNs. Once again lines representing the mechanical properties of the "best" NNDMA copolymers are shown for comparison. A discussion on the main factors which affect the mechanical properties of IPNs follows in Section 7.3

7.3 Conclusions

The initially poor mechanical properties of NNDMA coupled with its good solvent properties make it an excellent choice of monomer to form the matrix polymer in semi-IPNs of this type. It is apparent, from the results presented above, that the mechanical properties of NNDMA based systems may be greatly improved by the synthesis of IPNs. The IPNs are stiffer and stronger than comparable copolymers but many have a low elongation to break and may be classed as brittle polymers. As several different filler polymers, varying in both molecular weight and T_g, have been used in this work, this should help in the elucidation of some of the factors which influence σ_b, ε_b and E.

The phase transitions in the NNDMA-PVAc and NNDMA-PMMA systems, which have a profound effect on the water binding properties, also influence the mechanical properties of the IPNs. Thus, σ_b and E increase while ε_b falls subsequent to the phase transition in both systems. However, the increase in σ_b and E is more dramatic in the NNDMA-PMMA IPNs. As the matrix polymer (poly NNDMA) is identical in both these systems the filler polymer must be the major factor in determining the mechanical properties of the IPNs.

The T_g of the filler polymer may be one of the factors controlling the mechanical properties of the composite. In these systems the T_gs of PMMA and PVAc are 378K and 301K respectively. However, the major difference between these polymers is in their hydrophilicity. While PMMA has no water binding ability, PVAc although still a relatively hydrophobic polymer may be able to interact with the water present in the system. Non-freezing water lowers the T_g of the polymer it is associated with and only a small amount of non-freezing water would be necessary to reduce the T_g of PVAc to room temperature. In the PMMA and EPDCD systems the T_g of the filler polymers is high and will be unmodified by water as both are hydrophobic polymers. Therefore, these systems have the

highest E of all the IPNs studied. In the CA, CAB and polyurethane containing IPNs, however, the plasticising effect of freezing water is apparent. The T_g of CA is greater than that of CAB and both values are well above room temperature.Thus, it might be expected that because of the structural similarities between them E for the CA containing IPNs would be greater. However, although values of E for CA and CAB containing IPNs are similar, the Youngs modulus of CAB containing IPNs is generally higher. CA is more hydrophilic than CAB and there would be more filler-water interactions in the CA containing IPNs. This behaviour supports the hypothesis that in some systems the T_g of the filler polymer is reduced by interaction with water. Thus, the filler polymer is plasticised within the system.

PMMA incorporation has a similar effect on NNDMA as increasing the amount of crosslinking agent. Thus, σ_b and E are increased while ε_b falls. Therefore, the molecular weight of the filler polymer may be important in determining the mechanical properties of the IPNs. The effect of molecular weight (i.e. block length in a block copolymer) on the mechanical properties of NVP-MMA copolymers has been discussed previously in Chapter 4. However, unfortunately in this initial study too few IPN hydrogels were synthesised for any definitive results on the effect of molecular weight on mechanical properties to be obtained.

The differences in mechanical properties between the EPDCD and CA and CAB containing hydrogels can be explained by structural variations and the water binding ability of the filler polymers. The effect of the water binding ability of the filler polymer on its T_g has been discussed previously, however, the total amount of water present in the polymer will also have an effect on the mechanical properties. Thus, in the PMMA and EPDCD containing IPNs the filler polymer reduces the EWC both by acting as a filler and reducing the amount of NNDMA in the system and also by steric occlusion. However in the CA and CAB IPNs the filler polymer also has some water binding capability and therefore, there is a smaller

reduction in EWC in these systems.This manifests itself in terms of a higher σ_b and E and lower ε_b in EPDCD containing hydrogels.

If the results for all the IPNs are compared it is apparent that there are no simple rules which determine the mechanical properties in these systems. The compositions with the highest σ_b and E and lowest ε_b , for example, are the NNDMA-PMMA and NNDMA-EPDCD IPNs. These filler polymers have a high T_g, are sterically hindering and hydrophobic. In contrast, the IPNs with the highest ε_b but lowest σ_b and E are found in the incompatible NNDMA-PVAc system, where the filler polymer has a slight water binding capability. In systems of this type there is little or no interaction between the matrix and filler polymers and therefore, the PVAc has no reinforcing effect. However, when the water in IPNs is held in large pores, as is the case in this system, there is often excess water in the polymer. This excess freezing water will tend to have a plasticising effect and this accounts for the improvement of ε_b in this system. Therefore, factors such as the T_g, molecular weight and water binding capability of the filler polymer, EWC and the compatibility of the system all appear to have a part to play in controlling mechanical properties. Thus, the final mechanical properties of the IPNs will be a function of all the above properties with the relative contribution of each property being dependent on the composition of the system. Therefore, in the NNDMA-polyurethane IPNs, for example, the structural similarity of the filler polymers enables the EWC to be the controlling factor in determining E; while in the NNDMA-PMMA IPNs there is no linear correlation between EWC and E.

CHAPTER 8

Interpenetrating Polymer Network Hydrogels: Surface Studies: Physicochemical and Biological Probes

8.1 Introduction

The surface free energy of a polymer is thought to be important in determining its interactions with a biological environment. The surface studies completed on copolymer hydrogels (reported in Chapter 5) have indicated that surface properties vary regularly as a function of composition in the majority of systems investigated. However, previous work on the water binding and mechanical properties of these IPNs has indicted that phase changes can cause discontinuities in property (e.g. freezing water, EWC, tensile strength) versus composition curves. The results from surface studies on IPN hydrogels in both the hydrated and dehydrated states are presented in this Chapter and the effect of composition and phase changes on surface free energy will be discussed.

8.2 IPN Hydrogels: Dehydrated Surface Properties

Previously in this work it has been shown that changes in composition can produce marked differences in the mechanical and water binding properties of IPN hydrogels. In this section the use of the sessile drop technique to probe the the surface properties of IPNs in the dehydrated state will be discussed. Changes in surface properties will be related to changes in structure and the differences between IPN and copolymer hydrogels will also be examined. The majority of IPNs were clear throughout the whole composition range in the dehydrated state, however, there were some exceptions and these are shown on the appropriate Figures.

Figure 8.1 illustrates the dehydrated surface free energy of NNDMA-PVAc IPNs, the introduction of increasing amounts of PVAc causes a reduction in γ^p with an accompanying increase in γ^d. This behaviour is not unexpected as PVAc is more hydrophobic (i.e. has a lower γ^p and higher γ^d) than NNDMA. Therefore, PVAc addition moves the high γ^p of NNDMA towards the value of γ^p for PVAc. There is, however, very little change in γ^t

throughout the composition range as the decrease in γ^p is compensated for by the increase in γ^d in all the IPNs examined. The phase change, which is apparent by its effect on the water binding and mechanical properties, has no measurable effect on the surface properties of this system.

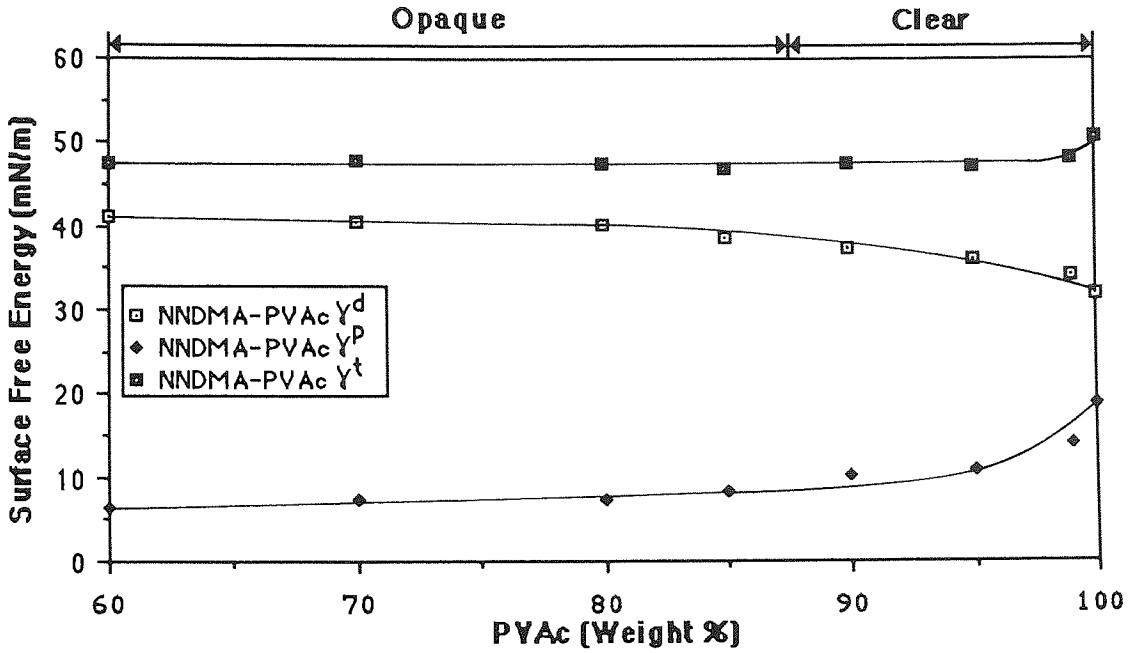

Figure 8.1 Effect of composition on the dehydrated surface free energy of NNDMA-PVAc IPN hydrogels

Figure 8.2 illustrates the surface free energy of NNDMA-PMMA IPNs presented in contrast with the NNDMA-MMA copolymers described previously. The total surface free energies of the NNDMA-PMMA IPNs are slightly higher than those of the corresponding NNDMA-PVAc polymers; this is reflected in the higher γ^p values and lower γ^d values of the PMMA containing IPNs. The measured surface energies of these two systems are surprising as PMMA has a higher γ^d and lower γ^p than PVAc. This difference in surface energy in moving from PVAc to PMMA is due to the α-methyl group on the PMMA which causes steric occlusion and restricts the expression (ie availability at the surface) of the polar groups

in PMMA.

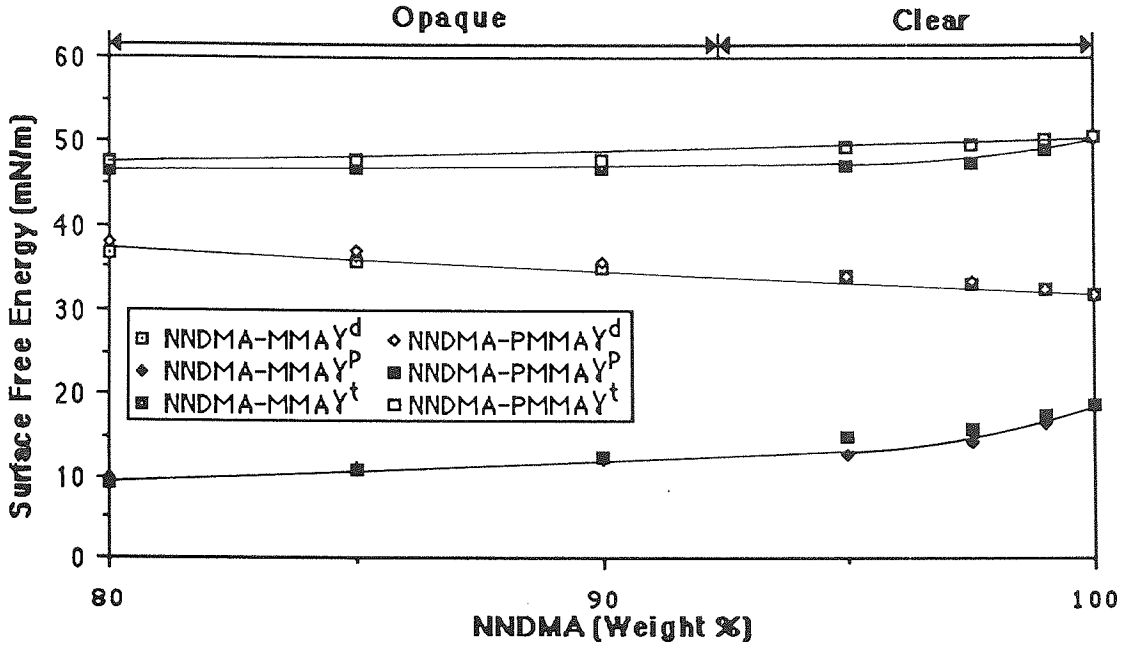

Figure 8.2 **Effect of composition on the dehydrated surface free energy of NNDMA-MMA copolymers (all clear) and NNDMA-PMMA IPN hydrogels**

In IPN systems, however, the distribution of the filler polymer within the matrix will also influence surface properties and this may account for the measured surface energies of these systems. The phase change which is apparent in its effect on the mechanical and water binding properties of both NNDMA-PMMA and NNDMA-PVAc IPNs does not manifest itself in terms of dramatic surface energy variations.

The difference in surface free energy between NNDMA-MMA copolymers and IPNs, is also illustrated in Figure 8.2. The total surface free energy for the IPNs is slightly higher throughout the whole composition range, decreasing as increasing amounts of PMMA are incorporated into the system, but the values of γ^t in both systems are similar. However, although the values of γ^p and γ^d for both systems are similar a slight difference between the

copolymers and IPNs is visible. In compositions prior to the 95:5 IPN (subsequent to which a phase change is seen) γ^d is virtually identical in the copolymer and IPNs, while γ^p is higher in the IPNs than in the copolymers. In subsequent compositions γ^p of the copolymer is identical or slightly higher than γ^p for the IPNs and the values of γ^d are higher in the IPNs than in the comparable copolymers. However, it could also be argued that given the 2° error in measuring contact angles that γ^p and γ^d are identical within the limits of experimental error.

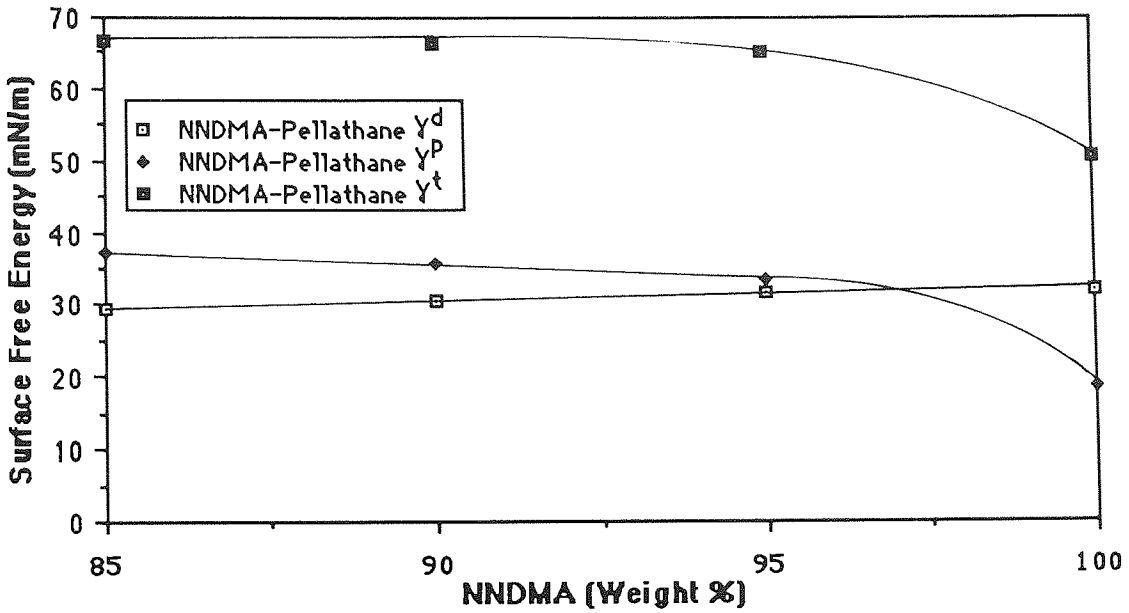

Figure 8.3 Effect of composition on the dehydrated surface free energy of NNDMA-Pellathane IPN hydrogels

The surface free energies of the dehydrated NNDMA-Pellathane IPNs studied, illustrated in Figure 8.3, display unusual trends. It is apparent from the Figure that Pellathane incorporation gives rise to a dramatic increase in γ^t with a slight increase in γ^d but a marked increase in γ^p. Similar behaviour is also observed with the NNDMA-Biomer and NNDMA-HPU25 IPNs. This behaviour is anomalous as the surface free energy of Biomer and Pellathane have been measured in the dehydrated state and the polar components are 14.4 mN/m and 7.1mN/m respectively. This confirms the assumption made by inspection of the

water contents of these IPNs that Pellathane is the most hydrophobic of the polyurethanes investigated. However, despite the fact that Pellathane is less polar than Biomer γ^p for the NNDMA-Pellathane 95:5 IPN is higher than the comparable Biomer containing IPN.

In these systems the IPNs have markedly different surface properties than would be expected from a simple addition of the surface energies of both components. There are two possible explanations for this phenomenon. As Pellathane has an excess of hydrophilic groups, the first, is the formation of an intramolecular complex which is oriented in such a way that all the hydrophilic groups are expressed at the surface, causing a rise in γ^p and γ^t. The other explanation for this behaviour is that these IPNs absorb the wetting liquids more rapidly than the other copolymers and IPNs investigated. Therefore, the high γ^p observed for the "dehydrated" surfaces may, in fact, be the measured polar component of a partially hydrated IPN. The NNDMA-Pellathane IPNs display greatly increased γ^p values and slightly lower γ^d values than either the NNDMA-PMMA or NNDMA-PVAc IPNs and there is obviously no simple relationship between composition and dehydrated surface energy in these NNDMA-polyurethane IPNs.

The NNDMA-EPDCD IPNs also display unusual behaviour in that the incorporation of increasing amounts of EPDCD causes a reduction in γ^p and γ^t with γ^d remaining relatively constant (Figure 8.4). This behaviour is consistent with the idea that EPDCD has a much lower surface free energy than poly NNDMA and its effect on the surface free energy is quite visible even at low levels of incorporation. The surface free energy of the EPDCD containing IPNs is appreciably lower than the γ^t of any of the previous IPN systems. This is due to the structure of EPDCD which is a substituted, epoxidised cycloheaxadiene ring, which would be expected to have a low polar component of the surface free energy. Therefore, it would be interesting to compare γ^t for this system with the surface energy of

other systems that contain filler polymers with ring systems in the backbone (e.g. CA and CAB).

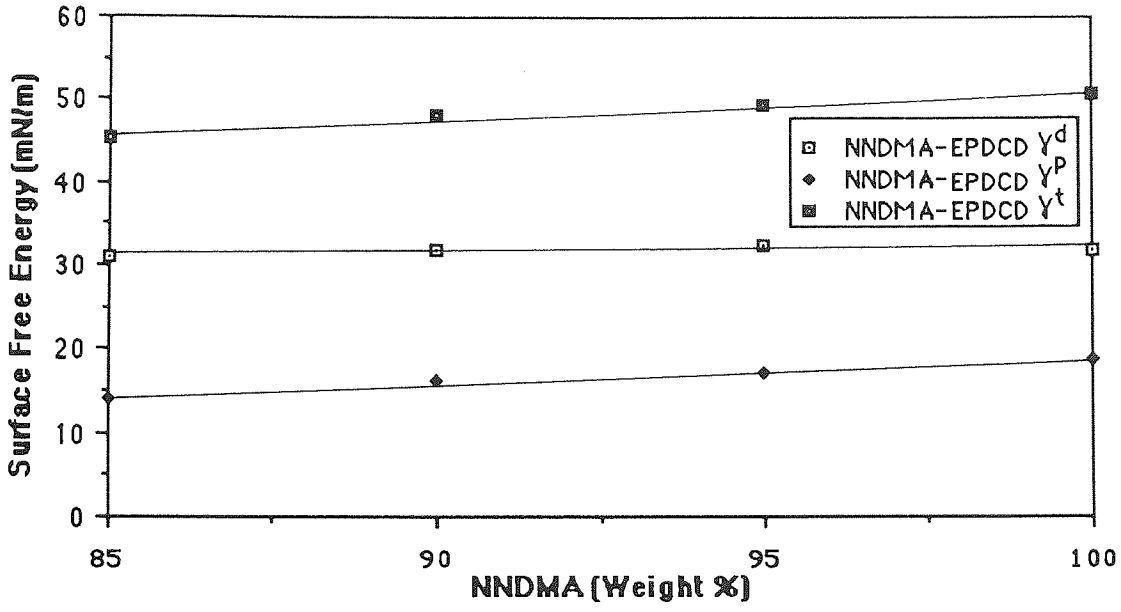

Figure 8.4 Effect of composition on the dehydrated surface free energy of NNDMA-EPDCD IPN hydrogels

The surface free energies of the NNDMA-CA and NNDMA-CAB IPNs are shown in Figure 8.5. Several points can be made about the behaviour in this system. Incorporation of increasing amounts of both CA and CAB causes a reduction in γ^p and γ^t with an increase in γ^d in all the IPNs examined. This behaviour is concomitant with the addition of a filler polymer which has a much lower concentration of polar groups / repeat unit and is sterically occluded. The increase in hydrophobicity of the IPNs also manifests itself in terms of water content reduction, discussed in Chapter 6.

Although the structure of CA and CAB are very similar, CAB has a slightly higher γ^t and γ^d and a slightly lower γ^p than CA. Although the values for surface free energy of the NNDMA-CA and NNDMA-CAB IPNs are similar the CAB containing IPNs have a lower

γ^t and γ^p and a higher γ^d than the comparable CA containing IPN. This demonstrates the accuracy it is possible to achieve with droplet techniques.

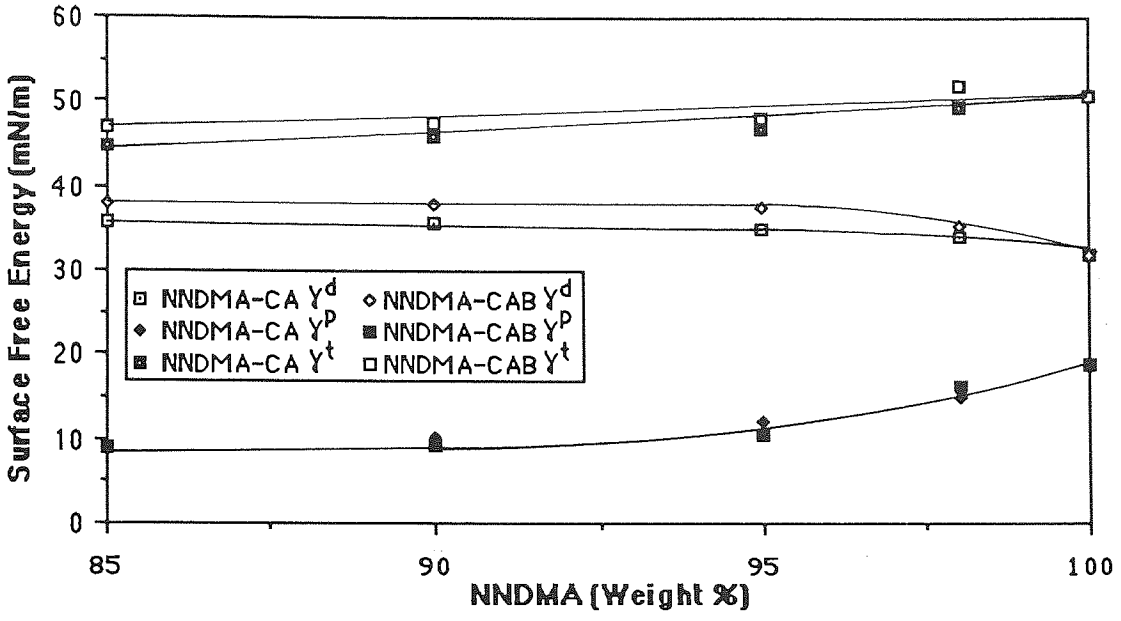

Figure 8.6 Effect of composition on the dehydrated surface free energy of NNDMA-CA and NNDMA-CAB IPN hydrogels

The total surface free energy of these systems is again lower than that found in the PVAc or PMMA containing hydrogels and comparable to the results obtained from the NNDMA-EPDCD system. Therefore, it appears that the surface free energy of these bulky polymers with a ring system in the backbone are lower than those of vinyl polymer such as PMMA and PVAc. This is reflected in the lower surface free energies of the IPNs containing these polymers.

The surface free energies of NNDMA-CA and NNDMA-CAB IPNs were compared with those of comparable IPNs based on NVP (illustrated in Figure 8.7). Several points can be made about the similarities and differences in these systems. The first is that CA or CAB incorporation once again causes a reduction in γ^t and γ^p with an increase in γ^d with CAB appearing to be slightly more hydrophobic than CA.

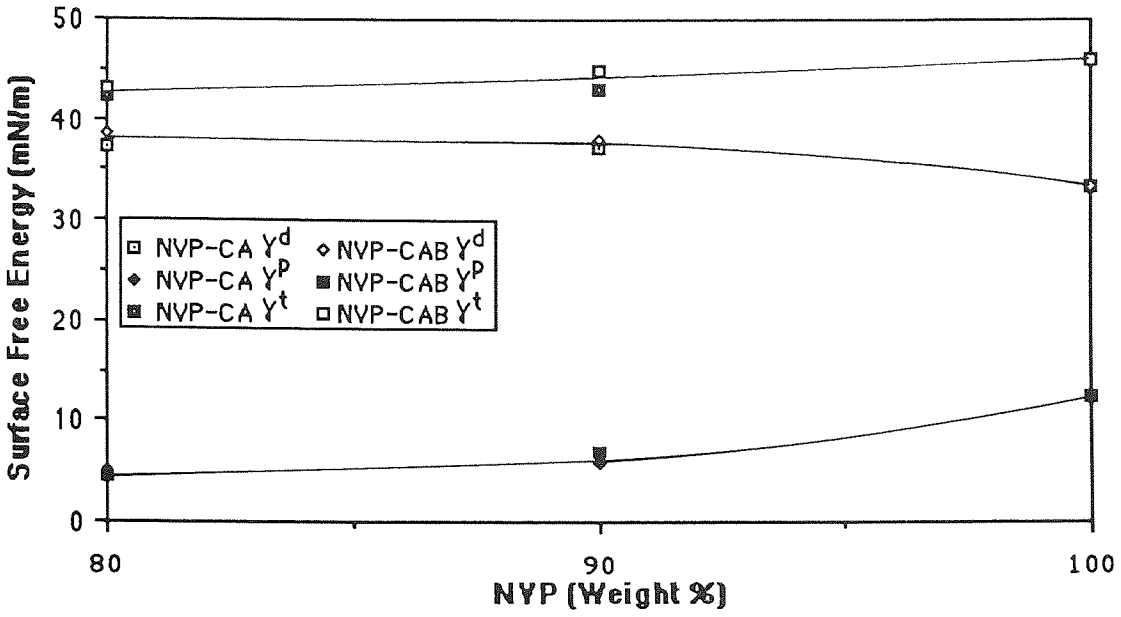

Figure 8.7 Effect of composition on the dehydrated surface free energy of NVP-CA and NVP-CAB IPN hydrogels

Poly NNDMA has a higher surface free energy than poly NVP and, therefore, it might be expected that the γ^t of the NNDMA-IPNs would be higher than a comparable IPN based on NVP. This is demonstrated by the IPNs examined in this work, with the major cause of this increased γ^t in the NNDMA system being the greater polar component of NNDMA. The steric occlusion and packing of the lactam ring in poly NVP causes this reduction in γ^p, which was discussed in more detail in section 5.8.1. The dispersive components of both IPN systems are similar as is the case in the homopolymers.

8.3 IPN Hydrogels: Hydrated Surface Properties

It is difficult to obtain information about events happening at a molecular level by using droplet techniques to examine the surface, particularly in the hydrated state. However, the surface properties of the IPN hydrogels in the hydrated state were probed using the Hamilton and captive air bubble techniques and the results are presented below.

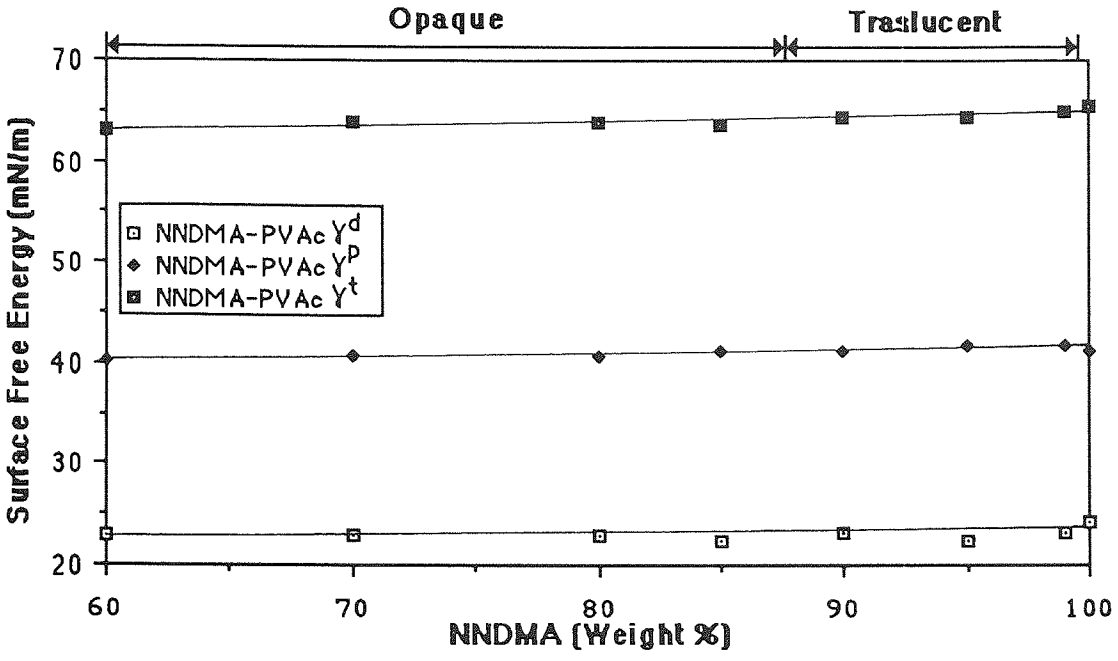

Figure 8.8 Effect of composition on the hydrated surface free energy of NNDMA-PVAc IPN hydrogels

Figure 8.8 illustrates the change in hydrated surface free energy with composition for NNDMA-PVAc hydrogels.There is very little change in the surface free energy of the NNDMA-PVAc system throughout the composition range γ^d remains constant (within the limits of experimental error) at a value just below that for poly NNDMA with a small reduction apparent in the values of γ^p and γ^t. The definite changes seen in γ^p and γ^d in the dehydrated state are undetected here and the phase change once again has no measurable effect on the surface properties. Thus, in the hydrated system it is apparent that NNDMA dominates the surface of the IPN with the measured values of γ^p, γ^d and γ^t being very similar to those of poly NNDMA. Even the incorporation of 40% PVAc leads to a value of γ^p only 1mN/m lower that that of poly NNDMA, while in the dehydrated state γ^p for PVAc is much lower than that of poly NNDMA. However, there is only a slight variation in water content throughout the composition range and in high water content hydrogels, water is one of the major factors controlling the surface free energy.

The hydrated surface free energies of IPNs based on NNDMA and PMMA are illustrated in Figure 8.9. The hydrated surface free energies of the NNDMA-MMA copolymers are also shown for comparison. Although, as is the case with NNDMA-PVAc IPNs, γ^t falls with increasing filler concentration and the values of γ^t in both systems are similar, marked differences are seen in the polar and dispersive contributions to γ^t. There is an increased polar contribution to the surface free energy in NNDMA-PVAc IPNs this can be explained, in part, by the higher EWCs in that system. However, at similar EWCs the NNDMA-PMMA IPNs have a higher γ^d and lower γ^p than those containing PVAc as the filler polymer.

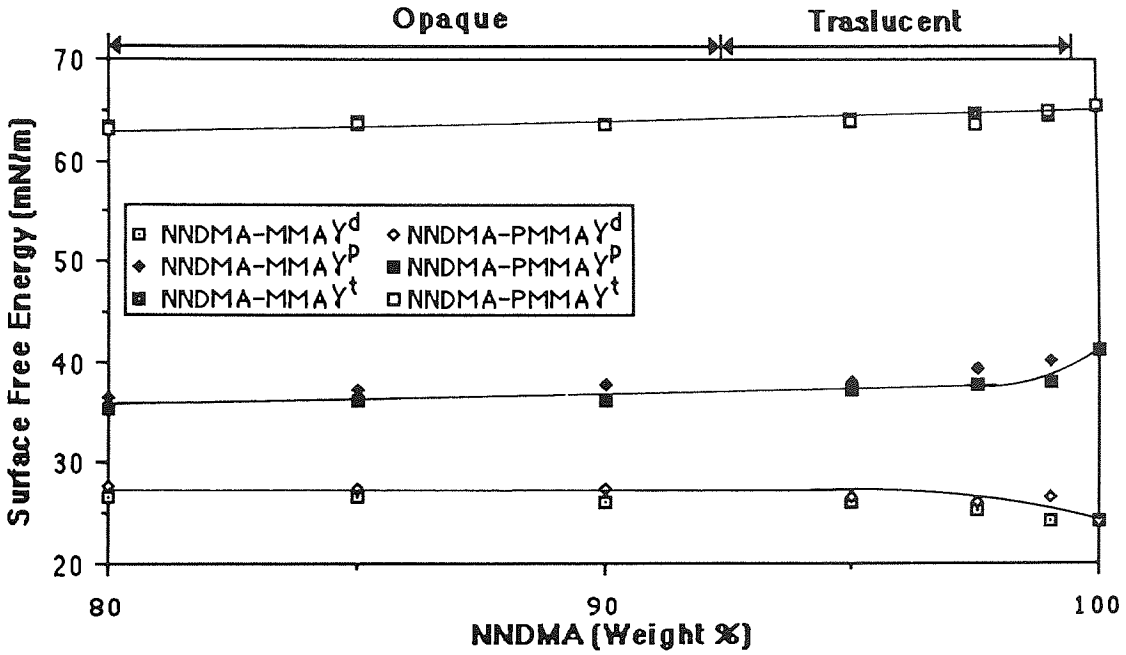

Figure 8.9 Comparison of the hydrated surface free energy of NNDMA-MMA copolymers and NNDMA-PMMA IPN hydrogels

Figure 8.9 also contrasts the surface free energies of NNDMA-MMA copolymers and NNDMA-PMMA IPNs. The usual differences between the hydrated and dehydrated surface energies are observed in this system. Thus, γ^t hydrated is greater than the dehydrated γ^t and whereas, in the the dehydrated IPNs γ^d is larger than γ^p the dramatic influence of water

means that the reverse is true in the hydrated state. The phase change apparent in the surface energy measurements on the dehydrated polymers is not visible in the hydrated state and may be masked by the water present in the IPNs. The γ^p of the copolymers is consistently higher, and γ^d consistently lower than those of the corresponding IPNs. The total surface free energies of both systems are similar, with γ^t of the NNDMA-MMA copolymers being slightly higher than those of the IPNs. This behaviour is consistent with the EWCs of the copolymers being higher than those of the IPNs and water being a major influence on the surface properties of both systems.

The unusual behaviour displayed by the NNDMA-polyurethane hydrogels in the dehydrated state is not apparent in the hydrated IPNs. All the hydrated surface free energies fall within the usual range for high water content hydrogels. The surface free energy of the NNDMA-Pellathane IPNs is illustrated below in Figure 8.10.

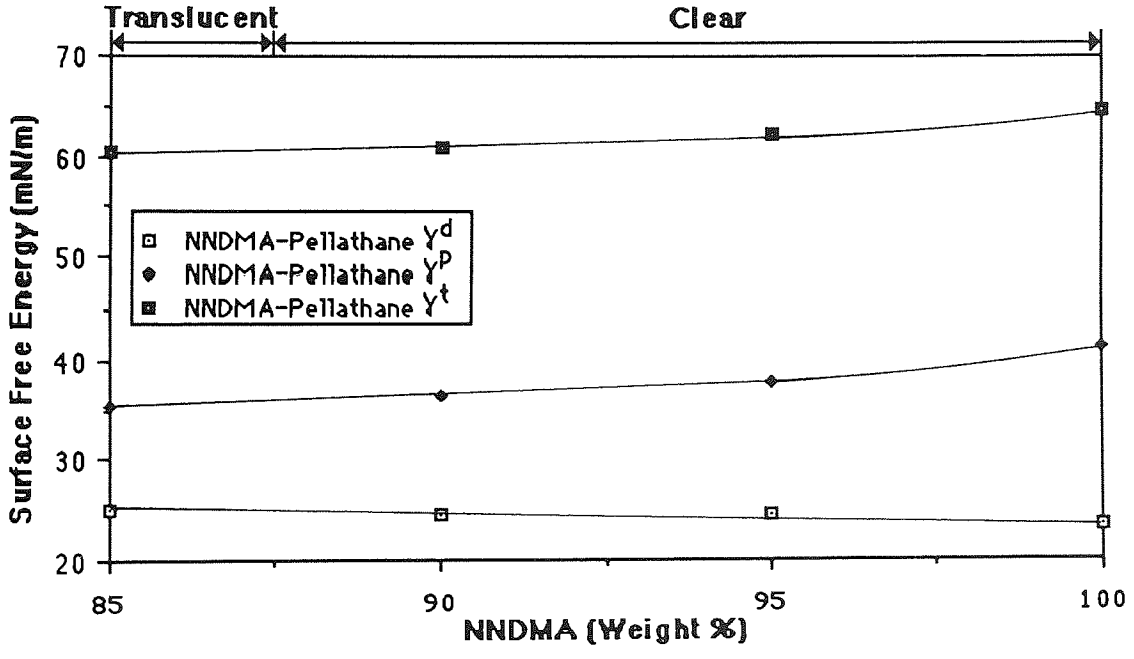

Figure 8.10 Effect of composition on the hydrated surface free energy of NNDMA-Pellathane IPN hydrogels

Pellathane incorporation causes a reduction in γ^p and γ^t with a slight rise in γ^d. Similar behaviour is also seen for the other hydrated polyurethane containing IPNs. However, γ^d and γ^p for hydrated Biomer have been reported as 48mN/m and 22mN/m respectively[220] but as the water content of Biomer is relatively low these values are not unreasonable. In the hydrated state water will have a great influence on the surface free energy of these IPNs. Thus, while in the dehydrated state γ^p appears to increase with Pellathane incorporation in the hydrated state the reverse is true. This behaviour is not unexpected as Pellathane incorporation increases the hydrophobicity of the system and decreases the EWC.

The total surface free energy of the Pellathane containing IPNs is slightly lower than those of the NNDMA-PMMA and NNDMA-PVAc IPNs discussed previously and in all the polyurethane containing IPNs the hydrated surface free energies are much lower than those predicted from the water content and the measured dehydrated surface energies.

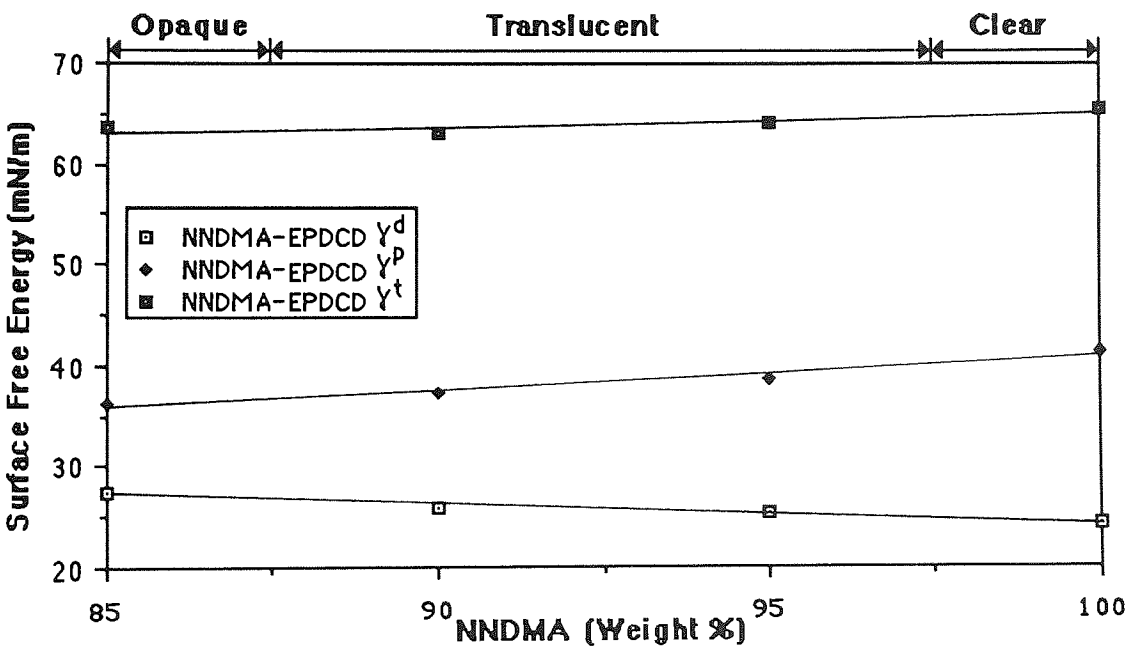

Figure 8.11 Effect of composition on the hydrated surface free energy of NNDMA-EPDCD IPN hydrogels

The hydrated surface properties of NNDMA-EPDCD IPNs are shown in Figure 8.11. It is clear that EPDCD is less polar than NNDMA as EPDCD incorporation is accompanied by a reduction in γ^p and γ^t and an increase in γ^d. This reduction in γ^p and γ^t is not as marked as in the dehydrated state due to the moderating influence of water. The increase in γ^d might be expected from the structure of EPDCD which has a large hydrophobic backbone with hydrophilic groups in the pendant side chain. However, the observed behaviour may be a secondary effect caused by the reduction in EWC which accompanies EPDCD incorporation. The values of γ^t, γ^p, and γ^d for this system are again in the range normally associated with high water content hydrogels.

The effect of IPN formation, using both CA and CAB as filler polymers, on the hydrated surface free energy and NNDMA is illustrated in Figure 8.12. There is a smooth transition in surface properties as increasing amounts of filler polymer are added, with the same trends being apparent in the hydrated state that were observed in the dehydrated state. This behaviour could be cited as a demonstration that imbibed water does not completely dominate the surface properties and that the polymer structure does have an effect. However, the values for γ^t are similar to those observed in the systems described previously. Thus, CA or CAB incorporation causes a reduction in γ^p and γ^t with an increase in γ^d but this behaviour may be due either to the structural changes in the IPNs or the differences in water contents or a combination of both factors. The accuracy of the technique is shown, however, as small changes in surface properties are detected.

The surface free energies of NVP based IPNs are shown in Figure 8.13 and these values may be usefully compared with the results for the NNDMA based IPNs. The important points which can be made about these systems will be reiterated but firstly, the differences between the hydrated and dehydrated surface energies of these IPNs will be discussed.

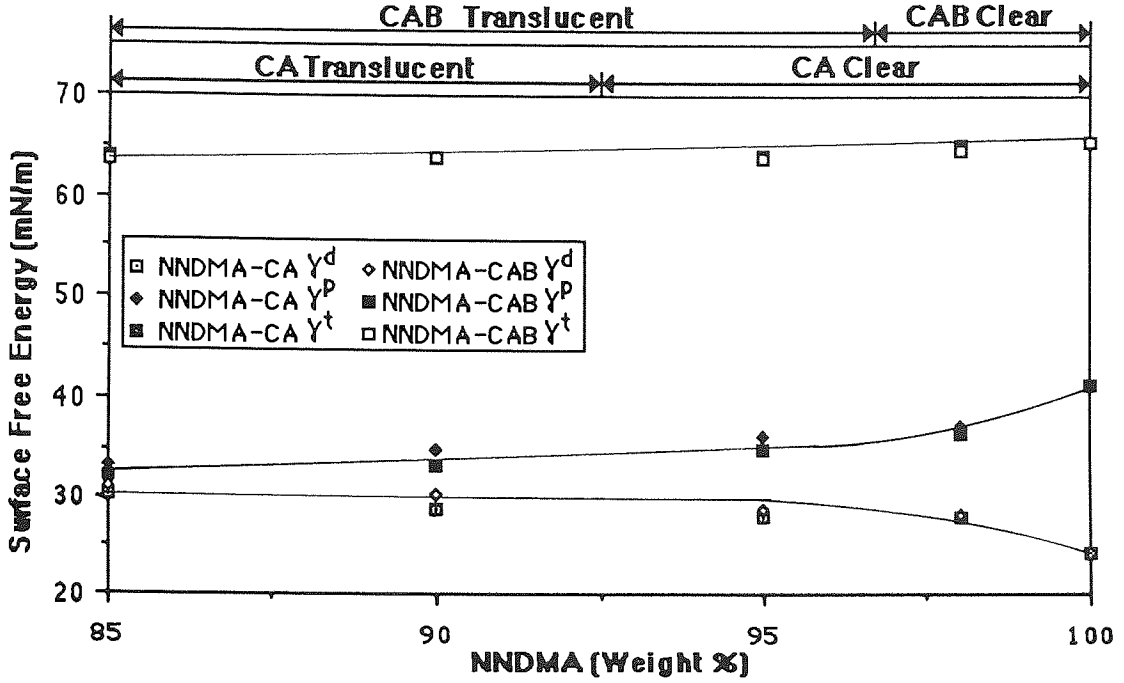

Figure 8.12 Effect of composition on the hydrated surface free energy of NNDMA-CA and NNDMA-CAB IPN hydrogels

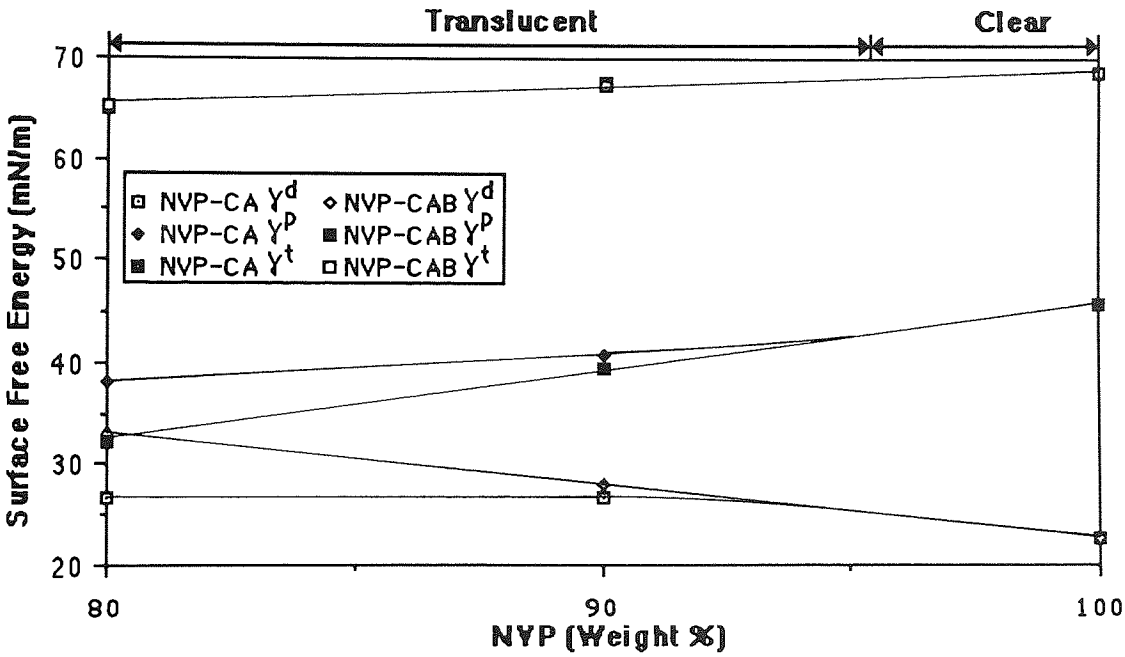

Figure 8.13 Effect of composition on the hydrated surface free energy of NVP-CA and NVP-CAB IPN hydrogels

Whereas, when dehydrated the NNDMA IPNs have a larger surface free energy, due to an increased γ^p and a reduced γ^d, the reverse is true in the hydrated polymers. This difference is not unexpected as poly NVP contains 98% water and only 2% organic material. Therefore, it might be assumed that the surface properties of poly NVP would be very similar to those of water (i.e. poly NVP should have a higher γ^p and lower γ^d than poly NNDMA). However, even after the incorporation of 15% or 20% filler polymer there are still noticeable differences in the surface energies of the NVP and NNDMA systems. In both the NVP and NNDMA systems the IPNs containing CAB as a filler polymer generally have a higher γ^d and a lower γ^p than the comparable IPN with CA.

8.4 Cell Adhesion Studies

Although sessile drop and droplet techniques may provide useful information about the changing surface properties of hydrogels they operate on a macroscopic scale rather than on a molecular level. However, one interesting investigative technique, which is often used in the biological field, has proved successful in many areas. Cell culture, often called tissue culture, makes use of the fact that under certain, well defined, conditions cells can be kept alive *in vitro*. This technique has been developed during the last decade and used successfully in many areas e.g. microbiology, biomaterials science and cancer research. In biomaterials science it may be used as a probe to investigate the response when a non-physiological material contacts a biological environment and of the process of interfacial conversion.

In this work the surface properties of a range of copolymer and IPN hydrogels with EWCs in the range 37.6% to 88.4% were investigated by cell adhesion studies with BHK fibroblast cells. Although a complete description of the techniques used for cell adhesion studies is beyond the scope of this thesis, they have been well documented by Thomas[221].

Initially, it was thought that the differences in cell response to these substrates might further the understanding of those polymer properties which affect cell adhesion. Furthermore, it was thought that a more sensitive surface probe technique might reveal differences in the surface properties of these hydrogels which were undetected by the droplet techniques.

The hydrogels chosen for cell adhesion studies are listed in Appendix 6 together with their EWC and the cell count. In the results presented graphically in this Chapter cell attachment is expressed as a percentage relative to the cell attachment on tissue culture plastic, which encourages complete cell attachment and spreading on its surface. The first point which can be made about these IPNs is that the majority of them can be classified as non-adhesive (-) and even in the cases where there is cell attachment, there is little spreading (+). This can be contrasted with the behaviour of tissue culture plastic on which there is a confluent monolayer of fully spread cells (+++) after the same time period. The consequences of this non-adhesive response to BHK fibroblast cells will be discussed in more detail after the trends in behaviour, of the various hydrogels examined, have been discussed. However, the fact that the specificity of a biological reaction cannot be regarded as being independent of surface chemistry is illustrated by a plot of cell adhesion to some of the hydrogels described in this thesis and expressed as a function of EWC (Figure 8.14). Clearly no correlation exists between EWC and cell attachment.

The hydrogels used in this work were then separated into groups according to their constituents to determine if polymer structure influenced cell attachment. Interesting differences in behaviour were observed in copolymers and IPNs with nitrogen containing monomers. The NVP and NNDMA copolymers show a dramatic fall in cell attachment as a function of EWC (Figure 8.15).

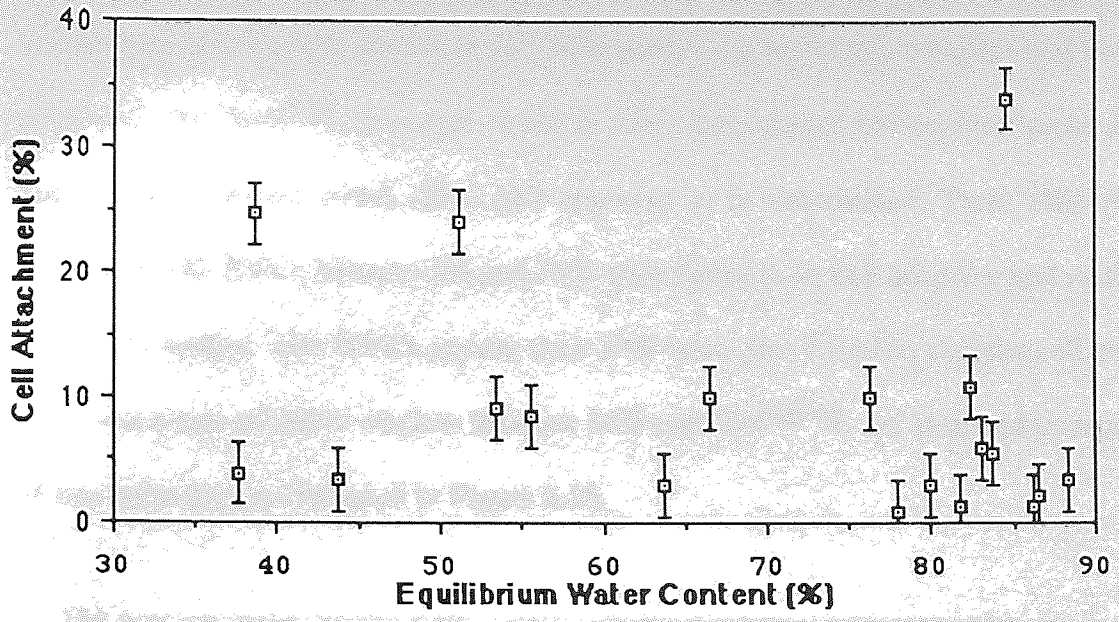

Figure 8.14 Effect of equilibrium water content on the cell attachment to a range of copolymer and IPN hydrogels

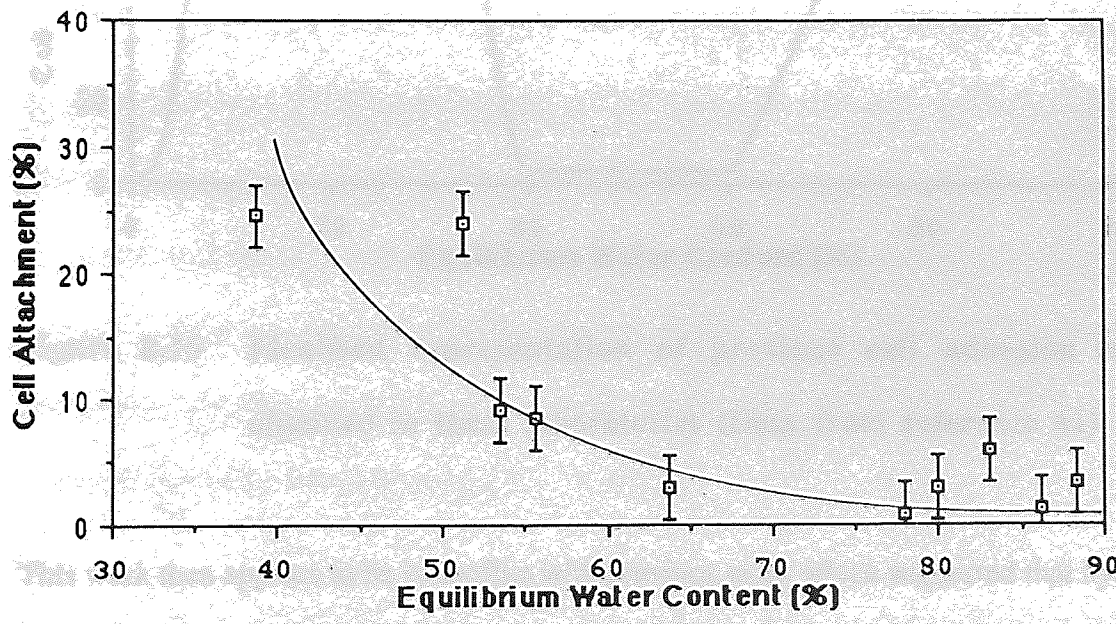

Figure 8.15 Effect of equilibrium water content on the cell attachment to NVP and NNDMA copolymer hydrogels

These results should be seen against those of previous workers. The factors governing the interactions of cells with polymers and biomaterials are extremely complex and have been reviewed elsewhere[222]. However, work in these laboratories has enabled some physical and chemical factors which affect cell response to be determined. Thus, HEMA based hydrogels with EWCs between 2% and 34% were found to be cell adhesive and while those hydrogels studied with EWCs greater than 70% were also found to support cell adhesion there was a non-adhesive window between 34% and 70%[40-42]. An idealised interpretation of this behaviour is illustrated in Figure 8.16.

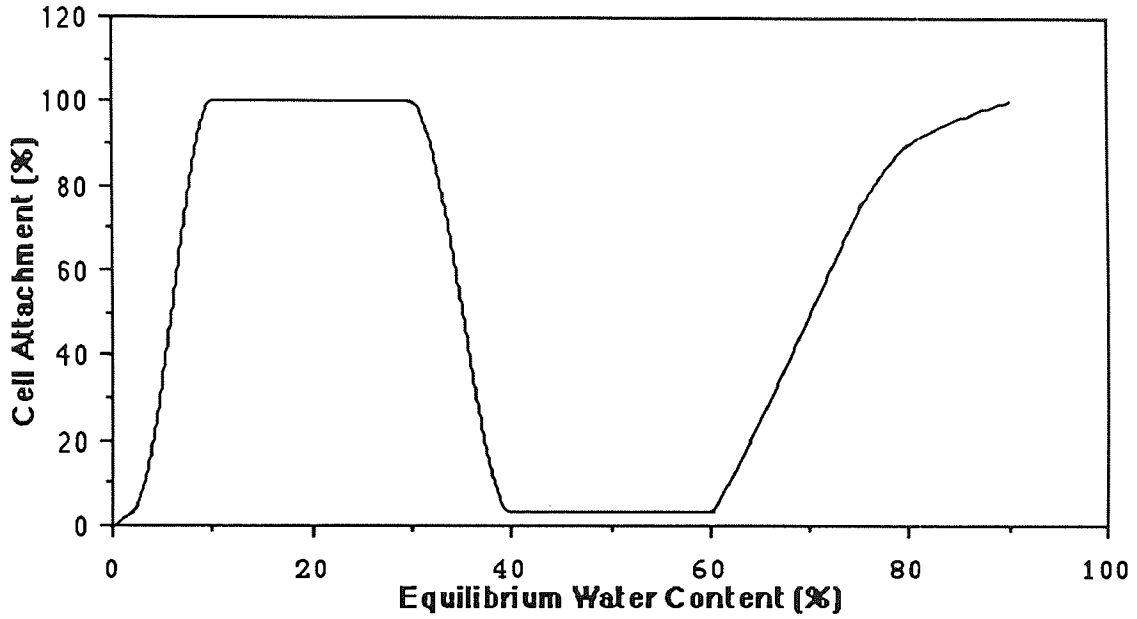

Figure 8.16 Idealised representation of previous cell adhesion results obtained in these laboratories (Data from reference 41)

This work then appears to be in conflict with previous work which suggested that hydrogels with EWCs of greater than 70% should be cell adhesive[41]. However, the high water content hydrogels used in that work were based on acrylamide and a recent study[221] has indicated that acrylamide hydrogels are adhesive in the EWC range 50%-90%. Therefore, it is reasonable to suggest that the point at which cell adhesion is inhibited in these hydrogels

is dependent not solely on EWC but also on the nature of the water structuring groups involved. Thus, the region of cell non-adhesion for HEMA based copolymers begins at an EWC of 34%, while for NVP and NNDMA based copolymers it begins at an EWC of approximately 50% and for acrylamide based copolymers at an EWC of greater than 90%.

The NNDMA based IPNs show interesting differences in behaviour and illustrate that cells can detect differences in surface properties which are undetected by droplet techniques. This is illustrated in Figure 8.17 which shows cell attachment, as a function of EWC and Figure 8.18 which shows cell attachment as a function of γ^p, the dehydrated polar component of surface free energy. It appears that the boundary layer of water in these IPN hydrogels masks differences in expression of water structuring groups (when droplet techniques are used to probe the surface) which are biologically active at the surface.

8.5 Conclusions

The surface properties of IPN hydrogels in both the hydrated and dehydrated states (with the exception of the NNDMA-polyurethane IPNs) are very similar to the surface properties of copolymer hydrogels and the same trends in behaviour are apparent. Thus, incorporation of a more hydrophobic filler polymer into NNDMA leads to a reduction in γ^p and an increase in γ^d in both the hydrated and dehydrated IPN. The magnitude of this change in γ^p and γ^d can be related to structural and steric changes in the IPN and this effect is more clearly visible in the dehydrated state.

Generally, the greatest reduction in γ^p is caused by the introduction of a bulky, sterically hindering monomer which reduces expression of the polar groups of NNDMA at the surface of the IPN. However, other factors must also be important as if γ^p for the three IPNs containing ring systems are compared, the EPDCD IPNs have the highest γ^p but

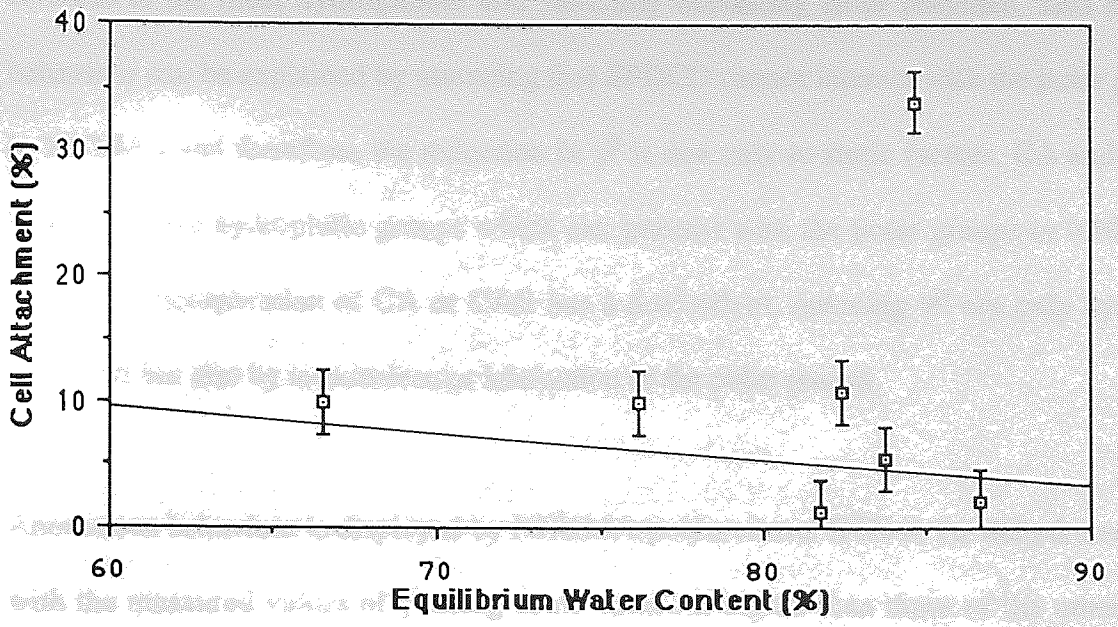

Figure 8.17 Effect of equilibrium water content on the cell attachment to NNDMA IPN hydrogels

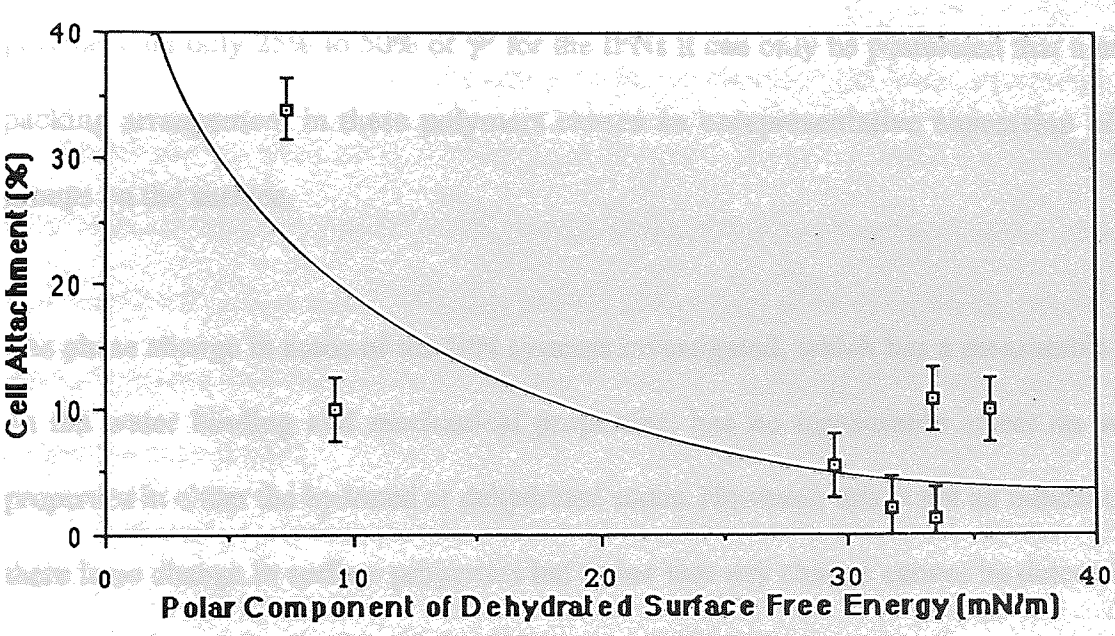

Figure 8.18 Effect of the polar component of the dehydrated surface free energy on the cell attachment to NNDMA IPN hydrogels

EPDCD is the most hydrophobic and sterically occluding filler polymer. This surface behaviour can be explained by assuming that EPDCD cannot interact with the polar groups in NNDMA and therefore, the reduction in γ^p is due only to steric factors. CA and CAB, however, have hydrophilic groups which can interact with the polar groups in NNDMA. Thus, the incorporation of CA or CAB has a duel effect, reducing γ^p not only by steric occlusion but also by intramolecular interaction of the polar groups.

Anomalous behaviour is displayed by NNDMA-polyurethane IPNs in the dehydrated state with the measured values of γ^t being some 15mN/m higher than those of the other IPNs examined in this work. The dispersive components of the surface free energy in these systems are similar to that of the other IPNs, however, the values of γ^p are nearly doubled. Interestingly, similar behaviour is displayed by Geliperm a commercially available wound dressing based on an acylamide-agar IPN. As the γ^p values for the polyurethane filler polymers are only 25% to 50% of γ^p for the IPNs it can only be postulated that a unusual packing arrangement in these polymers causes an unrepresentative expression of polar groups on the surface.

The phase change in some of the IPN systems investigated, which has a measurable effect on the water binding and mechanical properties, has no measurable effect on surface properties in either the hydrated or dehydrated states. However, this is not an indication that there is no change in surface properties but rather that any change cannot be detected on a macroscopic scale by the droplet techniques used in this work.

Marked differences in behaviour are observed in the mechanical and water binding properties of NNDMA-MMA copolymers and NNDMA-PMMA IPNs, however, the surface properties of both systems are similar. Although this can be easily explained for the

dehydrated polymers as the same groups will be present at the surface this is not the case in the hydrated systems. There is a 17% variation in EWC between the 80:20 copolymer and IPN but the surface free energies of both systems are similar, with the NNDMA-PMMA IPN having a slightly lower γ^p. These results suggest either that the surface of the hydrated IPN is dominated by NNDMA or that there is a surface layer of water present and the major contribution to γ^p and γ^t is coming from this water layer.

If the surface energies of the hydrated copolymers and IPNs based on NVP and NNDMA are compared the γ^p and γ^t values all lie within a narrow band. Thus, there is little measurable difference between a range of copolymers and IPNs. This behaviour leads to the impression that the surface properties of the hydrated materials are dominated by an adsorbed layer of water on the surface of the polymers. The results obtained from cell adhesion studies support this idea. It is apparent that in the region where droplet techniques detect little difference in surface properties, changes are occurring on a molecular level. The surface properties appear to be affected both by the nature of the water structuring group and by the amount and type of water present in the gel. However, these changes in surface properties are normally masked by the water layer present on the surface of the hydrogels. The correlation between cell adhesion and the dehydrated γ^p of the IPNs examined in this work, suggests that cell adhesion studies enable the underlying differences in surface properties to be probed.

CHAPTER 9

Conclusions and Suggestions for Further Work

9.1 Conclusions

A systematic study of the water binding, mechanical and surface properties of a series of copolymer and IPN hydrogels has been undertaken and the variations in these properties have been related to changes in structure and composition of the gels. Initially, the water binding capabilities of the hydrogels were investigated using the gravimetric method of determining EWC and differential scanning calorimetry, both of which have proved to be useful techniques. DSC reveals the complex water structuring that exists in hydrogel systems and that the water present in the gel exists in a continuum of states between the two experimentally determined extremes, freezing and non-freezing water.

Using the above techniques the EWC and water binding characteristics of poly HEMA were unambiguously determined by double extrapolation using the HEMA-MMA and HEMA-NVP systems. The values obtained for EWC, freezing and non-freezing water contents were 37.6%, 13.2% and 24.4% respectively. Poly HEMA was then used as a "standard" for the other systems studied. In work with both copolymers and IPNs based on HEMA and the more hydrophilic monomers NNDMA and NVP it became apparent that each water structuring group has a different, maximum water binding ability. The water binding ability is then modified by steric effects and the hydrophobicity of the comonomer or filler polymer. However, in IPNs there is the additional influence of the systems compatibility and the interaction between the water binding groups on the matrix and filler polymers. The regular variation in water binding properties with composition will be disrupted by a phase change in these systems as illustrated by the NNDMA-PMMA and NNDMA-PVAc IPNs. Therefore, incorporation of a more hydrophobic comonomer or filler polymer reduces the EWC, while the reverse is true for hydrophilic monomers. Steric occlusion of water structuring groups also causes a reduction in the water binding ability of the polymer system. Thus, in moving from HEA to HEMA the introduction of a hydrophobic, sterically

hindering α-methyl group reduces the EWC from 60.5% to 37.6% respectively. Furthermore, comparing the PMMA and PVAc IPNs although the structures of the polar groups are similar, PMMA has a much greater effect on the EWC because of the α-methyl group on the backbone. However, the water binding of a homopolymer, copolymer or IPN can normally be rationalised in terms of the structures of the constituents and the interactions between them.

NNDMA and NVP have the same water structuring groups and the water binding ability of both systems is similar at higher levels of crosslinker or comonomer incorporation. Results from cell adhesion studies also suggest that the surfaces (and water structuring groups) presented to the cell by both systems on a molecular level are very similar However, in the homopolymer with only 1% crosslinker, NVP has a much greater water binding capability the NNDMA. This is due to the helical packing of poly NVP which minimises the steric interactions between the lactam rings and enables more water to be associated with the molecule in the extra "space" in the chain, between the rings. This helical packing is also important in determining the surface energy of NVP containing polymers.

One of the great advantages of both copolymer and IPN hydrogel systems is that the ratio of freezing to non-freezing water may be altered both by varying the copolymer composition and the structure of the water binding group. Therefore, it is possible to synthesise a range of copolymers with varying EWCs and freezing to non-freezing water ratios. The transport properties of hydrogels are dependant on the above poperties and this abilty to control them is useful in applications where permselectivity is important.

Perhaps one of the most important aspects of hydrogel chemistry is the ability to move, in a simple copolymer series, from a composition where γ^d is the major component of the

surface free energy through to a composition where γ^p is dominates the surface properties. The results obtained from the surface studies on the hydrogels in both the hydrated and dehydrated states can be rationalised in terms of the hydrophobicity and structure of the copolymers. In the dehydrated state clear differences are observed between the polymers as a function of composition but these differences are sometimes masked in the hydrated state. Incorporation of a hydrophobic, sterically hindering comonomer will reduce γ^p and γ^d in both the hydrated and dehydrated copolymers, however, the effect will be less marked in the hydrated state because of the modulating effect of water. Some specific examples of the effect of polymer structure and interactions on the surface free energy will now be cited.

Poly NVP has a low polar component of surface free energy due to the helical packing in the homopolymer. The polar groups are oriented within the matrix and the CH_2 groups on the lactam rings are expressed at the surface. Incorporation of a sterically hindering monomer further reduces γ^p as the polar groups in poly NVP become more shielded and the percentage of hydrophobic molecules in the copolymer increases. Another factor which is important in determining the surface properties in hydrogel systems is polymer-polymer interactions. Thus, in the HEMA-NVP copolymers, for example, intramolecular interactions between the polar groups on both polymers reduces their expression at the polymer surface and leads to the 50:50 copolymer having a lower γ^p than either of the homopolymers. The surface properties of the IPNs vary regularly as a function of composition and the effect of the phase chage is undetected in these systems. The regular variation in surface properties of the semi-IPNs synthesised in this work is in contrast with the pronounced minima often found in the surface properties of full IPNs.

Many problems are encountered when attempting to measure the surface free energy of hydrogel polymers in both the hydrated and dehydrated states. Therefore, in this work

several predictive methods were used to assign a value to the surface free energy of a copolymer from its composition. The CED method which is based only on dispersive contributions gave values which were in poor agreement with γ^t in all the systems studied. However, the parachor technique produces values which are a close approximation to the experimentally determined values of surface free energy in the majority of dehydrated hydrogels. This method is, however, unable to take into account polymer-polymer interactions of the type described above and in systems where these interactions occur there is often a large disparity between the predicted and measured surface free energy. Although the parachor technique proves to be a reliable predictive method in the dehydrated state problems arise when it is used to predict the surface energy of hydrated polymers, as it is unable to account for the interactions between the polymer and water. Thus, these predicted values for the hydrated surface free energy are generally low. The second technique used for the prediction of hydrated surface free energies was based on a knowledge of the dehydrated surface energy of the hydrogels and the volume fraction of water in the gels. The relative contributions of polymer and water to the surface free energy were then calculated but the values obtained were again generally lower than the experimentally determined values of γ^t.

The similarity of all the measured values for the hydrated surface free energy and the low predicted values for γ^t in the hydrated state suggest that there may be an adsorbed surface layer of water on these polymers. This surface layer masks differences between the polymers which are not detected on a macroscopic scale using droplet techniques. Cell adhesion studies allow these the underlying differences in surface properties to be probed and the nature of the water structuring group is found to be important in determining adhesion Thus, there is a charcteristic curve of cell adhesion versus water content for each water structuring group with the cut off point being dependant on the nature of that group.

The results obtained from IPN hydrogels suggest that the cells are influenced by both the properties of the dehydrated material and the water structuring groups present in the system. However, the majority of the hydrogels studied can be classified as non-adhesive to BHK fibroblast cells, this may be advantageous for their use in wound dressing applications.

NNDMA is susceptible to chain transfer due to the readily abstractable hydrogens on the methyl groups. This often leads to the formation of brittle copolymers due to the low kinetic chain length of poly NNDMA. Thus, NNDMA proved to be an ideal monomer for use in the synthesis of IPNs as it has good solvent properties and any improvements in mechanical properties were clearly visible. The mechanical properties of the copolymer hydrogels were found to be a function of polymer composition, EWC and the mechanical properties of the copolymers in the dehydrated state. The mechanical properties of IPNs, on the other hand, are a complex function of the T_g, molecular weight and water binding capability of the filler polymer in conjunction with the compatibilty and EWC of the polymer system. Therefore, no precise correlation between filler polymer properties and the mechanical properties of IPNs has been found. However, this work has shown that synthesis of IPNs does provide a method of improving the mechanical properties of NNDMA based hydrogels. Another interesting property of the IPNs is that they display different stress strain envelopes to those of HEMA or NNDMA based copolymers of a similar tensile strength or Youngs modulus. Thus, it is possible to produce high tensile strength materials with varying degrees of flexibility or rigidity, by IPN formation.

Semi-IPN hydrogels of the type investigated in this work have the potential to further extend the use of hydrogels in biomedical applications. Although the initial interest in this work was in clear, homogeneous, compatible IPNs, it soon became apparent that the systems produced also had interesting and useful properties. These IPNs offer the

advantages of full IPN formation, which enables the production of polymers with EWCs of 70-80% which have higher tensile strengths and Youngs moduli than poly HEMA. However, there is a regular variation in surface properties in these semi-IPNs which contrasts with the marked deviations often seen in full IPN systems. The water binding properties also vary regularly with composition although, as is the case with mechanical properties, discontinuities are are apparent when phase changes occur in the system. Thus, by careful choice of matrix and filler polymers it should be possible to "design" IPNs for use in wound dressing and other biomedical applications.

9.2 Suggestions for Further Work

A systematic study of these polymers is necessary to determine the complex interdependence of the pH of the hydrating medium and tonicity on the water binding in these systems. Further work is also necessary with a range of monomers containing similar water binding groups to confirm the hypothesis that each water binding group has a specific water binding ability which is then modified by its environment.

Although the mechanical properties of these hydrogels have been investigated under tension, for some biomedical applications their behaviour under compression is also important. Therefore, micropenetrometry studies should be untertaken to determine the behaviour of these copolymers and IPNs under compression.

Poly NNDMA has proved to be a useful monomer for IPN formation having good solvent properties and being a particularly sensitive system because of chain transfer reactions. However, for commercial applications of IPNs of this type a matrix polymer with improved strength and flexibility would be advantageous. Therefore, the synthesis of new liquid monomers with similar solvent properties to NNDMA but with substituent groups which

are not susceptible to chain transfer reactions may help to in the achievement of this goal.

Although phase changes in some of the IPN systems studied are signalled by changes in appearance, these phase changes have not been fully investigated. Transmission electron microscopy studies would enable the morphology of the IPNs to be examined. It may then be possible to relate changes in morphology to changes in surface behaviour, as revealed by cell adhesion studies. Scanning electron microscopy studies would also be useful and would enable the surface structure of the IPNs to be investigated. Thus, it might be possible to see differences in pore size between IPN with varying water contents and compositions.

It has been postulated that the molecular weight, T_g and water binding ability of the filler polymer are important in determining the mechanical properties of IPNs. However, a systematic study of these systems with a carefully selected range of filler polymers would be able to confirm this hypothesis. Further work is also necessary to determine the precise factors affecting the mechanical properties of copolymer hydrogels.

The surface free energies of the hydrated copolymers and IPNs have been measured but the measurement of the friction and wear on the surface of the polymers would enable their suitability for use in articular cartilage applications to be determined.

Further use of cells as a biological probe technique may reveal interesting differences in surface properties of the hydrated hydrogels. The use of a wider range hydrogels with variations in water structuring groups would enable the cut off point for cell adhesion to each water structuring group to be determined. It would also be interesting to see the cell behaviour around the crossover point in hydrogel systems where the surface free energy is moving from being dominated by γ^d to being dominated by γ^p.

APPENDIX 1

Water Binding Data for Copolymer and IPN Hydrogels

Copolymer Hydrogel Composition	Equilibrium Water Content (%)	Freezing Water Content (%)	Non-Freezing Water Content (%)	Total Grams of Water / Gram of Polymer	Grams of Freezing Water / Gram of Polymer	Grams of Non-Freezing Water / Gram of Polymer
HEMA 0.0 % X-Linker	44.3	19.7	24.6	0.795	0.353	0.442
HEMA 0.1 % X-Linker	40.5	16.6	23.9	0.681	0.279	0.402
HEMA 0.25% X-Linker	39.4	15.5	23.9	0.650	0.255	0.394
HEMA 0.5 % X-Linker	38.5	14.4	24.1	0.626	0.234	0.392
HEMA 1.0 % X-Linker	37.6	13.2	24.4	0.603	0.211	0.391
HEMA 2.0 % X-Linker	36.0	11.2	24.8	0.563	0.175	0.388
HEMA 5.0 % X-Linker	31.5	5.2	26.3	0.460	0.076	0.384
HEMA 10.0% X-Linker	27.6	3.4	24.2	0.381	0.047	0.334
HEMA 15.0% X-Linker	23.0	2.6	20.4	0.299	0.033	0.265
HEMA 20.0% X-Linker	20.4	1.6	18.8	0.256	0.020	0.236
Poly HEMA	37.6	13.2	24.4	0.603	0.211	0.391
HEMA-MMA 95: 5	34.7	10.7	24.0	0.531	0.163	0.368
HEMA-MMA 90:10	32.5	7.2	25.3	0.481	0.106	0.375
HEMA-MMA 80:20	27.4	3.4	24.0	0.377	0.046	0.331
HEMA-MMA 70:30	24.1	1.6	22.5	0.318	0.021	0.296
HEMA-MMA 60:40	17.5	0.5	17.0	0.212	0.006	0.206
HEMA-MMA 50:50	12.3	0.0	12.3	0.140	0.000	0.140

Copolymer Hydrogel Composition	Equilibrium Water Content (%)	Freezing Water Content (%)	Non-Freezing Water Content (%)	Total Grams of Water / Gram of Polymer	Grams of Freezing Water / Gram of Polymer	Grams of Non-Freezing Water / Gram of Polymer
HEMA-St 95: 5	29.7	-	-	0.422	-	-
HEMA-St 90:10	25.2	2.2	23.0	0.337	0.029	0.307
HEMA-St 80:20	16.7	0.8	15.9	0.200	0.009	0.191
HEMA-St 70:30	11.2	0.0	11.2	0.126	0.000	0.126
HEMA-St 50:50	5.0	0.0	5.0	0.053	0.000	0.053
HEMA-NVP 95: 5	38.7	15.2	23.5	0.631	0.248	0.383
HEMA-NVP 90:10	41.1	17.1	24.0	0.698	0.290	0.407
HEMA-NVP 80:20	43.8	21.3	22.5	0.779	0.379	0.400
HEMA-NVP 70:30	49.6	24.9	24.7	0.984	0.494	0.490
HEMA-NVP 60:40	54.9	32.5	22.4	1.217	0.720	0.497
HEMA-NVP 50:50	64.3	47.2	17.1	1.801	1.322	0.479
HEMA-NNDMA 95: 5	41.3	15.1	26.2	0.704	0.257	0.446
HEMA-NNDMA 90:10	45.5	20.0	25.5	0.835	0.367	0.468
HEMA-NNDMA 80:20	53.6	31.6	22.0	1.155	0.681	0.474
HEMA-NNDMA 70:30	62.4	48.2	14.2	1.659	1.282	0.378
HEMA-NNDMA 60:40	70.5	54.6	15.9	2.390	1.850	0.539
Poly HPA	50.5	22.3	28.2	1.020	0.450	0.570
Poly HPMA	21.2	2.0	19.2	0.269	0.025	0.244

Copolymer Hydrogel Composition	Equilibrium Water Content (%)	Freezing Water Content (%)	Non-Freezing Water Content (%)	Total Grams of Water / Gram of Polymer	Grams of Freezing Water / Gram of Polymer	Grams of Non-Freezing Water / Gram of Polymer
NNDMA 1.0 % X-Linker	88.4	70.7	17.7	7.621	6.094	1.526
NNDMA 2.5 % X-Linker	78.8	58.5	20.3	3.717	2.759	0.958
NNDMA 5.0 % X-Linker	73.4	42.7	30.7	2.759	1.605	1.154
NNDMA 7.5 % X-Linker	69.1	35.0	34.1	2.236	1.132	1.104
NNDMA 10.0% X-Linker	60.9	26.2	34.7	1.558	0.670	0.887
NNDMA-LMA 90:10	78.0	55.6	22.4	3.545	2.527	1.018
NNDMA-LMA 80:20	69.2	39.1	30.1	2.247	1.269	0.977
NNDMA-LMA 70:30	63.7	29.7	34.0	1.755	0.818	0.937
NNDMA-LMA 60:40	53.5	21.7	31.8	1.150	0.466	0.684
NNDMA-MMA 99: 1	87.3	68.6	18.7	6.874	5.401	1.472
NNDMA-MMA 97.5:2.5	87.1	67.9	19.2	6.752	5.263	1.488
NNDMA-MMA 95:5	86.5	65.2	21.3	6.407	4.829	1.578
NNDMA-MMA 90:10	86.2	64.0	22.2	6.246	4.637	1.609
NNDMA-MMA 85:15	85.2	61.9	23.3	5.757	4.182	1.574
NNDMA-MMA 80:20	83.1	58.7	24.4	4.917	3.473	1.444
NVP 1.0% X-Linker	98.1	93.0	5.1	51.632	48.947	2.684
NVP 2.5% X-Linker	93.7	81.9	11.8	14.873	13.000	1.873
NVP 5.0% X-Linker	86.0	69.9	16.1	6.143	4.992	1.150
NVP 7.5% X-Linker	78.4	58.4	20.0	3.630	2.703	0.926
NVP 10.0% X-Linker	72.4	45.3	27.1	2.623	1.641	0.982

Copolymer Hydrogel Composition	Equilibrium Water Content (%)	Freezing Water Content (%)	Non-Freezing Water Content (%)	Total Grams of Water / Gram of Polymer	Grams of Freezing Water / Gram of Polymer	Grams of Non-Freezing Water / Gram of Polymer
NVP-LMA 90:10	80.0	57.8	22.2	4.000	2.890	1.110
NVP-LMA 80:20	68.0	37.7	30.3	2.125	1.178	0.947
NVP-LMA 70:30	58.4	23.0	35.4	1.404	0.552	0.851
NVP-LMA 60:40	51.2	18.8	32.4	1.049	0.385	0.664
NVP-MMA 90:10	82.3	53.4	28.9	4.650	3.017	1.633
NVP-MMA 80:20	76.7	43.1	33.6	3.292	1.849	1.442
NVP-MMA 70:30	67.8	31.3	36.5	2.106	0.972	1.134
NVP-MMA 60:40	55.6	24.6	31.0	1.252	0.554	0.698
NVP-MMA 50:50	38.6	3.5	35.1	0.629	0.057	0.572

IPN Hydrogel Composition	Equilibrium Water Content (%)	Freezing Water Content (%)	Non-Freezing Water Content (%)	Total Grams of Water / Gram of Polymer	Grams of Freezing Water / Gram of Polymer	Grams of Non-Freezing Water / Gram of Polymer
NNDMA-PMMA 99: 1	85.8	65.0	20.8	6.042	4.577	1.465
NNDMA-PMMA 97.5:2.5	86.1	63.7	22.4	6.194	4.582	1.612
NNDMA-PMMA 95:5	84.8	62.1	22.7	5.579	4.085	1.493
NNDMA-PMMA 90:10	75.2	48.9	26.3	3.032	1.971	1.060
NNDMA-PMMA 85:15	70.5	46.2	24.3	2.390	1.566	0.824
NNDMA-PMMA 80:20	66.5	40.8	25.7	1.985	1.218	0.767
NNDMA-PVAc 99: 1	86.4	64.0	22.4	6.353	4.705	1.647
NNDMA-PVAc 95: 5	86.9	64.2	22.7	6.634	4.900	1.733
NNDMA-PVAc 90:10	86.8	64.9	21.9	6.576	4.916	1.659
NNDMA-PVAc 85:15	85.3	65.7	19.6	5.803	4.469	1.333
NNDMA-PVAc 80:20	84.6	66.4	18.2	5.493	4.311	1.182
NNDMA-PVAc 70:30	82.7	65.1	17.6	4.780	3.763	1.017
NNDMA-PVAc 60:40	81.2	64.6	16.6	4.319	3.436	0.883
NNDMA-Biomer 95:5	83.7	59.2	24.5	5.135	3.632	1.503
NNDMA-Pellathane 95: 5	82.4	54.9	27.5	4.682	3.119	1.563
NNDMA-Pellathane 90:10	76.2	46.8	29.4	3.202	1.966	1.235
NNDMA-Pellathane 85:15	73.7	43.2	30.5	2.802	1.642	1.160
NNDMA-HPU25 95: 5	81.7	56.0	25.7	4.464	3.060	1.404
NNDMA-HPU25 90:10	86.6	53.7	32.9	6.463	4.007	2.455

IPN Hydrogel Composition	Equilibrium Water Content (%)	Freezing Water Content (%)	Non-Freezing Water Content (%)	Total Grams of Water / Gram of Polymer	Grams of Freezing Water / Gram of Polymer	Grams of Non-Freezing Water / Gram of Polymer
NNDMA-EPDCD 95: 5	85.6	67.7	17.9	5.944	4.701	1.243
NNDMA-EPDCD 90:10	80.7	57.2	23.5	4.181	2.963	1.218
NNDMA-EPDCD 85:15	70.0	39.3	30.7	2.333	1.310	1.023
NNDMA-CA 98: 2	84.7	64.8	19.9	5.536	4.235	1.301
NNDMA-CA 95: 5	86.1	69.5	16.6	6.194	5.000	1.194
NNDMA-CA 90:10	82.1	64.5	17.6	4.587	3.603	0.983
NNDMA-CA 85:15	79.8	59.1	20.7	3.951	2.925	1.025
NNDMA-CAB 98: 2	83.9	63.6	20.3	5.211	3.950	1.261
NNDMA-CAB 95: 5	84.3	67.9	16.4	5.369	4.324	1.044
NNDMA-CAB 90:10	80.0	61.0	19.0	4.000	3.050	0.950
NNDMA-CAB 85:15	77.6	57.2	20.4	3.464	2.553	0.911
NVP-CA 90:10	87.2	77.2	10.0	6.813	6.031	0.781
NVP-CA 80:20	79.1	62.9	16.2	3.785	3.009	0.775
NVP-CAB 90:10	81.8	69.8	12.0	4.494	3.835	0.659
NVP-CAB 80:20	72.6	57.8	14.8	2.650	2.109	0.540
Geliperm	98.0	96.4	1.6	49.000	48.200	0.800

IPN Hydrogel Composition	Equilibrium Water Content (%)	Freezing Water Content (%)	Non-Freezing Water Content (%)	Total Grams of Water / Gram of Polymer	Grams of Freezing Water / Gram of Polymer	Grams of Non-Freezing Water / Gram of Polymer
HEMA-Agar 99: 1	47.4	31.4	16.0	0.901	0.597	0.304
HEMA-Agar 95: 5	62.6	46.0	16.6	1.674	1.230	0.444
HEMA-Agar 90:10	67.1	50.8	16.3	2.040	1.544	0.495
NNDMA-CMC 98: 2	91.7	-	-	11.048	-	-
NNDMA-CMC 90:10	90.8	-	-	9.870	-	-
NNDMA-CMC 80:20	92.7	-	-	12.699	-	-
NNDMA-Gelatin 99: 1	93.3	-	-	13.925	-	-
NNDMA-Gelatin 98: 2	84.7	-	-	5.536	-	-
NNDMA-Gelatin 95: 5	93.3	-	-	13.925	-	-
NNDMA-Ch-6-sul 98: 2	83.9	-	-	5.211	-	-
NNDMA-Ch-6-sul. 92.5:7.5	91.9	-	-	11.346	-	-
NNDMA-HEC 98: 2	93.1	-	-	13.493	-	-
HEMA-HEC 98: 2	46.7	-	-	0.876	-	-
HEMA-Ch-6-sul 90:10	57.4	-	-	1.347	-	-

APPENDIX 2

Tensile Data for Copolymer and IPN Hydrogels

Copolymer Hydrogel Composition	E.W.C. (%)	Tensile Strength (MPa)	Elongation to Break (%)	Youngs Modulus (MPa)	Appearance
HEMA 1.0 % X-Linker	37.6	0.495	198	0.25	Clear
HEMA 2.0 % X-Linker	36.0	0.472	71	0.665	Clear
HEMA 5.0 % X-Linker	31.5	0.738	82	0.900	Clear
Poly HEMA	37.6	0.495	198	0.25	Clear
HEMA-MMA 95: 5	34.7	0.375	138	0.272	Clear
HEMA-MMA 90:10	32.5	0.345	160	0.216	Clear
HEMA-MMA 80:20	27.4	0.799	241	0.332	Clear
HEMA-MMA 70:30	24.1	0.921	282	0.327	Clear
HEMA-MMA 60:40	17.5	13.173	58	22.712	Clear
HEMA-MMA 50:50	12.3	13.259	21	63.138	Clear
HEMA-St 90:10	25.2	1.322	401	0.370	Clear
HEMA-St 80:20	16.7	7.840	324	2.440	Clear
HEMA-NVP 95: 5	38.7	0.476	194	0.245	Clear
HEMA-NVP 90:10	41.1	0.525	174	0.302	Clear
HEMA-NVP 80:20	43.8	0.321	74	0.434	Clear
HEMA-NVP 70:30	49.6	0.346	76	0.455	Clear
HEMA-NVP 60:40	54.9	0.249	117	0.213	Clear
HEMA-NVP 50:50	64.3	0.197	97	0.203	Clear

Copolymer Hydrogel Composition	E.W.C. (%)	Tensile Strength (MPa)	Elongation to Break (%)	Youngs Modulus (MPa)	Appearance
HEMA-NNDMA 95: 5	41.3	0.482	186	0.259	Clear
HEMA-NNDMA 90:10	45.5	0.394	131	0.301	Clear
HEMA-NNDMA 80:20	53.6	0.285	101	0.282	Clear
HEMA-NNDMA 70:30	62.4	0.247	116	0.213	Clear
HEMA-NNDMA 60:40	70.5	0.204	133	0.161	Clear
NNDMA 1.0 % X-Linker	88.4	0.136	141	0.097	Clear
NNDMA 2.5 % X-Linker	78.8	0.195	83	0.240	Clear
NNDMA 5.0 % X-Linker	73.4	0.225	47	0.541	Clear
NNDMA 7.5 % X-Linker	69.1	0.295	28	1.054	Clear
NNDMA 10.0% X-Linker	60.9	0.243	22	1.105	Clear
NNDMA-LMA 90:10	78.0	0.211	105	0.201	Clear
NNDMA-LMA 80:20	69.2	0.418	217	0.193	Clear
NNDMA-LMA 70:30	63.7	0.433	174	0.249	Clear
NNDMA-LMA 60:40	53.5	0.533	317	0.168	Clear
NNDMA-MMA 99: 1	83.7	0.094	120	0.078	Clear
NNDMA-MMA 97.5:2.5	87.1	0.066	62	0.106	Clear
NNDMA-MMA 95:5	86.5	0.131	149	0.088	Clear
NNDMA-MMA 90:10	86.2	0.161	170	0.095	Clear
NNDMA-MMA 85:15	85.2	0.142	129	0.110	Clear
NNDMA-MMA 80:20	83.1	0.127	130	0.103	Clear

Copolymer Hydrogel Composition	E.W.C. (%)	Tensile Strength (MPa)	Elongation to Break (%)	Youngs Modulus (MPa)	Appearance
NNDMA-EEMA 90:10	85.3	0.091	164	0.060	Clear
NNDMA-EEMA 80:20	84.5	0.125	112	0.112	Clear
NNDMA-EEMA 70:30	81.8	0.123	85	0.145	Clear
NNDMA-MPEGMA 95:5	85.4	0.065	68	0.096	Clear
NNDMA-MPEGMA 90:10	85.0	0.115	92	0.125	Clear
NNDMA-MPEGMA 85:15	84.7	0.106	71	0.149	Clear
NVP-LMA 90:10	80.0	0.103	117	0.088	Clear
NVP-LMA 80:20	68.0	0.162	115	0.141	Clear
NVP-LMA 70:30	58.4	0.341	93	0.367	Clear
NVP-LMA 60:40	51.2	0.324	117	0.277	Clear
NVP-MMA 90:10	82.3	0.026	57	0.046	Clear
NVP-MMA 80:20	76.6	0.129	110	0.117	Clear
NVP-MMA 70:30	67.8	0.807	145	0.557	Clear
NVP-MMA 60:40	55.6	2.651	157	1.689	Clear
NVP-MMA 50:50	38.6	4.746	72	7.210	Clear
EEMA-LMA 90:10	4.7	1.123	377	0.288	Clear
EEMA-LMA 80:20	2.4	1.086	465	0.234	Clear

IPN Hydrogel Composition	E.W.C. (%)	Tensile Strength (MPa)	Elongation to Break (%)	Youngs Modulus (MPa)	Appearance
NNDMA-PMMA 99: 1	85.8	0.110	99	0.111	Translucent
NNDMA-PMMA 97.5:2.5	86.1	0.116	110	0.105	Translucent
NNDMA-PMMA 95:5	84.8	0.136	61	0.272	Translucent
NNDMA-PMMA 90:10	75.2	0.532	75	0.718	Opaque
NNDMA-PMMA 85:15	70.5	0.782	66	1.185	Opaque
NNDMA-PMMA 80:20	66.5	1.740	64	2.719	Opaque
NNDMA-LMA-Poly MMA	46.2	0.965	115	0.839	Opaque
56.7 : 20 : 23.3					
NNDMA-PVAc 99: 1	86.4	0.091	107	0.085	Translucent
NNDMA-PVAc 95: 5	86.9	0.145	253	0.057	Translucent
NNDMA-PVAc 90:10	86.8	0.130	243	0.053	Translucent
NNDMA-PVAc 85:15	85.3	0.087	143	0.061	Opaque
NNDMA-PVAc 80:20	84.6	0.111	134	0.083	Opaque
NNDMA-PVAc 70:30	82.7	0.134	129	0.104	Opaque
NNDMA-PVAc 60:40	81.2	0.083	183	0.045	Opaque
NNDMA-Biomer 95:5	83.7	0.308	182	0.169	Translucent
NNDMA-Pellathane 95: 5	82.4	0.170	99	0.172	Clear
NNDMA-Pellathane 90:10	76.2	0.506	108	0.469	Clear
NNDMA-Pellathane 85:15	73.7	0.569	131	0.434	Translucent

IPN Hydrogel Composition	E.W.C. (%)	Tensile Strength (MPa)	Elongation to Break (%)	Youngs Modulus (MPa)	Appearance
NNDMA-HPU25 95:5	81.7	0.410	146	0.281	Translucent
NNDMA-HPU25 90:10	86.6	0.372	250	0.149	Translucent
NNDMA-EPDCD 95: 5	85.6	0.180	98	0.185	Translucent
NNDMA-EPDCD 90:10	80.7	0.344	70	0.499	Translucent
NNDMA-EPDCD 85:15	70.0	0.533	42	1.284	Opaque
NNDMA-CA 98: 2	84.7	0.120	97	0.124	Clear
NNDMA-CA 95: 5	86.1	0.149	89	0.167	Clear
NNDMA-CA 90:10	82.1	0.175	58	0.313	Translucent
NNDMA-CA 85:15	79.8	0.254	80	0.349	Translucent
NNDMA-CAB 98: 2	83.9	0.142	121	0.118	Clear
NNDMA-CAB 95: 5	84.3	0.184	100	0.184	Translucent
NNDMA-CAB 90:10	80.0	0.308	113	0.273	Translucent
NNDMA-CAB 85:15	77.6	0.479	107	0.458	Translucent
NVP-CA 90:10	87.2	0.120	107	0.112	Translucent
NVP-CA 80:20	79.1	0.183	136	0.163	Translucent
NVP-CAB 90:10	81.8	0.135	80	0.195	Translucent
NVP-CAB 80:20	72.6	0.375	79	0.590	Translucent
Geliperm	98.0	2.470	-	-	Translucent

APPENDIX 3

Measured and Predicted Surface Energies of Dehydrated Copolymer and IPN Hydrogels

Copolymer Hydrogel Composition	Water Contact Angle	Methylene Iodide Contact Angle	Dispersive Component of Surface Free Energy (mN/m)	Polar Component of Surface Free Energy (mN/m)	Total Surface Free Energy (mN/m)	Parachor Predicted Free Energy (Eqn. 5.26) (mN/m)	Parachor Predicted Free Energy (Eqn. 5.27) (mN/m)	CED Predicted Surface Free Energy (mN/m)
HEMA 1.0 % X-Linker	53	41	29.0	21.5	50.5	50.5	50.5	39.1
HEMA 2.0 % X-Linker	55	38	31.0	19.2	50.2	-	-	-
HEMA 5.0 % X-Linker	58	39	31.1	17.2	48.3	-	-	-
Poly HEMA	53	41	29.0	21.5	50.5	50.5	50.5	39.1
HEMA-MMA 95: 5	57	38	31.4	17.7	49.1	50.2	50.1	38.9
HEMA-MMA 90:10	58	35	33.1	16.3	49.4	49.9	49.7	38.8
HEMA-MMA 80:20	59	33	34.3	15.1	49.4	49.2	48.9	38.5
HEMA-MMA 70:30	61	32	35.3	13.6	48.9	48.6	48.2	38.2
HEMA-MMA 60:40	65	31	36.7	10.8	47.5	47.9	47.5	37.9
HEMA-MMA 50:50	67	29	38.1	9.3	47.4	47.3	46.8	37.6
Poly MMA	67	29	38.1	9.3	47.4			36.1
HEMA-St 90:10	57	41	29.8	18.5	48.3	49.3	49.2	38.7
HEMA-St 80:20	58	41	30.1	17.8	47.9	49.8	48.2	38.5
HEMA-St 50:50	59	42	29.7	17.3	47.0	45.5	45.0	37.5
HEMA-St 30:70	64	42	30.8	13.7	44.5	43.5	43.2	36.9
HEMA-St 10:90	73	40	34.1	7.7	41.8	41.6	41.4	36.5
Poly St	90	36	40.9	0.8	41.7	40.6	40.6	36.1

Copolymer Hydrogel Composition	Water Contact Angle	Methylene Iodide Contact Angle	Dispersive Component of Surface Free Energy (mN/m)	Polar Component of Surface Free Energy (mN/m)	Total Surface Free Energy (mN/m)	Parachor Predicted Free Energy (Eqn. 5.26) (mN/m)	Parachor Predicted Free Energy (Eqn. 5.27) (mN/m)	CED Predicted Surface Free Energy (mN/m)
HEMA-NVP 95: 5	67	36	34.7	10.5	45.2	50.5	50.4	39.1
HEMA-NVP 90:10	72	34	37.0	7.3	44.3	50.6	50.4	39.2
HEMA-NVP 80:20	75	32	38.8	5.5	44.3	50.6	50.4	39.2
HEMA-NVP 70:30	76	30	40.0	4.8	44.8	50.7	50.4	39.3
HEMA-NVP 60:40	76	29	40.5	4.7	45.2	50.7	50.4	39.3
HEMA-NVP 50:50	78	28	41.5	3.8	45.3	50.8	50.5	39.4
HEMA-NNDMA 95: 5	61	41	30.7	15.6	46.3	50.6	50.4	39.1
HEMA-NNDMA 90:10	63	40	31.7	13.9	45.6	50.7	50.4	39.0
HEMA-NNDMA 80:20	65	39	32.7	12.3	45.0	51.0	50.4	38.9
HEMA-NNDMA 70:30	68	38	33.9	10.2	44.1	51.2	50.4	38.8
HEMA-NNDMA 60:40	70	37	35.0	8.8	43.8	51.4	50.5	38.7
Poly HEA	50	35	31.5	22.1	53.6	57.0	57.0	45.1
HEA-St 90:10	50	35	31.5	22.1	53.6	55.4	56.1	44.2
HEA-St 80:20	50	35	31.5	22.1	53.6	53.7	54.1	43.3
HEA-St 50:50	51	37	30.7	21.9	52.6	48.8	49.3	40.7
HEA-St 40:60	52	37	30.9	21.2	52.1	47.2	47.6	39.8
HEA-St 30:70	53	37	31.1	20.4	51.5	45.6	45.9	38.9
HEA-St 10:90	60	37	32.6	15.3	47.9	42.3	42.5	37.1

Copolymer Hydrogel Composition	Water Contact Angle	Methylene Iodide Contact Angle	Dispersive Component of Surface Free Energy (mN/m)	Polar Component of Surface Free Energy (mN/m)	Total Surface Free Energy (mN/m)	Parachor Predicted Free Energy (Eqn. 5.26) (mN/m)	Parachor Predicted Free Energy (Eqn. 5.27) (mN/m)	CED Predicted Surface Free Energy (mN/m)
Poly HPMA	58	39	31.1	17.2	48.3	43.5	43.5	39.5
HPMA-St 50:50	62	39	32.0	14.4	46.4	42.1	41.2	37.7
Poly HPA	52	40	29.4	22.0	51.4	51.2	51.2	36.0
HPA-St 70:30	53	40	29.6	21.2	50.8	48.0	47.3	35.1
HPA-St 50:50	55	40	30.0	19.7	49.7	45.9	45.0	35.3
HPA-St 30:70	57	38	31.4	17.7	49.1	43.8	43.0	35.6
HPA-St 20:80	60	38	32.1	15.5	47.6	42.7	41.3	35.7
HPA-St 10:90	65	38	33.2	12.1	45.3	41.7	40.6	35.9
NNDMA 1.0 % X-Linker	55	36	32.0	18.7	50.7	52.9	52.9	38.1
NNDMA 2.5 % X-Linker	61	39	31.8	15.1	46.9	-	-	-
NNDMA 5.0 % X-Linker	63	42	30.6	14.4	45.0	-	-	-
NNDMA 7.5 % X-Linker	63	43	30.0	14.6	44.6	-	-	-
NNDMA 10.0% X-Linker	65	45	29.4	13.8	43.2	-	-	-
NNDMA-LMA 90:10	59	35	33.4	15.6	49.0	52.4	55.6	37.6
NNDMA-LMA 80:20	63	35	34.3	12.8	47.1	52.0	56.9	37.0
NNDMA-LMA 70:30	65	34	35.3	11.4	46.7	51.5	57.3	36.5
NNDMA-LMA 60:40	66	33	36.0	10.6	46.6	51.1	57.0	36.0

Copolymer Hydrogel Composition	Water Contact Angle	Methylene Iodide Contact Angle	Dispersive Component of Surface Free Energy (mN/m)	Polar Component of Surface Free Energy (mN/m)	Total Surface Free Energy (mN/m)	Parachor Predicted Free Energy (Eqn. 5.26) (mN/m)	Parachor Predicted Free Energy (Eqn. 5.27) (mN/m)	CED Predicted Surface Free Energy (mN/m)
NNDMA-MMA 99: 1	58	36	32.6	16.5	49.1	52.9	52.8	38.1
NNDMA-MMA 97.5:2.5	61	36	33.3	14.4	47.7	52.7	52.7	38.0
NNDMA-MMA 95:5	63	35	34.3	12.8	47.1	52.5	52.5	38.0
NNDMA-MMA 90:10	64	34	35.0	12.0	47.0	52.0	52.0	37.9
NNDMA-MMA 85:15	65	33	35.7	11.2	46.9	51.6	51.5	37.8
NNDMA-MMA 80:20	67	32	36.7	9.8	46.5	51.1	51.1	37.7
NVP 1.0% X-Linker	64	37	33.5	12.6	46.1	51.1	51.1	39.7
NVP-LMA 90:10	69	36	35.2	9.3	44.5	50.8	54.9	39.0
NVP-LMA 80:20	70	35	36.0	8.5	44.5	50.5	57.2	38.3
NVP-LMA 70:30	72	35	36.5	7.4	43.9	50.3	58.2	37.6
NVP-LMA 60:40	72	34	37.0	7.3	44.3	50.0	58.2	36.9
NVP-MMA 90:10	69	34	36.2	8.9	45.1	50.4	50.4	39.3
NVP-MMA 80:20	70	33	37.0	8.2	45.2	49.7	49.7	39.0
NVP-MMA 70:30	70	31	38.0	7.9	45.9	49.0	49.0	38.6
NVP-MMA 60:40	71	31	38.2	7.4	45.6	48.3	48.3	38.2
NVP-MMA 50:50	72	30	39.0	6.7	45.7	47.6	47.5	37.9

IPN Hydrogel Composition	Water Contact Angle	Methylene Iodide Contact Angle	Dispersive Component of Surface Free Energy (mN/m)	Polar Component of Surface Free Energy (mN/m)	Total Surface Free Energy (mN/m)	Parachor Predicted Free Energy (Eqn. 5.26) (mN/m)	Parachor Predicted Free Energy (Eqn. 5.27) (mN/m)	CED Predicted Surface Free Energy (mN/m)
NNDMA-PMMA 99: 1	56	35	32.7	17.7	50.4	-	-	-
NNDMA-PMMA 97.5:2.5	58	34	33.6	16.1	49.7	-	-	-
NNDMA-PMMA 95:5	59	33	34.3	15.1	49.4	-	-	-
NNDMA-PMMA 90:10	63	32	35.7	12.3	48.0	-	-	-
NNDMA-PMMA 85:15	65	30	37.1	10.7	47.8	-	-	-
NNDMA-PMMA 80:20	67	29	38.1	9.3	47.4	-	-	-
NNDMA-PVAc 99: 1	61	34	34.3	14.0	48.3	-	-	-
NNDMA-PVAc 95: 5	65	32	36.2	11.0	47.2	-	-	-
NNDMA-PVAc 90:10	66	30	37.4	10.1	47.5	-	-	-
NNDMA-PVAc 85:15	69	29	38.6	8.2	46.8	-	-	-
NNDMA-PVAc 80:20	70	26	40.2	7.3	47.5	-	-	-
NNDMA-PVAc 70:30	70	25	40.6	7.2	47.8	-	-	-
NNDMA-PVAc 60:40	71	24	41.2	6.5	47.7	-	-	-
NNDMA-Biomer 95:5	35	20	34.7	29.4	64.1	-	-	-
NNDMA-Pellathane 95: 5	31	27	31.8	33.4	65.2	-	-	-
NNDMA-Pellathane 90:10	28	29	30.6	35.7	66.3	-	-	-
NNDMA-Pellathane 85:15	27	32	29.3	37.2	66.5	-	-	-
Geliperm	35	25	33.1	30.4	63.5	-	-	-

IPN Hydrogel Composition	Water Contact Angle	Methylene Iodide Contact Angle	Dispersive Component of Surface Free Energy (mN/m)	Polar Component of Surface Free Energy (mN/m)	Total Surface Free Energy (mN/m)	Parachor Predicted Free Energy (Eqn. 5.26) (mN/m)	Parachor Predicted Free Energy (Eqn. 5.27) (mN/m)	CED Predicted Surface Free Energy (mN/m)
NNDMA-HPU25 95: 5	31	22	33.5	32.3	65.8	-	-	-
NNDMA-HPU25 90:10	33	28	31.7	32.4	64.1	-	-	-
NNDMA-EPDCD 95: 5	57	36	32.4	17.2	49.6	-	-	-
NNDMA-EPDCD 90:10	59	38	31.8	16.3	48.1	-	-	-
NNDMA-EPDCD 85:15	63	41	31.1	14.2	45.3	-	-	-
NNDMA-CA 98: 2	59	33	34.3	15.1	49.4	-	-	-
NNDMA-CA 95: 5	64	34	35.0	12.0	47.0	-	-	-
NNDMA-CA 90:10	67	34	35.7	10.1	45.8	-	-	-
NNDMA-CA 85:15	69	35	35.7	9.1	44.8	-	-	-
NNDMA-CAB 98: 2	56	28	35.9	16.2	52.1	-	-	-
NNDMA-CAB 95: 5	65	29	37.6	10.5	48.1	-	-	-
NNDMA-CAB 90:10	67	29	38.1	9.3	47.4	-	-	-
NNDMA-CAB 85:15	68	30	37.9	8.9	46.8	-	-	-
NVP-CA 90:10	75	35	37.3	5.9	43.2	-	-	-
NVP-CA 80:20	77	36	37.3	5.1	42.4	-	-	-
NVP-CAB 90:10	72	32	38.0	7.0	45.0	-	-	-
NVP-CAB 80:20	78	34	38.6	4.4	43.0	-	-	-

APPENDIX 4

Measured and Predicted Surface Energies of Hydrated Copolymer and IPN Hydrogels

Copolymer Hydrogel Composition	Air Contact Angle	n-Octane Contact Angle	Dispersive Component of Surface Free Energy (mN/m)	Polar Component of Surface Free Energy (mN/m)	Total Surface Free Energy (mN/m)	Surface Free Energy Predicted From Water Content (mN/m)	Parachor Predicted Surface Free Energy (mN/m)
HEMA 1.0 % X-Linker	27	145	23.2	42.2	65.4	60.0	58.1
HEMA 2.0 % X-Linker	36	133	24.3	36.1	60.4	59.4	-
HEMA 5.0 % X-Linker	36	130	26.4	34.4	60.9	57.2	-
Poly HEMA	27	145	23.2	42.2	65.4	60.0	58.1
HEMA-MMA 95: 5	31	140	23.4	39.8	63.2	58.5	56.5
HEMA-MMA 90:10	34	133	25.8	36.1	61.9	58.1	55.2
HEMA-MMA 80:20	36	126	29.6	32.2	61.8	56.9	52.3
HEMA-MMA 70:30	38	122	31.3	29.8	61.2	55.6	49.9
HEMA-MMA 60:40	40	118	33.2	27.5	60.7	52.7	48.0
HEMA-MMA 50:50	41	115	35.0	25.8	60.8	51.1	49.6
HEMA-St 90:10	31	135	26.7	37.2	63.8	55.8	53.8
HEMA-St 80:20	35	124	32.3	31.0	63.2	52.8	50.3
HEMA-NVP 95: 5	26	147	22.8	43.1	65.9	57.3	57.1
HEMA-NVP 90:10	26	149	21.8	44.0	65.8	57.5	56.4
HEMA-NVP 80:20	25	151	21.5	44.8	66.3	58.3	55.1
HEMA-NVP 70:30	25	151	21.5	44.8	66.3	60.1	56.4
HEMA-NVP 60:40	24	152	21.6	45.2	66.8	61.6	54.4
HEMA-NVP 50:50	23	153	21.7	45.6	67.3	64.0	56.5

Copolymer Hydrogel Composition	Air Contact Angle	n-Octane Contact Angle	Dispersive Component of Surface Free Energy (mN/m)	Polar Component of Surface Free Energy (mN/m)	Total Surface Free Energy (mN/m)	Surface Free Energy Predicted From Water Content (mN/m)	Parachor Predicted Surface Free Energy (mN/m)
HEMA-NNDMA 95: 5	26	142	25.5	40.8	66.3	58.6	57.7
HEMA-NNDMA 90:10	26	138	28.0	38.7	66.8	59.4	57.2
HEMA-NNDMA 80:20	27	136	28.8	37.7	66.5	59.5	56.6
HEMA-NNDMA 70:30	27	134	30.3	36.6	66.9	63.2	54.7
HEMA-NNDMA 60:40	27	133	31.0	36.1	67.1	65.1	55.4
NNDMA 1.0 % X-Linker	27	143	24.3	41.2	65.6	70.2	62.7
NNDMA 2.5 % X-Linker	28	141	24.9	40.2	65.1	67.6	-
NNDMA 5.0 % X-Linker	29	138	26.1	38.7	64.8	65.9	-
NNDMA 7.5 % X-Linker	29	133	29.6	36.1	65.7	64.7	-
NNDMA 10.0% X-Linker	30	131	30.4	35.0	65.4	62.0	-
NNDMA-LMA 90:10	28	140	25.4	39.8	65.2	67.8	60.8
NNDMA-LMA 80:20	29	137	26.7	38.2	65.0	65.3	58.5
NNDMA-LMA 70:30	30	135	27.4	37.2	64.6	63.7	56.3
NNDMA-LMA 60:40	31	133	28.1	36.1	64.2	61.0	54.1

Copolymer Hydrogel Composition	Air Contact Angle	n-Octane Contact Angle	Dispersive Component of Surface Free Energy (mN/m)	Polar Component of Surface Free Energy (mN/m)	Total Surface Free Energy (mN/m)	Surface Free Energy Predicted From Water Content (mN/m)	Parachor Predicted Surface Free Energy (mN/m)
NNDMA-MMA 99: 1	29	141	24.2	40.2	64.5	69.8	62.5
NNDMA-MMA 97.5:2.5	29	139	25.4	39.3	64.7	69.8	62.4
NNDMA-MMA 95:5	30	137	26.0	38.2	64.3	69.4	62.1
NNDMA-MMA 90:10	31	136	26.0	37.7	63.7	69.3	61.5
NNDMA-MMA 85:15	31	135	26.7	37.2	63.8	69.1	60.9
NNDMA-MMA 80:20	32	134	26.7	36.6	63.3	68.6	60.0
NVP 1% X-Linker	20	154	22.7	45.9	68.7	72.0	63.3
NVP-LMA 90:10	26	145	23.8	42.2	66.0	67.6	61.0
NVP-LMA 80:20	28	137	27.4	38.2	65.6	64.4	58.0
NVP-LMA 70:30	31	136	26.0	37.7	63.7	61.5	55.0
NVP-LMA 60:40	31	133	28.1	36.1	64.2	59.6	52.9
NVP-MMA 90:10	27	142	24.9	40.8	65.7	68.3	61.0
NVP-MMA 80:20	29	136	27.4	37.7	65.1	66.9	58.6
NVP-MMA 70:30	30	134	28.2	36.6	64.8	64.9	55.5
NVP-MMA 60:40	32	132	28.2	35.5	63.7	61.7	52.4
NVP-MMA 50:50	33	130	28.9	34.4	63.3	57.2	47.6

IPN Hydrogel Composition	Air Contact Angle	n-Octane Contact Angle	Dispersive Component of Surface Free Energy (mN/m)	Polar Component of Surface Free Energy (mN/m)	Total Surface Free Energy (mN/m)	Surface Free Energy Predicted From Water Content (mN/m)	Parachor Predicted Surface Free Energy (mN/m)
NNDMA-PMMA 99: 1	29	137	26.7	38.2	65.0	69.7	-
NNDMA-PMMA 97.5:2.5	31	136	26.0	37.7	63.7	69.6	-
NNDMA-PMMA 95:5	31	135	26.7	37.2	63.8	69.3	-
NNDMA-PMMA 90:10	32	133	27.4	36.1	63.5	67.0	-
NNDMA-PMMA 85:15	32	133	27.4	36.1	63.5	65.9	-
NNDMA-PMMA 80:20	33	132	27.4	35.5	62.9	64.9	-
NNDMA-PVAc 99: 1	28	144	23.1	41.8	64.9	69.5	-
NNDMA-PVAc 95: 5	29	144	22.5	41.8	64.3	69.5	-
NNDMA-PVAc 90:10	29	143	23.1	41.2	64.3	69.5	-
NNDMA-PVAc 85:15	30	143	22.5	41.2	63.7	69.1	-
NNDMA-PVAc 80:20	30	142	23.0	40.8	63.7	69.0	-
NNDMA-PVAc 70:30	30	142	23.0	40.8	63.7	68.7	-
NNDMA-PVAc 60:40	31	141	22.9	40.2	63.2	68.3	-
NNDMA-Biomer 95:5	29	132	30.4	35.5	65.9	71.2	-
NNDMA-Pellathane 95: 5	33	136	24.5	37.7	62.2	70.9	-
NNDMA-Pellathane 90:10	35	134	24.4	36.6	61.0	70.9	-
NNDMA-Pellathane 85:15	36	132	25.0	35.5	60.5	71.2	-
Geliperm	32	138	24.0	38.7	62.7	72.2	-

IPN Hydrogel Composition	Air Contact Angle	n-Octane Contact Angle	Dispersive Component of Surface Free Energy (mN/m)	Polar Component of Surface Free Energy (mN/m)	Total Surface Free Energy (mN/m)	Surface Free Energy Predicted From Water Content (mN/m)	Parachor Predicted Surface Free Energy (mN/m)
NNDMA-HPU25 95: 5	31	132	28.9	35.5	64.4	71.3	-
NNDMA-HPU25 90:10	33	139	22.7	39.3	61.9	71.4	-
NNDMA-EPDCD 95: 5	30	138	25.4	38.7	64.1	69.5	-
NNDMA-EPDCD 90:10	32	135	25.9	37.2	63.1	68.3	-
NNDMA-EPDCD 85:15	32	133	27.4	36.1	63.5	65.1	-
NNDMA-CA 98: 2	29	135	28.1	37.2	65.3	69.3	-
NNDMA-CA 95: 5	31	133	28.1	36.1	64.2	69.3	-
NNDMA-CA 90:10	32	131	28.8	35.0	63.8	68.1	-
NNDMA-CA 85:15	33	128	30.5	33.3	63.8	67.2	-
NNDMA-CAB 98: 2	30	134	28.2	36.6	64.8	69.5	-
NNDMA-CAB 95: 5	32	131	28.8	35.0	63.8	69.1	-
NNDMA-CAB 90:10	33	128	30.5	33.3	63.8	68.0	-
NNDMA-CAB 85:15	34	126	31.3	32.2	63.5	67.3	-
NVP-CA 90:10	24	142	26.7	40.8	67.4	69.2	-
NVP-CA 80:20	29	137	26.7	38.2	65.0	66.9	-
NVP-CAB 90:10	25	139	28.0	39.3	67.2	68.2	-
NVP-CAB 80:20	32	126	33.0	32.2	65.2	65.4	-

APPENDIX 5

Measured Surface Energies of Hydrated Copolymer and IPN Hydrogels

Copolymer Hydrogel Composition	Air Contact Angle	n-Octane Contact Angle	}'sv - }'sw (mN/m)	Isw (mN/m)	}'sv (d) (mN/m)	}'sv (p) (mN/m)	}'sv (t) (mN/m)	}'sw (mN/m)
HEMA 1.0 % X-Linker	27	145	64.9	92.8	23.1	42.2	65.3	0.4
HEMA 2.0 % X-Linker	36	133	58.9	85.8	24.2	36.1	60.3	1.4
HEMA 5.0 % X-Linker	36	130	58.9	83.8	26.3	34.4	60.7	1.8
Poly HEMA	27	145	64.9	92.8	23.1	42.2	65.3	0.4
HEMA-MMA 95: 5	31	140	62.4	90.1	23.3	39.8	63.1	0.7
HEMA-MMA 90:10	34	133	60.4	85.8	25.8	36.1	61.9	1.5
HEMA-MMA 80:20	36	126	58.9	81.0	29.5	32.2	61.7	2.8
HEMA-MMA 70:30	38	122	57.4	78.0	31.2	29.8	61.0	3.6
HEMA-MMA 60:40	40	118	55.8	74.9	33.1	27.5	60.6	4.8
HEMA-MMA 50:50	41	115	54.9	72.6	34.8	25.8	60.6	5.7
HEMA-St 90:10	31	135	62.4	87.1	26.5	37.2	63.7	1.3
HEMA-St 80:20	35	124	59.6	79.5	32.1	31.0	63.1	3.5
HEMA-NVP 95: 5	26	147	65.4	93.8	22.6	43.1	65.7	0.3
HEMA-NVP 90:10	26	149	65.4	94.7	21.7	44.0	65.7	0.3
HEMA-NVP 80:20	25	151	66.0	95.6	21.4	44.8	66.2	0.2
HEMA-NVP 70:30	25	151	66.0	95.6	21.4	44.8	66.2	0.2
HEMA-NVP 60:40	24	152	66.5	96.0	21.5	45.2	66.7	0.2
HEMA-NVP 50:50	23	153	67.0	96.4	21.6	45.6	67.2	0.2

Copolymer Hydrogel Composition	Air Contact Angle	n-Octane Contact Angle	}`sv - }`sw (mN/m)	lsw (mN/m)	}`sv (d) (mN/m)	}`sv (p) (mN/m)	}`sv (t) (mN/m)	}`sw (mN/m)
HEMA-NNDMA 95: 5	26	142	65.4	91.2	25.3	40.8	66.1	0.7
HEMA-NNDMA 90:10	26	138	65.4	88.9	27.9	38.7	66.6	1.2
HEMA-NNDMA 80:20	27	136	64.9	87.7	28.7	37.7	66.4	1.5
HEMA-NNDMA 70:30	27	134	64.9	86.4	30.2	36.6	66.8	1.9
HEMA-NNDMA 60:40	27	133	64.9	85.8	30.9	36.1	67.0	2.1
NNDMA 1.0 % X-Linker	27	143	64.9	91.7	24.3	41.2	65.5	0.6
NNDMA 2.5 % X-Linker	28	141	64.3	90.6	24.8	40.2	65.0	0.7
NNDMA 5.0 % X-Linker	29	138	63.7	88.9	26.0	38.7	64.7	1.0
NNDMA 7.5 % X-Linker	29	133	63.7	85.8	29.5	36.1	65.6	1.9
NNDMA 10.0% X-Linker	30	131	63.0	84.5	30.2	35.0	65.2	2.2
NNDMA-LMA 90:10	28	140	64.3	90.1	25.3	39.8	65.1	0.8
NNDMA-LMA 80:20	29	137	63.7	88.3	26.6	38.2	64.8	1.1
NNDMA-LMA 70:30	30	135	63.0	87.1	27.2	37.2	64.4	1.4
NNDMA-LMA 60:40	31	133	62.4	85.8	28.0	36.1	64.1	1.7
NNDMA-MMA 99: 1	29	141	63.7	90.6	24.2	40.2	64.4	0.7
NNDMA-MMA 97.5:2.5	29	139	63.7	89.5	25.3	39.3	64.6	0.9
NNDMA-MMA 95:5	30	137	63.0	88.3	25.9	38.2	64.1	1.1
NNDMA-MMA 90:10	31	136	62.4	87.7	25.9	37.7	63.6	1.2
NNDMA-MMA 85:15	31	135	62.4	87.1	26.5	37.2	63.7	1.3
NNDMA-MMA 80:20	32	134	61.7	86.4	26.5	36.6	63.1	1.4

Copolymer Hydrogel Composition	Air Contact Angle	n-Octane Contact Angle	}'sv - }'sw (mN/m)	lsw (mN/m)	}'sv (d) (mN/m)	}'sv (p) (mN/m)	}'sv (t) (mN/m)	}'sw (mN/m)
NVP 1% X-linker	20	154	68.4	96.8	22.6	45.9	68.5	0.1
NVP-LMA 90:10	26	145	65.4	92.8	23.6	42.2	65.8	0.4
NVP-LMA 80:20	28	137	64.3	88.3	27.3	38.2	65.5	1.2
NVP-LMA 70:30	31	136	62.4	87.7	25.9	37.7	63.6	1.2
NVP-LMA 60:40	31	133	62.4	85.8	28.0	36.1	64.1	1.7
NVP-MMA 90:10	27	142	64.9	91.2	24.8	40.8	65.6	0.7
NVP-MMA 80:20	29	136	63.7	87.7	27.3	37.7	65.0	1.3
NVP-MMA 70:30	30	134	63.0	86.4	28.0	36.6	64.6	1.6
NVP-MMA 60:40	32	132	61.7	85.1	28.0	35.5	63.5	1.8
NVP-MMA 50:50	33	130	61.1	83.8	28.8	34.4	63.2	2.1

IPN Hydrogel Composition	Air Contact Angle	n-Octane Contact Angle	$\gamma_{sv} - \gamma_{sw}$ (mN/m)	γ_{sw} (mN/m)	γ_{sv} (d) (mN/m)	γ_{sv} (p) (mN/m)	γ_{sv} (t) (mN/m)	γ_{sw} (mN/m)
NNDMA-PMMA 99: 1	29	137	63.7	88.3	26.6	38.2	64.8	1.1
NNDMA-PMMA 97.5:2.5	31	136	62.4	87.7	25.9	37.7	63.6	1.2
NNDMA-PMMA 95:5	31	135	62.4	87.1	26.5	37.2	63.7	1.3
NNDMA-PMMA 90:10	32	133	61.7	85.8	27.2	36.1	63.3	1.6
NNDMA-PMMA 85:15	32	133	61.7	85.8	27.2	36.1	63.3	1.6
NNDMA-PMMA 80:20	33	132	61.1	85.1	27.3	35.5	62.8	1.7
NNDMA-PVAc 99: 1	28	144	64.3	92.3	23.0	41.8	64.8	0.5
NNDMA-PVAc 95: 5	29	144	63.7	92.3	22.4	41.8	64.2	0.5
NNDMA-PVAc 90:10	29	143	63.7	91.7	23.0	41.2	64.2	0.5
NNDMA-PVAc 85:15	30	143	63.0	91.7	22.3	41.2	63.5	0.5
NNDMA-PVAc 80:20	30	142	63.0	91.2	22.8	40.8	63.6	0.6
NNDMA-PVAc 70:30	30	142	63.0	91.2	22.8	40.8	63.6	0.6
NNDMA-PVAc 60:40	31	141	62.4	90.6	22.8	40.2	63.0	0.6
NNDMA-Biomer 95:5	29	132	63.7	85.1	30.3	35.5	65.8	2.1
NNDMA-Pellathane 95: 5	33	136	61.1	87.7	24.5	37.7	62.2	1.1
NNDMA-Pellathane 90:10	35	134	59.6	86.4	24.3	36.6	60.9	1.3
NNDMA-Pellathane 85:15	36	132	58.9	85.1	24.9	35.5	60.4	1.5
NNDMA-HPU25 95: 5	31	132	62.4	85.1	28.8	35.5	64.3	1.9
NNDMA-HPU25 90:10	33	139	61.1	89.5	22.6	39.3	61.9	0.8

IPN Hydrogel Composition	Air Contact Angle	n-Octane Contact Angle	$\gamma_{sv} - \gamma_{sw}$ (mN/m)	γ_{sw} (mN/m)	γ_{sv} (d) (mN/m)	γ_{sv} (p) (mN/m)	γ_{sv} (t) (mN/m)	γ_{sw} (mN/m)
NNDMA-EPDCD 95: 5	30	138	63.0	88.9	25.2	38.7	63.9	0.9
NNDMA-EPDCD 90:10	32	135	61.7	87.1	25.8	37.2	63.0	1.3
NNDMA-EPDCD 85:15	32	133	61.7	85.8	27.2	36.1	63.3	1.6
NNDMA-CA 98: 2	29	135	63.7	87.1	28.0	37.2	65.2	1.5
NNDMA-CA 95: 5	31	133	62.4	85.8	28.0	36.1	64.1	1.7
NNDMA-CA 90:10	32	131	61.7	84.5	28.7	35.0	63.7	2.0
NNDMA-CA 85:15	33	128	61.1	82.4	30.4	33.3	63.7	2.6
NNDMA-CAB 98: 2	30	134	63.0	86.4	28.0	36.6	64.6	1.6
NNDMA-CAB 95: 5	32	131	61.7	84.5	28.7	35.0	63.7	2.0
NNDMA-CAB 90:10	33	128	61.1	82.4	30.4	33.3	63.7	2.6
NNDMA-CAB 85:15	34	126	60.4	81.0	31.2	32.2	63.4	3.0
NVP-CA 90:10	24	142	66.5	91.2	26.5	40.8	67.3	0.8
NVP-CA 80:20	29	137	63.7	88.3	26.6	38.2	64.8	1.1
NVP-CAB 90:10	25	139	66.0	89.5	27.9	39.3	67.2	1.2
NVP-CAB 80:20	32	126	61.7	81.0	32.8	32.2	65.0	3.3
Geliperm	32	138	61.7	88.9	23.8	38.7	62.5	0.8

APPENDIX 6

Cell Adhesion Results for IPN and Copolymer Hydrogels

Copolymer Hydrogel Composition	Equilibrium Water Content (%)	Polar Component of Dehydrated Surface Free Energy (mN/m)	No cells attached	No cells expressed as % of those on TC	Cell Spreading
Poly HEMA	37.6	21.5	5.1exp5	3.9	--
HEMA-NVP 80:20	43.8	5.5	4.4exp3	3.4	--
NVP-MMA 50:50	38.6	6.7	3.8exp4	24.6	+
NVP-LMA 60:40	51.2	7.3	3.1exp4	24.0	+
NVP-MMA 60:40	55.6	7.4	1.1exp4	8.5	--
NVP-LMA 90:10	80.0	9.3	3.9exp3	3.0	--
NNDMA-LMA 60:40	53.5	10.6	1.2exp4	9.2	--
NNDMA-LMA 70:30	63.7	11.4	4.3exp4	3.0	--
NNDMA-LMA 90:10	78.0	15.6	1.1exp3	0.8	--
NNDMA-MMA 80:20	83.1	9.8	7.8exp3	6.0	--
NNDMA-MMA 90:10	86.2	12.0	1.7exp3	1.3	--
Poly NNDMA	88.4	18.7	4.4exp3	3.4	--
NNDMA-PMMA 80:20	66.5	9.3	1.3exp4	10.0	+
NNDMA-Pellathane 90:10	76.2	35.7	1.3exp4	10.0	+
NNDMA-HPU25 95: 5	81.7	33.5	1.7exp3	1.3	--
NNDMA-Pellathane 95: 5	82.4	33.4	1.4exp4	10.8	+
NNDMA-Biomer 95:5	83.7	29.4	7.1exp3	5.5	--
NNDMA-PVAc 80:20	84.6	7.3	4.4exp4	33.9	+
NNDMA-HPU25 90:10	86.6	31.7	2.8exp3	2.2	--

References

1 Wichterle, O. and Lim, D., Hydrophilic gels for biological use, Nature 1960, 185, 117-118

2 Wichterle, O. and Lim, D., Process for producing shaped articles from three dimensional hydrophilic high polymers, U.S. Pat. 2,976,576 , 1961

3 Wichterle, O. and Lim, D., Cross-linked hydrophilic polymers and articles made there from, U.S. Pat. 3,220,960 , 1965

4 Jeronimidis, G., Natural Composite Materials, in Advances in Materials Science and Engineering, Ed. Cahn, R.W., Pergamon Press, In Press

5 Vincent, J.F.V., Structural Biomaterials, Macmillan Press, London 1982

6 Aplin, J.D. and Hughes, R.C., Complex carbohydrates of the extracellular matrix; structures, interactions and biological roles, Biochemica Biophisica Acta 1982, 694 , 375-415

7 Andrade, J.D. Ed., Hydrogels for Medical and Related Applications, ACS Symp. Ser. No. 31, ACS, Washington D.C. 1976

8 Ratner, B.D and Hoffman, A.S., Synthetic hydrogels for biomedical applications, in Hydrogels for Medical and Related Applications, Ed. Andrade, J.D., ACS Symp. Ser. No. 31, ACS, Washington D.C. 1976, 1-36

9 Wichterle, O., Hydrogels in Encyclopedia of Polymer Science and Technology Vol. 15, Eds. Mark, H. and Gaylord, N., Interscience , New York, N.Y. 1971, 273-291

10 Tighe, B.J., Biomedical applications of polymers in Macromolecular Chemistry, Eds. Jenkins A.D. and Kennedy, J.F., Specialist Periodical Reports No. 17, London: The Chemical Society 1980, 1 , 416-428

11 Tighe, B.J., Biomedical applications of polymers in Macromolecular Chemistry, Eds. Jenkins A.D. and Kennedy, J.F., Specialist Periodical Reports No. 18, London: The Chemical Society 1982, 2 , 347-360

12 Tighe, B.J., Biomedical applications of polymers in Macromolecular Chemistry, Eds. Jenkins A.D. and Kennedy, J.F., Specialist Periodical Reports No. 19, London: The Chemical Society 1984, 3 , 375-386

13 Ratner, B.D., Biomedical applications of hydrogels, a review and critical appraisal in Biocompatibility of Clinical Implant Materials Vol 2, Ed. Williams D.F., CRC Press, Boca Raton, Florida 1981, 145-175

14 Pedley, D.G., Skelly, P.J. and Tighe, B.J., Hydrogels in biomedical applications, Br. Polym. J. 1980, 12 , 99-110

15 Larke, J.R., Ng, C.O. and Tighe, B.J., Hydrogel polymers in contact lens applications: a survey of the existing literature - part 1, The Optitian 1971, 162 (4206) , 12-16

16 Larke, J.R., Ng, C.O. and Tighe, B.J., Hydrogel polymers in contact lens applications: a survey of the existing literature - part 2, The Optician 1971, 162 (4207) , 12-16

17 Refojo, M.F., A critical review of the properties and applications of soft hydrogel contact lenses, Sur. Opthal. 1972, 16 , 233-246

18 Hoffman, A.S., Hydrogels - A broad class of biomaterials, in Polymer Science and Technology. Vol 8. Polymers in Medicine and Surgery, Eds. Kronenthal, R.L., Oser, Z. and Martin, E., Plenum press, 1975, 33-44

19 Heitz, W., Krappitz, W., Stützel-Bilbao, C. and Neumann, B., Synthese und eigenschaften von polymeren hydrogelen, Angew. Makromol. Chem. 1984, 123/124 , 147-173

20 Roorda, W.E., Boddé, H.E., de Boer, A.G. and Junginger, H.E., Synthetic hydrogels as drug delivery systems, Pharm. Weekbl. (Sci) 1986, 8 , 165-189

21 Corkhill, P.H., Hamilton, C.J. and Tighe, B.J., Synthetic hydrogels VI: Hydrogel composites as wound dressing and implant materials, Biomaterials, In Press

22 Kudula, V., Hydrogels, in Encyclopedia of Polymer Science and Engineering, Vol 7, Ed. Kroschwitz, J.I., Wiley, New York, N.Y. 1987, 783-806

23 Peppas, N.A. Ed., Hydrogels in Medicine and Pharmacy. Vols. 1-3, CRC Press, Boca Raton, Florida 1987

24 Franks, F. Ed., Water a Comprehensive Treatise. Vols. 1-7, Plenum Press, New York - London 1972

25 Röntgen, W.K., Ueber der Constitution des flüssigen Wassers, Ann. Phys. 1892, 45 , 91-97

26 Bernal, J.D. and Fowler, R.H., A theory of water and ionic solution with particular reference to hydrogen and hydroxyl ions, J. Chem. Phys. 1933, 1 , 515-548

27 Samoilov, O. Ya, The coordination number in the structure of some liquids, Zh. Fiz. Khim. 1946, 20 , 1411-1414 (Russ)

28 Frank, H.S., Structural models, in Water a Comprehensive Treatise. Vol. 1, Plenum Press, New York - London 1972, 515-543

29 Frank, H.S. and Wen, W.Y., Structural aspects of ion solvent interactions in aqueous solutions: A suggested picture for water structure, Disc. Faraday Soc. 1954, 24 , 133-140

30 Stillinger, F.H., Water revisited, Science 1980, 209 , 451-457

31 Silberberg, A., The hydrogel-water interface, in Hydrogels for Medical and Related Applications, Ed. Andrade, J.D., ACS Symp. Ser. No. 31, ACS, Washington D.C. 1976, 199-205

32 Andrade, J.D., King, R.N. and Gregonis, D.E., Probing the hydrogel-water interface, in Hydrogels for Medical and Related Applications, Ed. Andrade, J.D., ACS Symp. Ser. No. 31, ACS, Washington D.C. 1976, 1-36

33 Miller, D.R. and Peppas, N.A., Bulk characterization and scanning electron microscopy of hydrogels of P(VA-co-NVP), Macromols. 1987, 20 , 1257-1265

34 Adamson, A.W. Physical Chemistry of Surfaces, 3rd edn., Wiley-Interscience, New York, N.Y. 1976

35 Andrade, J.D., King, R.N., Gregonis, D.E. and Coleman, D.L., Surface characterisation of poly (hydroxyethyl methacrylate) and related polymers I. Contact angle methods in water, J. Appl. Polym. Sci., Polym. Symp. 1979, 66, 313-336

36 Holly, F.J. and Refojo, M.F., Wettability of hydrogels I. Poly (2-hydroxyethyl methacrylate), J. Biomed. Mater. Res. 1975, 9 , 315-326

37 Ratner, B.D., Surface characterisation of materials for blood contact applications, in Biomaterials: Interfacial Phenomena and Applications, Eds., Cooper, S.L. and Peppas, N.A., ACS Symp. Ser. No. 199, ACS, Washington D.C. 1982

38 Baker, D.A., Corkhill, P.H., Ng, C.O., Skelly, P.J. and Tighe, B.J., Synthetic hydrogels II: Copolymers of carboxyl, lactam and amide-containing monomers: Structure property relationships, Polymer, In Press

39 Barnes, A., Corkhill, P.H. and Tighe, B.J., Synthetic hydrogels III: Hydroxyalkyl acrylate and methacrylate copolymers: Surface and mechanical properties, Polymer, In Press

40 Minett, T.W., Tighe, B.J., Lydon, M.J. and Rees, D.A., Requirements for cell spreading on poly HEMA coated culture substrates, Cell Biol. Int. Rep. 1984, 8 , 151-159

41 Lydon, M.J., Minett, T.W. and Tighe, B.J., Cellular interactions with synthetic polymer surfaces in culture, Biomaterials 1985, 6 , 396-402

42 Lydon. M.J., Synthetic hydrogels as substrata for cell adhesion studies, Br. Polym. J. 1986, 18 , 22-27

43 Magne, F.C., Portas, H.J. and Wakeham, H., A calorimetric investigation of the water in textile fibers, J.Am. Chem. Soc. 1947, 69 , 1896-1902

44 Watson, L.S., O'Neil, M.J., Justin, J. and Brenner, N., A differential scanning calorimeter for quantitative differential thermal analysis, Analytical Chem. 1964, 36 , 1233-1238

45 Yasuda, H., Olf, H.G., Christ, B. Lamaze, C.E. and Peterlin, A., Movement of water in homogeneous water swollen polymers, in Water Structure at the Water-Polymer Interface, Ed. Jellinek, H.H.G., Plenum, New York 1975, 39-55

46 Nelson, R.A., The determination of moisture transitions in cellulosic materials using differential scanning calorimetry, J. Appl. Polym. Sci. 1977, 21 , 645-654

47 Sterling, C. and Masuzawa, M., Gel water relationships in hydrophilic polymers: Nuclear magnetic resonance, Makromol. Chem. 1968, 116 , 140-145

48 Sung, Y.K., Gregonis, D.E., Jhon, M.S. and Andrade, J.D., Thermal and pulse NMR analysis of water in poly (2-hydroxyethyl methacrylate), J.Appl. Polym. Sci. 1981, 26 , 3719-3728

49 Aizawa, M. and Suzuki, S., Properties of water in macromolecular gels III. Dilatometric studies of the properties of water in macromolecular gels, Bull. Chem. Soc. Japan 1971, 44 , 2967-2971

50 Kim, E.H., Jeon, S.I., Yoon, S.C. and Jhon, M.S., The nature of water in tactic poly (2-hydroxyethyl methacrylate) hydrogels, Bull. Korean Chem. Soc. 1981, 2, 60-66

51 Mizuguchi, J., Takahashi, M. and Aizawa, M., Electrical conductivity of gels of natural macromolecular substances, Nippon Kagaku Zasshi 1970, 91 , 723-726

52 Hoffman, A.S., Modell, M. and Pan, P., Polyacrylic desalination membranes I. Synthesis and characterisation, J. Appl. Polym. Sci. 1969, 13 , 2223-2234

53 Jadwin, T.A., Hoffman, A.S. and Vieth, W.R., Crosslinked poly(hydroxyethyl methacrylate) membranes for desalination by reverse osmosis, J. Appl. Polym. Sci. 1970, 14 , 1339-1359

54 Sarbolouki, M.N., Probing the state of absorbed water by diffusion technique, J. Appl. Polym. Sci. 1973, 17 , 2407-2414

55 Frommer, M., Shporer, M. and Messalem, R., Water binding and irreversible dehydration processes in cellulose acetate membranes, J. Appl. Polym. Sci. 1973, 17 , 2263-2276

56 Shporer, M. and Frommer, M., Magnetic resonance studies of the water in cellulose acetate membranes, J. Macromol. Sci., Phys. 1974, B10 , 529-542

57 Krishnamurthy, S., Mc Intyre, D., Santee, E.R. and Wilson C.W., NMR of dissolved water in ultrathin and thick membranes of cellulose acetate, J. Polym. Sci., Polym. Phys. 1973, 11 , 427-448

58 Frommer, M.A. and Lancet, D., Freezing and non freezing water in cellulose acetate membranes, J. Appl. Polym. Sci. 1972, 16 , 1295-1303

59 Dehl, R.E., Collagen: Mobile water content of frozen fibers, Science 1970, 170 , 738-739

60 Froix, M.F. and Nelson, R.A., The interaction of water with cellulose from nuclear magnetic resonance relaxation times, Macromols. 1975, 8 , 726-730

61 Tanaguchi, Y. and Horigome, S., The states of water in cellulose acetate membranes, J. Appl. Polym. Sci. 1975, 19 , 2743-2748

62 Jhon, M.S. and Andrade, J.D., Water and hydrogels, J. Biomed. Mater. Res. 1973, 7 , 509-552

63 Lee, H.B., Jhon, M.S. and Andrade, J.D., Nature of water in synthetic hydrogels I. Dilatometry, specific conductivity and differential scanning calorimetry of polyhydroxyethyl methacrylate, J. Colloid Interface Sci. 1975, 51 , 225-231

64 Kim, E.H., Moon, B.Y., Jeon, S.I. and Jhon, M.S., The nature of water in copolymer hydrogels, Bull. Korean Chem. Soc. 1983, 4 , 251-256

65 Nakamura, K., Hatakeyama, T. and Hatakeyama, H., Studies on bound water of cellulose by differential scanning calorimetry, Textile Res.J. 1981, 51 , 607-613

66 Nakamura, K., Hatakeyama, T. and Hatakeyama, H., Relationship between hydrogen bonding and bound water in poly hydroxystyrene derivatives, Polymer 1983, 24 , 871-876

67 Hatakeyama, T., Yamauchi, A. and Hatakeyama, H., Studies on bound water in poly (vinyl alcohol) hydrogel by DSC and FT-NMR, Eur. Polym. J. 1984, 20 , 61-64

68 Higuchi, A. and Iijima, T., D.s.c. investigations of the states of water in poly (vinyl alcohol) membranes, Polymer 1985, 26 , 1207-1211

69 Higuchi, A. and Iijima, T., D.s.c. investigations of the states of water in poly (vinyl alcohol-co-itaconic acid) membranes, Polymer 1985, 26 , 1833-1837

70 Aizawa, M., Mizuguchi, J., Suzuki, S., Hagashi, S., Suzuki, T., Mitomo, N. and Toyama, H., Properties of water in macromolecular gels IV. Proton magnetic resonance studies of the properties of water in macromolecular gels, Bull. Chem. Soc. Japan 1972, 45 , 3031-3034

71 Filby, E. and Maass, O., The volume relations of the system cellulose and water, Can. J. Res. 1932, 7 , 162-177

72 Bosen, C.E., Bound water, Cellulose Chem. Technol. 1970, 4 , 149-164

73 Vincent, A.L., Barsh, M.K. and Kesting, R.E., Semi-permeable membranes of cellulose acetate for desalination in the process of reverse osmosis III. Bound water relationships, J. Appl. Polym. Sci. 1965, 9 , 2363-2378

74 Baresová, V., Structure and properties of hydrophilic polymers and their gels XII. Relaxation behaviour of the system poly (ethylene glycol monomethacrylate) - water below the glass transition temperature, Coll. Czech. Chem. Comm. 1969, 34 , 545-552

75 Baresová, V., Structure and properties of hydrophilic polymers and their gels XIII. Phase separation in the system poly (ethylene glycol monomethacrylate) - water at low temperatures, Coll. Czech. Chem. Comm. 1969, 34 , 707-710

76 Woessner, D.E. and Snowdon, B.S. Jr., Pulsed NMR study of water in agar gels, J. Colloid Interface Sci. 1970, 34 , 290-299

77 Woessner, D.E. and Snowdon, B.S. Jr., Pulsed NMR study of the temperature hysteresis in the agar water system, J. Colloid Interface Sci. 1970, 34 , 283-289

78 Katayama, S. and Fujiwara, S., NMR study of the spatial effect of polyacrylamide gel upon the water molecules confined in it, J. Am. Chem. Soc. 1979, 101 , 4485-4488

79 Choi, S., Jhon, M.S. and Andrade, J.D., Nature of water in synthetic hydrogels III. Dilatometry, specific conductivity and dielectric relaxation of poly (2,3-dihydroxypropyl methacrylate, J. Colloid Interface Sci. 1977, 61 , 1-8

80 Mack, E.J., Okano, T. and Kim, S.W., Biomedical applications of poly (2-hydroxyethyl methacrylate) and its copolymers, in Hydrogels in Medicine and Pharmacy Vol. III. Properties and Applications, Ed Peppas, N.A., CRC Press, Boca-Raton, Florida 1987, 65-93

81 Lee, J.W., Kim, E.H. and Jhon, M.S., The swelling and mechanical properties of hydrogels of tactic poly (2-hydroxyethyl methacrylate) Bull. Korean Chem. Soc. 1983, 4 , 162-169

82 Pedley, D.G. and Tighe, B.J., Water binding properties of hydrogel polymers for reverse osmosis and related applications, Br. Polym. J. 1979, 11 , 130-136

83 Nagura, M., Nagura, M. and Ishikawa, H., State of water in highly elastic poly (vinyl alcohol) hydrogels prepared by repeated freezing and melting, Polymer Comms. 1984, 25 , 313-314

84 Takaizawa, A., Kinoshita, T., Nomura, O. and Tsujita, Y., Characteristics of water in copoly (methyl methacrylate - N-vinyl pyrrolidone) membranes, Polymer J. (Tokyo) 1985, 6 , 747-752

85 Andrade, J.D., Interfacial phenomena and biomaterials, Medical Instrumentation 1973, 7 , 110-120

86 Drost-Hansen, W. and Clegg, J.S., Eds., Cell Associated Water, Academic Press, London 1979

87 Refojo, M.F., Hydrophobic interactions in poly (2-hydroxyethyl methacrylate) homogeneous hydrogel, J. Polym. Sci. Part A 1967, 5 , 3103-3113

88 Ilavsky, M. and Prins, W., Rheo-optics of poly (2-hydroxyethyl methacrylate) gels I. Effect of nature and amount of diluent, Macromols. 1970, 3 , 415-426

89 Warren, T.C. and Prins, W., Polymer-diluent interactions in cross-linked gels of poly (2-hydroxyethyl methacrylate), Macromols. 1972, 5 , 506-512

90 Cini, R., Logliu, G. and Ficalbi, A., Anomalies in the thermal properties of water, Nature 1969, 223 , 1148-1149

91 Drost Hansen, W., Structure of water near solid interfaces, Ind. Eng. Chem. 1969, 61 (11) , 10-47

92 Bowers, R.W.J. and Tighe, B.J., Studies of the ocular compatibility of hydrogels. A review of the clinical manifestations of spoilation, Biomaterials 1987, 8 , 83-88

93 Kleist, F.D., Appearance and nature of hydrophilic contact lens deposits-Part I: Protein and other organic deposits, Int. Contact Lens Clinic 1979, 6 , 120-130

94 Horbett, T.A., Protein adsorption on biomaterials, in Biomaterials: Interfacial Phenomena and Applications, Eds. Cooper, S.L. and Peppas, N.A., A.C.S. Symposium Series No. 199, A.C.S., Washington, D.C., 1982, 233-244

95 Horbett, T.A., Protein adsorption to hydrogels, in Hydrogels in Medicine and Pharmacy Vol. I. Fundamentals, Ed. Peppas, N.A., C.R.C. Press, Boca Raton, Florida 1986, 127-171

96 Baker, D. and Tighe, B.J., Polymers in contact lens applications (VIII). The problem of biocompatibility, Contact Lens J. 1981, 10 (3), 3-14

97 Castillo, E.J., Koenig, J.L., Anderson, J.M. and Lo, J., Characterisation of protein adsorption on soft contact lenses I. Conformational changes of adsorbed human serum albumin, Biomaterials 1984, 5 , 319-325

98 Hosaka, S., Ozawa, H., Tanzawa, H., Ishida, H., Yoshimura, K., Momose, T., Magatani, H. and Nakajima, A., Analysis of deposits on high water content contact lenses, J. Biomed. Mater. Res. 1983, 17 , 261-274

99 Wedler, F.C. Analysis of biomaterials deposited on soft contact lenses, J. Biomed. Mater. Res. 1975, 11 , 525-535

100 Karageozian, H.L., Use of the amino acid analyzer to illustrate the efficacy of an enzyme preparation for cleaning hydrophilic lenses, Contacto 1976, 20 (1), 5-10

101 Hasegawa, E., Yamada, A., Magatani, H., Hirano, A. and Atsuzawa, H., The possible role of human lysozyme in soft contact lens hygiene, J. Jpn. Contact Lens Soc. 1979, 21 , 128-133

102 Wedler, F.C., Illman, B.L., Horensky, D.S. and Mowrey-McKee, M., Analysis of protein and mucin components deposited on hydrophilic contact lenses, Clinical Experimental Optometry 1987, 70 (2), 59-68

103 Castillo, E.J., Koenig, J.L., Anderson, J.M. and Lo, J., Protein adsorption of hydrogels II. Reversible and irreversible interactions between lysozyme and soft contact lens surfaces, Biomaterials 1985, 6 , 338-344

104 Baier, R.E., Dutton, R.C. and Gott, V.L., Surface chemical features of blood vessels walls and of synthetic materials exhibiting thromboresistance, in Advances in Experimental Medicine, Vol. 7, Surface chemistry of biological surfaces, Plenum Press, New York, N.Y. 1970, 235-260

105 Ratner, B.D., Hoffman, A.S., Hanson, S.R., Harker, S.R. and Whiffen, J.D., Blood compatibility-water content relationships for radiation grafted hydrogels, J. Polym. Sci. Polym. Symp. 1979, 66 , 363-375

106 Coleman, D.L., Gregonis, D.E. and Andrade, J.D., Blood-materials interactions: The minimum interfacial free energy and the optimum polar / apolar ratio hypothesis, J. Biomed. Mater. Res. 1982, 16 , 381-391

107 Okano, T., Nishiyama, S., Shinohara, I., Akaike, T, Sakurai, Y., Kataoka, K. and Tsuruta, T., Effect of hydrophilic and hydrophobic microdomains on mode interaction between block polymer and blood platelets, J. Biomed. Mater. Res. 1981, 15 , 393-402

108 Okano, T., Aoyagi, T., Kataoka, K., Abe, M., Sakurai, Y., Shimada, M. and Shinohara, I., Hydrophilic-hydrophobic microdomain surfaces having an ability to suppress platelet aggregation and their *in vivo* antithrombogenicity, J. Biomed. Mater. Res. 1986, 20 , 919-927

109 Okano, T., Uruno, M., Sugiyama, N., Shimada, M., Shinohara, I., Kataoka, K. and Sakurai, Y., Suppression of platelet activity on microdomain surfaces of 2-HEMA-polyether block copolymers, J. Biomed. Mater. Res. 1986, 20 , 1035-1047

110 Okano, T., Nishiyama, S., Shinohara, I., Akaike, T, and Sakurai, Y., Interaction between plasma protein and microphase separated structure of copolymers, Polymer J. (Tokyo) 1978, 10 , 223-228

111 Horbett, T.A. and Weathersby, P.K., Adsorption of proteins from plasma to a series of hydrophilic-hydrophobic copolymers. I. Analysis with the *in situ* radioiodination technique, J. Biomed. Mater. Res. 1981, 15 , 403-423

112 Horbett, T.A., Adsorption of proteins from plasma to a series of hydrophilic-hydrophobic copolymers. II. Compositional analysis with the prelabeled protein technique, J. Biomed. Mater. Res. 1981, 15 , 673-695

113 Nakashima, T., Takakura, K. and Komoto, Y., Thromboresistance of graft-type copolymers with hydrophilic-hydrophobic microphase-separated structure J. Biomed. Mater. Res. 1977, 11 ,787-798

114 Tighe, B.J., Hydrogels as contact lens materials, in Hydrogels in Medicine and Pharmacy Vol. III. Properties and Applications, Ed Peppas, N.A., CRC Press, Boca-Raton, Florida 1987, 53-82

115 Park, G.B., Burn wound coverings - A review, Biomat. Med. Dev. Art. Org. , 1978, 6, (1) 1-35

116 Wang, P.Y. and Samji, N.A., Temporary skin substitute from non-antigenic dextran hydrogel, Polym. Sci. Technol. , 1981, 14 (Biomed. Dent. Appl. Polym.), 29-37

117 Wang, P.Y. and Samji, N.A., Characterisation of a dextran hydrogel wound dressing, Org. Coat. Plast. Chem. , 1980, 42 , 628-633

118 Widra, A., (to University of Illlinois Foundation), Hydrophilic biopolymeric electolytes for biodegradable wound dressings, Eur. Pat. Appl. EP 138385, 1985

119 Warne, K.J. (to United Kingdom Secretary of Defence, London), Hydrogel materials, Eur. Pat. Appl. EP 174849, 1986

120 Mason Jr., A.D., Johnson, A.A., Walker, H.C., Bowler, E.G. and Ritchey, G.R. (to United States Department of the Army), Protective Gel Composition for Wounds, U.S. Pat. 4,393,048, 1983

121 Nathan, P., Law, E.J., MacMillan, B.G., Murphy, D.F., Ronel, S.H., D'Andrea, M.J. and Abrahams, R.A., A new biomaterial for the control of infection in the burn wound, Trans. Amer. Soc. Artif. Int. Org. , 1976, 22, 30 - 41

122 D´Andrea, M.J., Moro, D.G. and Griffen, G.A. (to Nat. Pat. Dev. Corp.), Plastic Wound Bandage, S. African Pat. 79 03,825, 1980, U.S. Pat. 4,272,518, 1981

123 Curreri, P.W., Desai, M.H., Bartlett, R.H., Heimbach, D.M., Parshley, P. and Trunkey, D., Safety and efficiency of a new synthetic burn dressing (Hydron): a multicenter study, Arch. Surg. , 1980, 115, (8), 925-927

124 Warren, R.J. and Snelling, C.F.T., Clinical evaluation of the Hydron burn dressing, Plast. Reconstruct. Surg. , 1980, 66, 361-368

125 Brown, A.S., Hydron for burns, Plast. Reconstruct. Surg., 1981, 67, (8) 810 - 811

126 Husain, M.T., Akhtar, M. and Akhtar, N., Report on evaluation of Hydron as burn wound dressing, Burns , 1983, 9, 330-334

127 Robb, E.C., Fitz, D.G. and Nathan, P., Delivery of the topical antimicrobial agents silver sulfadiazine, gentamicin and nystatin to infected burn wounds in rats from preloaded synthetic dressings, Trans. Amer. Soc. Artif. Int. Org. , 1980, 26, 533-537

128 Fox jun., C., Moduk, S., Stanford, J.W. and Bradshaw, W., Silver sulphadiazine - poly hydroxyethyl methacrylate (PHEMA) dressing, Burns , 1981, 7, 295-297

129 Robb, E.C. and Nathan, P., Protective effect of a topical antimicrobial agent delivered to burn wounds from a preloaded synthetic dressing, Curr. Chemother. Infect. Dis. Proc. Int. Congr. Chemothem 11th, 1979 (Pub. 1980) Vol 2 (Eds Nelson, J.D.and Garassi, C.) 1980, 846-847

130 Nathan, P., Robb, E.C., Law E.J. and MacMillian, B.G., A clinical study of antimicrobial agents delivered to burn wounds from a drug loaded synthetic dressing, J. Trauma , 1982, 22, 1015-1018

131 Nathan, P., Robb, E.C. and MacMillian, B.G., A bacterial barrier dressing for skin donor sites, Burns , 1982, 7, 52-56

132 Migliaresi, C., Carfagna, C. and Nicolais, L., Laminates of poly (2-hydroxyethyl methacrylate) and polybutadiene as a potential burn covering, Biomaterials , 1980, 1, 205-208

133 Russo, F., d-Angelo, A., Vesce, C., Avallone, L., Roperto, F., Migliaresi, C., Carfagna, C., Nicodemo, L. and Nicolais, L., Prime osservazioni sulla biocompatibilita di un polimero utilizzabile quale protesi cutanea, Boll. Soc. Ital. Biol. Sper. , 1983, 59 (4), 560-564

134 Migliaresi, C., A poly-2-hydroxyethyl methacrylate based laminate as a potential burn wound covering, in Burn Wound Coverings Vol. 1 , (Ed. Wise D.L.), CRC Press, Boca Raton, Florida, 1984, 137-146

135 Wokalek, H., Schöpf, E., Vaubel, E., Kickhöfen, B., and Fischer, H., Erste Erfahrungen mit einem Transparent-Flüssigkeits-Gel bei der Behandlung frischer Operationswunden und cronischer Epitheldefekte der Haut, Akt. Dermatol. , 1979, 5, 255-265

136 Kickhöfen, B., Wokalek, H., Scheel, D. and Ruh, H., Chemical and physical properties of a hydrogel wound dressing, Biomaterials , 1986, 7, 67-72

137 Curtis, A.J., Covitch, M.J., Thomas D.A. and Sperling, L.H., Polystyrene / polybutadiene interpenetrating polymer networks, Polym. Eng. Sci. , 1972, 12, 101-108

138 Myers, J.A., Geliperm: A non-textile wound dressing, Pharmaceut. J., 1983, 230, 263-264

139 Gorkish, K., Fischer, H., Vaubel, H. and Kickhöfen, B., First experience with a plasma gel dressing, in Clinical Applications of Biomaterials, Eds. Lee, A.J.C., Albrektsson, T. and Branemark, P-I., John Wiley and Sons Ltd., New York, N.Y. 1982, 305-314

140 Knapp, U., Rahn, H.D. and Schauwecker, F., Klinische Erfahrungen mit einem neuen gelartigen Wundverband nach Hauttransplantationen, Aktuel.-Traumatol, 1984, 14 (6), 275-281

141 Leaper, D.J., Brennan, S.S., Simpson, R.A. and Forster, M.E., Experimental infection and hydrogel dressings, J. Hosp. Infection , 1984, 5 Suppl. A, 69-73

142 Behar, D., Juszynski, M., Rajbenbach, A. and Ben-Hur, N. (to Israel, State of), Synthetic wound covering, Eur. Pat. Appl. EP 91,129, 1983

143 Behar, D., Juszynski, M., Ben-Hur, N., Golan, J., Eldad, A., Tuchman, Y., Sterenberg, N. and Rudensky, B., Omniderm, a new synthetic wound covering: Physical properties and drug permeability studies, J. Biomed. Mater. Res. , 1986, 20,731-738

144 Golan, J., Eldad, A., Rudensky, B., Tuchman, Y., Sterenberg, N., Ben-Hur, N., Behar, D. and Juszynski, M., A new temporary synthetic skin substitute, Burns 1985, 11 , 274-280

145 Corkhill, P.H., Jolly, A.M., Ng, C.O. and Tighe, B.J., Synthetic hydrogels I: Hydroxyalkyl acrylate and methacrylate copolymers: Water binding studies, Polymer 1987, 28 , 1758-1766

146 Yocum, R.H. and Nyquist, E.B.(Eds) Functional Monomers, Vols. 1 & 2, Marcel Dekker, New York, 1973

147 Hamilton, W.C., A technique for the characterisation of hydrophilic solid surfaces, J. Colloid Interface Sci. 1972, 40 , 219-222

148 Owens, D.K. and Wendt, R.C., Estimation of the surface free energy of polymers, J. Appl. Polym. Sci. 1969, 13 , 1741-1747

149 Greenley, R.Z., Determination of Q and e values by a least squares technique, J. Macromol. Sci. Chem. 1975, A9 , 505-516

150 Varma, I.K. and Patnaik, S., Copolymerization of 2-hydroxyethyl methacrylate with alkyl acrylates, Eur. Polym. J. 1976, 12 , 259-261

151 Coover, H.W. Jr. and Wicker, T.H. Jr., Acrylic Ester Polymers, in Encyclopedia of Polymer Science and Technology, Vol. 1, Eds. Mark, H.F., Gaylord, N.A. and Bikales, N.M., Wiley-Interscience, New York, N.Y. 1964, 246-342

152 Al-Issa, M.A., Davis, T.P., Huglin, M.B. and Yip, D.C.F., Copolymerizations involving N-vinyl-2-pyrrolidone, Polymer 1985, 26 , 1869-1874

153 Reddy, B.S.R., Arshady, R. and George, M.H., Copolymerization of N-vinyl-2-pyrrolidone with 2,4,5-trichlorophenyl acrylate and with 2-hydroxyethyl methacrylate; Reactivity ratios and molecular weights, Eur. Polym. J. 1985, 21 , 511-515

154 Saini, G., Leoni, A. and Franco, S., Solvent effect in radical copolymerisation. II. N,N-dimethyl acrylamide, Makromol. Chem. 1971, 146 , 165-171

155 North, A.M. and Scallan, A.M., The free radical polymerisation of N,N dimethyl acrylamide, Polymer 1964, 5 , 447-455

156 Tamura, H., Tanaka, M. and Murata, N., Polymerisation by the active species produced from the charge transfer complex V. The thermal copolymerisation of N-vinyl-pyrrolidone and methyl methacrylate, Bull. Chem. Soc. Japan. 1969, 42 , 3042

157 Bork, J. F. and Coleman, L.E., Nitrogen containing monomers II. Reactivity ratios of N vinyl oxazoidone and N vinyl pyrrolidone with vinyl monomers, J. Polym. Sci. 1960, 43 , 413-421

158 Dandliker, W.B. and de Saussure, V.A., Stabilization of macromolecules by hydrophobic bonding: Role of water structure and of chaotropic ions, in Chemistry of Biosurfaces, Vol. 1, Ed. Hair, M.L., Marcel Dekker, New York, N.Y. 1981, 1-43

159 Okano, T., Ikemi, M. and Shinohara, I., Behaviour of oligo (2-hydroxy ethyl methacrylate) and its copolymers in water-organic solvents (Japan), Nippon Kagaku Kaishi 1977, 1 , 93-98

160 Ikemi, M., Odagiri, N. and Shinohara, I., Hydrophobic interaction of the the water soluble ABA-type block copolymer composed of 2-hydroxyethyl methacrylate and ethylene oxide and its conformational translation, Polymer J. (Tokyo) 1980, 12 , 777-784

161 Refojo, M.J. and Yasuda, H.J., Hydrogels from 2-hydroxyethyl methacrylate and propylene glycol monoacrylate, J.Appl. Polym. Sci 1965, 9 ,2425-2435

162 Kuriaki, M. and Harata, T., Temperature dependence of physical properties of crosslinked hydrogels, Makau 1983, 8 , 39-44

163 Starodubtsev, S.G., Boiko, O.K., Pavlova, N.R. and Ryabina, V.R., Properties of hydrogels of copolymers of N-vinylpyrrolidone with methacrylic esters, Kolloidn. Zh. 1982, 44 , 370-373 (Russ.)

164 Scheraga, H.A., Nemethy, G. and Steinberg, I.Z., The contribution of hydrophobic bonds to the stability of protein conformations, J. Biol. Chem. 1962, 237 , 2506-2508

165 Hamilton, C.J., Murphy, S.M. Atherton, N.D. and Tighe, B.J., Synthetic hydrogels IV: The permeability of poly (2-hydroxyethyl methacrylate) to cations, Polymer, In Press

166 Raab, M. and Janacek, J., Effect of chemical crosslinks on the ultimate tensile properties of water swollen poly (2-hydroxyethyl methacrylate), Int. J. Polymeric Mater. 1972, 1 , 147-156

167 Kolaarik, J. and Migliaresi, C., Mechanical properties of hydrophilic copolymers of 2-hydroxyethyl methacrylate with ethyl acrylate, n-butyl acrylate, and dodecyl methacrylate, J. Biomed. Mater. Res. 1983, 17 , 757-767

168 Hosaka, S., Yamada, A., Tanzawa, H. Momose, T., Magatani, H. and Nakajima, A., Mechanical properties of the soft contact lens of poly (methyl methacrylate-N-vinyl pyrrolidone), J. Biomed. Mater. Res. 1980, 4 , 557-566

169 Bowden, P.B., The yield behaviour of glassy polymers, in The Physics of Glassy Polymers, Ed. Haward, R.N., Applied Science, Barking, Great Britain, 1973, 279-339

170 Huglin, M.B. and Rehab, M.M.A-M., Mechanical and thermodynamic properties of butyl acrylate-N-vinyl pyrrolidone hydrogels, Polymer 1987, 28 , 2200-2206

171 Young, T., On the cohesion of fluids, Phil. Trans. Roy. Soc. (London) 1805, 95, 65-87

172 Dupré, A., Théorie méchanique de la chaleur, Gauthier Villars, Paris 1869, 369

173 Bangham, D.H. and Razouk, R. I., Adsorption and the wettability of solid surfaces, Trans. Faraday Soc. 1937, 33, 1459-1463

174 Melrose, J.C., Evidence for solid-fluid interfacial tensions from contact angles, in Contact angles, wettability and adhesion, Ed. Zisman, W.A., Advances in Chemistry Series No. 43, A.C.S., Washington D.C. 1964, 158-179

175 Fox, H.W. and Zisman, W.A., The spreading of liquids on low energy surfaces I. Polytetrafluoroethylene, J. Colloid Sci. 1950, 5 , 514-531

176 Fox, H.W. and Zisman, W.A., The spreading of liquids on low energy surfaces II. Modified tetrafluoroethylene polymers, J. Colloid Sci. 1952, 7 , 109-121

177 Fox, H.W. and Zisman, W.A., The spreading of liquids on low energy surfaces III. Hydrocarbon surfaces, J. Colloid Sci. 1952, 7 , 428-442

178 Ellison, A.H. and Zisman, W.A., Wettability of halogenated organic surfaces, J.Phys. Chem. 1954, 58 , 260-265

179 Bernett, M.K. and Zisman, W.A., Wetting properties of poly (hexafluoropropylene), J.Phys. Chem. 1961, 65 , 2266-2267

180 Kitazaki, Y. and Hata, T., Surface chemical criteria for optimum adhesion, J. Adhesion 1972, 4 , 123-132

181 Girifalco, L.A and Good, R.J., A theory for the estimation of surface and interfacial energies I. Derivation and application to interfacial tension, J. Phys. Chem. 1957, 61 , 904-909

182 Good, R.J., Girifalco, L.A. and Kraus, G., A theory for the estimation of surface and interfacial energies II. Application to surface thermodynamics of Teflon and graphite, J. Phys. Chem. 1958, 62 , 1418-1421

183 Good, R.J. and Girifalco, L.A., A theory for the estimation of surface and interfacial energies III. Estimation of surface energies of solids from contact angles, J. Phys. Chem. 1960, 64 , 561-565

184 Fowkes, F.M., Determination of interfacial tensions, contact angles and dispersion forces in surfaces by assuming additivity of intermolecular interactions in surfaces, J. Phys. Chem. 1962, 66 , 382

185 Kaelble, D.H., Physical chemistry of adhesion, Wiley-Interscience, New York 1971, 149-189

186 Kaelble, D.H., Dispersion-polar surface tension properties of organic solids, J. Adhesion 1970, 2 , 66-81

187 Panzer, J., Components of solid surface free energy from wetting measurements, J. Colloid Interface Sci. 1973, 44 , 142-161

188 Hamilton, W.C., Measurement of the polar force contribution to adhesive bonding, J. Colloid Interface Sci. 1974, 47 , 672-675

189 Bikerman, J.J., Physical Surfaces, Academic Press, London 1970

190 Fowkes, F.M., Additivity of intermolecular forces at interfaces I. Determination of the contribution to surface and interfacial tensions of dispersion forces in various liquids, J. Phys. Chem. 1963, 67 ,2538-2541

191 Tamai, Y., Makuuchi, K. and Suzuki, M., Experimental analysis of interfacial forces at the plane surface of solids, J. Phys. Chem. 1967, 71 , 4176-4179

192 Dettre, R.H. and Johnson, R.E, Contact angle hysteresis-Porous surfaces, in Wetting, SCI Monograph No. 25, SCI, London 1967, 144-163

193 El-Shimi, E. and Goddard, E.D., Wettability of some low energy surfaces II Oils on solids submerged in water, J. Colloid Interface Sci. 1974 48 , 249-255

194 Ottewill, R.H. and Vincent, B., Colloid and surface chemistry of polymer latices. Part I- Adsorption and wetting behaviour of n-alkanols, J.C.S. Faraday I 1972, 68, 1533 - 1543

195 Macleod, D.B., On a relation between surface energy and density, Trans. Faraday Soc. 1923, 19 , 38–42

196 Sugden, S., A relation between surface tension, density and chemical composition, J. Chem. Soc. 1924, 125 , 1177-1189

197 Rastogi, A.K. and St. Pierre, L.E., Interfacial phenomena in macromolecular systems, J. Colloid Interface Sci. 1969, 31 , 168-175

198 Hunten, K.W. and Maass, O., Investigation of surface tension constants in an homologous series from the point of view of surface orientation, J. Am. Chem. Soc. 1929, 51 , 153-165

199 Mumford, S.A. and Phillips, J.W.C., The evaluation and interpretation of parachors, J. Chem. Soc. 1929, 132 , 2112-2133

200 Quayle, O.R., The parachors of organic compounds. An interpretation and catalogue, Chem. Rev. 1953, 53 , 439-486

201 Hildebrand, J.H. and Scott, R.L., The Solubility of Nonelectrolytes, Reinhold, New York, 1950

202 Wu, S., Estimation of the critical surface tension for polymers from molecular constitution by a modified Hildebrand-Scott equation, J. Phys. Chem. 1968, 72 , 3332-3334

203 Small. P.A., Some factors affecting the solubility of polymers, J. Appl. Chem. 1953, 3 , 71-80

204 Barnes, A., Surface Properties of Hydrophilic Polymers, PhD Thesis, University of Aston 1976

205 Clay, C.S., Lydon, M.J. and Tighe, B.J., Surface energy measurements on protein layers adsorbed onto synthetic substrates, in Biomaterials and Clinical Applications, Eds., Pizzoferrato, A., Marchetti, P.G., Ravaglioli, A. and Lee, A.J.C., Elsevier Science Publishers B.V., Amsterdam 1987, 535-540

206 Mason, J.A. and Sperling, L.H., Polymer Blends and Composites, Plenum, New York, N.Y. 1976, 51

207 Sperling, L.H., Interpenetrating Polymer Networks and Related Materials, Plenum Press, New York, N.Y., 1981

208 Thomas, D.A. and Sperling, L.H., Interpenetrating Polymer Networks, in Polymer Blends Vol II, Eds. Paul, D.R. and Neuman, S., Academic Press, New York, N.Y., 1978, 1-33

209 Frisch, H.L., Frisch, K.C. and Klempner, D., Advances in interpenetrating polymer networks, Pure Appl. Chem. 1981, 53 , 1557-1566

210 Klempner, D., Yoon, H.K., Frisch, K.C. and Frisch, K.L., Polyurethane-polyacrylate pseudo-interpenetrating polymer networks, in Chemistry and Properties of Crosslinked Polymers, Ed. Labana, S.S., Academic Press, New York, N.Y. 1977, 243-256

211 Sperling, L.H., Pure and applied research on interpenetrating polymer networks and related materials, in Polymer Blends and Mixtures, NATO ASI Ser., Ser. E, Vol 89, Eds. Walsh, D.J., Higgins, J.S. and Maconnachie, A., Martinus Nijhoff, Dordrecht, The Netherlands 1985, 267-287

212 Klempner, D. and Berkowski, L., Interpenetrating polymer networks, in Encyclopedia of Polymer Science and Engineering, Vol. 8, Ed. Kroschwitz, J.I., Wiley-Interscience, New York, N.Y. 1987, 279-341

213 Falcetta, J.J., Frienos, G.D. and Niu, G.C-C, (to Bausch and Lomb Inc.), Solid article formed from a polymer network with simultaneous interpenetration, Fr. Demande 2,365,606 1978

214 Lee, E.S., Kim, S.W., Kim, S.H., Cardinal, J.R. and Jacobs, H., Drug release from hydrogel devices with a rate controlling barrier, J. Membrane Sci. 1980, 7 , 293-303

215 DeCrosta, M.T., Jain, N.B. and Rudnic, E.M. (to E.R. Squibb and Sons Inc.), Drug delivery systems including interpenetrating polymer networks, U.S. Pat. US 4575539 March 1986

216 Mueller, K.F. and Heiber, S.J. Gradient-IPN-modified hydrogel beads: Their synthesis by diffusion polycondensation and function as controlled drug delivery agents, J. Appl. Polym. Sci. 1982, 27 , 4043-4066

217 Dror, M., Elsabee, M.Z. and Berry, G.C., Gradient interpenetrating polymer networks I. Poly(ether urethane) and polyacylamide IPN, J. Appl. Polym. Sci. 1981, 26 , 1741-1757

218 Elsabee, M.Z., Dror, M. and Berry, G.C., Gradient interpenetrating polymer networks II. Polyacrylamide gradients in poly(ether urethane), J. Appl. Polym. Sci. 1983, 28 , 2151-2160

219 Hourston, D.J., Huson, M.G. and McCluskey, J.A., Semi and fully interpenetrating polymer networks based on polyurethane-polyacrylate systems IX. Properties of an isomerically related network, J.Appl. Polym. Sci. 1986, 31 , 709-716

220 Lelah, M.D., Lambrecht, L.K., Young, B.R. and Cooper, S.L., Physicochemical characterisation and *in vivo* blood tolerability of cast and extruded Biomer, J. Biomed. Mater. Res. 1983, 17 , 1-22

221 Thomas, K.D., Biological Interactions with Synthetic Polymers, PhD Thesis, University of Aston 1988

222 Ziats, N.P., Miller, K.M and Anderson, J.M., *In vitro* and *in vivo* interactions of cells with biomaterials, Biomaterials 1988, 9 , 5-13